IDENTIFYING GENE REGULATORY NETWORKS CONTROLLED BY BONE MORPHOGENETIC PROTEIN-SIGNALING IN *DROSOPHILA* AND MURINE GENOMES

by

Katerina Maria Othonos

B.Sc., University of Cyprus, 2013

A THESIS SUBMITTED IN PARTIAL FULFILLMENT OF

THE REQUIREMENTS FOR THE DEGREE OF

DOCTOR OF PHILOSOPHY

in

THE FACULTY OF GRADUATE AND POSTDOCTORAL STUDIES

(Neuroscience)

THE UNIVERSITY OF BRITISH COLUMBIA

(Vancouver)

February 2020

The following individuals certify that they have read, and recommend to the Faculty of Graduate and Postdoctoral Studies for acceptance, the dissertation entitled:

Identifying Gene Regulatory Networks Controlled by Bone Morphogenetic Protein-Signaling in *Drosophila* and Murine Genomes

submitted by Katerina Maria Othonos in partial fulfillment of the requirements for

the degree of Doctor of Philosophy

in Neuroscience

Examining Committee:

Dr. Douglas Allan

Supervisor

Dr. Timothy O`Connor

Supervisory Committee Member

Dr. Brad Hoffman

University Examiner

Dr. Daniel Goldowitz

University Examiner

Additional Supervisory Committee Members:

Dr. Michael Underhill

Supervisory Committee Member

Dr. Vanessa Auld

Supervisory Committee Member

Abstract

Bone morphogenetic proteins (BMPs) are a group of phylogenetically conserved signaling proteins, first identified to play important roles in bone formation. Since their discovery, they have been recognized to contribute to embryonic development and adult homeostasis in a multitude of tissues, by regulating cellular lineage commitment, morphogenesis, differentiation, proliferation, and apoptosis. BMPs transduce their signals through intracellular downstream effectors, primarily the Smad transcription factors, many of which bind to genomic BMP-responsive *cis*-regulatory elements (BMP-CREs) to direct gene expression. Despite their importance in cellular processes and maintenance, BMP-CREs remain largely unidentified at a genomic level for most BMP-dependent cellular processes.

The overall objectives of this thesis were to experimentally characterize the widespread function of a novel low-affinity BMP-CRE motif in the *Drosophila* nervous system and to identify the BMP-driven regulatory network underlying mammalian chondrogenesis.

To address the first goal, we used computational methods to identify this novel BMP-CRE through the *Drosophila* genome and used *in vivo* transgenic reporters to determine their function in the *Drosophila* nervous system. Our results show that this BMP-CRE is used within multiple enhancers to mediate their BMP-dependent activity. For our second goal, we used poly-A transcriptome sequencing (RNA-seq) to characterize differentially expressed genes (DEGs) during chondrogenesis in primary murine cells. Amongst these DEGs, we identified transcription factors/cofactors with previously unknown roles in chondrogenesis that are of interest for further study. Further, we used histone modification ChIP-seq to identify more than 2000 candidate

regulatory regions in the vicinity of BMP-responsive DEGs. Using computational tools, we examined these candidate regulatory regions for Smad-binding sites using BMP-CRE motifs identified in *Drosophila*. We then applied multiple selection criteria to prioritize likely BMP-responsive regulatory regions and assessed four novel regions for BMP-responsive reporter expression, using mouse primary limb mesenchymal (PLM) cells. Among these, we identified two BMP-responsive regulatory regions, including one within 50kb of the transcription factor *Jdp2*, a gene with previously unknown roles in chondrogenesis.

The genomic mapping of BMP-CREs remains incomplete. Mutations in these *cis*-regulatory sites and BMP-regulated genes could potentially result in disease, and therefore their identification is of critical importance to help further our understanding of disorders in various human tissues.

Lay Summary

From fruit flies to humans, bone morphogenetic protein (BMP) signaling plays critical roles in many tissues. Defects in this pathway are implicated in many human diseases; however, the exact roles of BMPs in these diseases are mostly unknown. BMPs control proteins called transcription factors that can direct gene expression through DNA sequence sites called *cis*-regulatory elements (CREs). Mutations occurring in CREs have been linked to several human disorders. Despite being extremely important, BMP-dependent CREs are not well characterized. This thesis identifies and studies CREs in fruit fly neurons, providing insight into BMP-dependent gene regulation. Further, it identifies important new genes and BMP-dependent CREs that regulate the process of cartilage formation during mouse embryonic development. This work will help us understand the process of cartilage formation in humans and lays the foundations for identifying cartilage-related BMP-dependent CREs that are associated with human disease.

Preface

The contents of this dissertation are my original work. All experiments were designed and conducted by me in conjunction with my supervisor, Dr. Douglas Allan, and the guidance of my supervisory committee.

Chapter 1 is a general introduction to my thesis, beginning with a review of the relevant literature and ending with the main objectives and overarching hypothesis of my research.

Chapter 2: "Genomic identification and validation of a novel BMP *cis*-regulatory element in the *Drosophila* CNS"

The work entailed in this chapter is part of a manuscript currently under review, following the first round of review. The publication is entitled: **A low affinity *cis*-regulatory BMP response element confers subtype-specific gene activation in *Drosophila* neurons,** Anthony J.E. Berndt*, Katerina M. Othonos*, Tianshun Lian, Mo Miao, Shamsuddin Buiyan, Raymond Y. Cho, Justin S. Fong, Seo Am Hur, Paul Pavlidis, Douglas W. Allan *= co-first authorship

Dr. Douglas Allan, Dr. Anthony Berndt and I conceptualized the study and the required experiments that are detailed in Chapter 2. The initial experiments were conducted by Dr. Anthony Berndt, as part of his Ph.D. research. This included cloning of the initial transgenic flies which was done with the help of Raymond Y. Cho, Justin S. Fong, and Seo Am Hur. I generated all further transgenic lines used in the study, performed all dissections and immunocytochemistry, collected data and prepared figures/graphs. Mo Miao assisted with transgenic fly maintenance and dissections. Computational motif discovery was performed by Shamsuddin Bhuiyan, a Ph.D. candidate in the Pavlidis lab, UBC and Dr. Stephane Flibotte. Tianshun performed all EMSAs. Along with Dr. Douglas Allan and Dr. Anthony Berndt, I helped write and revise the manuscript.

Chapter 3: "Determining the BMP-dependent regulatory network underlying the early stages of chondrogenesis in the murine limb bud." is a manuscript in preparation, the title of which is currently tentative. I am the first author on this manuscript, co-authored by Mo Miao, Stephane Flibotte, Shamsuddin Bhuiyan, Ryan Vander Werff, Paul Pavlidis, Michael T. Underhill, and Douglas W. Allan.

Dr. Douglas Allan, Dr. Michael Underhill and I conceptualized the study. I prepared samples for all experiments, conducted the GO term analyses, analyzed the data and prepared figures. RNA-seq sample Bioanalyzer Quality Control and PolyA-RNA-seq library preparation and sequencing were performed by Ryan Vander Werff, at the BRC-Seq Next Generation Sequencing Core, UBC. For the histone ChIP-seq experiments I prepared all samples that were used for chromatin immunoprecipitation and library preparation. These were conducted in the Laboratory of Epigenomics and Chromatin Biology, UBC, under the supervision of Dr. Martin Hirst. Sequencing was performed at the BC Cancer Genome Sciences Centre. RNA-seq and ChIP-seq raw data analysis, as well as the generation of all corresponding quality control figures, were performed by Dr. Stephane Flibotte in the Allan lab. Computational motif discovery was performed by Shamsuddin Bhuiyan, a Ph.D. candidate in the Pavlidis lab, UBC and Dr. Stephane Flibotte. Mo Miao, a graduate student in the Allan lab, assisted with the construction of reporter plasmids and cloning of genomic fragments.

Chapter 4 is a summary of the overall conclusions of my thesis, including contributions and significance to the field, and future directions.

Table of Contents

List of Tables

List of Figures

List of Abbreviations

AE	Activating Element
ACAN	Aggregan
bHLH	basic helix-loop-helix
BMP	Bone Morphogenetic Protein
BMPR1A	BMP Receptor 1A
BMPR1B	BMP Receptor 1B
BMPRII	BMP Receptor II
CDC	Centers for Disease Control and Prevention
ChIP	Chromatin Immunoprecipitation
CHRD	Chordin
Ci	Cubitus interruptus
CNS	Central Nervous System
Col2a1	Collagen type II alpha 1
CRE	*cis*-Regulatory Element
CRISPR	Clustered Regularly Interspaced Short Palindromic Repeats
CRM	*cis*-Regulatory Module
Dad	*Daughters against dpp*
DEG	Differentially expressed gene
dfd	*deformed* (*dfd*) enhancer
DLX2	Distal-Less Homeobox 2
DNA	Deoxyribonucleic Acid
Dpp	Decapentaplegic
ECM	Extracellular matrix
EGFP	Enhanced Green Fluorescent Protein
ENCODE	Encyclopedia of DNA Elements
EVI1	Ecotropic Viral Integration Site 1 Protein Homolog
FAIRE-Seq	Formaldehyde-Assisted Isolation of Regulatory Elements Sequencing
FDR	False Discovery Rate

FMRFa	FMRFamide (*Drosophila* neuropeptide)
Gbb	Glass bottom boat
GDF	Growth Differentiation Factors
GFP	Green Fluorescent Protein
GMR	eye-specific glass multimer reporter (GMR) enhancer
GO	Gene Ontology
GWAS	Genome-Wide Association Studies
HAT	histone acyteltransferase
HDAC	histone deacetylase
HD-RE	Homeodomain-Response Element
Hh	Hedgehog
HMT	Histone methyltransferases
IHH	Indian Hedgehog
JDP2	Jun Dimerization Protein 2
Mad	Mothers against *dpp*
Matn1	Matrilin-1
MEF2	Myocyte Enhancer actor-2 family transcription factors
MH1	Mad Homolog 1
MH2	Mad Homolog 2
MSC	Mesenchymal Stem Cells
MSX2	Msh Homeobox 2
NKX	NKX-homeodomain factors
NMJ	Neuromuscular junction
NOG	Noggin
OA	Osteoarthritis
OAZ	Ornithine Decarboxylase Antizyme 1
PANTHER	Protein ANalysis THrough Evolutionary Relationships
PLM	Primary Limb Mesenchymal

PRC2	Polycomb Repressive Complex 2
PRMT	Protein arginine methyltransferases
PTHrP	Parathyroid Hormone-related Peptide
RNA	Ribonucleic Acid
RT	Room Temperature
RUNX	Runt-related transcription factors
Sax	Saxophone
SBE	Smad binding element
SE	Silencer Element
seq	Sequencing (usually referring to high throughput methods)
Shn	Schnurri
Smad	acronym from the fusion of the *C.elegans* **S**ma and *Drosophila* **Mad** genes
Sog	Short gastrulation
SOX	Sex-Determining Region Y-Box family transcription factors
STARR-Seq	Self-Transcribing Active Regulatory Region Sequencing
STRING	Search Tool for the Retrieval of Interacting Genes/Proteins
svb	shavenbaby
TCF4	Transcription Factor 4
TF	Transcription factor
TFBS	Transcription factor binding site
TGFβ	Transforming Growth Factor β
Tkv	Thickveins
TSS	Transcription start site
UTR	Untranslated region
VNC	Ventral Nerve Cord
wit	*wishful thinking*
WT	Wildtype
ZEB2	Zinc Finger E-Box Binding Homeobox 2
Zen	zerknüllt

Acknowledgements

First and foremost, I would like to express my gratitude to my supervisor, Dr. Douglas Allan, for his continuous support during my Ph.D. work. I am grateful for his patience, guidance, motivation and for consistently inspiring me with his passion for science. Thank you for taking a chance on me and for investing all this time and effort to ensure my development as a student and scientist. I could not have imagined having a better advisor for my Ph.D. I would like to extend my appreciation to my supervisory committee members Drs. Tim O`Connor, Michael Underhill and Vanessa Auld, for their time, encouragement and feedback that helped shape this thesis and my progress as a researcher. To our collaborators, the Underhill lab, the Hirst lab, Dr. Stephane Flibotte, Shamsuddin Bhuiyan and Margot Gunning, I am fortunate to have had the opportunity to work with you and learn from you. This research would not have been possible without the passion and knowledge of all of the aforementioned.

I would also like to thank all members of the Allan lab, past and present, for their friendship and support during my time here. Thank you from the bottom of my heart for the countless hours you have spent training, teaching and troubleshooting with me. Special thanks go to past lab members: Anthony, Monica, Kathleen, Justin, Katiana and Ray. To all of my present lab members: Payel, Mo, Robin, Helen, Tian, Mriga and Aarya, I have enjoyed working with all of you and will always cherish our friendships. It is rare to find a lab where you not only enjoy the science, but also appreciate all the people you work with.

Last but not least, I would like to thank my friends and family for their continuous support, love and guidance. To my old lab-mates, Sarah, Tissa, Adam and Negar, thank you for helping me when I first moved to Canada and for supporting me through some tough times. To my closest friends and partners-in-crime, Payel, Lakshana and Aarya, thank you for being there for all the ups and downs over the years. I am fortunate to have found such wonderful friends that I can work with every day.

To my amazing partner and best friend, Abhinav, thank you for coming into my life so unexpectedly and for keeping me sane during this degree. Words cannot express how much your love, patience, devotion and never-ending support has meant to me over the years. You are the best thing that has ever happened to me and I am excited to see what the future will bring.

To my family, thank you for your unconditional love and support through the years. To my baby brothers, Χρήστο, Αλέξη and Μάρκο, thank you for your encouragement and love, even from so far away. Το γιαγιά Αναστασία, παππού Σπύρο and γιαγιά Παναγιώτα thank you for believing in me. Το θείο Γιώργο, θεία Ελεάνα, Χριστίνα, Σπύρο and Μαρία, thank you for making the move to Canada worth it. Finally, to my parents Αντρέα and Δήμητρα, thank you for being the most encouraging, inspirational and supportive people in my life. Thank you for always believing in me and telling me that I can make all my dreams come true. Your generosity is truly amazing, and I would not have been able to survive this degree without your help. I am forever indebted to you and can only hope that I make you proud every day.

to my parents,

for always encouraging me to follow my dreams

and

to my partner,

for keeping me sane and pushing me to always do my best

Chapter 1: Introduction

1.1 *cis*-Regulatory Modules and *cis*-Regulatory Elements

The focus of my thesis is identifying and experimentally verifying *cis*-regulatory regions that regulate gene expression in bone morphogenetic protein (BMP)-dependent cellular differentiation. To this end, the next section provides a basic background on the nature of *cis*-regulatory elements in transcription regulation.

Differential gene expression is a fundamental process that underlies cellular development and differentiation. An important step in this process is the transcription of a DNA sequence into mRNA by the RNA polymerase II (Pol II). Transcription requires the recruitment of Pol II and the formation of the pre-initiation complex (i.e. general TFs, Mediator complex) at the core promoter, which is comprised of genomic sequences around the transcription start site (TSS). However, control of the recruitment of this basal transcriptional machinery and/or clearance of this complex from the promoter to initiate transcription is regulated by transcription factor (TF) complexes bound to non *cis*-regulatory regions, commonly referred to as enhancers or silencers (Shlyueva et al., 2014).

Cis-regulatory elements (CREs) are short 4-12bp DNA binding sites for TFs (Shlyueva et al., 2014; Suryamohan and Halfon, 2015; Guo and Huo, 2017). TFs that bind CREs act to enhance or repress transcription, depending on the factors recruited and/or their post-translational modifications. One of the defining hallmarks of a CRE is that they can influence transcription regardless of their location or orientation relative to the promoter of the gene they regulate (Banerji et al., 1981; Ong and Corces, 2011; Shlyueva et al., 2014). CREs are typically organized in 50bp-2kb clusters (Levine 2010; Cho 2012; Long et al., 2016; Hojo et al., 2017), termed *cis*-regulatory

modules (CRMs, i.e. enhancers, silencers, insulators, promoters; Hardison and Taylor, 2012). CRMs may be up to 1Mb away from the TSS they regulate, in intergenic non-coding sequence or 5′ UTR, 3′ UTR or introns relative to their target genes (Lettice et al., 2008; Spitz and Furlong, 2012; Evans et al., 2012; Hardison and Taylor, 2012; Suryamohan and Halfon, 2015; Long et al., 2016). Thus, there are CREs that are located within a few kb of the promoter, referred to as promoter-proximal CREs, and those that interact with distally located promoters, called distal CREs. DNA looping allows distal CRM complexes to come into proximity with their target promoters, where they help recruit or stabilize interactions with the core transcriptional machinery (Weake and Workman, 2010; Bulger and Groudine, 2011; Beagrie and Pombo, 2016). The modular nature of CRMs allows the integration of signaling and tissue-specific inputs via the assembly of several TFs, which then recruit co-activators or co-repressors and chromatin modifiers, including post-translational modifiers or nucleosome-remodeling complexes (Levine, 2010; Weake and Workman, 2010; Mathelier et al., 2015). The combined regulatory input of all bound factors results in the spatiotemporal-specific regulation of target gene transcription (Levine, 2010; Yanez-Cuna et al., 2013).

1.1.1 *cis*-Regulatory Element Tuning and Specificity

As Chapter 2 deals largely with a novel pSmad CRE binding site that relies upon a low-affinity interaction for its appropriate function, here I will be discussing some of our current knowledge on CRE specificity, how it arises and the use of low-affinity binding sites in transcriptional regulation.

The binding of TFs to CREs is dependent upon the specific DNA sequence of the CRE. Historically, CREs have been defined and searched as high affinity, stringent binding sites.

However, most TFs can tolerate a degree of sequence diversity, or degeneracy, at the CRE (Mathelier et al., 2015). Beyond the linear organization, spacing and number of transcription factor binding sites, the relative strength/quality of regulatory binding sites is key for tuning enhancer activity for appropriate expression. For each TF, there is an optimal motif with highly constrained nucleotide composition conferring the lowest possible binding free energy, and thus, making the binding between TF and DNA more stable, favorable and high affinity. Since each nucleotide within a sequence contributes additively to the free energy of the binding site, it stands to reason that there are multiple nucleotide substitutions that can convert a sequence to a lower affinity binding site (Badis et al., 2009; Slattery et al., 2012; Ramos and Barolo, 2013; Farley et al., 2015; Crocker et al., 2016). Thus, CREs that exhibit high degeneracy have been called low-affinity motifs.

A growing body of literature has identified low-to-moderate affinity binding sites that are required for regulating spatiotemporal gene expression. Importantly, in these cases, conversion to a high affinity site often disrupts gene expression, or results in ectopic expression, indicating that low-affinity sites are necessary to specify precise gene expression patterns (Swanson et al., 2011; Farley et al., 2015; Crocker et al., 2015; Lorberbaum et al., 2016; Crocker et al., 2016). One such example is from the *Drosophila* Cubitus interruptus (Ci) TF that mediates gene expression in response to a Hedgehog (Hh) morphogen signaling gradient (Von Ohlen et al., 1997). Depending on the intensity of Hh signaling, Ci activates or actively represses the transcription of Hh responsive genes. Multiple low-affinity binding sites for Ci in Hh-responsive enhancers were found to be required for normal activation in regions with relatively low Hh signaling. Changing these low-affinity sites into optimal Ci binding motifs resulted in a switch from Ci-mediated activation to Ci-mediated repression (Parker et al. 2011). Therefore, the low-affinity nature of the

binding sites contributed to limiting the response to a pleiotropic and broadly active pathway, allowing for adjustment of that response in specific tissues and cells (Ramos and Barolo 2013). Another example is the regulation of the shavenbaby (*svb*) gene by (homotypic) clusters of low-affinity binding sites for the Ultrabithorax TF in *Drosophila*. Clustering of many low-affinity sites was shown to confer robustness of *svb* regulation and replacing these sites with high affinity ones not only resulted in ectopic expression, but it also decreased normal expression patterns (Crocker et al. 2015).

Even with sequence tolerance, we cannot explain how a family of TFs, with overlapping or similar sequence recognition, can carry out distinct functions *in vivo*. In other words, how can each of the nearly 60 basic helix-loop-helix (bHLH) transcription factors that bind to a variation of the sequence "CACGTG" carry out their discrete functions (Murre et al., 1989; Jones, 2004)? Spatiotemporal differences in expression, as well as the small variances in binding sequence preference between TF family members alone, cannot explain how TFs can regulate their unique set of target genes. A mechanism called "latent specificity" could account for the added TF specificity observed *in vivo*. Based on work with the *Drosophila* Hox homeodomain TFs, it was shown that individual members of the same TF family acquire novel DNA binding sequence preferences by forming complexes with cofactors (Joshi et al., 2007; Slattery et al., 2011). Further work with a larger set of TFs verified that interactions between cofactors can significantly alter a TF's sequence preference (Jolma et al. 2015). This added complexity further hinders our ability to identify CREs, as TFs form different complexes under different contexts and bind to degenerate sequences, making it challenging to define universal and computationally identifiable consensus sequences.

1.1.2 Chromatin Modifications and their use in CRM Discovery

Another layer of transcriptional regulation is epigenetic regulation by modification of chromatin structure. DNA is compacted into repeated structures termed nucleosomes; these are the basic subunits of chromatin and consist of 147bp of packaged DNA wrapped around a histone octamer. Two copies of each H2A, H2B, H3, and H4 core histone proteins form this octamer. The core histones are mainly globular with unstructured N-termini (histone tails). The linker histone H1 binds on the outside and stabilizes the folding on the nucleosome (Luger et al., 1997).

Chromatin structure can be altered to facilitate or suppress transcription; for example, actively transcribed regions tend to be in looser chromatin structures so that transcription factors and RNA polymerases can access the genes. Post-translational modifications on histone tail residues have a large impact, by disrupting chromatin structure or by recruiting non-histone proteins, such as a class of co-factors called histone-modifying enzymes, described below. For instance, acetylation of a lysine residue can neutralize its positive charge and weaken the binding between the histone and the negatively charged DNA, exposing the DNA to regulatory proteins (Kouzarides 2007), and facilitate the recruitment of transcriptional machinery.

Histone modifying enzymes promote covalent modifications of histone protein tails. Out of the many distinct types of modifications (e.g. phosphorylation, ubiquitylation, sumoylation; Butler et al., 2012), here I will only focus on acetylation and methylation since these are commonly used to identify active/repressed genes and enhancers. Histone acetylation was first identified in the 60s (Allfrey et al., 1964) and is characterized by the addition of an acetyl moiety to the ε-amino group of a conserved lysine residue (Postberg et al., 2010). Acetylation is controlled by histone acetyltransferases (HATs) and histone deacetylases (HDACs). As both HATs and HDACs are

unable to directly bind to DNA, they are recruited to the promoter or regulatory regions along with other multiprotein complexes by DNA-bound activators. Histone methylation can occur at both lysine and arginine residues. Lysines may be mono-, di-, or tri-methylated and arginines may be mono- or di-methylated. Methylation of lysine on histone subunits H3 and H4 is catalyzed by histone methyltransferases (HMTs), and methylation of arginines is catalyzed by the protein arginine methyltransferases (PRMT) family. (Whetstine 2010; Burke and Grant 2010)

Examining histone modification patterns during various stages of cell development in many tissues and organisms revealed that certain marks correlate with specific gene expression or transcriptional states (Bernstein et al., 2006; Calo and Wysocka, 2013) (Figure1.2). While a significant number of histone post-translational modifications have been identified to date (Huang et al., 2014; Zhao and Garcia, 2015), the most extensively studied H3 methylation sites are lysines 4, 9, 27, 36, 79 and acetylation sites at lysines 9, 14, 18, 23, 27, 56 (Lennartsson and Ekwall, 2009; Greer and Shi, 2012). The following section will outline what is currently known about H3 post-translational modifications at K4me1, K4me3, K27ac, and K27me3, as they are widely used to identify active/repressive enhancer function or gene expression.

Methylation of histone H3K4 is predominantly found at CREs and promoters during transcription. Monomethylated H3K4 (H3K4me1) marks active, primed and poised enhancers, while H3K4me3 is found at the promoters/TSS of actively transcribed genes (Santos-Rosa et al., 2002; Bernstein et al., 2006). Histone H3 lysine 27 acetylation (H3K27ac) identifies both actively transcribed gene promoters/TSS and active enhancers (Wang et al., 2008; Tie et al., 2009). In fact, active enhancers bear both the H3K4me1 and H3K27ac marks and are typically bound by the histone acetyltransferase P300 (Heintzman et al., 2007; Heintzman et al., 2009; Creyghton et al.,

2010; Zentner et al., 2011). Primed enhancers drive low levels of gene expression and are characterized by a lack of H3K27ac and retention of H3K4me1 and P300 (Creyghton et al., 2010; Zentner et al., 2011). Finally, at repressed genes, regulatory elements are enriched for H3K27me3, a mark which is also associated with Polycomb Repressive Complex 2 (PRC2) silencing, and are depleted of other activating modifications (Bernstein et al., 2006; Boros et al., 2014). However, a bivalent modification pattern containing the "opposing" H3K4me3 and H3K27me3 marks was identified in ES cells and found to keep certain developmental genes in a silent but poised-for-activation state (Bernstein et al. 2006). This type of chromatin modification pattern tends to be resolved during ES cell differentiation, with differentiated cells only maintaining one of the two marks on each given gene. Poised enhancers are inactive, and are marked by H3K4me1 and P300 while also bearing the repressive H3K27me3 mark (Rada-Iglesias et al., 2011; Shlyueva et al., 2014). During differentiation, these poised enhancers transition to their active state and H3K27me3 residues replace their methylation with acetylation marks (Rada-Iglesias et al. 2011).

In short, combinations of H3K4me1, H3K27ac, and H3K27me3 are widely used to classify active enhancers (containing both H3K4me1 and H3K27ac), inactive enhancers (containing H3K4me1 but lacking H3K27ac) or poised enhancers (containing both H3K4me1 and H3K27me3) (Heintzman et al. 2007; Creyghton et al. 2010; Rada-Iglesias et al. 2011).

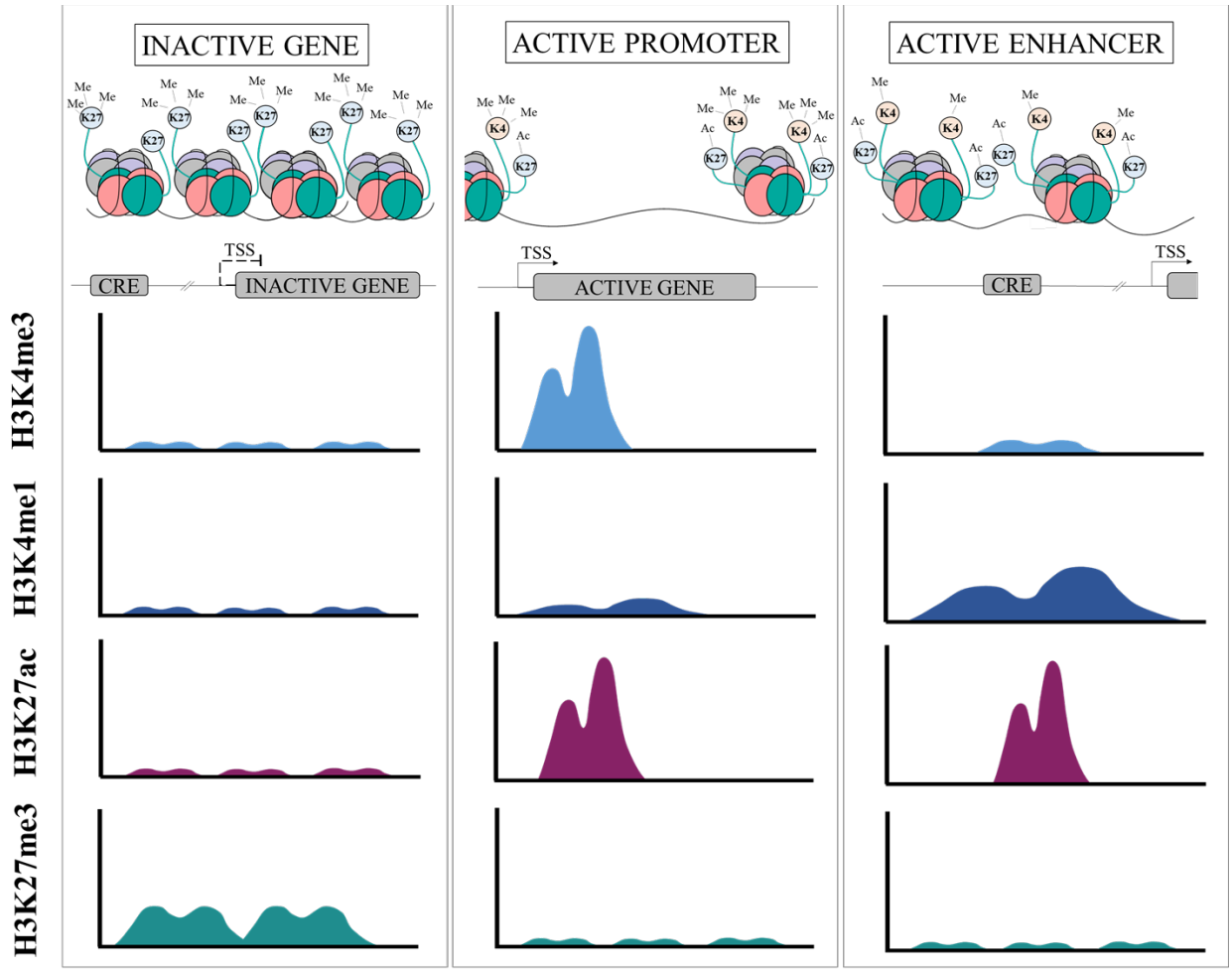

Figure 1.1: ***Representation of genome browser tracks for histone modifications corelated to gene and enhancer activity.*** Each column represents the transcriptional state of a gene/enhancer region and the histone modification marks we expect to observe in each case. Figure generated using (Pundhir et al., 2015) as source material.

1.2 Bone Morphogenetic Protein Signaling

BMPs were first identified in 1965 (Urist, 1965), but were only characterized as critical components of bone extract that direct cartilage and *de novo* bone formation in the late 1980s (Wozney et al. 1988). Since then, multiple studies have confirmed the role of BMPs in cartilage and bone formation, and expanded our understanding of their important functions in the formation, maintenance and regeneration of multiple tissues and organs (Mehler et al. 1997; Whitman 1998; Massague et al., 2000; Liu and Niswander 2005; Wang et al. 2014). As would be expected by these diverse functions, altered BMP signaling is associated with several human diseases including amyotrophic lateral sclerosis, arthritis, osteoporosis, kidney diseases, fibroses, multiple cancers and pulmonary hypertension (Wang et al. 2014).

BMPs belong to the highly conserved transforming growth factor (TGF) β superfamily of signaling molecules, which also includes activins, inhibins and nodal, growth differentiation factors (GDFs) and the TGFβ subfamily (Massagué et al., 2005; Mueller, 2015). Although BMPs can signal via a variety of pathways, they do so primarily through the canonical Smad transduction pathway. In this pathway, BMP ligand dimers bind to a heterotetrameric complex of transmembrane receptors comprised of two dimers each of type I and type II receptor kinases. Ligand binding allows type II receptor kinases to transphosphorylate the glycine/serine rich domain of type I receptors (Miyazono et al., 2010). Receptor engagement results in type I receptor-driven phosphorylation of the conserved C-terminal SXS (Ser-X-Ser) motif of Receptor-Smads (R-Smad), which are Smad1/5/9 in vertebrates and Mad in *Drosophila*. Phosphorylated R-Smads form a 2:1 complex with their cofactor, the Co-Smad (Smad4 in vertebrates and Medea in *Drosophila*), that translocates to the nucleus to act as the sequence specific transcription factor pSmad complex (Fig.1.1) (Zawel et al., 1998; Massagué et al., 2005; Mueller, 2015). While in the

nucleus, the activated pSmad complex binds to a CRE (BMP-CREs are described in Section 1.3.1) and interacts with various transcriptional co-activators and co-repressors to fine-tune cell-type specific transcription of target genes (Miyazono et al., 2006; Ross and Hill, 2008; Hill, 2016).

R-Smads and co-Smads both have two conserved domains that are connected by a proline-rich linker. These domains are the Mad Homolog 1 (MH1) domain, which contains the sequence-specific DNA binding domain, and the MH2 domain, which contains transactivation and protein-protein interaction domains (Heldin et al., 1997; Kretzschmar and Massagué, 1998).

Canonical BMP signaling can be regulated at all steps along the pathway (Zhu et al., 1999; Massagué et al., 2005; Xu, 2006); however, here I will only briefly discuss those directly relevant to this thesis. Extracellular molecules, such as *Drosophila* Short gastrulation (Sog) and vertebrate Noggin (NOG) act as extracellular antagonists of BMP signaling via sequestering of ligand and suppression of receptor activation. In addition, intracellular regulators of BMP signaling such as inhibitory Smads (I-Smads; Smad6, Smad7 in vertebrates and Dad in *Drosophila*) can compete with R-Smads for binding to the activated type I receptors and thereby reduce R-Smad phosphorylation (Mulloy and Rider, 2015). Smad complex co-regulators, such as Schnurri (Shn) in *Drosophila*, will be discussed further in Sections 1.2.2 and 1.3.1.

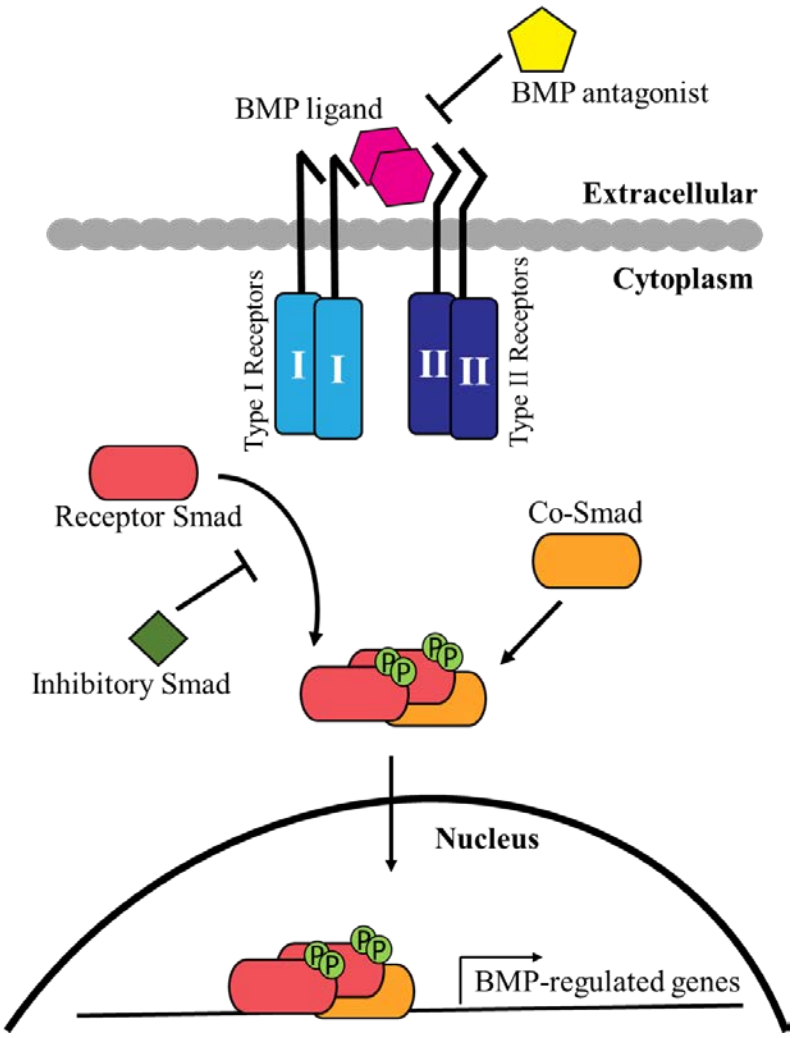

Signaling Component	***Drosophila***	**Mouse**
BMP Ligand	Decapentaplegic (Dpp), Glass bottom boat (Gbb), Screw (Scw)	BMP2/4/5/8
BMP Antagonist	Short gastrulation (Sog), Twisted gastrulation (Tsg)	Chordin (CHRD), Noggin (NOG)
Type I Receptor	Thickveins (Tkv), Saxophone (Sax)	BMPR1A,BMPR1B,ACVRL1
Type II Receptor	Punt (Pnt), Wishful thinking (Wit)	BMPRII, ACTRIIA,ACTRIIB
R-Smad	Mothers against decapentaplegic (Mad)	SMAD1/5/9
Co-Smad	Medea	SMAD4
Inhibitory Smad	Daughters against *dpp* (Dad)	SMAD6/7

Figure 1.2: **Summary of the BMP Signaling Pathway in *Drosophila* and mouse.**

Schematic representation of the canonical BMP signaling pathway. Table containing the orthologues of relevant BMP signaling components in *Drosophila* and mouse.

1.2.1 BMP-CREs, Smads, and their Co-factors

One of the long-term goals of this project is to identify TFs that act together with Smads to define cell-type specific gene expression. Smads have weak affinity for DNA relative to many other TFs (Shi et al., 1998; Shi et al., 1999), and have often been found to require cooperative or collaborative interactions with other TFs or cofactors for high-affinity and specificity in recruitment to CRE binding sites (Ross and Hill, 2008; Blitz and Cho, 2009). This is seen by many as a mechanistic basis for diversifying Smad transcriptional activities in a wide variety of cellular processes.

Homeodomain TFs, such as HOXC8 (Shi et al., 1999) and Zen (Xu et al., 2005), and BMP-activated Smads have been commonly observed to maintain cooperative or collaborative interactions (Henningfeld et al., 2002; Li et al., 2006; Walsh and Carroll, 2007; Zhou et al., 2008; Liang et al., 2012). There are several other well-documented examples of TFs that interact with Smads. Some of these include: transcriptional coactivators like EP300/CREB binding protein (CBP) (Pouponnot et al., 1998) and OAZ (Hata et al. 2000), transcriptional corepressors like ZEB2 (Verschueren et al. 1999) and EVI1 (Alliston et al. 2005), as well as other transcription factors like RUNX2 (Hanai et al. 1999), NKX3-2 (Kim and Lassar, 2003), YY1 (Lee et al., 2004), TCF4 (Hu and Rosenblum, 2005), GATA4 (Brown et al. 2004), GATA5 and GATA6 (Benchabane and Wrana, 2003). More recently, SOX5 was shown to physically interact with R-Smads and that it is essential for the recruitment of Smad1/4 to BMP response elements during *Xenopus laevis* ectodermal patterning (Nordin and LaBonne, 2014). While we still do not have a comprehensive list of all potential cofactors that cooperate with Smads, according to the BioGRID database (version 3.5.170; Oughtred et al., 2019) it is estimated that human SMAD1, SMAD5, and SMAD9 interact with 126, 62 and 114 proteins, respectively. While these estimates may not be completely

reliable, due to potential false-positives, it opens up the possibility of identifying many more Smad coregulators.

1.3 Conservation of Bone Morphogenetic Protein *cis*-Regulatory Elements

BMP signaling is highly conserved from invertebrates to vertebrates and used to regulate a diverse array of processes across development (Schmierer and Hill, 2007; Blitz and Cho, 2009). Likewise, evidence suggests that BMP-CREs are also highly conserved. Studies have shown that BMP-CREs from one organism can recapitulate the function of autologous enhancers in another organism. For instance, Weiss et al. showed that a multimerized BMP-CRE from the *Drosophila Dad* gene enhancer induced reporter expression in zebrafish embryos (Weiss et al., 2010). Additionally, the Allan lab demonstrated that a BMP-CRE taken from the Xenopus *bambi* BMP-responsive enhancer functionally replaced a fly BMP-CRE *in vivo* and a multimerized fly *Dad* BMP-AE could drive reporter expression in chick spinal cord (Vuilleumier et al. 2018).

The following subsections discuss current knowledge on BMP-CREs in *Drosophila* and vertebrate systems.

1.3.1 Bone Morphogenetic Protein *cis*-Regulatory Elements in *Drosophila*

The pMad-binding consensus motif GCCGnCGC was originally identified in *Drosophila* in the promoters of *Vestigial* (Kim et al., 1997) and *Tinman* (Xu et al., 1998). Since then, work primarily in the wing imaginal disc has identified two bipartite BMP-CREs sequences for Mad and Medea binding found in the regulatory regions of *Drosophila* BMP-regulated genes. These are termed the BMP-Silencer Element (BMP-SE) (Pyrowolakis et al., 2004) and the BMP-Activation Element (BMP-AE). These motifs have since been found to be operational in other

tissues of developing *Drosophila*; however, it is notable that less than 10 of these motifs had been identified and functionally analyzed prior to recent work by the Allan lab in the fly nervous system (Vuilleumier et al. 2018). Thus, we still do not know how broadly they are used to regulate gene expression in other tissues.

The BMP-SE and BMP-AE motifs operate to pattern BMP-regulated gene expression across a gradient of BMP ligand availability across the developing wing imaginal disc. Phosphorylated Mad (pMad; *Drosophila* R-Smad) binds to GRCGNC or GGCGCC motifs, while Medea (*Drosophila* co-Smad) binds to GTCT or GNCV. Two additional regulators are also recruited to these motifs, the conserved co-regulator Schnurri and the Dipteran specific repressor Brinker, that play critical roles in BMP-dependent developing wing imaginal disc patterning.

BMP-Silencing Element (BMP-SE)	GRCGNC(N_5)GTC**T**	(R= G or A)
BMP-Activating Element (BMP-AE)	GGCGCCA(N_4)GNC**V**	(V= A, C or G)

Recruitment of the conserved co-repressor Schnurri requires the N_5 spacer and the terminal thymidine of GTC**T** of the BMP-SE. This recruitment makes the BMP-SE a repressor motif. The lack of Schnurri recruitment to the BMP-AE, due to the lack of the terminal thymidine in the GNCV motif, allows the pMad and Medea complex to activate gene expression (Pyrowolakis et al., 2004; Gao et al., 2005; Weiss et al., 2010). In many tissues of the fly, a major gene silenced by the BMP-SE is *brinker*. Brinker is itself a sequence-specific transcriptional repressor. In the wing disc and other tissues, *brinker* repression by BMP signaling results in de-repression of genes that would be otherwise repressed by Brinker. Notably, many BMP-activated genes in the developing wing imaginal disc are in fact de-repressed via BMP-dependent *brinker* repression (Sivasankaran et al., 2000; Zhang et al., 2001; Weiss et al., 2010). However, Brinker not only acts

to promote BMP-dependent gene activation through de-repression but also competes with pMad binding to BMP-AE motifs to counteract pMad/Medea-driven gene activation from this motif. Brinker binds sequences with the consensus sequence GGCGYY (Y=C, T). This overlaps with the pMad binding site of the BMP-AE (GGCGCC), serving as a template for competitive binding to this motif, placing gene activation from the BMP-AE under the control of the relative expression of pMad and Brinker. This serves to finely tune gene expression across the BMP ligand gradient of the developing wing imaginal disc (Rushlow et al., 2001). In addition to the work in the imaginal wing disc, the Allan lab has recently verified the widespread use of the BMP-AE motif in the *Drosophila* CNS, by identifying and experimentally verifying 34 BMP-AE containing genomic fragments near BMP-activated genes (Vuilleumier et al. 2018). This is the first study to show that the BMP-AE motif is utilized by a large number of BMP-responsive genes in any tissue.

Despite mounting evidence that the BMP-SE and BMP-AE are widespread motifs governing BMP-regulated genes, several diverse pMad/Medea-responsive motifs have been identified in *Drosophila* (Xu et al., 1998; Rushlow et al., 2001; Lin et al., 2006; Walsh and Carroll, 2007; Deignan et al., 2016). The deviation of some of these motifs from the AE/SE consensus sequences may be required in order to enable pMad/Medea interactions with other TFs and cofactors (Ross and Hill, 2008; Blitz and Cho, 2009). Adding to this body of work, we have identified and characterized a novel BMP-CREs motif that we have termed the BMP-AE2 in the *Drosophila* CNS (see Chapter 2). This motif has a low affinity, compared to the BMP-AE and BMP-SE, and our evidence indicates that this lowered affinity is required for cell-specific activation of the nearby gene. Additionally, biochemical studies have shown Smad complex binding to the bipartite BMP-CRE sequence with varying linker spacing, demonstrating that linker ranges of 5±1bp and even 5+ multimers of 10bp may be tolerated (Gao and Laughon, 2007). This

further indicates that novel BMP-CREs with varying sequences or linker site lengths may exist and should be further investigated. Studying the deployment and roles of these varied motifs will deepen our understanding of BMP-dependent gene regulation.

1.3.2 Bone Morphogenetic Protein *cis*-Regulatory Elements in Vertebrates

Early insight into the DNA-binding specificity of human Smads came from oligonucleotide binding screens, where the palindromic 5`-GTCTAGAC-3` termed Smad binding element (SBE), was identified as a binding site for Smad4 (vertebrate co-Smad) and Smad3 (TGFβ pathway R-Smad) (Zawel et al. 1998). This was further corroborated by the identification of SBE sites that bind Smads and regulate the expression of genes like Nkx2.5, the mammalian homologue of the BMP-responsive *Drosophila* transcription factor Tinman (Lien et al., 2002; Brown et al., 2004). Furthermore, the X-ray crystal structure of the N-terminal MH1 domain of Smads 1, 3, 4 and 5 indicated that they all recognize and bind to the GTCT motif (Shi et al., 1998; Baburajendran et al., 2010; Baburajendran et al., 2011; Chai et al., 2015).

Though able to bind to the SBE (GTCT) motif as cited above, Smad1 binds to GC-rich sequences with higher affinity (Kim et al., 1997; Korchynskyi and Ten Dijke, 2002). X-ray crystallography of the Smad5 MH1 domain confirms that it binds to GC-rich sequences (in addition to the SBE sequence) (Chai et al. 2015). Additionally, canonical BMP pathway Smads1/5/9 were shown to bind GC-rich sequences (such as GCCG, GGCGCC), termed a BMP Response Element (BRE), near well-known BMP-regulated genes such as the *Id1*, *Id2*, *Id3* and *Id4* genes (Ishida et al., 2000; López-Rovira et al., 2002; Korchynskyi and Ten Dijke, 2002; Karaulanov et al., 2004). There are many variations of this GC-rich BRE sequence, for example,

a ChIP-seq study mapping SMAD1/5 occupancy in primary human cells revealed enrichment for both GGCGCC and GGAGCC sequences (Morikawa et al. 2011).

Akin to *Drosophila* BMP-CREs, bipartite arrangements of SBE and GC-rich sequences (i.e. TGGCGGC(N_5)GTCT) have been observed in the regulatory regions of numerous vertebrate BMP-regulated genes such as *Ihh, Bambi*, *Smad7* (I-Smad) and *Id* genes (Katagiri et al., 2002; Korchynskyi and Ten Dijke, 2002; Karaulanov et al., 2004; Seki and Hata, 2004; Nakahiro et al., 2010). A notable difference between the fly and vertebrates is that these BMP-CREs serve as activators (Yao et al., 2006), despite the fact that these are BMP-SE silencers in the *Drosophila* wing imaginal disc and early embryonic blastoderm (Gao et al., 2005; Pyrowolakis et al., 2004; Weiss et al., 2010). For a more detailed description of these vertebrate BMP-CREs see Table 3.10 in Chapter 3, Section 3.3.3. Recently, published work by the Allan lab demonstrated that a multimerized fly BMP-AE-type motif functions as a functional activator element in the vertebrate CNS (Vuilleumier et al. 2018). This opens the possibility that BMP-AE-type BMP-CREs may regulate BMP-responsive genes in vertebrates.

If these more ‘complex’ bipartite motifs are widely utilized in vertebrates, as opposed to a degenerate “GC-rich” sequence, this would improve our ability to use computational methods to detect putative BMP-CREs, as was previously done in *Drosophila*. However, the question remains as to the fraction of BMP-CREs that have this bipartite structure and conform to the BMP-SE consensus. This has not been examined directly.

Experimentally validating the existence of diverse bipartite BMP-CRE sequence types, perhaps with different functions, will be an important step in understanding BMP-gene regulation in vertebrates. Identifying discrete sequences and the extent to which each of these is utilized in

vertebrates will help us further elucidate BMP regulatory mechanisms, as well as improve our ability to accurately detect such motifs by purely computational methods. My project partially aims to identify such motifs, and ultimately test their contribution to the BMP-regulatory landscape.

1.4 Challenges in Studying *cis*-Regulatory Modules and *cis*-Regulatory Elements

Mutations in non-coding CREs are known to cause or contribute to human disease, resulting in a growing class of diseases classified as “enhanceropathies” (Smith and Shilatifard, 2014; Mathelier et al., 2015). Mapping BMP-CREs on a genomic scale and defining their sequence variation tolerances would help interpret disease susceptibility arising from sequence variants in non-coding regions (Mathelier, Shi, and Wasserman 2015). CRE discovery has been historically challenging, as CREs are located at varying distances to the genes they regulate and can have high sequence degeneracy. However, their crucial role in gene regulation makes their identification very important, particularly in light of human genome sequencing efforts to identify disease susceptibility loci in the genome (Wasserman and Sandelin, 2004; Petersen et al., 2017).

1.4.1 Combining Computational and Experimental Methods to Detect CREs

Several computational and experimental methods have been developed to predict and identify CREs; however, none of these strategies alone can confidently identify functional CREs. In this section, I will be discussing the advantages and disadvantages of using some of these methods.

Computational methods include enrichment and clustering of characterized transcription factor binding sites (TFBS), as well as comparative genomics based on sequence conservation

between species. TFBS are typically short (4-12bp), and such short motifs can be frequently found in the genome, with only a few functioning as *in vivo* binding sites. Searching for clusters of short TFBS motifs can improve predictions but these can also be widespread in large genomes, resulting in many false-positive predictions. Chromatin context, cell type, developmental stage, as well as the presence or absence of regulatory co-factors, all contribute to whether a predicted binding site is occupied *in vivo* (Gaulton et al., 2010; Kaplan et al., 2011), making it almost impossible to experimentally verify a false-positive prediction as false. The high variability in TFBS sequences, especially when TFs act cooperatively (Jolma et al. 2015) can also result in a high degree of false negatives. Incorporation of sequence conservation information can improve prediction accuracy, assuming that important non-coding functional DNA sequences are more likely to be conserved across multiple species during evolution. However, CRE evolution is a driving force of evolutionary change, hence phylogenetic conservation can also be misleading (Long et al., 2016; Douglas and Hill, 2014; Rebeiz and Williams, 2011). Additionally, as many computational methods of enhancer prediction rely on the strongest biochemical TF binding signals (high-affinity binding sites), they typically fail to detect low to moderate affinity binding sites (Jaeger et al., 2010; Ramos and Barolo, 2013).

Experimentally, one of the ways occupies CREs can be identified is by using ChIP-seq either against transcription factors or against histone post-translational modifications characteristic of active transcription (Hardison and Taylor, 2012; Shlyueva et al., 2014). This provides experimentally verified, unbiased, genome-wide detection of CREs in a systematic manner. Using ChIP-seq, we can recover binding sites of a transcription factor with a resolution of 150-300bp (Park 2009). However, this method only allows the study of single factors in a snapshot of time and space. This hinders the detection of cell-specific CREs unless they are directly examined

(Schmidt et al. 2010). An additional caveat of this method is the recovery of a substantial number of candidate CREs, many of which are false positives and do not contribute to gene regulation. Finally, it is possible that more "rare" binding sites can be dismissed as false-positives or "background". In order to better discriminate functional TF binding sites, one can also assess chromatin accessibility and histone modifications that mark genomic regions areas by their functional status, such as the enrichment of H3K4me1 and H3K27ac. H3K4me1 enrichment at enhancers can be quite broad, extending 1kb or more on either side of the CREs, thereby providing a large sequence area to identify the actual TF binding site (Heintzman et al., 2007; Creyghton et al., 2010).

In isolation, any single strategy is limited in its ability to confidently predict functional CREs. However, predictions can be improved by the combined use of ChIP-seq data for TF occupancy and chromatin modifications, coupled with TF binding motif models and multi-species sequence comparisons. In addition to data generated in-house, public datasets such as those available through the ENCODE projects can be added to enhance CRE prediction. These available datasets include, but are not limited to, DNA-seq and FAIRE-seq data (from various cell types and conditions) to identify nucleosome-depleted and open chromatin regulatory regions (Dailey 2015), as well as STARR-seq data which are massively parallel functional assays for the discovery of active enhancers in vertebrates and invertebrates (Arnold et al., 2013). Combining all these complimentary methods to identify and experimentally verify TF binding sites will markedly enhance the predictive power of any CRE characterization project.

1.5 Thesis Research Objectives and Aims

Despite the importance of BMP-CREs to BMP-driven genomic responses and the potential for BMP-CRE sequence variants in disease susceptibility, they remain largely unidentified on a genomic scale. The overall objective of my thesis is two-fold; to characterize the widespread deployment of a novel low-affinity BMP-CRE motif our lab found to be active in the *Drosophila* central nervous system and to start the process of identifying the BMP-driven gene regulatory network underlying mammalian chondrogenesis.

My specific experimental aims were to:

1) Experimentally validate a novel set of BMP-CRE motifs in *Drosophila*.
2) Perform genomic identification of BMP-regulated genes and active enhancer regions during mouse chondrogenesis.
3) Experimentally verify candidate BMP-CREs that are active during mouse chondrogenesis.

Chapter 2:

Genomic Identification and Validation of a Novel BMP *cis*-Regulatory Element in the *Drosophila* CNS.

2.1 Introduction

Neurogenesis is a complex and tightly regulated process driven by local extrinsic cues and genetically encoded intrinsic programs that control cell fate (Hobert et al., 2010; Allan and Thor, 2015). Late stages of neural circuitry differentiation and maturation, such as the formation and growth of synapses, arborization of axons and dendrites and acquisition neurotransmitter phenotype, also require "retrograde" signaling from dendritic and axonal targets (Hippenmeyer et al., 2004; Marqués, 2005; da Silva and Wang, 2011). A well-studied example of retrograde signaling in *Drosophila* is retrograde BMP signaling in efferent neurons. Retrograde BMP-signaling is required for the induction and maintenance of neuronal subtype-specific gene expression including neuropeptide genes, such as *FMRFa*, in developing and mature neurons in the VNC (Allan et al., 2003; Marqués et al., 2003; Eade and Allan, 2009; Veverytsa and Allan, 2011). Additionally, retrograde BMP signaling is required in motor neurons for increased neuromuscular junction (NMJ) growth and neurotransmission to homeostatically match muscle growth (Aberle et al., 2002; Marqués, 2005; Goold and Davis, 2007; Berke et al., 2013).

In *Drosophila* efferent neurons, retrograde BMP-signaling is triggered by Glass bottom boat (Gbb) ligand engagement at a presynaptic BMP-Receptor complex of Wishful thinking (Wit), Thickveins (Tkv) and Saxophone (Sax) that phosphorylates Mad (Aberle et al., 2002; Rawson et al., 2003; Allan et al., 2003; Mccabe et al., 2004). Phospho-Mad binds Medea to form the Smad complex (Gao, Steffen, and Laughon 2005) Gao and Laughon, 2006) that translocates to the

nucleus and regulates transcription by binding DNA in a sequence-specific manner at BMP-response elements (Kim et al., 1997; Xu et al., 1998; Shi and Massague, 2003; Berndt et al., 2015; Vuilleumier et al., 2018).

The role of retrograde BMP-signaling in neuronal gene regulation is best defined for the neuropeptide gene *FMRFa.* This gene is selectively initiated and maintained in Tv4 neurons through the integration of BMP-activated Smad transcription factors with a Tv4-specific transcription factor code at two closely spaced *cis*-elements, a homeodomain-response element (HD-RE) and a BMP-response element (BMP-CRE, within a Tv4-neuron specific enhancer of the *FMRFa* gene (Allan et al., 2003; Miguel-Aliaga et al., 2004; Allan et al., 2005; Berndt et al., 2015). These results lead to a model wherein retrograde signaling contributes a BMP input to complete a combinatorial transcription factor code that determines selective gene expression in differentiating neurons (Allan et al., 2003; Berndt et al., 2015).

Studies primarily in the *Drosophila* wing imaginal disc have established core principles regarding BMP-CRE sequence and function. *Drosophila* BMP-dependent gene activation is mediated directly by Smads acting as activators, or indirectly through de-repression whereby BMP/Smad-dependent repression of the transcriptional repressor *brinker* reduces its activity, and de-represses numerous genes (Affolter and Basler, 2007; Hamaratoglu et al., 2014).

The existence of activating/repressing BMP *cis*-Response Element motifs (see Section 1.3.1) in *Drosophila* suggests that the nature of the BMP-mediated gene regulation can be textured by the specific BMP-CRE sequence contained within a gene's *cis*-regulatory region. Therefore, in addition to a model where the BMP-CRE is a simple docking site for BMP input to a combinatorial transcription factor code, a second model presents itself in which the BMP-CRE sequence plays

an additional functional role to diversify the regulatory outcomes of BMP input. These models have not been tested for their relevance in diversifying BMP-dependent gene expression in neurons.

2.2 Preliminary Work

This section summarizes work performed by a former graduate student, Anthony Berndt, upon which my work for Chapter 2 builds on, for manuscript submission. In studying the highly restricted expression of the *FMRFa* neuropeptide gene, our lab identified a minimal BMP-responsive *cis*-regulatory element (BMP-CRE) that mediates BMP-dependent *FMRFa* gene transcription in the 6 Tv4 neurons of the *Drosophila* VNC (Berndt et al., 2015). Follow-up work revealed that this BMP-CRE is a novel Activating-like Element (BMP-AE2; GGCGCCA(N_4)GT**A**T) that differs from the previously identified BMP-SE and BMP-AE sequences (see Section 1.3.1), mainly by virtue of a C > A transversion of a functionally critical C nucleotide in the Medea binding site (GT**A**T vs. GT**C**T/GN**C**V), that confers reduced Smad recruitment compared to BMP-AE (GNCV) or BMP-SE-type (GTCT) motifs (see attached manuscript for details). Regardless of reduced Smad recruitment, functional testing of BMP-AE2 mutants demonstrated that this atypical motif directly mediates Smad recruitment and *FMRFa* expression, without the contribution of *brinker* or *schnurri* co-regulators. Moreover, conversion of GTAT to an optimal BMP-AE sequence GNCV-type motif (GACG) enhanced Smad recruitment *in vitro* and led to substantial ectopic BMP-dependent reporter expression in other neuronal populations. This indicates that the low affinity of the BMP-AE2 motif directly contributes to the high neuronal subtype-specific expression of BMP-dependent *FMRFa*. Mutational analysis further revealed that the T in position two of the Medea binding site (G**T**AT) is the only nucleotide that

can be replaced without eliminating reporter activity. Taken together, this suggests that a BMP-AE2 consensus sequence (GGCGCCA(N_4) G**N**AT) may be a novel BMP-CRE motif.

2.3 Materials and Methods

2.3.1 Fly Genetics

Strains used: *med* ^{C246} (McCabe et al., 2004), *med*^{13} (Hudson et al., 1998), *med*^{1} (Das et al. 1998), *wit*^{A12} and *wit*^{B11} (Aberle et al. 2002) were provided by the Bloomington *Drosophila* Stock Center. Mutants were kept over *TM3, Sb, dfd-GMR-nvYFP* (Le et al. 2006) *TM3,Sb,Ser,twiGAL4,UAS-2xEGFP* (Halfon et al. 2002) or *TM6B* (Craymer 1984). *w*^{1118} was used as the control genotype. Flies were reared on standard medium 25°C, 70% humidity.

2.3.2 EGFP Reporter Transgene and Transgenic Fly Construction

A list of all primers used for the construction of these transgenic flies can be found in Table 2.1. To generate reporter constructs, approximately 2kb genomic DNA fragments (see Table 2.1) were amplified by PCR and cloned into an empty pThunderbird EGFP vector (Berndt et al. 2015). These fragment sizes correspond with those tested in other studies performing large scale enhancer identification in *Drosophila* (Weiss et al., 2010; Kvon et al., 2014; Pfeiffer et al., 2008; Vuilleumier et al., 2018) and are sufficiently large fragments to reduce the chance of excluding important enhancer elements on either side of the putative BMP-CREs. Coordinates of the fragments amplified, as well as the primers used for fragment amplification from genomic DNA, are summarized in Table 2.2.

Mutagenesis was performed by Q5® Site-Directed Mutagenesis Kit (New England Biolabs), using primers designed to introduce specific base pair substitutions to the Mad binding site (GCCGGC

> tgatga), according to manufacturer`s protocols. Primers were designed using the NEBase Changer v1.2.8 tool and are summarized in Table2.1. All constructs were verified by sequencing before the generation of transgenic fly lines.

For fly transgenesis, constructs were inserted via PhiC31 mediated site-specific integration (Bischof et al., 2007) into the *attP2* site (Groth et al, 2004) on chromosome 3 by Rainbow Transgenics Flies Inc. (CA, USA).

Table 2.1: **Q5 mutagenesis primers**

DNA fragment	*Primer Sequence (5`→ 3`)*	*Mutated BMP-AE2 site*
Atyp3	F: GGC**GTAT**ACGTGATAAGTGGCGCTA R: AT**tcatca**GTCACCAGATTCGGTGGTT	**tgatga**ATGGC**GTAT**
Atyp8	F: ACT**GTAT**CTGTATCTGTGTTTCTTTTTTTTG R: CT**tcatca**TCTTGCAGCTCGAATGTG	**tgatga**AGACT**GTAT**
Atyp9	F: TTT**GTAT**TTCGAGGGTAAGGCCGAA R: AT**tcatca**AATGGGTTTCAATGGTCCC	**tgatga**ATTTT**GTAT**
Atyp11	F: T**tcatca**TCTAATGTTTGCTCGGTTTG R: AAAA**GTAT**GCAACACTACAGAAGCCC	**tgatga**AAAAA**GTAT**
Atyp15	F: T**tcatca**AGCACTTTGTCGTGGGCG R: AAAA**GTAT**GCTATAATATTTAAAGCTCACGCAAGC	**tgatga**AAAAA**GTAT**

2.3.3 Immunocytochemistry

Standard protocols were used throughout (Eade and Allan, 2009; Vuilleumier et al., 2018). Primary antibodies used: rabbit anti-pSmad1/5 (1:100; 41D10; Cell Signaling Technology). Secondary antibodies used: donkey anti-rabbit conjugated to Cy3 or Cy5 (1:250; Jackson ImmunoResearch).

2.3.4 Bioinformatic Detection of BMP-AE2

HOMER v4.10 software suite (Heinz et al. 2011) was used to scan the reference dm6 *Drosophila* genome for the BMP-AE2 ($GGCGCCN_5GTAT$) motif. Base-specific PhastCons scores (Siepel et al., 2005; 27-insect conservation) were obtained from the UCSC genome browser (https://genome.ucsc.edu/) to annotate each motif instance with evolutionary conservation scores.

Table 2.2: **Cloned AE2 fragment genomic coordinates and they primer sequences used for their amplification**

DNA fragment	CRE genomic coordinates (dm6 – BDGP Release 6 plus ISO1 MT)	Average phastCONs	Primer Sequence (5`→ 3`)	Genomic coordinates of fragment cloned	Fragment size
Atyp1	**chr2R:9905662-9905676**	**1**	F: CAATTTTCGGGCCAGTAGCGCGTGCGTT R: AAACTGCAGCGAAAATCAGTTCCATTG	**chr2R:9904061-9906149**	**2089bp**
Atyp2	chr3R:17053115-17053129	1	F: GGCTTTCAAGAGCTCAAAGGCCAGACA R: ATTACCGCGTTAGCCAACACTATTTCC	chr3R:17051370-17053599	2230bp
Atyp3	**chrX:15616808-15616822**	**0.998643**	F: TTTCGCAAGTGCGTAGCATACGAAATAG R: CAGGGACAGAGCGAAGTGCCTTTGAAA	**chrX:15616292-15618623**	**2332bp**
Atyp4	chr3R:18498566-18498580	0.999857	F: CAATGAAACCTGGCGGATGTGGCCCGC R: TCGCAATGAAGACGACATCCCCCACAC	chr3R:18498121-18500496	2376bp
Atyp5	chr3R:28698786-28698800	1	F: GCGTGTAACGGCCAAATACTAAGCC R: CGACAAATAAGCGGAGACAAGCGGCC	chr3R:28697790-28699915	2126bp
Atyp6	chr2L:15189633-15189647	0.988429	F: CGAAATATCTCTTTGGTCTGGGCAAAT R: CGCAGGCAAAGAAAGCGGCCGCAGAG	chr2L:15187760-15189856	2097bp
Atyp7	chrX:14450410-14450424	0.957214	F: TCTTTGGTCGGCTTAATTGCTGATCTA R: TCTTTGAGCCAAAATTCTAAATATGCC	chrX:14450016-14452157	2142bp
Atyp8	**chrX:14696740-14696754**	**0.554643**	F: GAGTTGTTATTGGTGAAGAAATTGTG R: GGGCAAAGCTGCGAATTTAAGGGTCCG	**chrX:14695051-14697141**	**2091bp**
Atyp9	chr3L:14589745-14589758	1	F: TGACTGAACAATCAGGACCAAAATG R: TGCCTCTTCCGCCATTTTTATGAGTT	chr3L:14587810-14589922	2113bp
Atyp10	chr3R:9836926-9836940	1	F: CACCACCACCACACCTTAAAAACCGT R: GATTCTTTTGGGATCTTGTGCCTTAG	chr3R:9835985-9838072	2088bp
Atyp11	**chr2L:9319175-9319189**	**1**	F: CGGAACGGGTATCAATCAATAGCCA R: GCATTTTCAATTTGGACCCGTCAGC	**chr2L:9318297-9320893**	**2597bp**
Atyp12	chr3R:18357071-18357085	0.999929	F: TTTGCTGTTATTGCTGTTATTGCTATCGC R: TTAATTGTTGTTTCCGAGTGCGCTCAAT	chr3R:18355808-18358004	2197bp
Atyp13	chr3R:15594263-15594277	1	F: GTACTTTGACAGCTCACGCAAAGGTTG R: GATGCCAACAAATTGCCTCTGCGGCCGC	chr3R:15592738-15595782	3045bp
Atyp14	chr3L:2836246-2836260	0.997214	F: TTTTCCCCACTGTGCTCAGACGGAAAC R: CGAAATAAATTGCGATCTCTGCGGCCGC	chr3L:2835299-2836800	1502bp
Atyp15	**chr2R:19199705-19199719**	**1**	F: GCTCAATTGTTTGGAAAATCCCAAGCAA R: GTCATTCAGTCAGGCGCTCTGCGGCCGC	**chr2R:19198829-19200842**	**2014bp**
Atyp16	chr2R:24694131-24694145	0.999643	F: TTCATCTTATATTCAACCAAATTGTGA R: GCAGCCCGCAAAACTCGGAAAAGC	chr2R:24693621-24694315	695bp
Atyp17	chr3L:11348427-11348441	0.6135	F: GTTTCATCGTTCTGCTGTTTTAGCTGT R: CAATCCAGCAACCACCCTCTGCGGCCGC	chr3L:11347382-11349454	2073bp
Atyp18	**chr2L:11595432-11595445**	**1**	F: GAGAAATTCCACTTCGGCAACATATTTG R: CCGCTTGTGTACATAACTCTGCGGCCGC	**chr2L:11594630-11596060**	**1431bp**
Atyp20	chr3R:10449056-10449070	0.969214	F: CCACCCATGAGTGTGCGTGCATGTGT R: TTAGGGGGAAAATAATATAAGACCAA	chr3R:10447961-10450057	2097bp
Atyp21	chr2R:23517681-23517695	0.922	F: GCTATAGTCGAGAATATATGACCAATC R: ATAGCCACCAACACATTAGGCAATCGA	chr2R:23516524-23518211	1688bp
Atyp22	chr2R:13835553-13835567	0.997357	F: CTCCTCGATAAGCCGACGTTGGTAGGA R: ATAGCCACCAACACATTAGGCAATCGA	chr2R:13835299-13836232	934bp
Atyp23	**chr3L:15776762-15776776**	**1**	F: CAGACTAGAAAATCTCCCAGTGTGGGC R: TGTCAATAGTTCGTTTTGACAGGCTGA	**chr3L:15775869-15777334**	**1466bp**
Atyp24	chrX:10180864-10180878	0.588214	F: CTATAAATGGGCCAAAAAGGCTGTTTTG R: CGAAATTGAATTGCATATGAGCTTTAGG	chrX:10180102-10182068	1967bp
Atyp25	chrX:1649111-1649125	0.997143	F: CACCGGCAGCCTACTCAGTGGCGTCAT R: AAATGCGCTGAATGTCATCACCCATCG	chrX:1647378-1649894	2517bp
Atyp26	**chr3L:13570864-13570878**	**0.756857**	F: GCCGCGAGACTCATGAAATATTTATGC R: TTTGAGGGAGAATGAAACCCTTTGCTGC	**chr3L:13569638-13572061**	**2424bp**

2.3.5 Imaging Analysis and Quantification of Reporter Expression

Images were acquired as z-stacks on an Olympus FluoView FV1000 confocal microscope or a Zeiss Axio Imager VIS LSM880 confocal microscope. We examined native GFP reporter expression (without anti-GFP immunoreactivity enhancement) in late L3 larval VNCs, in the context of anti-pMad immunoreactivity (to mark nuclei with active BMP-signaling). In all cases, four or more VNC were dissected and imaged for each genotype. All tissues to be compared were processed with the same reagents, imaged and analyzed in identical ways. To quantitate reporter activity, we used Bitplane: Imaris v9.2 software (in Spots Mode) to identify reporter-positive nuclei in the VNC (excluding the brain lobes). When comparing control and pMad-binding site mutant genomic fragment reporters, we additionally assessed GFP positive nuclei that were co-marked by pMad immunoreactivity (by mean intensity thresholding). Imaris settings were established independently for each set of reporters, in order to provide optimal 'spot' marking of the GFP reporter and pMad co-immunoreactive nuclei, with minimal background fluorescence spot marking. Each image was further subtracted, manually, for spots that erroneously labelled background fluorescence.

2.3.6 Statistical Analysis

Statistical analysis and graphing were performed with GraphPad Prism Version 8.0.1 (GraphPad Software, San Diego, CA). The normality of sample distribution was determined with Shapiro-Wilk normality tests. All multiple comparisons were done with One-Way ANOVA and a Tukey post-hoc test or Student's two-tailed t-test when only two groups were compared. Mann-Whitney *U* test was used when the samples were not normally distributed. Differences between genotypes were considered significant when p-value < 0.05. Data are presented as mean ± Standard Error of Mean (SEM).

2.4 Results

2.4.1 Identification of 128 Highly Conserved AE2 Genomic Fragments in *Drosophila*

Following the identification of the novel BMP-AE2 regulating *FMRFa* expression in Tv4 neurons, we examined if this *cis*-regulatory motif was widely distributed through the genome to regulate numerous neuronal genes in a BMP-dependent manner. Therefore, I examined the distribution of conserved BMP-AE2 motifs in the genome and tested the BMP-dependent activity of a 2kb genomic fragment surrounding the motif, following established methods (Vuilleumier et al. 2018).

We identified all 178 BMP-AE2 motifs in the *D. melanogaster* genome using the motif discovery tool HOMER (v4.10) (Heinz et al. 2011). These were filtered for high sequence conservation across 24 sequenced *Drosophila* species using PhastCons scores, limiting the list to 128 BMP-AE2 with an average PhastCons score over 0.55 (Supplemental Table S1). Out of these 128 motifs, we found that 68% (87/128) are located within an intron or UTR, while the remaining 32% (41/128) are intergenic relative to the nearest gene.

Towards selecting a subset of these for functional testing *in vivo*, we prioritized 24 of the BMP-AE2 motifs based on their proximity to genes expressed in the larval nervous system (Chintapalli et al., 2007; Weiszmann et al., 2009) (see Table 2.3). Out of the 24 selected motifs, we selected 20 highly conserved with an average PhastCons score above 0.9 in order to optimize the chance of characterizing functional BMP-CRE's, but also added 4 motifs with scores 0.75-0.55 in order to test of lesser conserved motifs were also functional (Table2.3, Supplemental Table S1). We additionally identified the nearest *wit*-responsive gene TSS for each motif (unpublished data, Allan lab). These data are included in Table 2.3.

Table 2.3: **Cloned AE2 fragment conservation, genomic location, and corresponding nearby genes**

DNA fragment	CRE genomic coordinates (dm6 – BDGP Release 6 plus ISO1 MT)	Average phastCons*	Nearby CNS expressed gene	Distance in bp (CRE to nearby CNS-expressed gene TSS)	Position relative to nearest gene	Nearest BMP-regulated gene**	Distance in bp (CRE to nearest BMP-regulated gene TSS)
Atyp1	**chr2R:9905662-9905676**	**1**	***FMRFa***	**618**	**intergenic**	***FMRF***	**618**
Atyp2	chr3R:17053115-17053129	1	*Dad*	878	intergenic	*Dad*	878
Atyp22	chr2R:13835553-13835567	0.997357	*CG6357*	4486	intergenic	*CG6357*	4486
Atyp21	chr2R:23517681-23517695	0.922	*RabX1*	5918	intergenic	*RabX1*	5918
Atyp11	**chr2L:9319175-9319189**	**1**	***Eaat1***	**14378**	**intergenic**	***Eaat1***	**14378**
Atyp24	chrX:10180864-10180878	0.588214	*CG43902*	22431	intronic	*CG43902*	22431
Atyp3	**chrX:15616808-15616822**	**0.998643**	***sog***	**13535**	**intronic**	***CG9220***	**23275**
Atyp12	chr3R:18357071-18357085	0.999929	*CG31235*	28085	intergenic	*CG31235*	28130
Atyp20	chr3R:10449056-10449070	0.969214	*Cyp12e1*	14252	intergenic	*CG6325*	41772
Atyp16	chr2R:24694131-24694145	0.999643	*ST6Gal*	255bp	intronic	*Mid1*	42512
Atyp8	**chrX:14696740-14696754**	**0.554643**	***NetA***	**42813**	**intronic**	***NetA***	**42813**
Atyp10	chr3R:9836926-9836940	1	*Teh1*	31308	intronic	*CG8507*	45444
Atyp13	chr3R:15594263-15594277	1	*AOX3*	46528	intergenic	*AOX3*	46528
Atyp9	chr3L:14589745-14589758	1	*HGTX*	9814	intronic	*Mpcp2*	52094
Atyp15	**chr2R:19199705-19199719**	**1**	***Hppy***	**21070**	**intronic**	***CG15118***	**62537**
Atyp26	**chr3L:13570864-13570878**	**0.756857**	***bru-3***	**96083**	**intronic**	***CG10089***	**96078**
Atyp6	chr2L:15189633-15189647	0.988429	*CG4168*	10850	intronic	*CG15270*	114858
Atyp23	**chr3L:15776762-15776776**	**1**	***Comm***	**48800**	**intergenic**	***pHCl-1***	**122253**
Atyp14	chr3L:2836246-2836260	0.997214	*Tet*	43090	intronic	*Fife*	124557
Atyp17	chr3L:11348427-11348441	0.6135	*CG6163*	16516	intergenic	*Ube3a*	137845
Atyp7	chrX:14450410-14450424	0.957214	*dpr8*	11990	intronic	*sbm (CG9413)*	152156
Atyp4	chr3R:18498566-18498580	0.999857	*fru*	47233	intronic	*CG31235*	169625
Atyp25	chrX:1649111-1649125	0.997143	*Br*	74545	intronic/3`UTR	*futsch*	240043
Atyp18	**chr2L:11595432-11595445**	**1**	***kek2***	**13580**	**intronic**	***CG42486***	**247692**
Atyp5	chr3R:28698786-28698800	1	*htt*	36100	intronic	*beat-VI*	280579

* Average evolutionary conservation score of a motif calculated based on the base-by base conservation score of each position in the motif.

** Color indicates whether genes were upregulated or downregulated in *wit* mutant background. Green labeled genes are downregulated, and blue ones are upregulated.

Reporters were sorted based CRE distance to nearest BMP-regulated gene TSS.

2.4.2 Identification of 7 BMP-Responsive Genomic Fragments in Neurons

To test the *in vivo* activity of these BMP-AE2s, 24 genomic DNA fragments (of~2kb) each containing one of these motifs were cloned in front of a minimal promoter and a nuclear-localizing GFP reporter.

We examined reporter activity driven from these genomic fragments in wandering third instar larvae. Out of the 24 reporters, 5 showed no expression in the VNC, but only 1 of these exhibited no reporter expression in any of the other tissues examined (Table 2.4, Figure 2.1). The remaining 19 reporters exhibited low to robust reporter activity in the VNC (Table 2.4). Additionally, a subset of the 19 reporters exhibited reporter expression in the optic lobes and/or other larval tissues, indicating that these reporters may not only have a restricted function in the CNS but may have roles outside the CNS during larval development.

Of these active reporters, 10 exhibited expression in subsets of pMad-positive cells in the VNC (which at this developmental stage comprises motor and neuropeptidergic neurons) (Allan et al., 2003), as well as pMad-negative glia and neurons (Figures 2.3, 2.4, 2.5). The other 9 active reporters only exhibited reporter expression in pMad-negative glia and neurons (Figures 2.2).

We tested the BMP-responsiveness of the 10 reporters expressed in subsets of pMad-positive cells reporters, by placing all 10 into a *wit* mutant background. The transgenic flies were crossed to a *wit* mutant allele line (wit^{A12}) to create recombinant animals that would contain both the enhancer reporter and *wit* mutant allele on the third chromosome. As third instar larvae heterozygous for wit^{A12} are viable and have normal BMP signaling in the VNC ($pMad^{+}$ stain) they were used as controls ($wit^{A12}/+$). The corresponding *wit* mutants were made by crossing with another *wit* mutant line (wit^{B11}), generating wit^{A12}/wit^{B11} transheterozygotes that are pupal lethal

(Veverytsa and Allan, 2011) and lack normal BMP signaling and pMad stain in the VNC. Out of those 10 reporters, 7 showed partial to total loss of reporter expression, and 3 reporters showed no significant change (Figures 2.3, 2.4, 2.5).

Three of these *wit*-responsive fragments were Atyp18, Atyp23, and Atyp26 (Figure 2.4). Atyp18 reporter was expressed in 339±15 nuclei, of which 134±25 (34%) nuclei were pMad-positive (n=16). In *wit* mutants, reporter activity was reduced by 47% to 181±5 nuclei (n=17) (Figure 2.4-A,D). Atyp26 reporter had very robust and widespread expression across the whole L3 brain. In the VNC it was expressed in 805±22 nuclei, of which 217±10 (27%) nuclei were pMad-positive (n=6). In *wit* mutants, reporter activity was reduced by 30% to 592±39 nuclei (n=6) (Figure 2.4-B,E). Finally, Atyp23 had a sparser expression pattern and was expressed in 61±6 nuclei (n=5). In *wit* mutants, reporter activity was reduced by 50% to 30±5 nuclei (n=5) (Figure 2.4-C,F).

We next tested whether the activity of the identified *wit*-responsive fragments was dependent on the AE2 Mad binding site included in these fragments. We selected 4 *wit*-responsive fragments (Atyp3, 8, 11 and 15) and one non-*wit* responsive fragment (Atyp9, Figure 2.3-C,F), to introduce specific mutations into the pMad-binding site of the AE2 (GGCGCC > TGATGA). We placed these mutant genomic fragment reporters into the same *attP2* site as the corresponding WT reporter. In all 4 *wit*-responsive fragments tested, there was a significant loss of reporter expressing cells; however, this loss was less pronounced than the loss in *wit* mutants (Figure 2.5-A-C, E-G). *Atyp15*^{mad} was the only fragment with the same loss of cell numbers in the pMad-binding site mutant compared to the *wit* mutant (Figure 2.5-D,H).

We quantified the number of cells in which reporters were expressed for these 4 *wit*-responsive fragments (Atyp3, 8, 11 and 15). In the VNC, Atyp3 reporter was expressed in 224±16 nuclei, of which 56±6 (25%) nuclei are pMad-positive (n=7). In *wit* mutants, reporter activity was reduced by 61% to 88±10 nuclei (n=12). Once the pMad-binding site was mutated (*Atyp3*^{mad}), reporter activity was reduced by 27% to 159±9 nuclei (n=15) compared to controls that had reporter expression in 218±19 nuclei (n=6) (Figure 2.5-A,E). Atyp8 reporter was expressed in 49±5 nuclei, of which 9±2 (18%) nuclei are pMad-positive (n=5). In *wit* mutants, reporter activity was reduced by 75% to 12±1 nuclei (n=5). In the pMad-binding site mutant (*Atyp8*^{mad}), reporter activity was reduced by 50% to 23±3 nuclei (n=7) compared to controls that had reporter expression in 46±5 nuclei (n=6) (Figure 2.5-B,F). Atyp11 reporter was expressed in 228±17 nuclei, of which 118±10 (52%) nuclei are pMad-positive (n=10). In *wit* mutants, reporter activity was reduced by 88% to 24±8 nuclei (n=9). In the pMad-binding site mutant (*Atyp11*^{mad}), reporter activity was reduced by 41% to 131±8 nuclei (n=9) compared to controls that had reporter expression in 221±15 nuclei (n=6) (Figure 2.5-C,G). Finally, Atyp15 reporter was expressed in 212±17 nuclei, of which 68±7 (32%) nuclei are pMad-positive (n=9). In *wit* mutants, reporter activity was reduced by 64% to 77±5 nuclei (n=9). In the pMad-binding site mutant (*Atyp15*^{mad}), reporter activity was reduced by 67% to 76±7 nuclei (n=9) compared to controls that had reporter expression in 228±17 nuclei (n=9), of which 68±8 are pMad-positive (Figure 2.5-D,H). Coincidently, Atyp15 reporter is the only case where a near complete loss (90%) of pMad^{+} stain and reporter expression overlap were observed in the pMad-binding site mutant (Figure 2.6). Taken together, the data strongly suggest that these 4 motifs are functional BMP-AE2 where binding to the Mad-binding site plays an important role in driving reporter expression in the VNC.

Next, we examined reporter intensity effects in all 7 *wit*-dependent motifs and found that only 4 of these exhibited altered reporter intensities (Figure 2.7). Both Atyp18 and Atyp26 had a significant reduction in mean relative reporter intensity when comparing controls to their respective *wit* mutants. For Atyp18, control mean relative reporter activity per nucleus was measured at 120±11, while in *wit* mutants it dropped by 63% to 45±7 (Figure 2.7-C). The reduction was even more significant in Atyp26, where control mean relative reporter activity was measured at 260±30, while in *wit* mutants it dropped by 88% to 32±3 (Figure 2.7-D). In Atyp15, while there was no significant mean relative reporter intensity reduction between *wit* controls (64±2) and *wit* mutants (66±3), there was a 27% reduction in Atyp15^{mad} mutants (49±2) compared to the controls (67±8) (Figure 2.7-A). In this case, we were also able to measure relative reporter intensities of pMad^{+} stained nuclei only, where the mean relative reporter intensity of controls (70±4) was reduced by 54% in the Mad-binding site mutants (32±2) (Figure 2.7-B). Finally, Atyp23 had the most surprising result, with the *wit* mutants exhibiting a 24% increase in mean relative reporter expression compared to the controls (Figure 2.7-E). Based on the distribution in the Atyp23 graph (Figure2.7-F), the highest reporter-expressing cells appear to be maintained in the *wit* mutants, suggesting that the increase in mean relative reporter intensity observed in Figure2.6-E could be a result of a loss of mainly low reporter-expressing cells.

Having established the necessity of Medea for the BMP-dependent activity of the *FMRFa* BMP-RE (Berndt et al., manuscript pending resubmission), we decided to test the necessity of Medea for reporter expression in a subset of the 7 BMP-dependent AE2 motifs. We placed Atyp3, Atyp8, Atyp11, and Atyp15 in a null *Medea* background, and in all these cases, reporter expression was lost with the same pattern observed when the reporters were placed in a *wit* mutant background (Figure 2.8).

Overall, we have identified 7 BMP-dependent AE2 motifs out of the 10 motifs with reporter expression overlap with pMad stain in the L3 VNC tested, which gives our approach a discovery rate of 70%. This discovery rate is in line with previous studies done using other BMP-motifs (Vuilleumier et al. 2018).

Table 2.4: **AE2-enhancer genomic fragment-driven GFP reporter expression patterns.**

DNA Fragment	Expression* in: VNC	Expression* in: Optic lobes	Reporter/pMad stain overlap	*wit* responsive	VNC Expression Details	Expression in Other Tissues
Atyp26	+++	+++	√	√	neurons and glia	glial cells, cells in trachea
Atyp3	+++	++	√	√	medial and lateral neurons	fat body, muscle tissue, salivary glands
Atyp18	+++	+	√	√	medial and lateral neurons	salivary glands
Atyp15	+++	-	√	√	medial and lateral neurons	cells in trachea
Atyp11	++	+	√	√	medial and lateral neurons	salivary glands
Atyp8	+	+	√	√	sparse	tip of mouth hooks
Atyp23	+	+	√	√	sparse	none
Atyp13	+++	+	√	-	medial neurons	none
Atyp9	++	++	√	-	lateral neurons	none
Atyp7	+	+	√	-	sparse	none
Atyp17	++	+	-	-	neurons and glia	cells in midgut, pharynx and glial cells
Atyp22	+	++	-	-	sparse	brain glial cells, Malpighian tubule cells
Atyp14	+	++	-	-	sparse	none
Atyp24	+	+	-	-	sparse	none
Atyp20	+	+	-	-	sparse	none
Atyp21	+	-	-	-	sparse	none
Atyp5	+	+	-	-	low intensity	none
Atyp10	+	+	-	-	low intensity	none
Atyp12	+	-	-	-	low intensity	ring of cells in proventriculus
Atyp2	-	+++	-	-	none	disc cells
Atyp16	-	+	-	-	none	cells in midgut
Atyp25	-	-	-	-	none	epidermis (specifically cells in segment borders)
Atyp6	-	+	-	-	none	none
Atyp4	-	-	-	-	none	none

***** Expression pattern was assessed in wandering third Instar larvae.

Reporters were sorted based on VNC expression intensity and pattern, *wit* responsiveness and expression in other tissues.

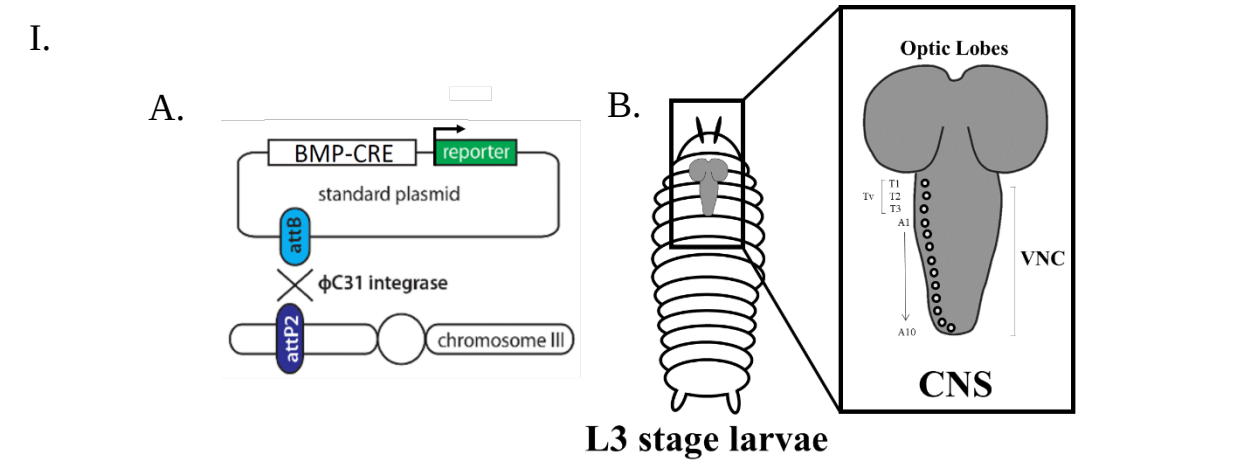

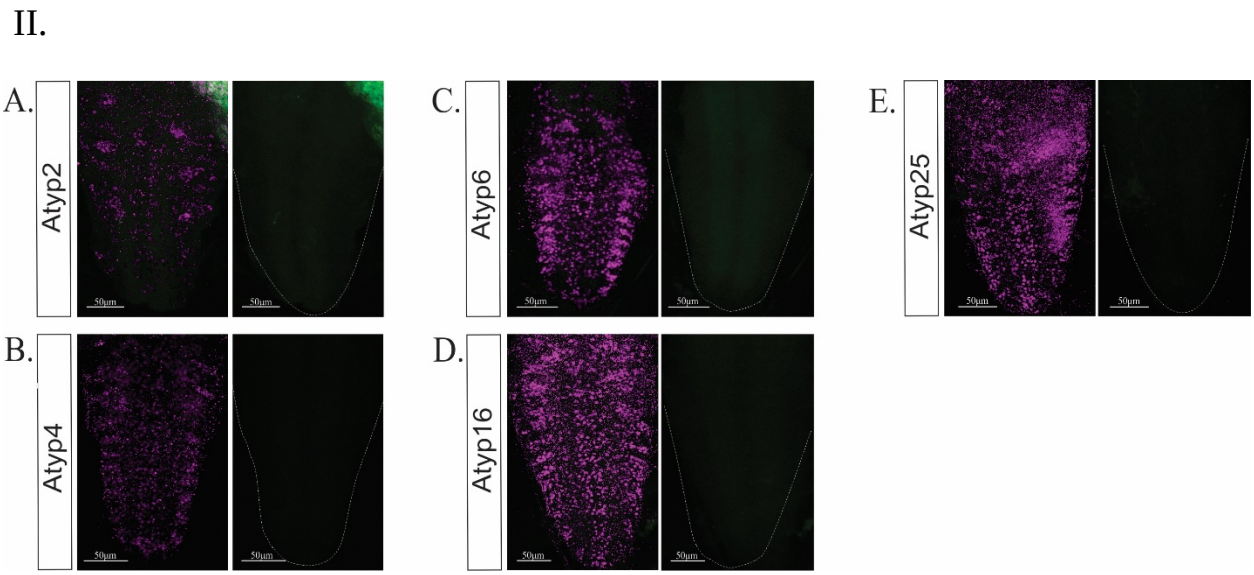

Figure 2.1 ***AE2 motifs with no detectable expression in the CNS of third Instar (L3) larvae.*** **I. (A)** Generation of the transgenic flies required the generation of plasmids containing the AE2 motifs of interest upstream of a minimal promoter driving a GFP reporter. Using φC31 integrase, the plasmid was placed in an *attP2* site on the 3rd chromosome. **(B)** Schematic representation of the L3 larvae Central Nervous System (CNS). **II. (A-E)** Transgenic reporter lines Atyp2, 4, 6, 16, 25 exhibit no GFP reporter expression in wandering L3 larvae brains. *Genotypes:* All lines examined here were heterozygous (*w;;AtypX/+*).

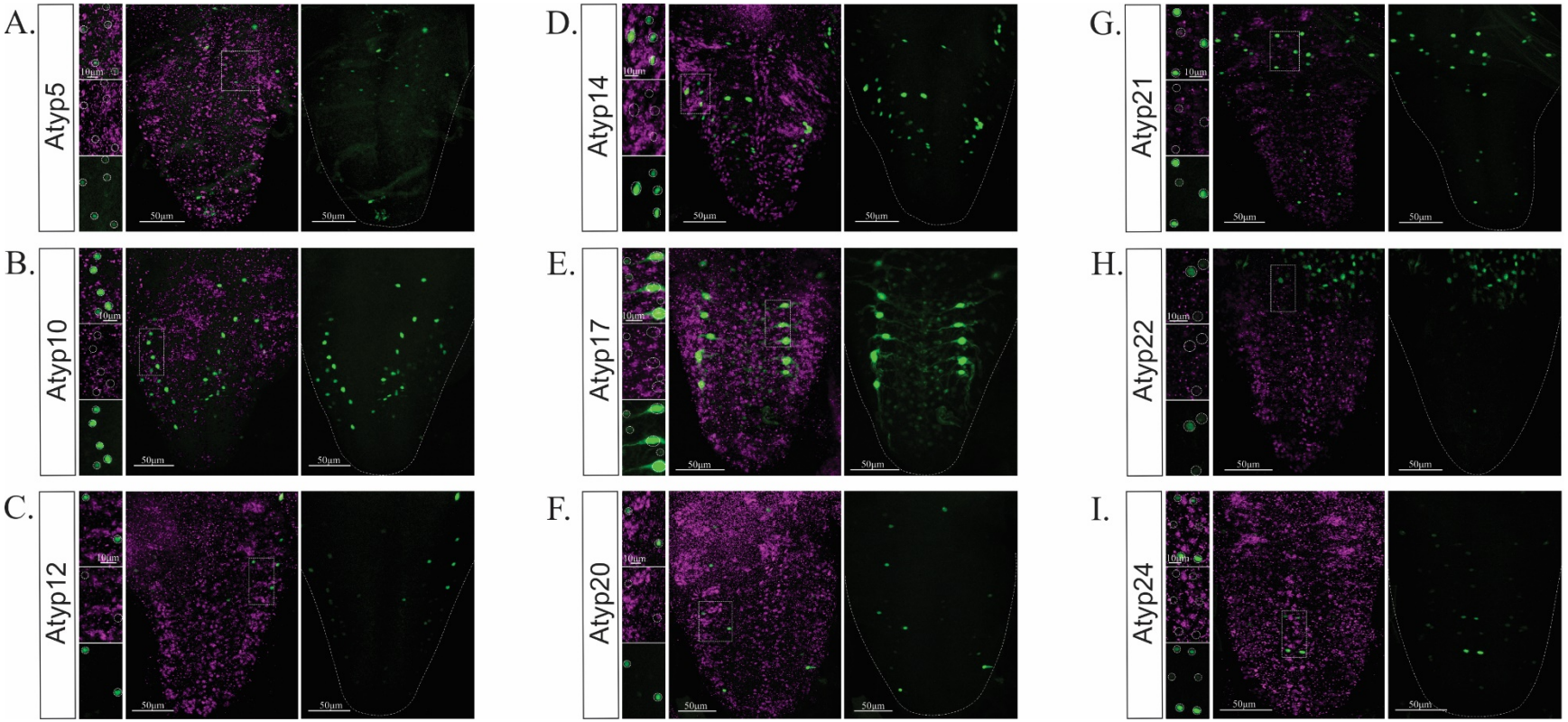

Figure 2.2: ***Non-BMP responsive AE2 motifs with expression in the VNC of third Instar larvae.***

Transgenic reporter lines Atyp5, 10, 12, 14, 17, 20, 21, 22, 24 exhibit GFP reporter expression in L3 larvae VNCs, with no observed overlap of GFP reporter (green) and pMad (magenta). *Genotypes:* All lines examined here were heterozygous (*w;;AtypX/+*).

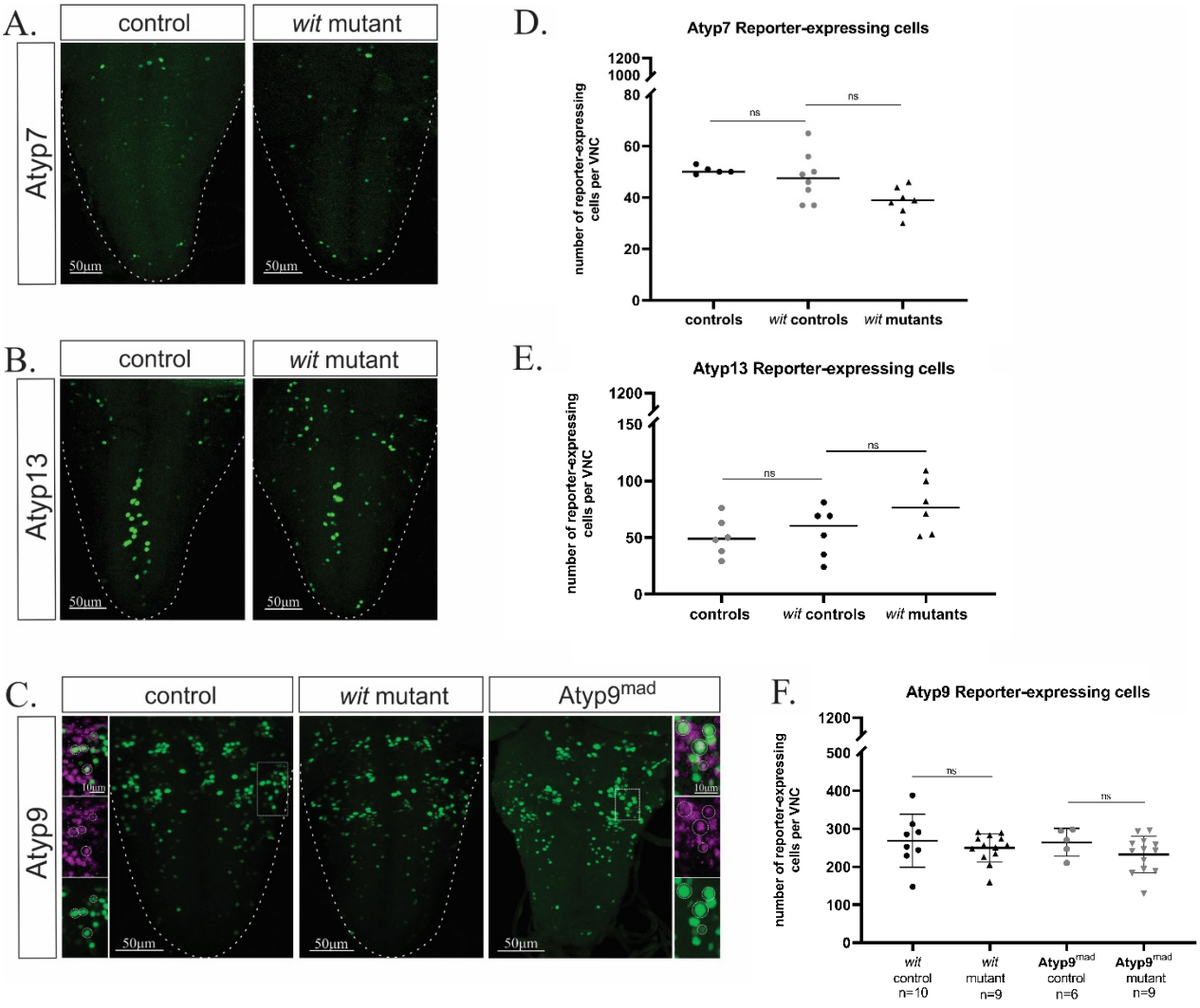
A.
control
wit mutant
Atyp7
50µm
50µm
B.
control
wit mutant
Atyp13
50µm
50µm
C.
control
wit mutant
Atyp9mad
Atyp9
10µm
50µm
50µm
50µm
D.
Atyp7 Reporter-expressing cells
number of reporter-expressing cells per VNC
1200
1000
80
60
40
20
0
ns
ns
controls
wit controls
wit mutants
E.
Atyp13 Reporter-expressing cells
number of reporter-expressing cells per VNC
1200
150
100
50
0
ns
ns
controls
wit controls
wit mutants
F.
Atyp9 Reporter-expressing cells
number of reporter-expressing cells per VNC
1200
500
400
300
200
100
0
ns
ns
wit control n=10
wit mutant n=9
Atyp9mad control n=6
Atyp9mad mutant n=9

Figure 2.3: ***Three of the fragments tested are non wit-responsive in the L3 VNC.*** **(A-B)** Representative images of transgenic reporter lines Atyp7 and Atyp13, along with their respective *wit* mutants. (**C)** Representative images of reporter line Atyp9 control, *wit* mutant and pMad-binding site mutant (*Atyp9^{mad}*). Side panels indicate overlap of GFP reporter (green) and pMad stain (magenta). (**D-F)** Quantification revealed non-significant change of number of reporter-expressing cells in the mutant genotypes compared to the controls, indicating that these reporters do not have BMP-dependent expression in the L3 VNC, despite observed overlap of reporter and pMad stain in some cells. Each point in the graph represents the total number of reporter-expressing cells in the VNC of a single animal. Significance was calculated with one-way ANOVA with a Tukey post-hoc test: no was significance detected in any of the comparisons. *Genotypes:* All control and pMad-binding site mutant lines examined here were heterozygous (*w;;AtypX/+*); *wit* mutants (*w;;AtypX,wit^{A12}/wit^{B11}*).

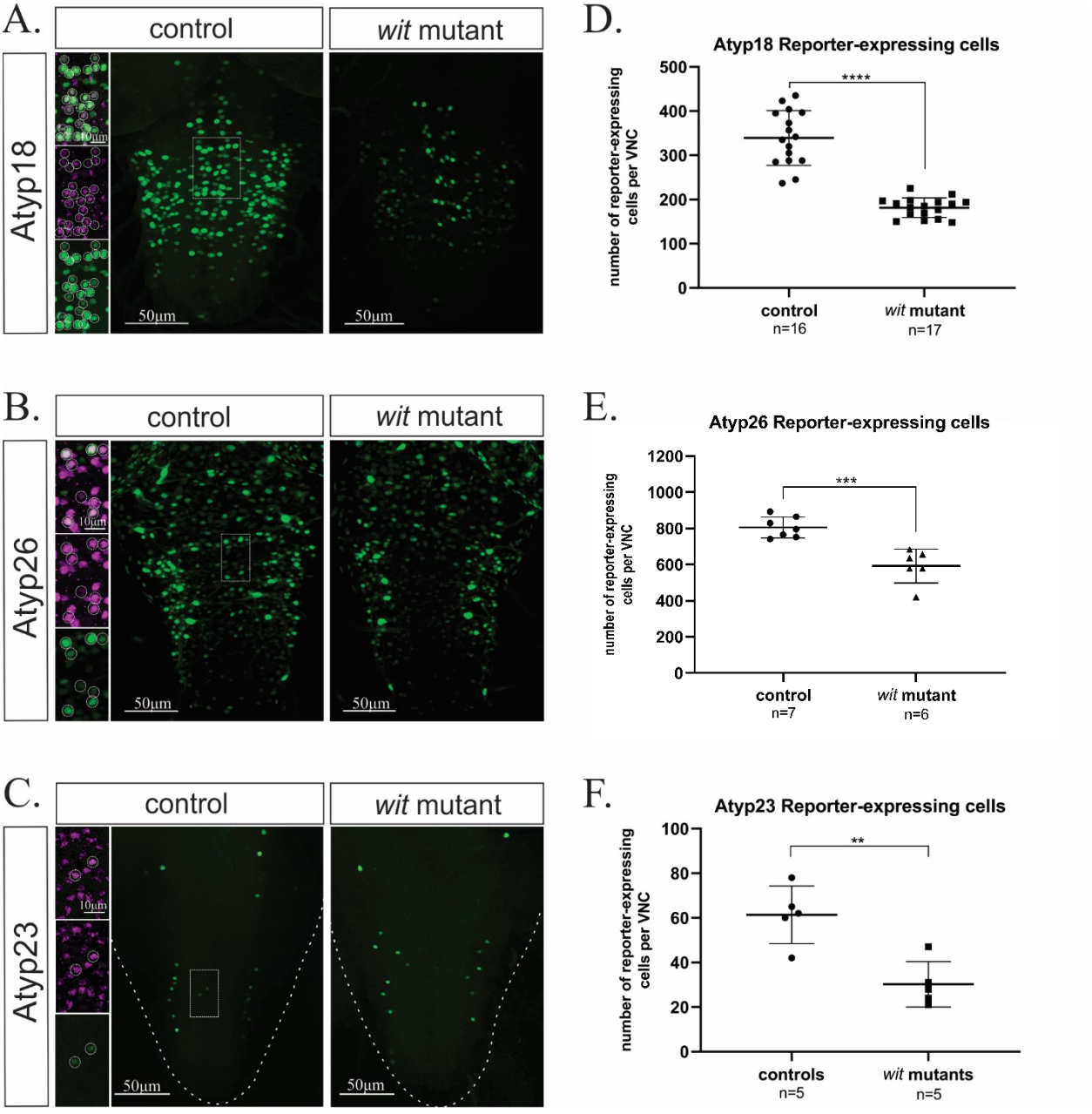
A.
control
wit mutant
Atyp18
10µm
50µm
50µm
D.
Atyp18 Reporter-expressing cells
number of reporter-expressing cells per VNC
500
400
300
200
100
0
****
control
n=16
wit mutant
n=17
B.
control
wit mutant
Atyp26
10µm
50µm
50µm
E.
Atyp26 Reporter-expressing cells
number of reporter-expressing cells per VNC
1200
1000
800
600
400
200
0
***
control
n=7
wit mutant
n=6
C.
control
wit mutant
Atyp23
10µm
50µm
50µm
F.
Atyp23 Reporter-expressing cells
number of reporter-expressing cells per VNC
100
80
60
40
20
0
**
controls
n=5
wit mutants
n=5

Figure 2.4: ***wit-mutants exhibit a significant loss in reporter-expressing cells compared to controls in the VNC of third Instar larvae.***

(A-C) Representative images of transgenic reporter lines Atyp18, Atyp26 and Atyp23 where reporter expression is significantly altered in *wit* mutants (wit^{A12}/wit^{B11}). Side panels indicate nuclei with overlapping GFP reporter (green) and pMad stain (magenta). **(D-F)** Quantification of numbers of reporter-expressing cells indicates a significant difference in the mutant genotypes compared to their controls (Atyp18 controls: 339±15 cells and *wit*: 181±5 cells; Atyp26 controls: 805±22 cells and *wit*: 592±39 cells; Atyp23 controls: 61±6 cells and *wit*: 30±5 cells). Data shown as mean±SEM and n indicate the number of VNCs analyzed. Significance was calculated with Student`s t-test: Atyp18 $p<0.0001$; Atyp26 $p=0.0004$; Atyp23 $p=0.0028$. Each point in the graphs represents the total number of reporter-expressing cells in the VNC of a single animal. *Genotypes:* All control lines examined here were heterozygous (*w;;AtypX*); *wit* mutants ($w;;AtypX,wit^{A12}/wit^{B11}$).

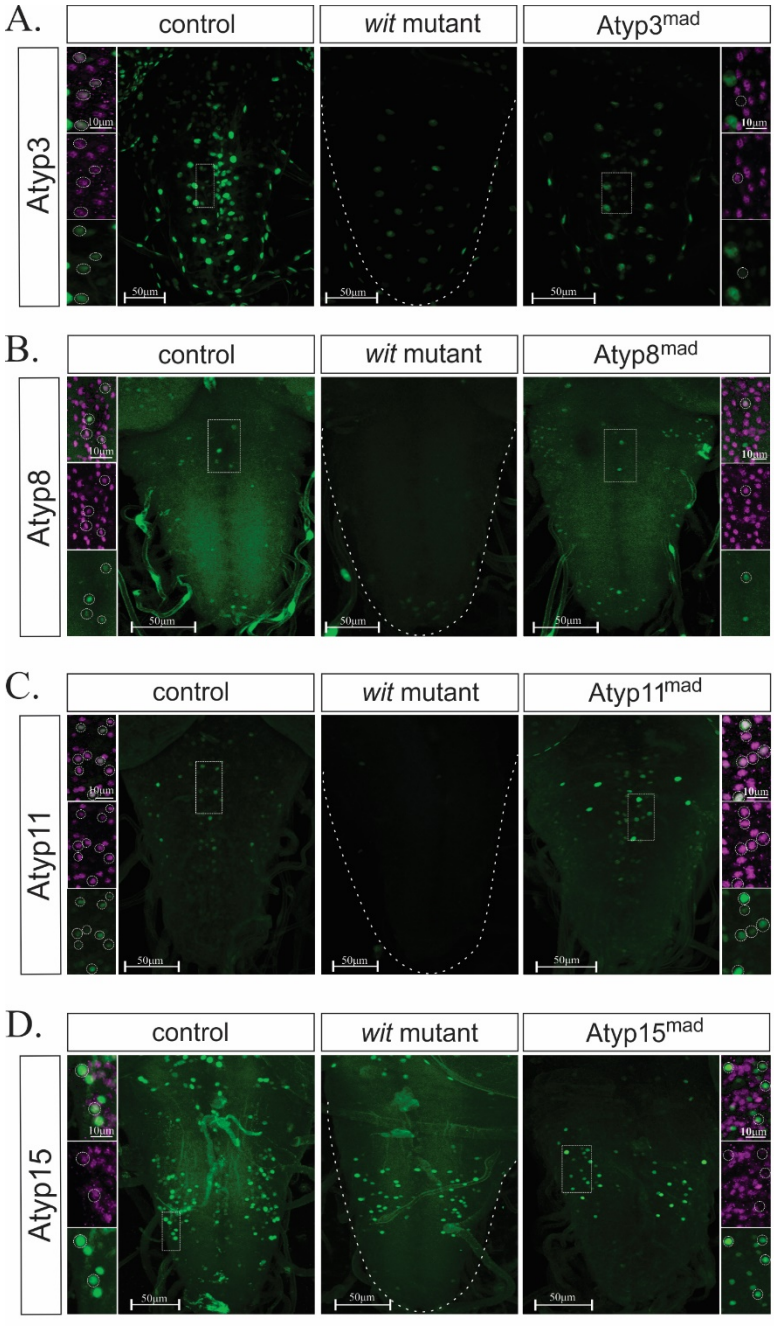
A.
control
wit mutant
Atyp3mad
Atyp3
B.
control
wit mutant
Atyp8mad
Atyp8
C.
control
wit mutant
Atyp11mad
Atyp11
D.
control
wit mutant
Atyp15mad
Atyp15
50µm
10µm

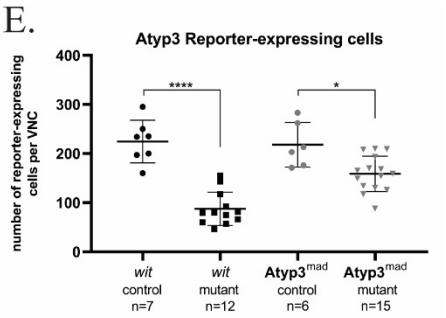
E.
Atyp3 Reporter-expressing cells
number of reporter-expressing cells per VNC
****
*
wit control n=7
wit mutant n=12
Atyp3mad control n=6
Atyp3mad mutant n=15

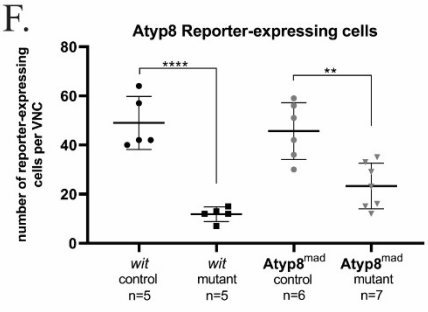
F.
Atyp8 Reporter-expressing cells
number of reporter-expressing cells per VNC
****
**
wit control n=5
wit mutant n=5
Atyp8mad control n=6
Atyp8mad mutant n=7

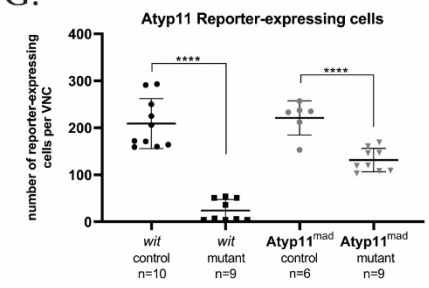
G.
Atyp11 Reporter-expressing cells
number of reporter-expressing cells per VNC
****
****
wit control n=10
wit mutant n=9
Atyp11mad control n=6
Atyp11mad mutant n=9

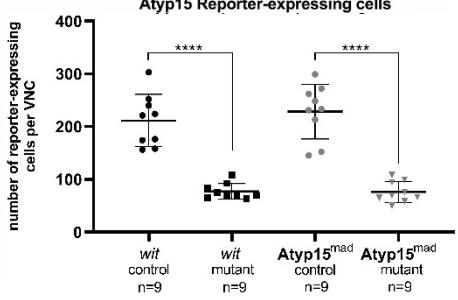
H.
Atyp15 Reporter-expressing cells
number of reporter-expressing cells per VNC
****
****
wit control n=9
wit mutant n=9
Atyp15mad control n=9
Atyp15mad mutant n=9

Figure 2.5: ***wit-mutants and AE2 Mad-binding site mutants exhibit significant loss of reporter-expressing cell numbers compared to controls in the VNC of third Instar larvae.***

(A-D) Representative images of transgenic reporter lines Atyp3, Atyp8, Atyp11 and Atyp15, where reporter expression was significantly altered in *wit* mutants (wit^{A12}/wit^{B11}) and pMad-binding site mutants ($AtypX^{mad}$). Side panels indicate nuclei with GFP reporter (green) and/or pMad stain (magenta). **(E-H)** Quantification of numbers of reporter-expressing cells indicates a significant difference in the *wit* and pMad-binding site mutant genotypes compared to their controls. Significance was calculated with one-way Anova with a Tukey multiple comparisons test for the following genotypes: Atyp3 control *vs wit* mutants $p<0.0001$ and control *vs* pMad-binding site mutants $p=0.0143$; Atyp8 control *vs wit* mutants $p<0.0001$ and control *vs* pMad-binding site mutants $p=0.0021$; Atyp15 control *vs wit* mutant and control *vs* pMad-binding site mutants $p<0.0001$. For Atyp11, as the *wit* control samples were non-normally distributed, significance was calculated with Mann-Whitney *U* test for control *vs wit* mutants $p<0.0001$; Student`s t-test was used for control *vs* pMad-binding site mutants $p<0.0001$. In all cases, *wit* control and AtypX controls had non-significant differences in reporter-expressing cell numbers. Each point in the graphs represents the total number of reporter-expressing cells in the VNC of a single animal and n indicates the number of VNCs analyzed. *Genotypes:* All control and pMad-binding site mutant lines examined here were heterozygous (*w;;AtypX/+*); *wit* mutants ($w;;AtypX,wit^{A12}/wit^{B11}$).

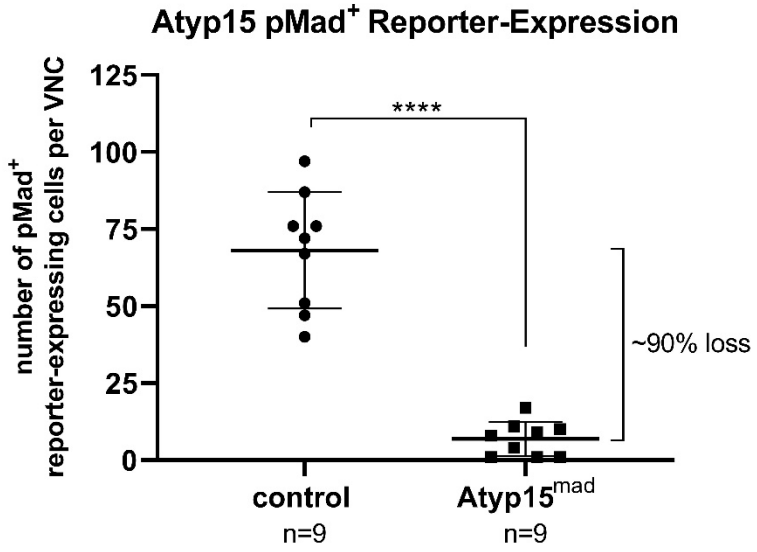

Figure 2.6: ***Near complete loss of pMad stain and reporter-expression overlap in pMad-binding site mutant Atyp15^{mad}.***

Quantification of reporter-expressing pMad^{+} cells reveals a 90% loss in pMad-binding site mutant *Atyp15^{mad}* (average of 7±2 cells per VNC) compared to controls. Significance was calculated with Student`s t-test: $p<0.0001$.

Data shown as mean±SEM and n indicate the number of VNCs analyzed. Each point in the graph represents the number of pMad^{+} reporter-expressing cells in the VNC of a single animal and n indicates the number of VNCs analyzed. Genotypes: All control and pMad-binding site mutant lines examined here were heterozygous (*w;;AtypX/+*).

A.

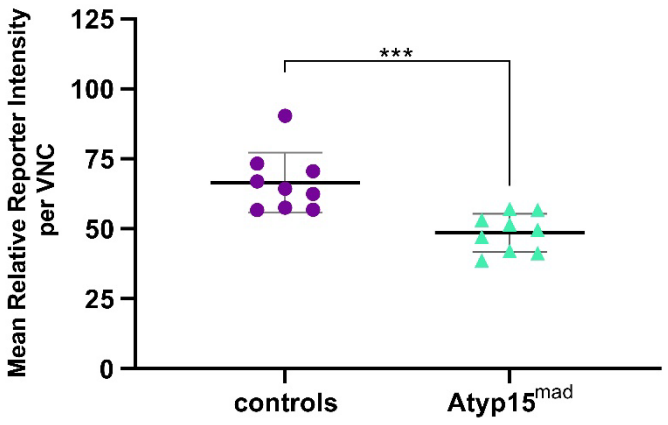
Atyp15 Mean Relative Reporter Intensity
Mean Relative Reporter Intensity per VNC
125
100
75
50
25
0
***
controls
Atyp15mad

B.

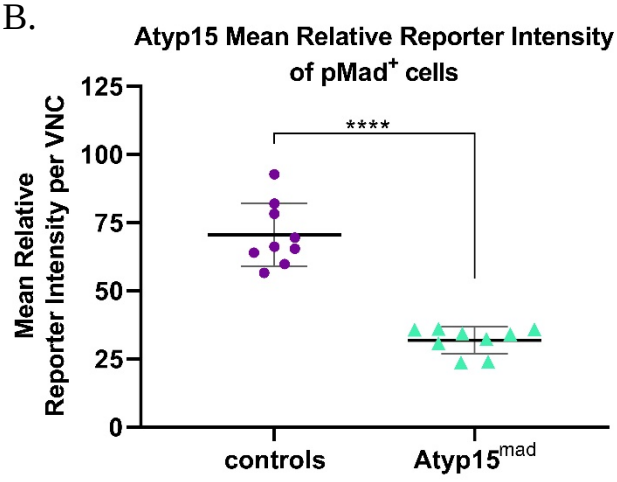
Atyp15 Mean Relative Reporter Intensity of pMad+ cells
Mean Relative Reporter Intensity per VNC
125
100
75
50
25
0
****
controls
Atyp15mad

C.

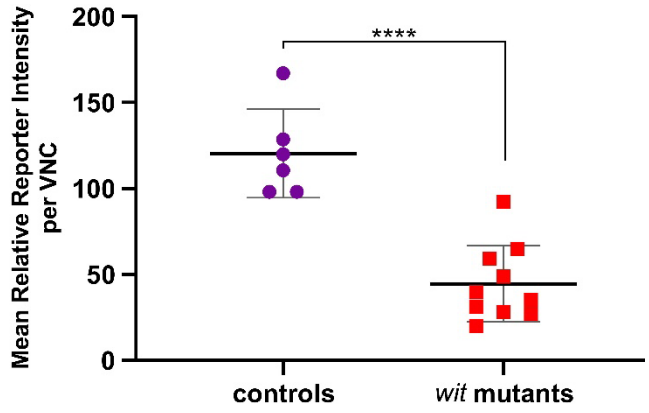
Atyp18 Mean Relative Reporter Intensity
Mean Relative Reporter Intensity per VNC
200
150
100
50
0
****
controls
wit mutants

D.

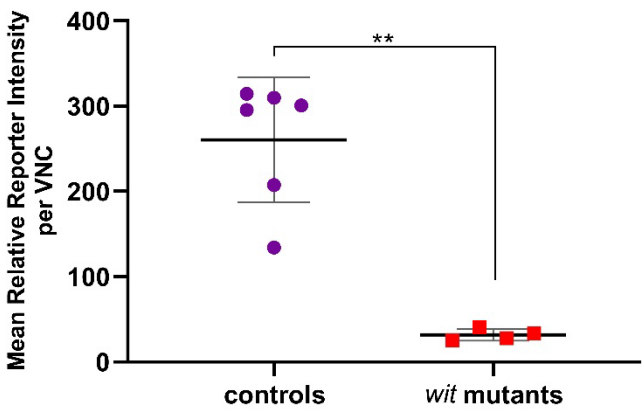
Atyp26 Mean Relative Reporter Intensity
Mean Relative Reporter Intensity per VNC
400
300
200
100
0
**
controls
wit mutants

E.

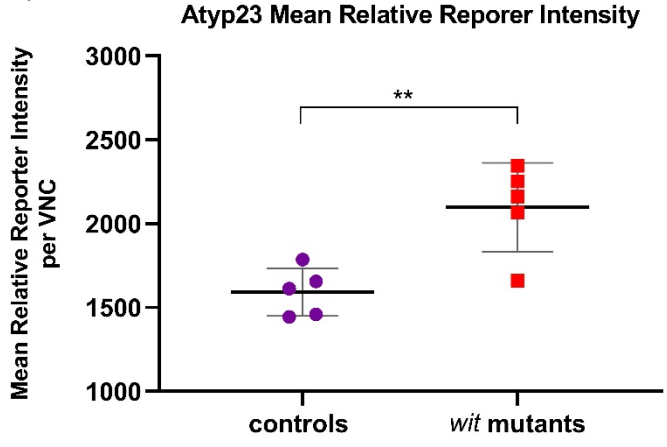
Atyp23 Mean Relative Reporer Intensity
Mean Relative Reporter Intensity per VNC
3000
2500
2000
1500
1000
**
controls
wit mutants

F.

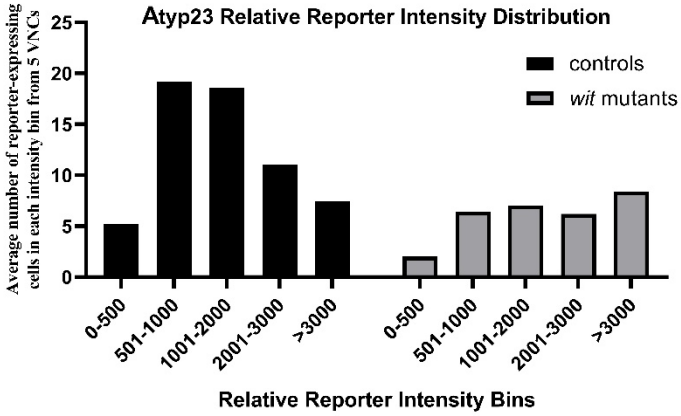
Atyp23 Relative Reporter Intensity Distribution
Average number of reporter-expressing cells in each intensity bin from 5 VNCs
25
20
15
10
5
0
controls
wit mutants
0-500
501-1000
1001-2000
2001-3000
>3000
0-500
501-1000
1001-2000
2001-3000
>3000
Relative Reporter Intensity Bins

Figure 2.7: ***Significant change in relative reporter intensity was observed in 4 mutant genotypes compared to their respective controls.***

(A-B) Quantification of mean relative reporter intensity for Atyp15 indicates a significant difference of reporter expression in the controls and pMad-binding site mutant genotypes. Graph (A) plots the mean relative reporter intensity (in arbitrary units) of all reporter-expressing cells in the VNC. Significance was calculated with Student`s t-test: p=0.006. Graph (B) represents the mean relative reporter intensity of $pMad^+$ cells only, indicating that the BMP-dependent cells exhibit a larger reporter intensity loss (54% loss) than all the reporter expressing cells combined (27% loss). Significance was calculated with Mann-Whitney U test: p<0.0001. It is important to note here that there was an average of 7±2 $pMad^+$ with reporter overlap per VNC (FigureS1). **(C)** Quantification of mean relative reporter intensity for Atyp18 indicates a significant loss of reporter expression in *wit* mutants compared to controls (63% loss). Significance was calculated with Student`s t-test: p<0.0001. (**D)** Quantification of mean relative reporter intensity for Atyp26 indicates a significant loss of reporter expression in *wit* mutants compared to controls (88% loss). Significance was calculated with Mann-Whitney U test: p=0.0095. (**E)** Quantification of mean relative reporter intensity for Atyp23 indicates a significant increase of reporter expression in *wit* mutants compared to controls (24% increase). Significance was calculated with Student`s t-test: p=0.0057. **(F)** All reporter-expressing cells from the 5 VNCs of controls and *wit* mutants were distributed into groups based on their relative reporter intensity. Each column represents the average number of cells in each bin across the 5 VNCs that were quantified. Despite the significant loss of reporter-expressing cells in Atyp23 *wit* mutants (Figure2.4-F), the highest expressing cells appear to be maintained.

Each point in the graphs (A-E) represents the mean relative reporter intensity of reporter-expressing cells in the VNC of a single animal.

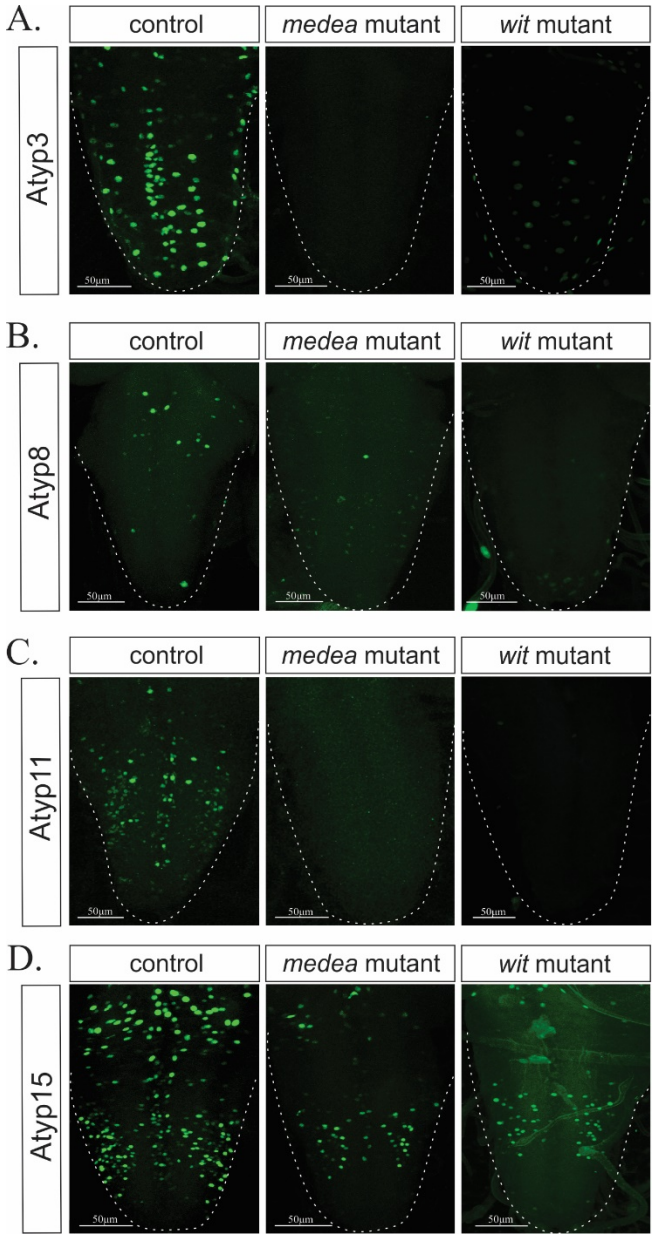

Figure 2.8: ***Medea is necessary for BMP-dependent activity of 4 wit-responsive BMP-AE2s.***

(**A-D)** Representative images of Atyp3, Atyp8, Atyp11 and Atyp15 control reporter expression compared to the same lines in a *Med* and *wit* mutant backgrounds. In all cases, reporter expression loss in both mutants exhibit the same pattern. Genotypes: All control lines examined here were heterozygous (*w;;AtypX/+*); *wit* mutants (*w;;AtypX*, wit^{A12}/wit^{B11}); *Med* mutants (*w;;AtypX*, Med^{c246}/Med^{13}).

2.4.3 Identification of other BMP-CRE Binding Sites within the BMP-AE2 Fragments

Evaluation of the genomic fragments cloned into our reporter lines for additional or high-affinity BMP-CREs revealed that the Atyp11 fragment contains a BMP-AE type enhancer previously cloned and characterized (Vuilleumier et al. 2018). This previously identified and characterized fragment, called Van23, includes the same BMP-AE but only partially overlaps with the Atyp11 genomic fragment (Figure 2.9-A). Van23 was shown to be *wit*-responsive in (Vuilleumier et al. 2018), as the reporter expression (Figure 2.9-B,C) was completely lost in a *wit* mutant background. Comparing Van23 reporter with Atyp11, we observe a striking difference between the two expression patterns with regards to the numbers of reporter expressing cells, as well as distribution of reporter expressing cells (Figure 2.9-B-D).

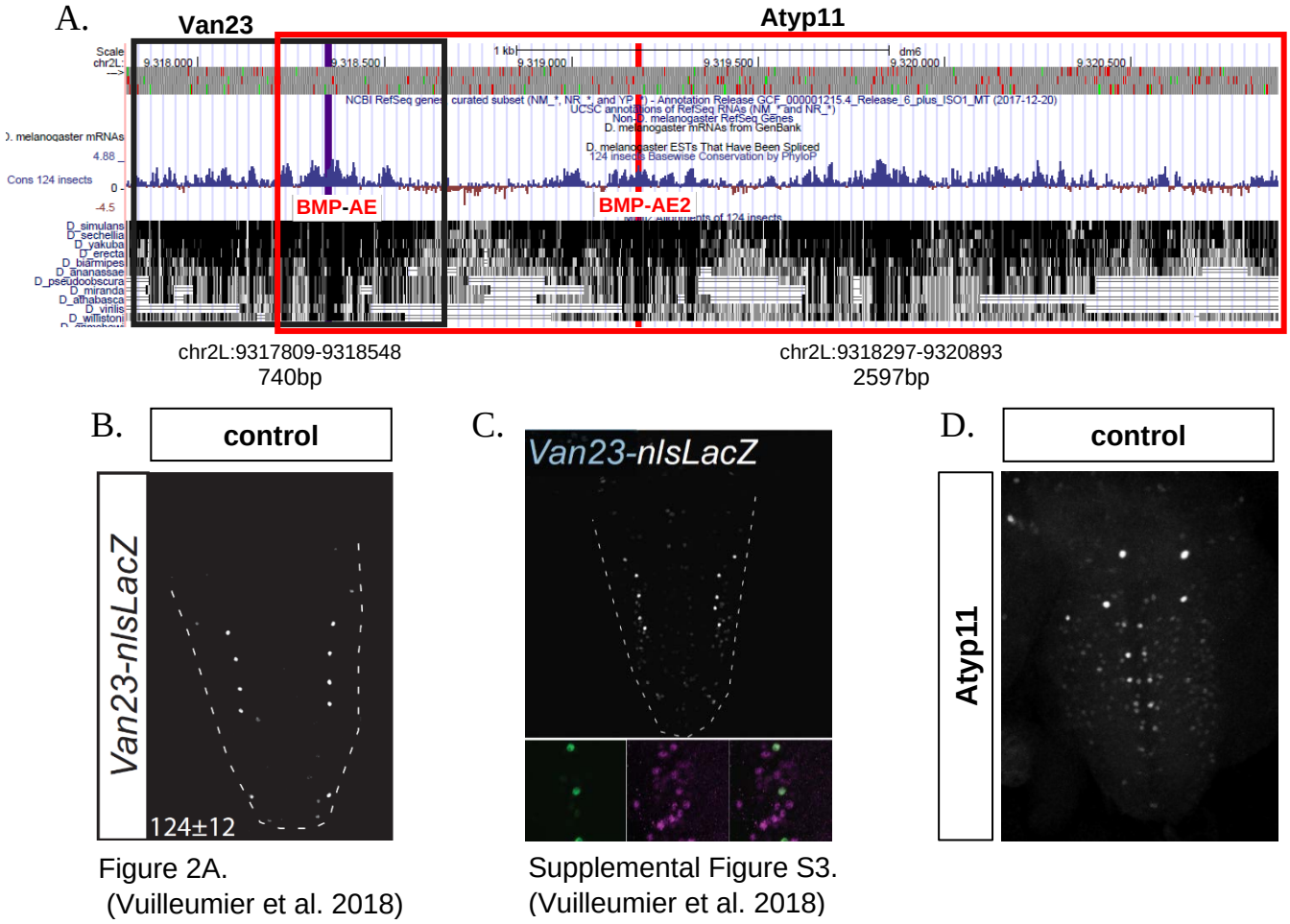

Figure 2A.
(Vuilleumier et al. 2018)

Supplemental Figure S3.
(Vuilleumier et al. 2018)

Figure 2.9: ***Comparison of two reporter lines with a common BMP-CRE binding site reveals strikingly different expression patterns.***

(A) Represents a USCS genome browser (https://genome.ucsc.edu/, dm6 - Aug.2014-Release 6 plus ISO1 MT) snapshot with the location and size of the genomic fragments contained in the reporter lines Atyp11 and Van23 (Vuilleumier et al. 2018). The position of the BMP-AE2 and BMP-AE motifs are also indicated in red text. **(B, C)** Images taken from (Vuilleumier et al. 2018) indicating the expression pattern of the reporter line Van23, which only contains a BMP-AE. Permission to use data was granted via email. **(D)** Representative image of Atyp11 reporter line, which contains two CREs, one BMP-AE2 and one BMP-AE.

2.5 Discussion

In this Chapter, we show that many instances of conserved BMP-AE2 motifs exist in the *Drosophila* genome. Functionalizing a subset of these *in vivo* revealed that several have a *wit*-dependent expression in the L3 VNC. In the case of Atyp3, Atyp8, and Atyp11, *wit* mutants exhibit a more severe loss of reporter-expressing cells compared to their respective Mad-binding site mutants. This suggests that additional *wit*-dependent co-factors could contribute to reporter expression. Another possibility is that alternative BMP-CRE binding sites compensate for the loss. In fact, for Atyp11, we have identified an additional BMP-CRE included in the genomic fragment cloned (Section 2.4.3). The difference in reporter expression between Van23 and Atyp11 could reflect the combinatorial effect of BMP-AE and BMP-AE2 binding sites. On the other hand, since the Atyp11 fragment (2597bp) is significantly larger than the Van23 fragment (740bp), it may include additional cofactor binding sites that may be missing in Van23, thereby strengthening reporter expression. The partial loss of reporter-expressing cells in the pMad-binding site mutant of the BMP-AE2 in the Atyp11 line compared to the *wit*-mutant reporter loss in Atyp11 could reflect compensation by the still intact BMP-AE in the pMad-binding site mutant.

In the case of Atyp15, loss of reporter-expressing cells in *wit* mutants and the pMad-binding site mutants is comparable. This suggests that in this genotype, the BMP-AE2 motif could be the sole or most important driver of *wit*-dependent reporter expression. Intriguingly though, *wit* mutants maintain wild-type (control level) mean relative reporter intensity while reporter intensity significantly diminishes in the pMad-binding site mutants. A possible explanation for this is the existence of *wit*-independent cofactors that help maintain reporter intensity expression in populations of $pMad^-$ cells that maintain reporter expression in a *wit* background (see Figure 2.10 for a schematic model). The need for other BMP-dependent cofactors could explain the loss of

reporter expression in pMad^{-} cells in *wit* mutants. In pMad-binding site mutants, the ability of the activated Smad-complex to bind to the BMP-AE2 motif is impaired, resulting in loss of reporter expression in almost 90% of the pMad^{+} cells. Remaining reporter-expressing cells have decreased mean relative reporter intensity, suggesting that the cofactors driving expression in these cells may also be impaired due to the pMad-binding site mutation. This could be due to direct interaction with the BMP-AE2 motif or, more likely due to conformational changes to the immediately flanking sequence of the AE2. There is increasing evidence that DNA structural parameters such as bendability, curvature, groove shape, of flanking sequences of a TF binding site play an important role in DNA-TF recognition and binding for some TF families (Yella et al. 2018). Therefore, it stands to reason that cofactors that bind to the immediate vicinity of the BMP-AE2 would be affected by the mutation of the pMad-binding site.

In line with what we observed with the *FMRFa* BMP-AE2, *Medea* is required for the expression of the reporter, as putting the Atyp BMP-AE2s in a *med*-mutant background phenocopied the reporter loss observed in a *wit*-mutant background. Since the exact grammar of the Medea binding site was crucial to restricting FMRFa expression to the TV4 neurons, it is possible that the Medea binding site (GTAT) plays an important role in directing the pattern of reporter expression in the Atyp BMP-AE2s as well.

It is becoming increasingly clear that the use of low affinity *cis*-regulatory sequences is a common mechanism for spatiotemporal restriction in gene expression (Crocker et al., 2016). While most other low affinity cis-regulatory elements are highly degenerate, we find that the BMP-AE2 motif is very well conserved. Furthermore, based on my work described in this chapter, we now know that FMRFa might not be the only gene controlled by a BMP-AE2 motif CRE. The

conservation of this motif, especially the C>A conversion in the Medea binding site that distinguishes the AE2 motif from the previously described AE and SE motifs, could be attributed to sequence specificity for a cofactor. However, due to the fact that many other functional BMP-AE2 motifs were identified, it is somewhat unlikely that the same cofactor is used in all these scenarios and different types of cells. The differences in expression pattern and intensity between the BMP-AE2 reporters tested in this chapter could be conferred partially by the combination of TFs present and contributing to each scenario. It is also likely that the specific sequence encoded by the BMP-AE2 motif may provide additional critical information that guides TF binding and dictates some of the effect observed in intensity and expression pattern. Detailed bioinformatic work could help us identify other degenerate BMP-CREs, as many low-affinity (redundant) binding sites have been identified as clusters, as well as cofactors and other transcription factors that directly interact with or bind sequences that flank the BMP-AE2 motif.

In the end, having a detailed understanding of the regulatory motif network utilized in different tissues, under different conditions will help build better bioinformatic prediction models for regulatory elements. With our growing understand of the contribution of non-coding sequences to disease, every effort to understand how regulatory elements are used across the genome is important.

2.6 Strengths and Limitations

This is the first study to systematically search for and identify low-affinity non-canonical versions of the well-established BMP-AE and BMP-SE.

Preliminary, unpublished work in our lab (by both Dr. Berndt and Dr. Vuilleumier) indicates that Brinker is not be involved in the BMP-responsiveness of AE2 sequences in the CNS.

No orthologue of Brinker has been identified in any metazoan other than insects (Blitz and Cho, 2009), suggesting that BMP signaling in the *Drosophila* CNS may be more similar to that of mammals, compared to the better-studied *Drosophila* wing disc. This gives us the means to study the use of a low-affinity BMP-CRE in a more similar context to that of mammals, thereby enabling us to more easily transition this work in vertebrates.

However, our approach to identifying and characterizing these CREs has its limitations. By using a biased approach and restricting our search to the BMP-AE2 "GGCGCC(N_5)GTAT" sequence we are potentially disregarding other non-canonical low-affinity BMP-CREs that could be employed in the *Drosophila* CNS. Additionally, the use of chromosomal reporter integration to a non-native site takes each tested BMP-CRE out of its native chromatin context. This could result in false-positive or more likely false-negative results.

Here we utilize episomal reporters assays to functionally characterize the genomic regions we have identified, and though this is the most commonly used tool in the field to test candidate CREs, episomes lack native chromatin features, which may affect our ability to identify all real CREs. Comparison between genomically-integrated *versus* episomal reporter assays, of the same sequence, show higher reproducibility and better correlation with ENCODE annotations based on chromatin accessibility assays and TF ChIP-seq for the integrated reporters (Inoue et al. 2017). Despite this, episomal reporter assays remain useful since active sequence-fragments in these assays are likely to also be active in a genomically-integrated context (Inoue et al. 2017).

2.7 Conclusions

In conclusion, we have identified 7 conserved BMP-CREs with the same sequence as the newly identified *FMRFa* BMP-AE2 binding site, supporting that this CRE type is not a unique feature of *FMRFa* regulation.

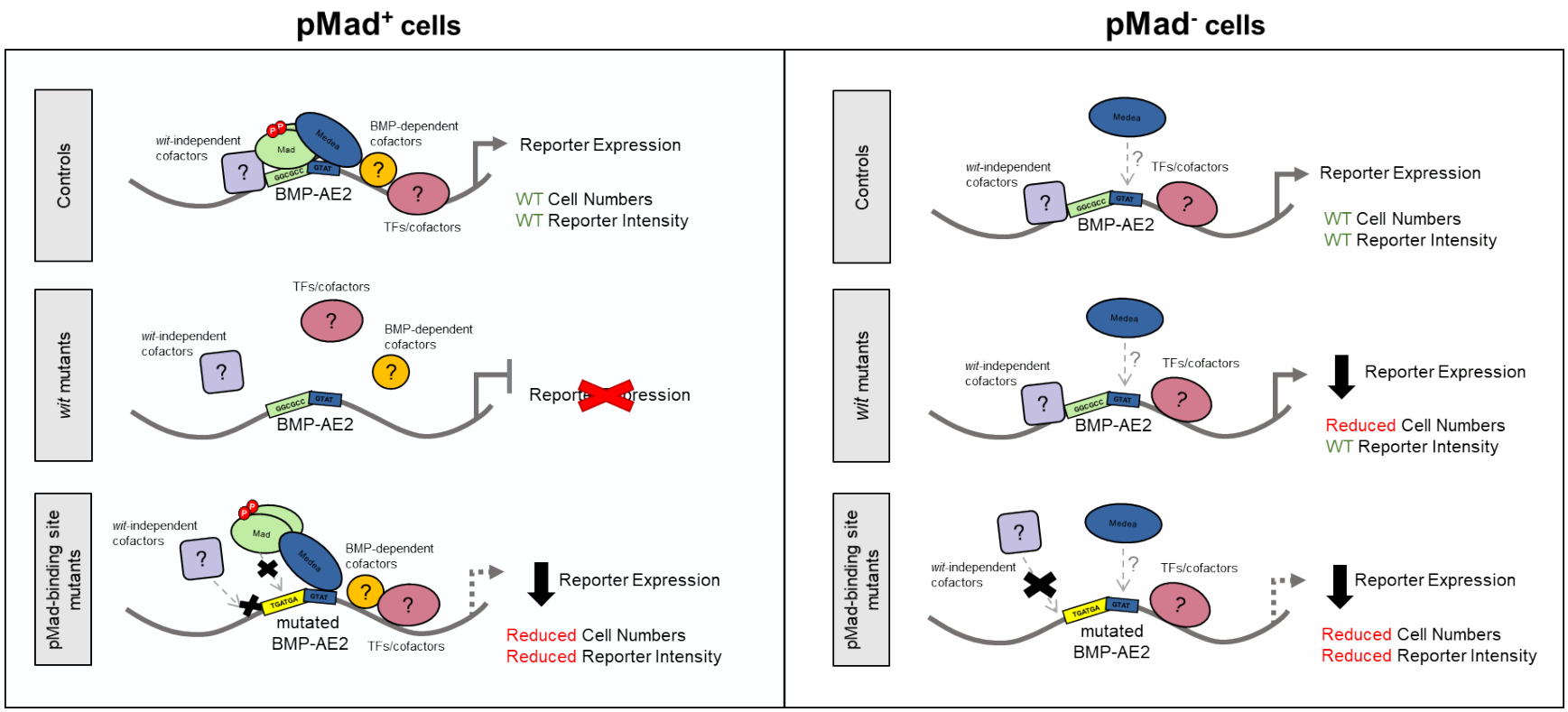

Figure 2.10: ***Schematic representation of gene regulation model in the Atyp15 reporter line.***

Genotypes represented here should be considered the same as in the experimental figures described previously: controls (*w;;AtypX/+*); *wit* mutants (*w;;AtypX*, wit^{A12}/wit^{B11}); pMad-binding site mutants ($w;;AtypX^{mad}/+$).

Chapter 3:

Determining the BMP-Dependent Regulatory Network Underlying the Early Stages of Chondrogenesis in the Murine Limb Bud.

3.1 Introduction

Musculoskeletal conditions are the second leading cause of disabilities globally. Disrupted or enhanced cartilage and bone formation or regeneration underlie the majority of this global burden, including arthritis, osteoporosis, chondrodysplasias and heterotopic ossification. Deciphering the molecular steps required to regulate chondrogenesis is essential in understanding the cause of various cartilage diseases, including skeletal malformations, chondrodysplasias, as well as osteoarthritis. According to the CDC (Centers for Disease Control and Prevention; https://www.cdc.gov/arthritis/data_statistics/index.htm), osteoarthritis (OA) is the most common form of arthritis affecting not just older adults, but also athletes and others with physically demanding jobs (Allen and Golightly, 2015). Progressive and irreversible degradation of articular cartilage plays an important role in the pathology of osteoarthritis (Bentley 1975). Being an avascular tissue, articular cartilage lacks access to necessary nutrients. Thus, cartilage is unable to sufficiently heal post trauma or chronic damage (Huey et al., 2012).

Current strategies to repair or replace damaged cartilage have many limitations and disadvantages (Zuscik et al., 2008; Smith et al., 2011; Solchaga et al., 2011; Huang et al., 2018). It is widely believed that a better understanding of chondrogenesis will provide novel therapeutic strategies. Concentrated efforts in the past two decades to understand the process of chondrocyte differentiation has led to the identification of numerous important factors in this process (reviewed in Section 3.1.1; (Akiyama and Lefebvre, 2011; Liu et al., 2017)).

Despite this wealth of discoveries, our understating of the chondrogenic transcriptional networks is far from complete. Therefore, further elucidating the molecular and regulatory mechanisms that control and direct chondrogenesis will provide us with a better foundation to enhance current and develop novel therapeutics.

3.1.1 Chondrogenesis

Chondrogenesis is the process by which cartilage is formed during the development and maintenance of the vertebrate skeleton (Kozhemyakina et al., 2015; Liu et al., 2017). Almost all mammalian skeletons are (mainly) cartilaginous during early fetal development. This cartilage matrix serves as a template for bone formation and is slowly replaced by bone through a process known as endochondral ossification until only a few cartilaginous tissues remain in skeletally-mature animals. Though endochondral ossification accounts for the development of the majority of the vertebrate skeleton, not all bones are formed via this process. The skull and facial bones develop through a process called intramembranous ossification, where mesenchymal cells directly differentiate into osteoblasts, without the cartilage matrix “intermediate” stage (Hojo et al., 2016).

The chondrogenic process is initiated by the recruitment and migration of embryonic mesenchymal cells (MSC) committed to the chondrogenic lineage. These pre-chondrogenic cells aggregate and form pre-cartilaginous condensations, where cells begin to differentiate into ovoid-shaped chondroblasts. Chondroblasts secrete molecules such as type II collagen, hyaluronic acid, glycoproteins, and proteoglycans (including aggrecan) to form the extracellular matrix (ECM) of the cartilage. Pre-hypertrophic chondrocytes proliferate within the condensations until they exit the proliferative phase to undergo hypertrophy. Terminal differentiation of chondrocytes into

hypertrophic chondrocytes is characterized by cartilage matrix calcification/mineralization and vascular invasion. (Goldring et al., 2006; Underhill et al., 2014)

Historically, it was widely accepted that hypertrophic chondrocytes undergo programmed cell death, initiating the process of endochondral ossification where bone marrow-derived osteoblast cells migrate and replace the apoptotic chondrocyte population (Gibson, 1998; Kronenberg, 2003; Mackie et al., 2011). However, recent cell lineage tracing techniques revealed that a significant portion of bone cells are derived directly via transformation of chondrocytes into osteoblasts (Ono et al., 2014; Zhou et al., 2014; Yang et al., 2014). This suggests that chondrogenesis and osteogenesis are not separate processes, but rather sequential phases of the same process, where hypertrophic chondrocytes transdifferentiate into bone cells.

3.1.2 Current Knowledge of Chondrogenic Regulatory Mechanisms

3.1.2.1 SOX9, the "Master" Regulator of Chondrogenesis

SOX9 (or Sex-Determining Region Y-Box 9) is a key transcription factor involved in chondrogenesis. It is essential for mesenchymal condensation, proliferation, and differentiation of chondrocytes (Bi et al., 1999; Bi et al., 2001; Akiyama et al., 2002). At the onset of chondrogenesis, Sox9 induces expression of two other Sox family members, *Sox5* and *Sox6*, and together as the 'Sox trio', these three TFs direct transcription of a multitude of chondrogenic genes (Smits et al., 2001; Smits et al., 2004; Akiyama et al., 2007). For example, during the early stages of chondrogenesis, SOX9 directly induces the expression of cartilage matrix components and markers of committed chondrocytes, like collagen type II alpha 1 (COL2A1), COL9A1 and aggregan (ACAN). In addition to SOX5 and SOX6, several other regulators have been reported to function with SOX9 in the transcriptional control of targets, including the co-regulators WWP2,

SIK3, ARID5A, and the histone deacetylase HDAC4 (Akiyama and Lefebvre, 2011; Lefebvre and Dvir-Ginzberg, 2017).

From the pre-hypertrophic stage onwards, further differentiation of chondrocytes is mainly directed by RUNX2 (and RUNX3 to some extent), and by the MADS-box-containing transcription factor MEF2C, with MEF2D enhancing MEF2C`s action (Takeda et al., 2001; Yoshida and Komori, 2005; Arnold et al., 2007). SOX9 delays pre-hypertrophy and prevents osteoblastic differentiation by downregulating Runt domain transcription factor RUNX2 (CBFA1) and β-catenin (Akiyama et al., 2004; Zhou et al., 2006; Topol et al., 2009; Cheng and Genever, 2010; Dy et al., 2012). During hypertrophy, SOX9 still has important functions as it cooperatively transactivates expression of Col10a1 (hypertrophic chondrocyte-specific collagen gene) along with MEF2C (Dy et al. 2012).

3.1.2.2 BMP Signaling in Chondrogenesis

BMPs are necessary for chondrogenesis, skeletal development, and fracture repair. Disrupted BMP signaling causes many debilitating human disorders of bone, vasculature, as well as many cancers and fibroses (Gazzerro and Canalis, 2006; García et al., 2016; Morrell et al., 2016). Conditional deletion of BMPs, BMP receptors, Smads or even BMP antagonists leads to a failure of chondrogenesis, severe chondrodysplasia and bone malformations (Gong et al., 1999; Yoon et al., 2005; Bandyopadhyay et al., 2006; Tsuji et al., 2006), and even embryonic lethality in some cases (Retting et al., 2009). For example, the targeted deletion of BMP Receptor 1a (BMPR1A) in chondrocytes results in severe cartilage defects and halts the process of endochondral bone formation (Jing et al. 2014).

BMPs control nearly every aspect of chondrogenesis (Song et al., 2009). Components of the BMP signaling pathway are highly expressed in growth plates with specific temporal-spatial patterns that correlate with functions during growth plate development and homeostasis (Minina et al. 2001). *In vitro,* BMPs can promote primary mesenchymal cells to differentiate into chondrocytes in high-density cultures (e.g mesenchymal limb bud-derived micromass cultures; Karamboulas et al., 2010). *In vivo,* conditional deletion of *Bmp2* and *Bmp4* in prechondrogenic limb mesenchyme revealed that they are both essential for the initiation of mesenchymal condensations (Bandyopadhyay et al. 2006). Additional *in vivo* experiments revealed a role for BMPs in chondrocyte differentiation, as well as a potential role in maintaining Sox (*Sox9*, *Sox5*, and *Sox6*) protein expression (Yoon et al. 2005). After chondrocytes have differentiated, continued TGF-β-mediated SMAD1/5/9 signaling leads to terminal differentiation hypertrophy, potentially via interaction with RUNX2 (Leboy et al., 2001; Bandyopadhyay et al., 2006; van der Kraan et al., 2009). To further support this, a recent study has demonstrated that SMAD4 controls chondrocyte hypertrophic differentiation by directly binding to regulatory elements in the Runx2 promoter and upregulating its expression during skeletal development (Yan et al. 2018). Finally, BMP7 has a pivotal role in postnatal maintenance of articular cartilage and has been shown to delay cartilage degeneration, such as when induced by excessive running in rats (Sekiya et al. 2009).

Despite advancements in understanding the impact of BMP signaling, many questions remain unanswered regarding the specific regulatory contributions of the canonical BMP pathway during the initial stages of chondrogenesis. Remarkably, we do not know how BMP signaling and Smad TFs control chondrogenesis. How do Smads fit in with the other known TFs and cofactors mediating this process? The goal of this thesis is to provide a more comprehensive report on the

molecular players involved in embryonic chondrocyte development. Specifically, we aimed to identify transcription factors and regulatory regions, and subsequently characterize downstream gene regulatory processes involved in chondrogenesis.

3.1.2.3 Signaling Pathway Crosstalk During Chondrogenesis

At the molecular level, several signaling pathways such as WNT/β-catenin, Notch, Retinoid, Hedgehog, FGF, and TGF-β/BMP regulate the initiation of the chondrogenic process, chondrocyte maturation and subsequent bone formation during embryonic skeletogenesis (Goldring et al., 2006; Long and Ornitz 2013; Kozhemyakina et al., 2015).

Sonic hedgehog (SHH), along with BMPs, is able to promote chondrogenesis of the somitic mesoderm by inducing the expression of both *Sox9* and *Nkx3.2* (Zeng et al., 2005). NKX3.2 is a BMP-dependent transcriptional repressor that blocks BMP-dependent expression of GATA 4, 5 and 6 (Daoud et al. 2014). These same GATA TFs were shown to block SHH-dependent induction of *Sox9* gene expression, thus NKX3.2 effectively de-represses *Sox9* and promotes chondrogenesis (Daoud et al. 2014). WNT signaling proteins were shown to inhibit chondrocyte differentiation (Rudnicki and Brown, 1997), potentially by repressing *Sox9* via methylation of its promoter by the methyltransferase DNMT3. Fibroblast growth factor (FGF) signaling was shown to block the recruitment of DNMT3 (Kumar and Lassar, 2014). In addition, FGF signals have been demonstrated to boost the expression of *Sox9* in chondrocytes via a mitogen-associated protein kinase (MAPK)-dependent pathway (Murakami et al., 2000). Retinoid and Notch signaling, on the other hand, were both shown to suppress chondrogenesis (Cash et al., 1997; Hardingham et al., 2006; Dong et al., 2010).

BMP signaling is also required for the condensation of chondroprogenitor cells and chondrocyte differentiation. *In vitro* studies suggest that TGF-β signaling operates prior to BMPs and regulates the formation of pre-cartilaginous condensations, potentially via a SMAD3-driven regulation of *Sox9* (Leonard et al., 1991; Furumatsu et al., 2005; Lorda-Diez et al., 2009; Karamboulas et al., 2010). TGF-β can also signal via the MAPK proteins p38, ERK, and JNK in MSC cells and contribute to the progression from condensation to chondrocyte differentiation by blocking WNT-mediated β-catenin nuclear translocation, thereby reducing N-cadherin and cell-cell interactions (Tuli et al., 2003; Zhang, 2009; Mu et al., 2012). TGF-β also mediates the end of proliferation (by counteracting the FGF-mediated cell proliferation) and the subsequent initiation of chondrocyte differentiation (Cleary et al., 2015).

The parathyroid hormone-related peptide/Indian Hedgehog (PTHRP/IHH) signaling pathway has been defined as an important negative regulator of chondrocyte maturation. IHH is mainly expressed in pre-hypertrophic and early hypertrophic chondrocytes and regulates

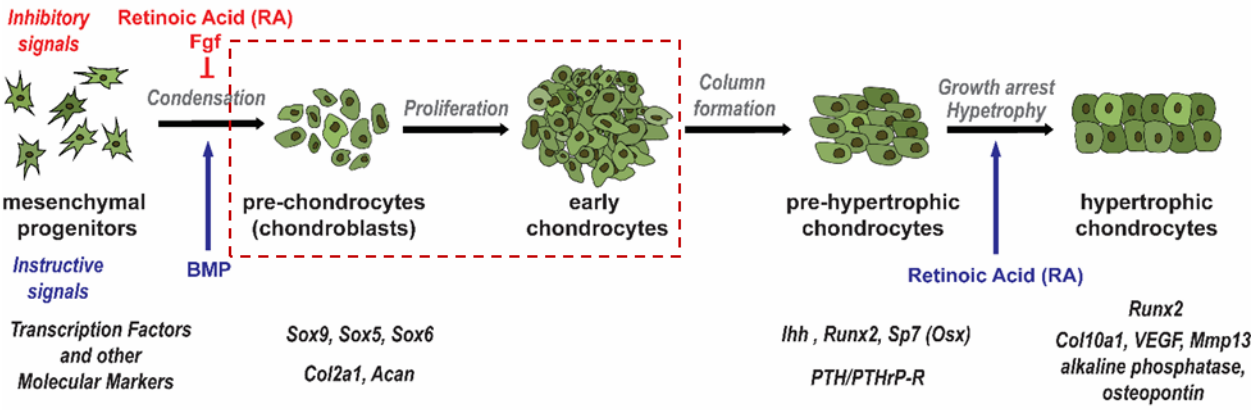

Figure 3.1: ***Chondrocyte differentiation***

A general schematic representation of differentiating chondrocytes from mesenchymal stem cells. This is a non-exhaustive list of key TFs, extracellular matrix components and signaling molecules characteristic of the cells at each of the differentiation steps. The red box indicates the stages of chondrogenesis during which we are conducting our experiments.

chondrocyte maturation by maintaining expression of PTHRP (Vortkamp et al., 1996). PTHRP signals repress chondrocyte hypertrophy by inhibiting the activity of both Mef2 and Runx family members (Kozhemyakina et al., 2009; Correa et al., 2010).

Taken together, although we have a much better understanding of regulatory mechanisms that take place during the maturation process of already committed chondrocytes, the same cannot be said about molecular events that induce and regulate the initial steps of mesenchymal cell differentiation into chondrocytes. Although some of the signaling molecules necessary for the induction of this sequential process (chondrogenesis) have been identified, our understanding of the exact regulatory mechanisms at play and the extent of crosstalk between these pathways are yet to be clarified.

3.1.2.4 *cis*-Regulatory Elements in Chondrogenesis

Some of the earliest work in identifying the *cis*-regulatory elements that are utilized during chondrogenesis focused on extracellular matrix components, starting with Col2a1 (Horton et al., 1987; Mukhopadhyay et al., 1995; Krebsbach et al., 1996). It was later shown that SOX9, along with SOX5, SOX6, and NKX3.2, were bound to this enhancer and directed Col2a1 expression in chondrocytes (Bell et al., 1997; Lefebvre et al., 1997; Lefebvre et al., 1998; Leung et al., 1998; Kawato et al., 2012). Subsequent studies revealed that other extracellular matrix components like Col11a2, Col9a1, Col27a1, Col10a1, Acan (AGC1), MIA (Cd-rap), Hapln1 (CRTL1) and Matn1 (Matrilin-1), owed their cartilage-specific expression to SOX9, SOX5, SOX6 as well (Bridgewater et al., 1998; Xie et al., 1999; Bridgewater et al., 2003; Kou and Ikegawa, 2004; Jenkins et al., 2005; Rentsendorj et al., 2005; Han and Lefebvre, 2008; Liu and Lefebvre, 2015; Li et al., 2018).

In the era of genome-scale ChIP-seq experiments, hundreds to thousands of putative binding sites for chondrogenic and osteogenic transcription factors have been identified (Hojo et al., 2016). Many of these experiments were conducted in various cell-lines, whole limbs or other primary tissues, in different organisms (mice, rats, humans) and at various timepoints during development, which makes it difficult to utilize in conjunction with our experiments and analyses. Several SOX9 ChIP-seq experiments have been done in the developing mouse limb (Oh et al., 2014; Liu and Lefebvre, 2015; Liu et al., 2018), revealing many putative *cis*-regulatory elements relevant to our work (Garside et al. 2015; Yamashita et al. 2019). One of these studies further revealed that SOX9 binds to low-affinity motifs and that many of these binding sites are grouped together and form "super-enhancer like" clusters providing insights into specific regulatory strategies that might be employed by Sox9 (Ohba et al., 2016). While ChIP-seq experiments have been conducted in chondrogenic cells for SMAD2/SMAD3 (Wang et al., 2016) and more recently SMAD4 (Yan et al. 2018), there are no such published experiments for SMAD1/5/9.

3.1.2.4.1 BMP *cis*-Regulatory Elements in Chondrogenesis

Over the years there have been some attempts to identify *bona fide* chondrogenic BMP-CREs and Smad-binding sites; however, very few have been successful thus far.

One of the first attempts was by Kusanagi et al. who showed that SMAD1 and SMAD4 could bind to the GCCG motif (derived from the early GCCGnCGC consensus identified in flies) in a BMP-dependent manner (Kusanagi et al. 2000). They then constructed a multimerized version of this motif, placed it upstream of a minimal *Col10a1* promoter and transfected two cell lines that can be differentiated into chondrocytes (the C3H10T1/2 mesenchymal progenitor cells and the murine teratocartinoma ATDC5 cells). The reporter responded to a combination of canonical BMP

signaling components (transfection with SMAD1/BMPRII/constitutively active BMPRIB receptor) in both cell lines, but not to a combination of TGF-β signaling components (transfection with SMAD3/TβRII/constitutively active TβRI receptor). It is important to note the authors did not describe the use of differentiation culture protocols for the C3H10T1/2 and ATDC5 cell lines during their experiments, which is what is normally done with these cells to differentiate them into chondrocytes (Shukunami et al. 1997; Andrew et al. 1999). Therefore, the multimerized GCCG motif was not studied in a chondrogenic context, but rather in a mesenchymal cell/teratocarcinogenic context.

A subsequent study identified a Smad1 binding site in the promoter of the chicken *COL10A1* gene with the sequence 'CAGAGATTATTCACCTCTCT' that was responsive in chicken embryonic chondrocytes (Drissi et al. 2003). Unfortunately, the promoter region upstream of the chicken *COL10A1* gene (Appendix, Figure S2A) is not very well conserved to the murine and human genomes and no such putative binding sites have been identified in other vertebrates.

A study utilizing an *in vivo* approach identified a 560bp fragment upstream of the *Msx2* gene that was able to drive BMP-responsive lacZ-expression in 10T1/2 mouse embryonic fibroblasts, as well as various tissues in E11.5 mouse embryos, including the developing limb bud (Brugger et al. 2004). Deletion analysis narrowed down the BMP-responsive region to a 52bp fragment that drove weaker lacZ-reporter expression in a subset of the original 560bp fragment expression tissues. Further study of a multimerized 52bp fragment revealed that it responded to BMP4 stimulation in the anterior mouse limb bud, but it did not respond to stimulation in the proximal or posterior regions of the limb. This suggests that other sequences within the larger 560bp fragment help mediate BMP-responsiveness in a subset of tissues/developmental stages

(Appendix, Figure S2B). Finally, mutation of the 4 “GCCG” sequences or “AATTAA” sequence within the 52bp fragment revealed that they are necessary for BMP-responsiveness.

Deletional analysis, using a luciferase reporter in P19 embryo-derived murine teratocarcinoma cells, identified a 163bp BMP7-responsive region upstream of the *Ihh* gene (Seki and Hata, 2004). Mutation of the 6 GCCGNGC-like motifs and the palindromic “GGCGCC” sequence within this region revealed that each of these motifs contributes to the overall BMP-responsiveness of the 163bp fragment. Reviewing the promoter/enhancer fragments in their deletional assay revealed that the initial “2HC8” fragment had a much higher BMP7 response than any subsequent fragments tested and that deletion of the +1 to -123 region resulted in a substantial loss of reporter activity. However, this region (+1 to -123 from the *Ihh* gene TSS) was not studied further for BMP-responsiveness and potential Smad-binding sites. See Section 3.3.3, Table 3.10 for more details.

A 28bp GC-rich BMP-responsive sequence, with two overlapping GCCGNCGC-like sequences in the 5`end and another GCCGNCGC-like sequence in the 3`end, was identified upstream of the Smad6 gene via deletional analysis in P19 cells (Ishida et al., 2000). This sequence was multimerized (3x) and placed in a luciferase reporter plasmid with a core Col10 promoter and tested for reporter transcriptional activation in P19 and mouse mesenchymal C2C12 cell lines, as well as human HaCaT keratinocytes and Mv1Lu mink lung epithelial cells. Luciferase reporter activity was increased in all cases with the addition of Smad1/5 and constitutively active BMP type I receptors or BMP7. Mutation of the 5`end and 3` end GCCGNCGC-like sequences revealed that the overlapping sequence in the 5`end was the one important for BMP-driven reporter activity. Another region just upstream of the 28bp GC-rich BMP-responsive sequence was also shown to

have significant BMP-responsive activity, however, this region was not studied further for potential Smad-binding sites (Appendix, Figure S3; Section 3.3.3, Table 3.10). A subsequent study in C2C12 and 2T3 (mouse osteoblast cell line) cells was able to identify a BMP2/SMAD1/RUNX2 responsive sequence within the region upstream of *Smad6*, however, in this case, it is likely that SMAD1 doesn't directly bind DNA but rather interacts with RUNX2 to mediate an effect its *Smad6* expression (Wang et al. 2007).

In addition to a lack of information regarding the contribution of BMP signaling to the chondrogenic regulatory network, there is insufficient research identifying BMP-CREs and Smad-binding elements. Most of the aforementioned studies, except for the one conducted by Brugger et al., were conducted using cell lines from different animals, with only a few of them using chondrocytes and/or cell precursors with chondrogenic potential. Utilizing primary mouse chondrogenic cells, our study provided a robust, reliable, and consistent system to identify and test the function of several regulatory regions important in different stages of chondrogenesis.

3.1.3 Project Rationale

Reviewing current literature on chondrogenesis, it is clear there are important unanswered questions regarding the contribution of canonical BMP signaling to chondrogenesis. Recent work by Liu et al. has revealed that while SOX9 plays important roles during early chondrogenesis, it is not absolutely required to activate transcription (Liu et al., 2018). Therefore, there must be some other activating factors that function upstream or alongside SOX9 to enable chondrogenic gene activation. This new insight further underscores the need to study the transcriptional network of early chondrogenesis. Additionally, there is very little knowledge available on the gene regulatory role of Smads in chondrogenesis and the CREs that the Smads utilize.

We chose to use high-density micromass cultures from embryonic mesenchymal cells as they have been proven a reliable and robust *in vitro* model for studying the chondrogenic program and identifying important factors and elements involved. Murine embryonic limb micromass cultures are one of the best studied, and they can provide insights into the BMP-regulated molecular cascade involved in directing chondrogenic lineage differentiation (Underhill et al., 2014).

3.2 Materials and Methods

3.2.1 Animals and Timed Mating

Mice with a CD1 background were housed on a 12-hr light-dark cycle in a controlled climate according to protocols approved by the UBC Animal Care Committee and in accordance with guidelines established by the Canadian Council on Animal Care. Single male mice were paired with female mice between the ages of 7-10 weeks old and vaginal plugs were assessed the following morning. Plugged female mice were set as embryonic day E0.5 at midday of discovery and isolated in a separate cage until embryonic day E11.5.

3.2.2 Primary Cell Culture and Treatments

Primary limb mesenchymal (PLM) cell micromass cultures were established, as previously described (Hoffman et al., 2006; Karamboulas et al., 2010; Underhill et al., 2014). Briefly, whole limbs were harvested from E11.5 mouse embryos and dissociated in media containing 1U/mL Dispase (Life Technologies). Dissociated cells were pelleted and re-suspended to a density of ~$2x10^7$ cells/mL. Cells were then seeded at a density of ~$2x10^5$ cells/micromass 10uL droplet into 12-well or 24-well plates. This cell density allowed chondrogenic differentiation and the formation

of cartilage nodules. Following 1-2 hours incubation, media containing BMP4 or Noggin (NOG) was added to each well and replaced every 24 hours. PLM cells were treated with 20ng/mL BMP4 (Calbiochem) or 100ng/mL NOG (StemCell Technologies) for 0, 12 and 24 hours, to drive and block BMP signaling, respectively. For each experiment, additional cultures treated with BMP4 or NOG were stained with Alcian blue (protocol described in Section 3.2.3) on day 4 post-seeding to confirm treatment efficacy. Alcian blue stains proteoglycans and other extracellular matrix components produced by mature chondrocytes. We confirmed the doses of 20ng/mL BMP4 and 100ng/mL NOG were sufficient to induce or inhibit differentiation (Appendix, Figure S4A).

3.2.3 Alcian Blue Staining

Cells were washed with PBS, fixed for 10 min with 4% paraformaldehyde, rinsed with PBS, followed by a wash with 0.2M HCl. Cells were stained with a 4:1 mixture of 0.2M HCl:0.5% Alcian blue solution (Alcian Blue 8 GX, BioShop; 0.5gr Alcian Blue powder in 95% ethanol) overnight and rinsed with 70% ethanol. Stained cultures were stored dry, but for imaging purposes, stained cells were placed in 70% ethanol. Images were taken on a Motic SMZ-168 light microscope with the Moticam 2300 digital camera (3.0M Pixel USB2.0).

3.2.4 Plasmids

The pCAGGS-SmadSD-IRES-H2B-RFP (constitutively active pSmad1) and pCAGGS-IRES-H2B-RFP plasmids were kindly gifted by Dr. E.Marti (Dréau et al., 2014); 7xBRE-Id3-Luciferase was a gift from Dr. Ken Cho (Javier et al. 2012). The 8 times repeat concatemer of the fly dad13 BMP-AE plasmid, BMP-AE8x-EGFP, and the Mad-binding site mutant version BMP-AE8x$^{\Delta mad}$ were generated in the Allan lab and published (Vuilleumier et al. 2018).

A custom destination vector (pGL3-Gateway-mpId3-eGFP; Appendix Figure S1) was created using a pGL3-Promoter luciferase reporter vector (Promega) as the backbone. A ccdB-Gateway cassette (Invitrogen) with attR recombination sites flanking a chloramphenicol-resistance gene was cloned upstream of the minimal SV40 promoter to enable easy transfer of enhancer fragments from the MCS-TOPO entry vector. The minimal SV40 promoter was replaced with the minimal Id3 promoter from the 7xBRE-Id3-Luciferase plasmid, and the Luciferase reporter gene was replaced with eGFP to allow easy visualization of reporter expression. As a positive control plasmid, we generated the pGL3-7xBRE-mpId3-eGFP vector with the 7xBRE enhancer placed in the custom destination vector, using the Gateway LR-Clonase exchange reaction. Finally, as a negative control, the minimal SV40 promoter from the pGL3-Basic luciferase reporter vector (Promega) was replaced with the minimal Id3 promoter and the luciferase reporter with eGFP.

3.2.5 Reporter Construction

A list of all primers used for the construction of the reporter lines can be found in Table 3.1. Genomic DNA extraction from CD1 mice E11.5 PLM cells (isolated as described above) was performed with a QIAamp DNA Mini kit (Qiagen) following the manufacturer`s protocols. To generate reporter constructs, approximately 1.5kb genomic DNA fragments (see Table 2.1) were PCR-amplified, verified for correct band size via agarose gel, prepped by restriction digest and ligated into the MCS-TOPO entry vector (Appendix, Figure S1). We used Acc65I and BglII restriction enzymes to digest the forward and reverse primers, respectfully, except for the Dlx2-SE reverse primer, where we used MfeI instead. Homemade electrocompetent *E.coli* were transformed with 1uL of the ligated entry vector with a BioRad MicroPulser Electroporator using standard protocols. Transformed cells were topped up to 500uL with SOC media and placed in a 37^{o}C shaking incubator for 1 hour. Cells were plated at a 1:50 or 1:5 dilution and incubated

overnight at 37ºC on spectinomycin-containing LB plates. Several colonies were picked and grown in 5mL spectinomycin-containing LB cultures at 37ºC overnight for colony screening. For the colony screen, 100uL of each culture was pelleted, lysed for 10min at 37ºC and run on an agarose gel. A comparison with an empty vector (~3kb) enabled us to identify colonies that contained the enhancer fragments (~4.5kb). Colonies with the correct size vector were mini-prepped, verified with a restriction digest and sent for sequencing (Genewiz; https://www.genewiz.com/). Following sequence verification, Gateway LR Clonase II reactions were performed to transfer the enhancer fragments to the pGL3-Gateway-mpId3-GFP destination vector, according to manufacturer's protocols. Electrocompetent *E.coli* were transformed as described above, plated at a 1:50 or 1:5 dilution and incubated overnight at 37ºC on ampicillin-containing LB plates. Colonies were picked, grown, screened for correct plasmid size, and used to inoculate 100mL cultures for midi-preps. Midi-prep samples were finally re-sequenced to verify that the correct enhancer fragment was intact in the destination vector.

Mutagenesis was performed by Q5® Site-Directed Mutagenesis Kit (New England Biolabs), using primers designed to introduce specific base pair substitutions to the Mad binding site (GCCGGC > tgatga), according to manufacturer`s protocols. Primers were designed using the NEBase Changer v1.2.8 tool and are summarized in Table3.1. Mutagenesis was performed using the MCS-TOPO plasmid, with subsequent cloning steps as described above. Verification of the mutations, however, was done only via sequencing (no size differences between WT and mutant enhancer).

Table 3.1: **Reporter Plasmid PCR and Q5 mutagenesis primers**

Name	***Primer Sequence (5`→ 3`)***	
PCR primers	*(mm10)*	*Genomic coordinates*
Dlx2-AE.SE	F: **ACTGATGGTACC**GAACGTGTCATCATCAGCCTAAAATGGGA R: **ACTGATAGATCT**GTGACCAGGTAACCACATTGGACAGTACA	chr2:71,628,376-71,630,508
Dlx2-SE	F: **ACTGATGGTACC**CACCTCTGACTTTCAGCGTCTCCTCTT R: **ACTGATCAATTG**CTTGAACTTGGAGCGTTTGTTCTGGA	chr2:71,531,303-71,532,305
Dlx2-AE	F: **ACTGATGGTACC**GGGTTGCCCAGCATTCCAAAGCAGCCA R: **ACTGATAGATCT**GGAGTGTGTGCTTTTTCCTTGGTGCCA	chr2:71,542,844-71,543,410
Msx2-SE	F: **ACTGATGGTACC**CAGAGAAGGCTGTAGACGGGCC R: **ACTGATAGATCT**TGAGCTCAGAGAGGTGCCATC	chr13:53,476,035-53,476,474
Jdp2-AE	F: **ACTGATGGTACC**GGATTTGTCTCACCTCCAGCCCACGAGA R: **ACTGATAGATCT**GCAGTCTGAAAAGAATCAGGCCCAGGGCT	chr12:85,548,072-85,549,296
Q5 mutagenesis primers		*Mutant BMP-CRE sequence*
Jdp2mut	F: TCCCAAGCAG**tgatga**CGCCAGTCAGTCTGGCCAGG R: GCTGCGCCACACTGGAGA	**tgatga**CGCCAGTCA

Bold capital letters indicate the restriction cut sites added to each PCR amplified fragment.

Bold lowercase letters indicate the BMP-CRE Mad-binding site mutations.

3.2.6 PLM Cell Transfections

Cells were transfected as previously described (Weston et al., 2002). Briefly, PLM cells were harvested and resuspended at a density of ~2x10^7 cells/mL, as described above. For transfection purposes, cells were mixed with a DNA/FuGene6 (Promega) mixture in a 2:1 ratio. FuGene6-DNA mixtures were prepared according to the manufacturer`s instructions. Cells were seeded as ~2x10^5 cells/micromass droplet into 24-well plates. Following a 1 hour incubation in a humidified 37^{o}C incubator, cells were supplemented with media containing BMP4 or Noggin (same concentrations as above). The media was replaced every 24 hours. Cells were monitored for reporter expression with the IncuCyte ZOOM™ software until Day4 post-seeding when cells were fixed and stained with Alcian Blue to confirm chondrogenic differentiation (treatment efficacy).

3.2.7 Poly-A RNA-seq

RNA from PLM cultures was used for poly-A (enriched for mRNA) RNA-seq to identify differentially expressed genes upon BMP4 and NOG exposure. This experiment was repeated for

3 biological replicates. To collect enough total RNA from PLM cells for RNA-seq, 9 x ~2 x 10^5 cells/micromass droplet were seeded per well in 12-well plates, resulting in ~1.8 x 10^6 cells/sample. Wells were rinsed twice with sterile PBS, homogenized in TRIzol (Invitrogen) by pipetting and vortex, incubated at room temperature (RT) for 5min and stored at -80^{o}C until they could be further processed. Total RNA isolation was carried out using a TRizol/RNAeasy kit (Qiagen) hybrid protocol. Briefly, 0.2mL Chloroform (Sigma) per 1mL TRIzol was added to samples, followed by vigorous shaking and a 3min RT incubation. Samples were centrifuged at 13,000 rpm for 15min at 4^{o}C to allow for phase separation. The upper aqueous phase (containing the RNA) was collected and mixed with an equal volume of 100% EtOH. Samples were then transferred to RNAeasy spin columns. Subsequent steps were performed as per the RNAeasy kit "RNA Isolation from Animal Cells using Spin technology" protocol by Qiagen. Quality control (QC) and sample integrity were validated via 18s and 28s ribosomal RNA fragment sizes using the Agilent 2100 Bioanalyzer (Agilent Technologies). High quality samples were reverse transcribed to cDNA with the High Capacity cDNA Reverse Transcription Kit (Applied Biosystems) according to manufacturer's specifications using the Eppendorf MasterCycler EP Gradient S Thermal Cycler. Real time PCR (qPCR) was performed to confirm that cultured cells responded as expected to the BMP4 or NOG treatments (description below). PolyA-RNA-seq sequencing libraries were prepared for select, high quality samples using standard Illumina protocols. Sequencing was performed on the Illumina NextSeq500 using a NextSeq 75cycle High Output v2 kit sequencing at 42x42 Paired End.

3.2.8 qPCR Validation

Quantitative real time PCR was performed on a 7900HT Fast Real-Time PCR system (Applied Biosystems) using validated IDT (Integrated DNA Technologies) primer sets for Sox9

(Mm.PT.58.42739087), Acan (Mm.PT.58.10174685), Nog (Mm.PT.58.30936710.g), Aldh1a2 (Mm.PT.58.12196815) and Tbp1 (Mm.PT.39a.22214839), and the TaqMan Fast Universal PCR master mix kit (Applied Biosystems). PCR consisted of one cycle at 95°C for 20 seconds followed by 40 cycles at 95°C for 1 second and 60°C for 20 seconds, as per the manufacturer's instructions. Tbp1 was used as a reference to normalize gene expression across samples. Standard curves were generated using serial dilutions of pooled control samples. Gene expression levels were quantified using the absolute quantification-standard curve method.

3.2.9 RNA-seq Data Analysis

Multiple analysis RNA-seq pipelines have been applied and their results combined. Briefly, for the alignment stage, we used both STAR (Dobin et al. 2013) and HISAT2 (Pertea et al., 2016), as well as the pseudo-aligners kallisto (Bray et al., 2016) and Salmon (Patro et al., 2017). Quantification was performed directly with STAR, kallisto, and Salmon or with RSEM (Li and Dewey, 2011) and StringTie (Pertea et al. 2016) for the pipelines producing real alignments. RNA-

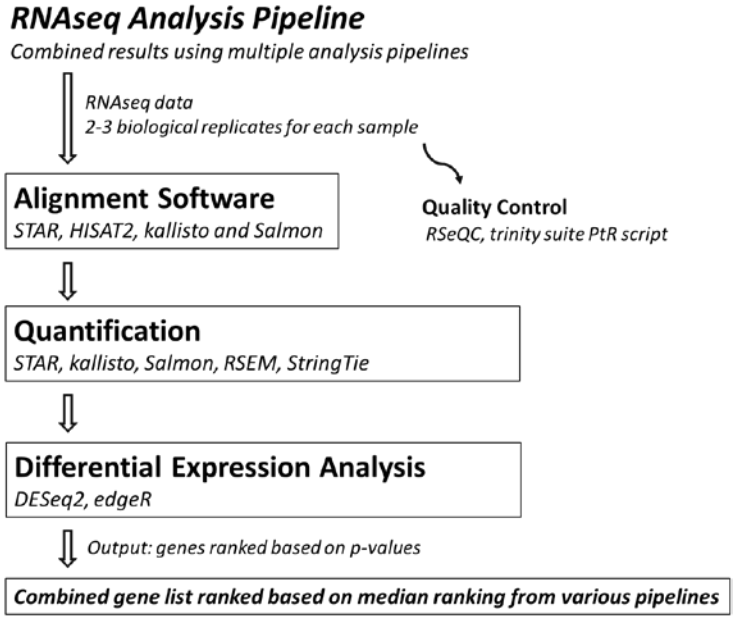

Figure 3.2: ***RNA-seq Analysis Pipeline***

seq reads were mapped/aligned against the mouse reference genome (GRCm38.p5, http://www.ensembl.org). In-house Perl scripts were used to sum the read counts at the transcript level for each gene and create matrices comprising the read counts for all the genes in each sample. Differential expression analysis was then performed using the R package DESeq2 (Love et al., 2014) and edgeR (Robinson et al., 2010). Each sample was assessed using the quality-control software RSeQC (Wang et al., 2012) and the PtR script from the trinity suite (Grabherr et al. 2011). The output for each pipeline is a list of genes ranked by the p-value for differential expression after correction for multiple testing. A combined list was obtained by ranking the genes according to their median rank from the various analysis pipelines. Genes with a differential expression not going in a consistent direction between pipelines were eliminated from that combined list.

3.2.10 Gene Ontology Term Analysis

Gene Ontology (GO) Enrichment Analysis PANTHER (Protein ANalysis THrough Evolutionary Relationships) Version 14.1 (http://pantherdb.org/; Thomas et al. 2006; Mi et al. 2019) and STRING (Search Tool for the Retrieval of Interacting Genes/Proteins) Version 11 database (https://string-db.org/; Szklarczyk et al., 2019) were used to perform gene annotations and overrepresentation (enrichment) analysis for the differentially expressed genes (DEGs) from our RNA-seq experiment. In PANTHER we used the default statistical settings (Fisher`s Exact test to calculate the p-value and False Discovery Rate (FDR) $p<0.05$) and the whole mouse transcriptome (22296 genes) as the reference list. The Gene Ontology database browsing tool AmiGO 2 version: 2.5.12 was also used to verify GO terms associated with certain genes (http://amigo.geneontology.org/amigo; Carbon et al., 2009).

3.2.11 Histone Modification ChIP-seq

Histone modification ChIP-seq was used to identify chromatin marks associated with the state of enhancer and promoter activity. PLM cell samples for histone modification ChIP-seq were prepared, as described (Lorzadeh et al. 2016). Each sample was split into tubes, one to be used for pellet cell number quantification and one to carry out the ChIP-seq protocol. One biological replicate of this experiment was carried out. Briefly, cells were lysed in mild non-ionic detergents (0.1% Triton X-100 and Deoxycholate) and protease inhibitor cocktail (Calbiochem) in order to preserve the integrity of histones harboring epitopes of interest during cell lysis. Cells were pelleted, flash-frozen and stored at -80^{o}C. Frozen cell pellets were cross-linked by 1% formaldehyde and lysed, following chromatin shearing. Chromatin fragments were incubated with protein G and A Sepharose beads (GE Healthcare) to eliminate non-specific binding. Unbound chromatin fragments were incubated with beads and validated antibodies against the following histone markers: H3K4me1 (Diagenode: Catalogue#pAb-037-050, lot#A1657D), H3K4me3 (Cell Signaling Technology: Catalogue#9751S, lot#8), H3K27me3 (Diagenode: Catalogue#pAb-069-050, lot#A1811-001P), H3K27ac (CMA309 monoclonal antibody, (Kimura et al. 2008)). DNA fragments were then stripped from histones, purified using the QIAquick PCR Purification Kit (Qiagen) and subjected to Illumina library construction by end repair, 3′ A-addition, and Illumina sequencing adaptor ligation. Libraries were PCR amplified and sequenced on Illumina HiSeq 2500 sequencing platforms, with paired-end 75bp, following the manufacturer`s protocols. We conducted one biological replicate of this experiment.

3.2.12 ChIP-seq Data Analysis

ChIP-seq sequence reads were aligned to the mouse reference genome (GRCm38.p5) using Burrows-Wheeler Aligner (BWA; Li and Durbin, 2009). Peak calling and differential peak

comparisons were performed with MACS2 (Model-based Analysis for ChIP-seq) version 2.1.2 (Zhang et al., 2008). Plots for histone mark distributions around TSS`s were made with deepTools2 (Ramirez et al. 2016). Annotation of histone modification markers at promoter sites, as well as of active and repressed regulatory regions, against the list of differentially expressed genes (RNA-seq data) was performed using custom scripts. Data were visualized with the IGV genome browser (Robinson et al., 2011).

3.2.13 Graphs

Graphs were made using GraphPad Prism Version 8.0.1 (GraphPad Software, San Diego, CA) and R packages. The heatmap for Appendix Figure S7 was made with the web tool ClustVis (https://biit.cs.ut.ee/clustvis_large/; (Metsalu and Vilo 2015)).

3.2.14 Bioinformatic Detection of BMP-CREs

The Perl script scanMotifGenomeWide.pl from the HOMER v4.10 software suite (Heinz et al. 2011) was used to scan the reference mm10 mouse genome for the BMP-AE (GGCGCCN$_5$GNCV), BMP-SE (GRCGNCN$_5$GNCT) and BMP-AE2 (GGCGCCN$_5$GTAT) motifs. Base-specific PhastCons scores (Siepel et al., 2005; 60-vertebrate conservation) were obtained from the UCSC genome browser (https://genome.ucsc.edu/) to annotate each motif instance with evolutionary conservation scores. Using a custom Python script, each motif was annotated with the average PhastCons score across all bases of the motif instance. Motifs with an average PhastCons conservation score above 0.7 across placental mammals were kept for the correlation analysis with the RNA-seq results.

3.3 Results

3.3.1 Differential Gene Expression During BMP4-Driven Chondrogenesis

We performed polyA-RNA-seq assays on primary limb mesenchymal (PLM) micromass cultures prepared from murine E11.5 forelimbs and hindlimbs, treated with BMP4, NOG or vehicle control and harvested at 0hrs, 12hrs, and 24hrs post-seeding, in order to identify changes in gene expression during early chondrogenesis. We used BMP4 to induce chondrogenesis and NOG (a potent inhibitor of BMP signaling) to block chondrogenesis. Genes with enhanced and opposite responses to these treatments are likely to be direct BMP targets, especially if there are induced as early as 12hrs post treatment.

Before sequencing, we decided to test the quality and proper induction of our samples by qPCR. We looked at the RNA expression of a number of key chondrogenic markers (*Sox9, Acan*), Noggin (as it is upregulated during chondrogenesis to oppose BMPs), as well as genes that respond to NOG treatment (*Aldh1a2* – part of the retinoid signaling pathway that opposes chondrogenesis). Results from our qPCRs are summarized in Figure 3.3. As expected, *Sox9* is already expressed at relatively high levels by ~E11.5 during the development of the limb bud. BMP4 progressively increases Sox9 expression, while Noggin has the opposite effect. Furthermore, BMP4 upregulates the expression of Noggin and *Acan* at 12hrs and 24hrs compared to controls, while NOG downregulates them. Finally, *Aldh1a2* has the opposite response, BMP4 abolishes expression, while NOG increases it over time. Alcian blue stain of Day 4 cultures from these experiments further verifies that the treatments successfully induced or blocked chondrogenesis (Appendix, Figure S4-B).

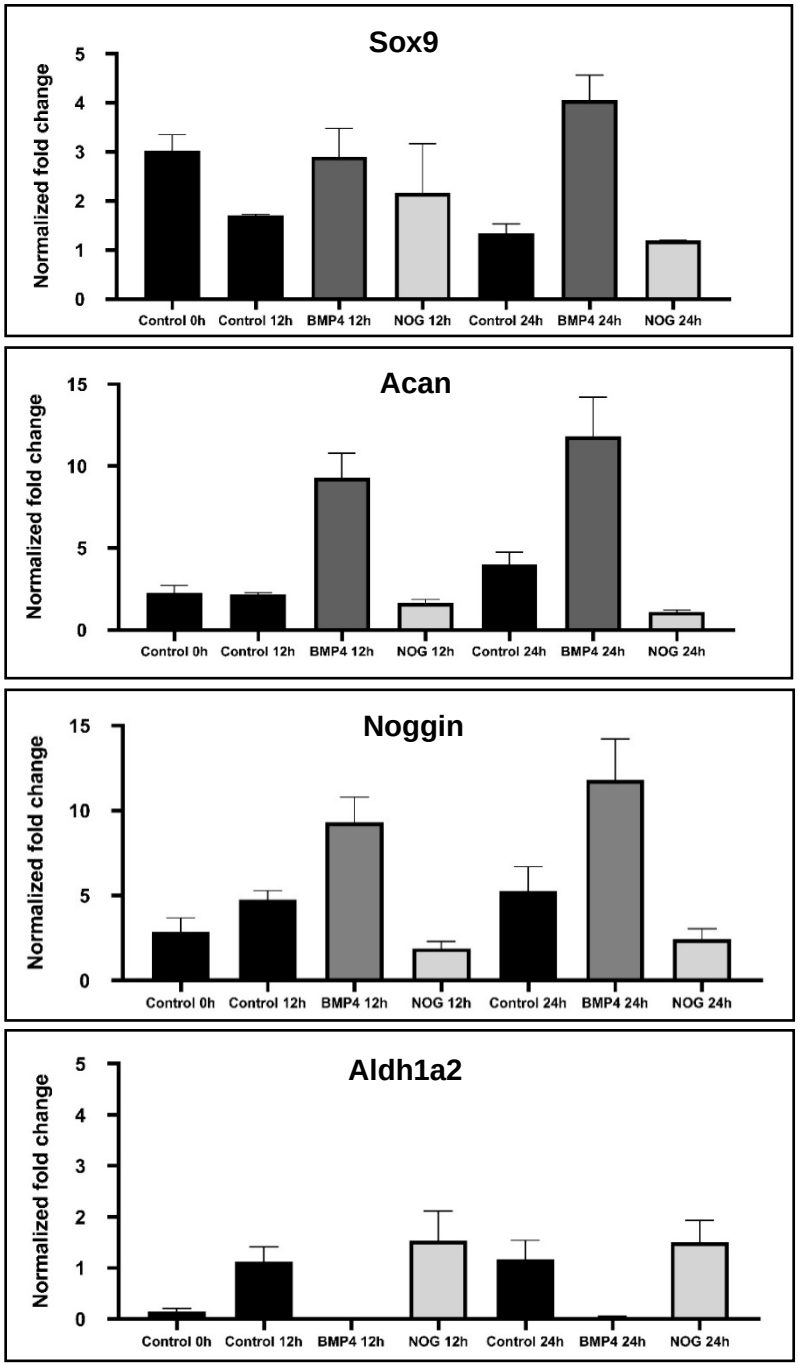

Figure 3.3: ***Key chondrogenic genes respond to our treatments as expected, based on previously published work.*** Each graph represents the average of 2 biological replicates per sample and treatment (each biological replicate value is the average of 2 technical replicates). All samples are normalized to the reference gene.

3.3.1.1 Identification of Differentially Expressed Genes Between BMP4, NOG and Control Treatments

Prior to downstream analysis and data interpretation, we performed quality assessment steps, including coverage uniformity plots and sample matrix correlation plots that verified our sample quality (Appendix, Figures S5 and S6).

Utilizing multiple analysis pipelines, we generated a combined gene list based on the median ranking across all the pipelines used, increasing our confidence in the 'differentially expressed genes' (DEGs) in our samples (Figure 3.2).

Comparing our samples at the 12-hour and 24-hour time points with the 0h Control, we find significant numbers of genes that are differentially expressed (Figure3.3-A,B). The largest change is observed in the BMP4-treated samples both at 12hours and 24hours compared to the equivalent Control and NOG-treated samples. Based on our RNA-seq DEG expression levels and previously published data (Karamboulas et al., 2010) it is likely that the cells in our culture system at 24-hours are proliferating chondrocytes.

We also identified many genes that are differentially regulated at 12-hours and 24-hours post-treatment when comparing BMP4 and NOG samples against the 0h Control (Figure 3.4-C). The most highly differentially regulated genes at 24-hours were mainly extracellular matrix related genes, transcription factors/cofactors, signaling proteins and growth factors/cytokines (heatmap plot, Appendix Figure S7).

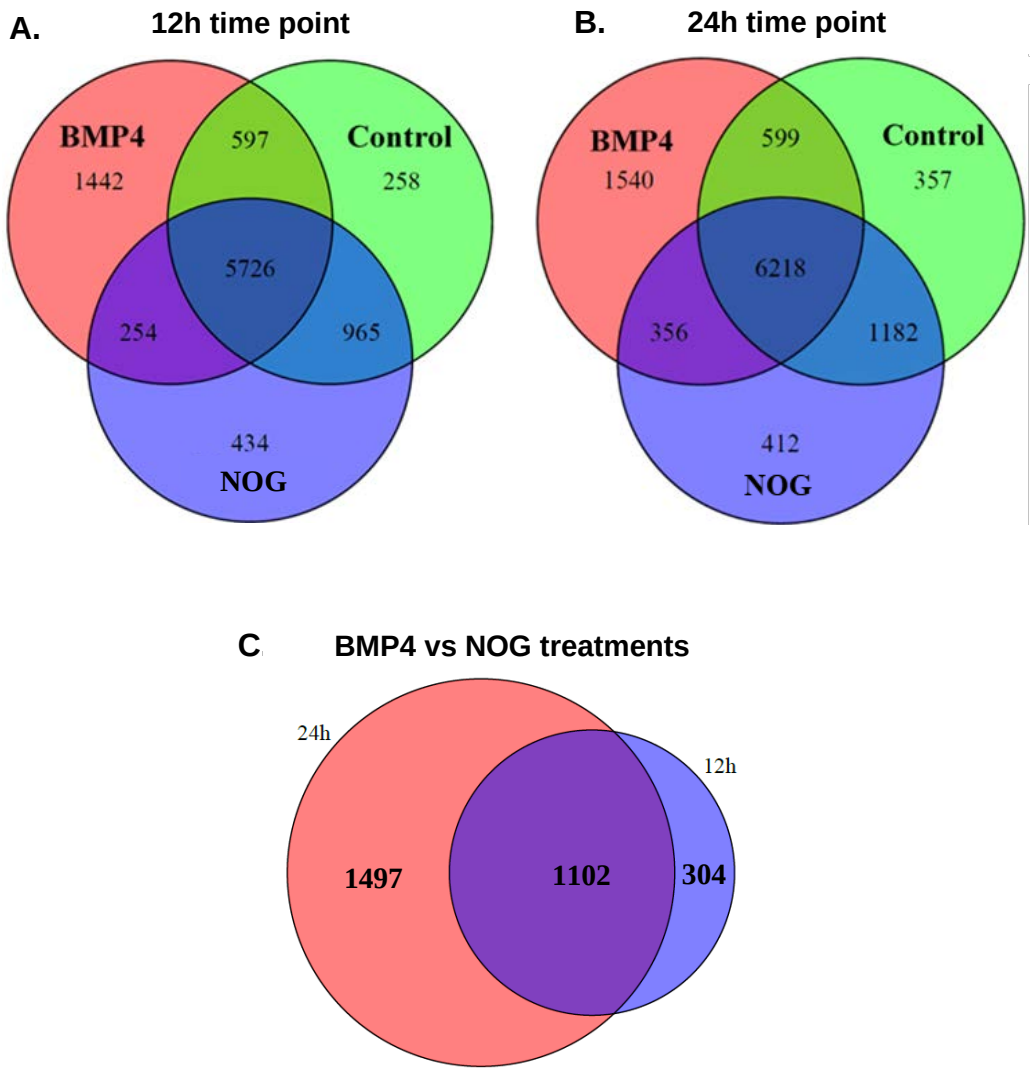

Figure 3.4: ***Venn diagrams representing the number and overlap of differentially expressed genes with different treatments and at different time points.***

3.3.1.2 Gene Ontology Terms used to Identify Genes Regulated via BMP-Signaling

To elucidate the regulatory network proteins involved in early chondrogenesis and determine the contribution of BMP signaling to this process, we decided to focus on genes that were differentially expressed between BMP4 or NOG treatments at 12-hours and 24-hours. Specifically, we were interested in genes that had an opposite response to BMP4 and NOG treatments (i.e. BMP4 induces, but NOG reduces gene expression), as we postulated that they were likely to be directly regulated by BMP signaling.

To achieve this, we generated "strict" lists of genes for both BMP4 and NOG (Figure 3.5). For instance, the BMP4 list included DEGs at 24-hours post-treatment compared to Control at 0 hours and excluded DEGs present in the 24-hours Control or NOG treatment, unless they responded differently in the BMP4-treated samples. The list was separated into upregulated and downregulated DEGs. A similar process was followed to generate the NOG lists. We did not repeat the process for the 12-hour DEGs since most of the genes that this workflow would capture were already included in our 24-hour list analyses.

The workflow generated 4 lists of genes: 1) BMP4-upregulated (total 417 genes; Appendix Table S2), 2) BMP4-downregulated (total 319 genes; Appendix Table S3), 3) NOG-upregulated (total 77 genes; Appendix Table S4), and 4) NOG-downregulated (total 93 genes; Appendix Table S5).

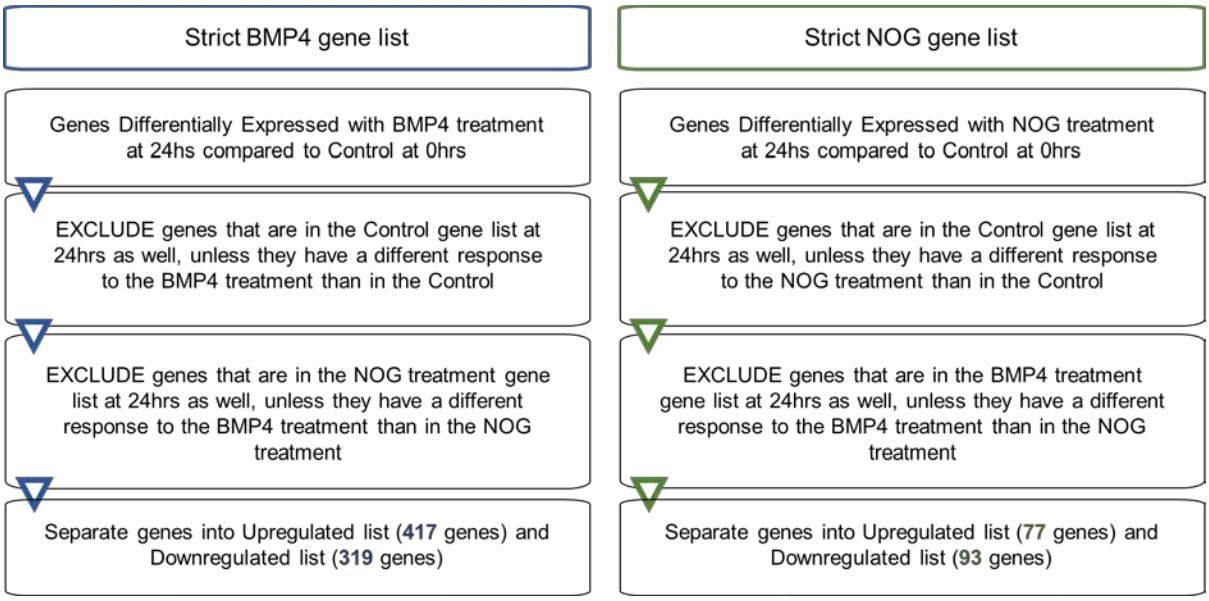

Figure 3.5: ***Workflow for generating the "strict" gene lists from the RNA-seq results.***

We used the PANTHER and STRING databases to conduct functional profiling and enrichment analysis of genes within each of the 4 "strict" lists, and identified genes already annotated as chondrogenic. We selected PANTHER for our analyses, as it integrated into the GO curation process (updated monthly) and is the most reliable GO term database (Mi et al. 2019). We selected STRING to confirm data gathered from PANTHER, as it is a widely used, well-maintained and regularly updated database and contains information from several sources, including experimental data, computational prediction methods and public text collections (Szklarczyk et al. 2019). Although less reliable, the text-mining feature of STRING makes it possible to obtain more up-to-date information.

First, we looked for enrichment of chondrogenic and osteogenic-related GO terms with the PANTHER Annotation Data Set "Biological Process Complete". This allowed us to identify genes

previously known to have a role in chondrogenesis or osteogenesis, enabling their exclusion from downstream analyses and helped establish novel chondrogenic genes.

Within the BMP4-upregulated list, we identified a total of 71 previously annotated chondrogenic/osteogenic genes (GO term list is summarized in Figure 3.6). These results were confirmed by searching for "Biological Process" chondrogenic and osteogenic-related GO terms in STRING, which yielded a ~99% overlap between the two tools. We then looked at the "Molecular Function Complete" GO terms of these 71 genes and found that 24/71 (34%) were enriched with TF function, transcription regulation and cofactor function terms (Figure 3.6). This could either mean that many transcription factors/cofactors are involved in the initial stages of chondrogenesis or, more likely, that most studies focus on chondrogenic TFs/cofactors, resulting in an overestimation of the number of such genes being annotated with GO terms.

We then wished to identify new TFs/cofactors important in chondrogenesis, among the remaining 316 genes without any chondrogenic/osteogenic GO annotations (Figure 3.6). Using the "Molecular Functions Complete" annotations we identified 31 potentially new TFs/cofactors that may have a role in early chondrogenesis. Literature review confirmed that 13/31 (42%) of these TFs/cofactors were previously shown to have important roles during chondrogenesis such as functioning as SOX9 transcriptional coactivators, regulating the expression of RUNX2 and SOX9 TFs, and regulating cartilage ECM genes such as *Col2a1* and *Mmp-13* (Table 3.2). Additionally, 6 of the remaining 18 TFs/cofactors (*Rorc*, *Nr4a3*, *Grhl1*, *Isl2*, *Pouf3f3*, and *Cux2*) displayed a ≥1.5-fold increase in RNA levels by 24hrs (BMP4 vs NOG sample comparison), and this may indicate a likely role in the chondrogenic pathway.

Following the same workflow for the BMP4-downregulated list, we identified a total of 20 previously annotated chondrogenic/osteogenic genes, of which 7 were TFs/cofactors (Figure 3.6). From the remaining 286 genes without any chondrogenic/osteogenic GO annotations, we identified 29 TFs/cofactors (Table 3.3). Literature review revealed only 4/29 (14%) to have been previously studied in chondrogenesis. Of the remaining 25 genes, 4 (*Hic1*, *Ebf2*, *Ebf3*, and *Scrt1*) displayed a ≥1.5-fold decrease in RNA levels by 24hrs, suggesting that their downregulation is important in the chondrogenic process.

A similar analysis was performed with the NOG-upregulated and NOG-downregulated gene lists (Figure 3.7; Table 3.4). For the NOG-upregulated list, we identified a total of 7 previously annotated chondrogenic/osteogenic genes, of which 2 were TFs/cofactors (*Gsc* and *Cebpa*). From the remaining 33 non-signaling genes without a chondrogenic/osteogenic GO annotation, we identified 7/33 TFs/cofactors, one of which (*Nfkbia*) has been previously implicated in chondrogenesis (Table 3.3). Likewise, for the NOG-downregulated list, we identified a total of 16 previously annotated chondrogenic/osteogenic genes, of which 6 were TFs/cofactors (*Runx3*, *Msx2*, *Id4*, *Hey1*, *Gli1*, and *Maf*). From the remaining 49 genes without a chondrogenic/osteogenic GO annotation, we identified 8 TFs/cofactors, and once again, two of these (*Dlx3*, *Gata2*) have been previously linked to chondrogenesis. The remaining newly identified genes may potentially be involved in the chondrogenic pathway and warrant further investigations.

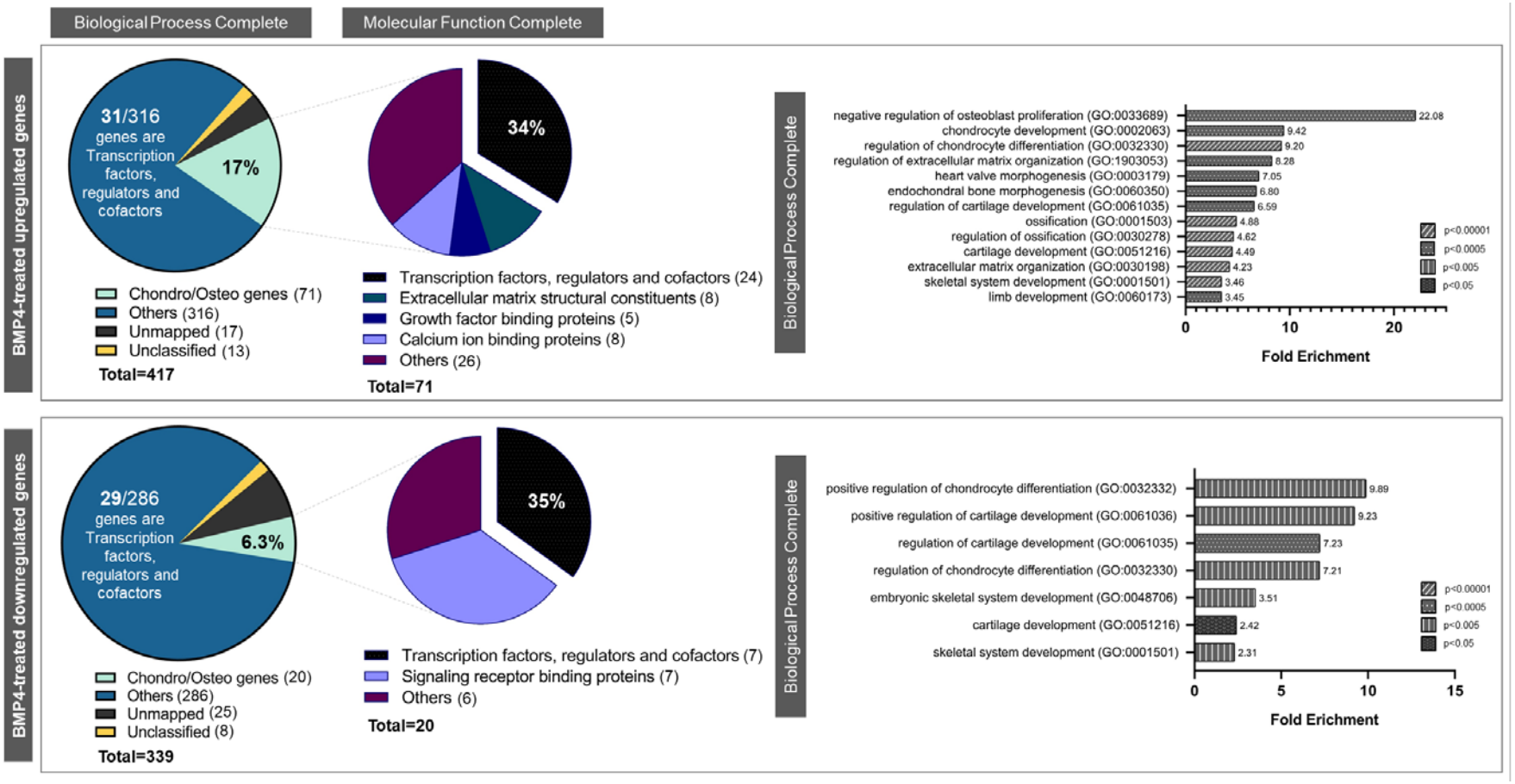

Figure 3.6: ***Gene Ontology Term analysis of genes from the BMP4-treated list of differentially regulated genes identifies several potentially uncharacterized transcription factors and cofactors that may be involved in chondrogenesis.***

Table 3.2: **Transcription Factors and Cofactors with no chondrogenic GO annotations, upregulated with BMP4 treatment.**

TFs/cofactors with no chondrogenic GO annotations	RNA-seq (log2FoldChange)	Manual literature search associations with chondrogenesis/osteogenesis
Sox10	6.26	(Chimal-Monroy et al. 2003)
Rorc	3.28	-
Nr4a3	3.18	[1]
Dlx3	2.67	(Hassan et al. 2006)
Klf4	2.21	(Gurusinghe et al. 2019)
Grhl1	2.07	[2]
Ppargc1a (aka PGC1A)	2.06	(Kawakami et al. 2005)
Isl2	2	[3]
Pou3f3	2	[4]
Plagl1 (aka *Zac1*)	1.69	(Tsuda et al. 2004)
Cux2	1.65	[5]
Prickle1	1.52	(Yang et al., 2013)
Nupr1	1.42	(Yammani and Loeser, 2014)
Nacc2	1.37	[6]
Ebf4	1.36	[7]
Vgll2	1.33	[8]
Klf15	1.32	(Song et al., 2017)
Ets2	1.03	[9]
Pir	0.97	-
Sox13	0.8	(Wang et al., 2006)
Tox2	0.8	-
Bsn	0.79	-
Ssbp2	0.74	-
Wipi1	0.68	-
Ezh1	0.67	(Lui et al. 2016)
Optn	0.66	[10]
Litaf	0.54	-
Klf3	0.42	-
Atf6	0.4	(Guo et al., 2016)
Atf4	0.39	(Wang et al., 2009)
Nfe2l1	0.36	(Kim et al., 2010)

[1] *Nr4a3* may have a role in the inflammatory-related loss of cartilage/bone in human joint disease (Marzaioli et al. 2012). A conference abstract indicated that NR4A3 may be involved in the regulation of *Mmp-13* and *Adamts-5* expression (Angerer et al. 2012).

[2] No direct association of *Grhl1* with chondrogenesis, but GRHL3 was shown to act upstream of SP7 (OSX1) in a BMP-dependent manner, to regulate osteoblast formation (Salazar et al., 2016).

[3] Tzchori et al., noted the presence of Islet2 during limb bud patterning (Tzchori et al. 2009), but no association with chondrogenesis specifically.

[4] No direct association with chondrogenesis but implicated in craniofacial development and the formation of some of the maxillary arch-derived skeleton (Jeong et al. 2008).

[5] No direct association with chondrogenesis, but a recent publication showed that *Cux2* is involved in the specification of the limb forming fields by regulating the Hoxb TF and retinoic acid synthesis (Ueda et al. 2019).

[6] No direct association with chondrogenesis, but its paralog *Nacc1* has been implicated in chondrocyte migration and differentiation (Yap et al. 2013).

[7] No direct association with chondrogenesis, but its paralog (*Ebf1*) has been shown to have a crucial role in promoting the differentiation of MSCs into adipocytes and osteocytes (Almalki and Agrawal, 2016).

[8] *Vgll2a* (zebrafish ortholog of Vgll2) was shown to be required for craniofacial development and pharyngeal cartilage development in zebrafish (Johnson et al. 2011).

[9] *Ets2* is known to be expressed in the developing cartilage, but it has been studied more in the context of osteogenesis (Raouf and Seth, 2000). We do not know if it has any other chondrogenesis specific functions.

[10] No direct association with chondrogenesis; however, mutations in *Optn* have been associated with Paget`s disease of bone (PDB), the second most frequent metabolic bone disorder (Silva et al., 2018).

Table 3.3: **Transcription Factors and Cofactors with no chondrogenic GO annotations, downregulated with BMP4 treatment.**

TFs/cofactors with no chondrogenic GO annotations	RNA-seq (log2FoldChange)	Manual literature search associations with chondrogenesis/osteogenesis
Hic1	-5.64	[1]
Scrt1	-2.38	-
Ebf2	-2.05	-
Ebf3	-1.65	-
Glis3	-1.56	(Beak et al., 2007)
Dio3	-1.35	[2]
Etv4	-1.26	-
Prkcb	-1.22	-
Pls1	-0.94	-
Hdac7	-0.92	(Bradley et al., 2015)
Jazf1	-0.75	-
H2afy	-0.71	-
Zcchc12	-0.67	-
Id3	-0.66	(Asp et al., 1998)
Nrip1	-0.62	-
Wwc1	-0.61	-
Etv6	-0.52	-
Zfp90	-0.51	-
Sox12	-0.5	[3]
Zfp395	-0.48	-
Pmf1	-0.47	-
Tead3	-0.46	-
Phf6	-0.45	-
Ncoa3	-0.43	(Zhang et al., 2018)
Ybx3	-0.43	-
Pttg1	-0.39	-
Kpna2	-0.35	-
Stip1	-0.27	-
Tcf20	-0.26	-

[1] No direct association with chondrogenesis. HIC1 attenuates Wnt signaling (Valenta et al., 2006), which is an important pathway in chondrogenesis.

[2] No direct association with chondrogenesis; however, *Dio2* is upregulated in osteoarthritic cartilage (compared to normal cartilage) and there is speculation on *Dio3* having a role in chondrogenesis (Reynard and Loughlin, 2013).

[3] No direct association with chondrogenesis or osteogenesis; however, *Sox12* belongs to the SoxC family along with *Sox4* and *Sox11*. SOX11 was shown to positively regulate osteogenesis (Gadi et al. 2013).

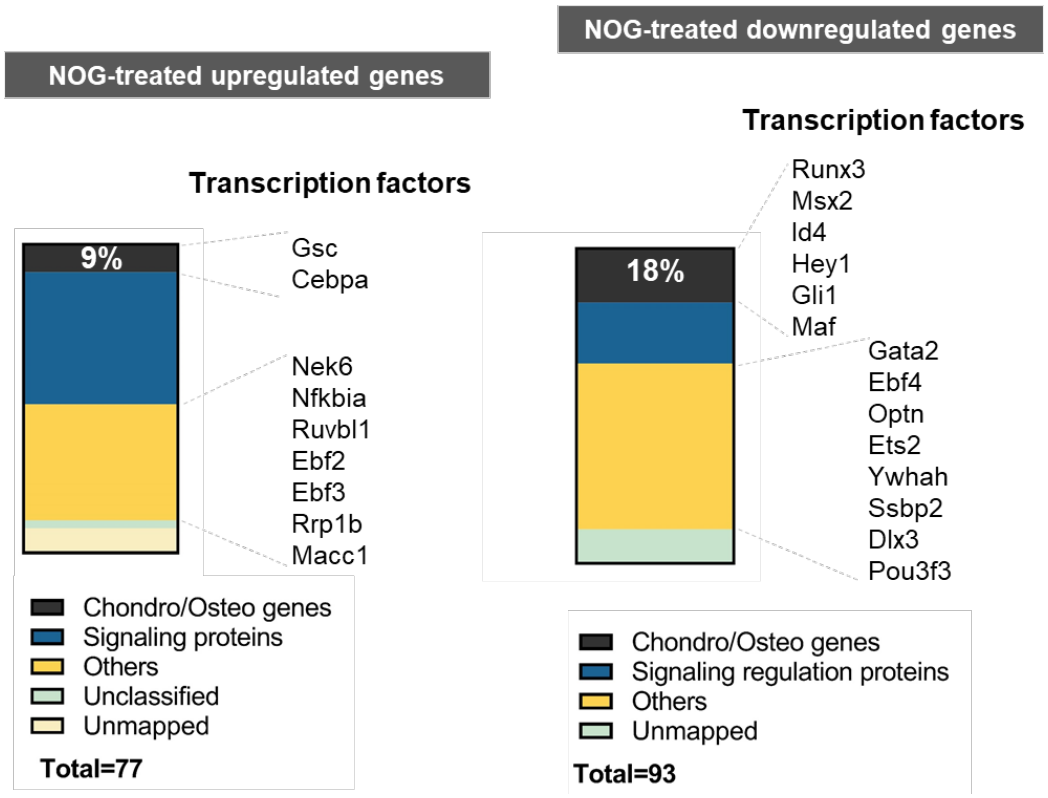

Figure 3.7: ***Gene Ontology Term analysis of genes from the NOG-treated list of differentially regulated genes identifies several potentially uncharacterized transcription factors and cofactors that may be involved in chondrogenesis.***

Table 3.4: **Transcription Factors and Cofactors with no chondrogenic GO annotations, upregulated or downregulated with NOG treatment**
*excludes genes that were captured by the BMP4 lists above

TFs/cofactors with no chondrogenic GO annotations	RNA-seq (log2FoldChange)	Manual literature search associations with chondrogenesis/osteogenesis
Upregulated with NOG	*Downregulated with BMP4*	
Macc1	-1.27	-
Nfkbia	-0.57	(Dehne et al. 2010)
Nek6	-0.4	-
Rrp1b	-0.33	-
Ruvbl1	-0.33	-
Downregulated with NOG	*Upregulated with BMP4*	
Gata2	0.72	[1] (Karamboulas, et al. 2010)
Ywhah	0.36	-

[1] In mesenchymal cells, GATA2 blocks adipogenesis (Tong et al. 2000; Tong et al. 2005; Kamata et al. 2014). According to (Tolkachov et al. 2018) GATA2 also affects bone turnover and inhibits osteoblastogenesis of MSCs by blocking SMAD1/5/8 signaling.

3.3.1.3 Gene Ontology Terms used to Identify Chondrogenic Regulatory Proteins

Our "strict" lists aimed to identify genes most likely to be directly regulated by BMP signaling. However, a host of other genes that could also be involved in chondrogenesis were excluded from our previous analysis. Here, we aimed to characterize the other important chondrogenic-regulatory genes in order to create a comprehensive list of all genes expressed during the early stages of chondrogenesis.

Genes differentially regulated with BMP4 and NOG treatments were separated into 3 lists based on their expression time-points: a) "12-hours only", b) "24-hours only" DEGs, c) "Overlap" DEGs between 12 and 24-hours. For each of these lists, we performed functional profiling and enrichment analysis with the PANTHER and STRING software, as described in Section 3.3.1.3. As before, we looked for enrichment of chondrogenic and osteogenic-related GO terms using the "Biological Process Complete" and then the "Molecular Function Complete" functions to identify the TFs/regulators/cofactors (Figure 3.8). In all 3 lists, the Molecular Function GO terms "Transcription factor binding", "Transcription regulator activity", "Extracellular matrix structural constituents" and "Signaling receptor binding" were significantly enriched, an expected result, since many transcription factors as well as signaling and ECM components are required to initiate most cellular differentiation programs, including chondrogenesis.

Within the "12-hours only" list we identified 24 chondrogenic/osteogenic annotated genes out of which 7 were annotated with GO terms relating to transcription factor function, transcription regulation, and cofactor functions. Genes identified in this set may be necessary only for a short period during the chondrogenic process since they were not detected as DEGs in the 24hrs post-treatment samples.

From the list of 254 genes without known roles in chondrogenesis/osteogenesis, we identified 25 potentially new TFs/cofactors that may be involved in the early stages of chondrogenesis (Table 3.5). An extensive literature review revealed that 8/25 of these TFs/cofactors have been previously studied in chondrogenesis. The remaining 17 TFs/cofactors could be pursued further to understand their potential contributions to chondrogenic lineage commitment and differentiation.

Within the "24-hours only" list we identified 145 chondrogenic or osteogenic annotated genes out of which 62 (43%) were annotated with TFs/cofactors GO terms. From the remaining 1234 genes without chondrogenic/osteogenic annotations, we identified 92 potentially new TFs/cofactors that may have a role during chondrogenesis. A subset of these genes is listed in Table 3.6. This includes 32 genes with a ≥0.55-fold increase in RNA levels, out of which 10 have been previously associated with chondrogenesis. From the remaining 22 TFs/cofactors, 7 display ≥|1.0-fold increase| in RNA levels (*Ddn*, *Dmrta1*, *Nfe2l3*, *Lpin3*, *Myrf*, *Klf14*, and *Nr2f1*) and could be pursued in the future to understand their potential contributions to the pre-hypertrophic/hypertrophic stages of chondrocyte development.

Finally, within the "Overlap" list we identified 187 chondrogenic or osteogenic annotated genes out of which 88 (47%) were annotated with TFs/cofactors GO terms. From the remaining 840 genes without chondrogenic/osteogenic annotations, we identified 97 potentially new TFs/cofactors that may have important roles during chondrogenesis since they exhibited sustained upregulation/downregulation in both tested time points. A subset of these genes was listed in Table 3.7. This includes 32 genes with a ≥1.0-fold increase in RNA levels, out of which 15 have been previously linked to chondrogenesis. The remaining 17 TFs/cofactors (*Hr*, *Dusp26*, *Rbpjl*, *Jdp2*,

Klf2, *Ss18l2*, *Nr4a1*, *Fam129b*, *Isl1*, *Nr6a1*, *Smarca2*, *Esrrg*, *Mdfic*, *Eya2*, *Esrrb*, *Pdlim1* and *Ikzf3*), are identified as highly differentially expressed genes that are maintained upregulated/downregulated over at least 12-hours, which makes them likely to have important roles in chondrogenesis that need to be studied in the future.

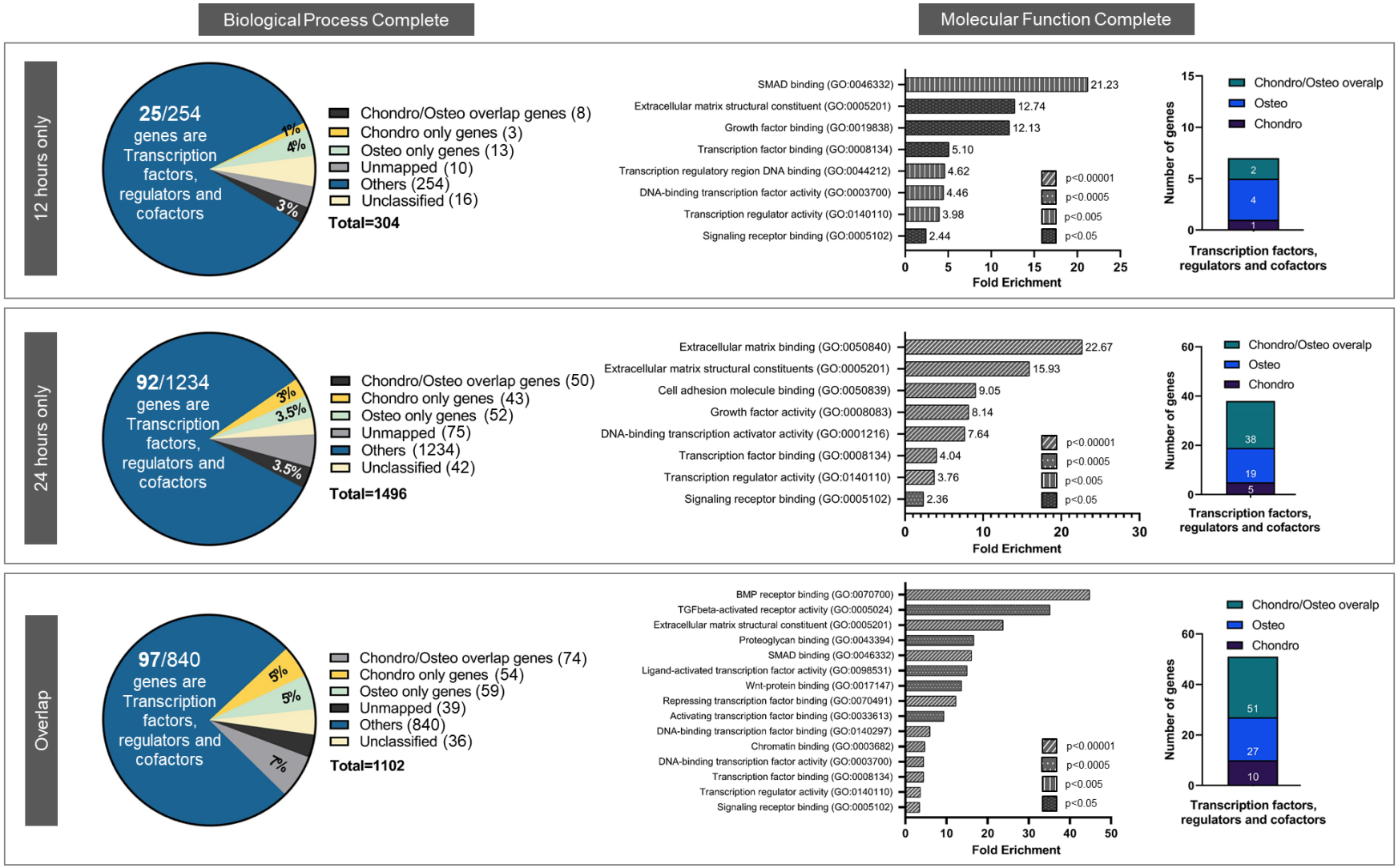

Figure 3.8: ***Gene Ontology Term analysis of genes separated into 3 lists based on their expression time (only at 12hrs, only at 24hrs or at both 12hrs and 24hrs) identifies several potentially uncharacterized transcription factors and cofactors that may be involved in chondrogenesis.***

Table 3.5: **Transcription Factors and Cofactors with no chondrogenic GO annotations, differentially expressed only at 12hrs**

TFs/cofactors with no chondrogenic GO annotations	Manual literature search associations with chondrogenesis/osteogenesis
Actn2	(James et al. 2005)
Bcl6	[1]
Bhlhe40 (aka DEC1)	(Shen et al. 1997)
Cbfa2t3	-
Crym	-
Dact2	(Sensiate et al. 2014)
E2f2	(Yanagino et al. 2009)
Egr3	[2]
Glis2	-
Hdac11	[3]
Hmga1	[4]
Hmga2	[5]
Klf12	[6]
Plscr1	-
Pou2f2	-
Prmt5	(Norrie et al. 2016)
Rxrg	-
Sik1	-
Sim2	(Qiryaqoz et al. 2019)
Smad7	(Zhao et al. 2017)
Sox17	-
Taf9b	-
Tfap4	-
Trib2	(You et al. 2019)
Zeb2	-
Actn2	-

[1] BCL6 was identified as a regulator of early adipose commitment (Hu et al. 2016).

[2] While there is a focus on the function of *Egr1* during chondrogenesis (Spaapen et al. 2013), there is some indication that *Egr3* has increased expression in ATDC5 cells at the onset of chondrogenic differentiation. Additionally, EGR3 was shown to be involved in myoblast proliferation (Kurosaka et al. 2016).

[3] *Hdac11* ectopic expression was shown to inhibit myoblast differentiation (Byun et al. 2017).

[4] Down-regulation of *Hmga1* is necessary to initiate the myogenic (or osteogenic) program after induction of C2C12 differentiation (Brocher et al. 2010).

[5] HMGA2 was shown to promote adipogenesis (Xi et al. 2016).

[6] *Klf12* was expressed in MSC but not in lineage-committed mesenchymal cells (Zhang et al. 2012).

Table 3.6: **Transcription Factors and Cofactors with no chondrogenic GO annotations, differentially expressed only at 24hrs and with RNA-seq |log2foldChange| ≥ 0.55**
*excludes genes that were captured by the lists above

TFs/cofactors with no chondrogenic GO annotations	RNA-seq (log2FoldChange)	Manual literature search associations with chondrogenesis/osteogenesis
Ddn	2.36	-
Sfmbt2	1.73	(Hussain et al. 2018)
Dmrta1	1.56	-
Nfatc2	1.36	(Ranger et al. 2000; Chen et al. 2011)
Nfe2l3 (aka *Nrf3*)	1.21	[1]
Lpin3 (aka *Lipin-3*)	1.2	[2]
Myrf	1.19	-
Pax3	1.1	(Cairns et al. 2012)
Klf14	1.04	[3]
Dcc	1.01	(Schubert et al. 2009)
Dll1	0.94	[4]
Trib3	0.93	[5]
Ell3	0.92	-
Glis1	0.87	[6]
Ccnd1	0.86	(Ito et al. 2014)
Prdm16	0.8	(Warner et al. 2013)
Pbxip1 (aka HPIP)	0.77	(Ji et al. 2019)
Stat5a	0.77	[7]
Meis3	0.74	-
Sertad2 (aka TRIP-Br2)	0.69	[8]
Sorbs1	0.63	-
Klf13	0.59	-
Anxa4	0.57	-
Tsc22d1	-0.55	-
Med12l	-0.64	-
Tle6	-0.68	-
Nmi	-0.71	-
Rora	-0.86	(Woods et al. 2009)
Meis2	-0.97	[9]
Erbb4	-1.61	(Nawachi et al. 2002)
Esr2 (aka *Erβ*)	-1.61	(Zeng et al. 2016)
Nr2f1 (aka COUP-TFI)	-1.73	[10]

[1] No direct association with chondrogenesis; however, according to (Pepe et al. 2010) NFE2L3 has an important role in smooth muscle cell (SMC) differentiation from stem cells.

[2] No direct association with chondrogenesis; however, according to (Csaki et al. 2014) *Lpin3* is expressed in adipose tissue and is induced during adipogenesis.

[3] No direct association with chondrogenesis; however, KLF14 was shown to act as a master trans-regulator of adipose gene expression (Small et al. 2011).

[4] *Dll1* expression was observed in a chondrogenic (ATDC5) cell line (Watanabe et al. 2003), while (Zhang et al. 2018) have more recently shown that inhibition of *Dll1* expression in rat chondrocytes and chondrosarcoma cells triggered cell death/senescence and suppressed proliferation.

[5] No direct association with chondrogenesis; TRIB3 was shown to play an important role in proliferation and osteogenic differentiation in human bone marrow-derived mesenchymal stem cells (Zhang et al. 2017).

[6] No direct association with chondrogenesis; GLIS1 was identified as a regulator of mesenchymal multipotency that represses lineage-specific genes (specifically adipocyte and osteoblast differentiation) (Gerard et al. 2019).

[7] No direct association with chondrogenesis; STAT5A inhibition was shown to enhance bone formation by promoting osteogenesis of BMSCs (Lee et al. 2018).

[8] No direct association with chondrogenesis; TRIP-Br2 was identified as a transcription co-regulator for adiposity and energy metabolism (Liew et al. 2013).

[9] Restriction of *Meis2* expression is essential for limb outgrowth/development, and disruption of its expression resulted in limb alterations, many of which developed into cartilage pattern alterations; therefore, MEIS2 may have a role during chondrogenesis (Capdevila et al. 1999). MEIS2 was shown to repress osteoblastic transdifferentiation of cells in the heart (Sun et al. 2019).

[10] *Nr2f1* was implicated in osteogenesis (Tsai and Tsai 1997; Manikandan et al. 2018).

Table 3.7: **Transcription Factors and Cofactors with no chondrogenic GO annotations, differentially expressed at both 12hrs and 24hrs and with RNA-seq |log2foldChange| ≥ 1**
*excludes genes that were captured by the lists above

TFs/cofactors with no chondrogenic GO annotations	RNA-seq (log2FoldChange)	Manual literature search associations with chondrogenesis/osteogenesis
Hr	3.35	-
Dusp26	3.1	-
Wwp2	2.74	[1] (Zou et al. 2011; Nakamura et al. 2011)
Rbpjl	2.73	-
Jdp2	2.26	[2]
Klf2	1.99	[3]
Pparg	1.65	(Wang et al. 2005; Ma et al. 2015)
Ss18l2	1.44	-
Nr4a1	1.35	[4]
Fam129b	1.19	[5]
Isl1	1	[6]
Nr6a1	-1.02	-
Smarca2	-1.02	-
Esrrg	-1.09	[7]
Bcl11a	-1.11	(Yamamoto et al. 2019)
Mdfic (aka HIC)	-1.16	[8]
Foxp2	-1.33	(Zhao et al. 2015)
Epas1 (aka HIF2A)	-1.35	(Preitschoph et al. 2016)
Foxp1	-1.43	(Zhao et al. 2015)
Eya2	-1.51	[9]
Esrrb	-1.52	-
Agtr2	-1.55	(James et al. 2005)
Ebf1	-1.63	(El-Magd et al. 2015)
Atf3	-1.68	(James et al. 2006)
Nfia	-1.7	(Pratap Singh et al. 2018)
Pax9	-1.82	(Rodrigo et al. 2003)
Barx1	-1.88	(Nichols et al. 2013)
Zic3	-2	(Zhu et al. 2007)
Pdlim1	-2.02	[10]
Hhex (aka *Hex*)	-2.16	(Morimoto et al. 2011)
Meox1 (aka *Mox1*)	-2.29	(Candia et al. 1992; Candia et al. 1996)
Ikzf3	-3.13	-

[1] WWP2 forms a complex with SOX9 and the transcription enhancer MED25 to enhance SOX9 transcriptional activity during chondrogenesis. Additional studies have recognized *Wwp2* as an important target for cartilage diseases such as osteoarthritis (Rice et al. 2019; Chantry 2011).

[2] No direct association with chondrogenesis; however (Kawaida et al. 2003; Maruyama et al. 2012) showed JDP2 plays a role in osteoclast differentiation and bone homeostasis, while (Nakade et al. 2007) demonstrated that JDP2 represses adipogenesis.

[3] *Klf2* was found to be upregulated in diseased (osteoarthritis) chondrocytes (Aki et al. 2018; Teramura et al. 2015; Yuan et al. 2017). Additionally, it was demonstrated that KLF2 regulates osteoblast differentiation by targeting *Runx2* (Hou et al. 2019). KLF2 was identified as a negative regulator of adipogenesis (Sen Banerjee et al. 2003; Wu et al. 2005).

[4] *Nr4a1* expression was significantly elevated in OA cartilage, and while it is normally located in nuclei of chondrocytes, it translocated to mitochondria in OA chondrocytes (Shi et al. 2017).

[5] No direct association with chondrogenesis; FAM129B was identified as a Wnt/β-catenin regulator (Conrad et al. 2013), which offers a potential role for FAM129B to negatively regulate Wnt signaling, thereby enabling chondrogenesis.

[6] Some indication of association with chondrogenesis; (Kawakami et al. 2011) showed Islet1 as a hindlimb-specific transcriptional regulator that regulates hindlimb outgrowth along with β-catenin, while (Akiyama et al. 2014) confirmed that loss of ISL1/β-catenin in the hindlimb results in failure to expand chondrogenic precursor cells and skeletal defects.

[7] No direct association with chondrogenesis; however, work by (Jeong et al. 2009; Cardelli and Aubin 2014) suggests that ESRRG (aka ERRG) negatively regulates bone formation and osteoblast differentiation (potentially in a sex-dependent manner).

[8] No direct association with chondrogenesis; but a paralog of MDFIC called MDFI or I-mfa has been shown to have important roles in chondrogenic differentiation (Kraut et al. 1998).

[9] No direct association with chondrogenesis; but a EYA2 has been implicated in myogenesis and tenogenesis (Xu et al. 1997).

[10] *Pdlim1* expression was detected in human articular chondrocytes (Joos et al. 2008).

3.3.2 Identification of Active Regulatory Regions with Histone Modifications

To complement our transcriptomic data from Section 3.3.1, we performed histone ChIP-seq assays to identify genome-wide histone modification profiles on PLM micromass cultures prepared as described previously. Cultures were treated with BMP4, NOG or vehicle control and harvested at 0hrs, 12hrs and 24hrs post-seeding, in order to identify histone modification mark changes during the time course corresponding to our RNA-seq data.

To validate the biological relevance of the ChIP-seq peak calls from MACS2, we analyzed the profiles of the H3K27ac and H3K4me3 ChIP-seq peaks in the vicinity (±1.5kb) of all TSSs for all times points and treatments (Figure 3.9). We verified that the regions covered exhibited a bimodal pattern, as expected from observations in other studies of H3K27ac and H3K4me3 marks, and this confirmed the quality of our data (Wang et al. 2008; Nie et al. 2013). Additionally, the ratio of fold enrichment between upregulated and downregulated genes is reversed with BMP4 and NOG treatments, confirming that the histone peaks are enriched near the expected gene`s TSS as per our RNA-seq data.

We investigated potential regulatory regions utilizing the H3K27ac peak calls that were differentially regulated with BMP4 and NOG treatments (Figure 3.10). At 12hrs post-treatment we identified a total of 888 peaks within 50kb of DEG TSS, of which 563 were near upregulated DEGs and 325 near downregulated DEGs. Exclusion of the promoter-proximal peaks (±1.5kb from DEG TSS) helped locate potential enhancer regions within 50kb from the TSS. In doing so we identified 385 peaks near 234 upregulated DEGs and 212 near 122 downregulated DEGs. At 24hrs, a total of 2354 peaks were located within 50kb of DEG TSSs; 1035 peaks near upregulated DEGs and 1317 near downregulated DEGs. When promoter-proximal peaks were excluded, we

identified 856 peaks near 446 upregulated DEGs and 838 peaks near 410 downregulated DEGs within 1.5kb-50kb from the TSSs. We then combined all H3K27ac mark data within this range at both time points and removed duplicated gene entries and overlapping histone peaks. This resulted in a total of 1118 H3K27ac marks near 556 upregulated DEGs and 976 marks near 459 genes within 1.5kb-50kb from the TSS. An additional 398 peaks for the 12hr time point and 1153 peaks for the 24hr time point were located within 50-100kb. This substantial number of H3K27ac peaks in close proximity to DEGs provides a great starting point to locate candidate regulatory regions active during the initial stages of chondrogenesis when chondrocytes transition from condensation to active proliferation.

For example, the TF Sox5 is known to be activated by Sox9 during chondrogenesis. Figure 3.11 depicts the Sox5 locus, along with the RNA-seq data and pertinent histone mark data we generated, along with sequence conservation data and some previously published Sox9 ChIP-seq data from E12.5/E13 murine whole limb buds. Using our own data, we identified two potential regulatory sites for Sox5 that are used during early chondrogenesis and coincide with Sox5 differential expression upregulation. One of these sites (A`) also contains Sox9 binding sites, identified by two separate studies (Garside et al. 2015; Yamashita et al. 2019) around the same developmental stage as our PLM cultures, further validating our data.

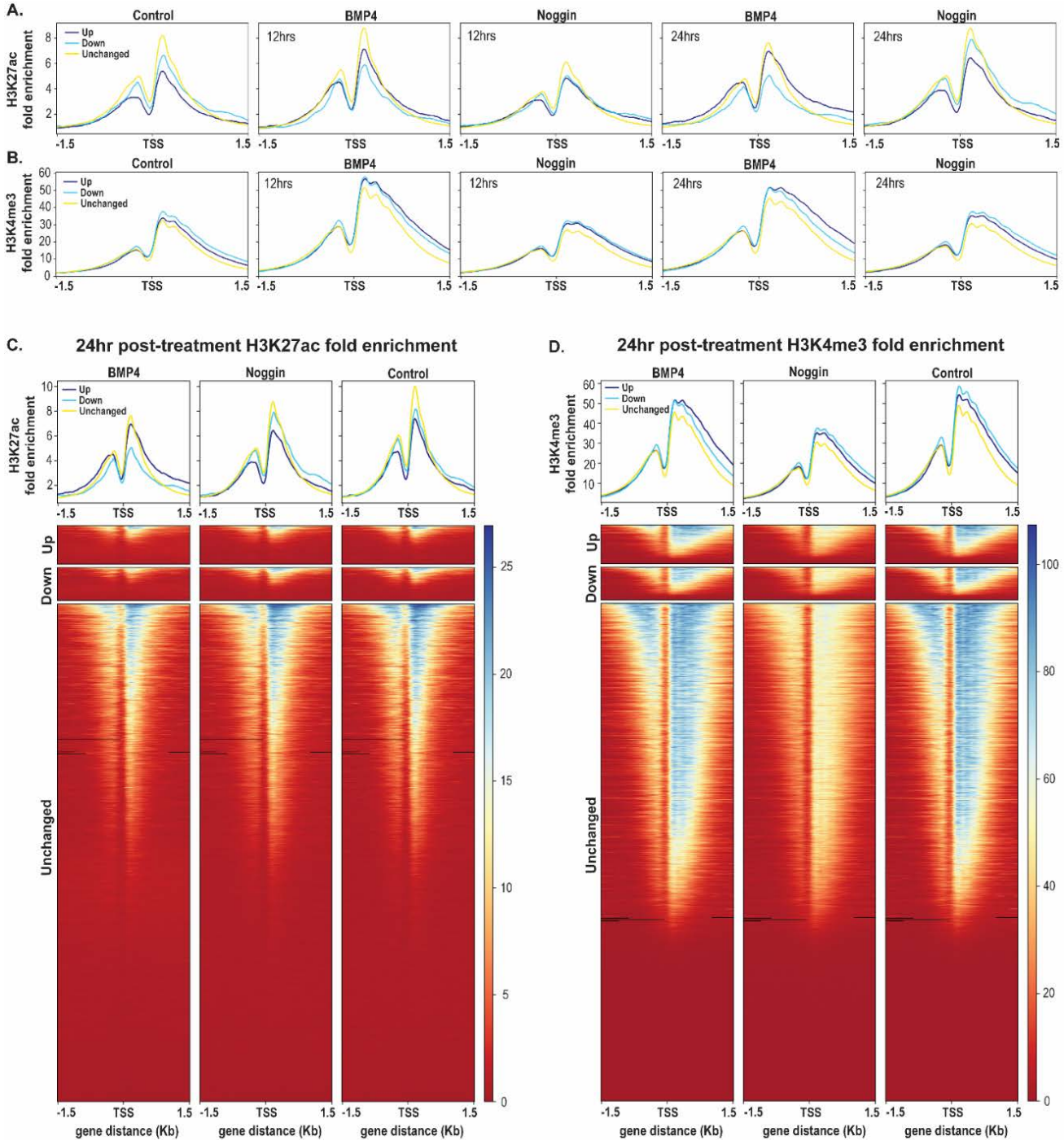
A.
Control
BMP4
Noggin
BMP4
Noggin
12hrs
12hrs
24hrs
24hrs
Up
Down
Unchanged
H3K27ac fold enrichment
B.
H3K4me3 fold enrichment
-1.5
TSS
1.5
C.
24hr post-treatment H3K27ac fold enrichment
D.
24hr post-treatment H3K4me3 fold enrichment
Up
Down
Unchanged
gene distance (Kb)

Figure 3.9: ***Histone mark enrichment distribution near the TSS of differentially regulated genes identified via RNA-seq.***

The average genome-wide histone enrichment calculated by MACS2 near TSSs (±1.5 Kb) was plotted for all genes detected from our RNA-seq analysis for each individual histone modification: H3K27ac (A,C) and H3K4me3 (B,D) and shown for individual treatments [Up (dark blue), Down (light blue) and Unchanged (yellow)]. Controls in (A,B) are from time point 0h and controls in (C,D) are from 24hrs. The relative fold enrichment was calculated with the MACS2 algorithm, accounting for the background signal by comparing the ChIP peaks within an individual sample to its own input control. The scale of fold enrichment distribution for individual samples is on the right of each enrichment matrix. Projection analysis (C,D) graphically shows each gene in each

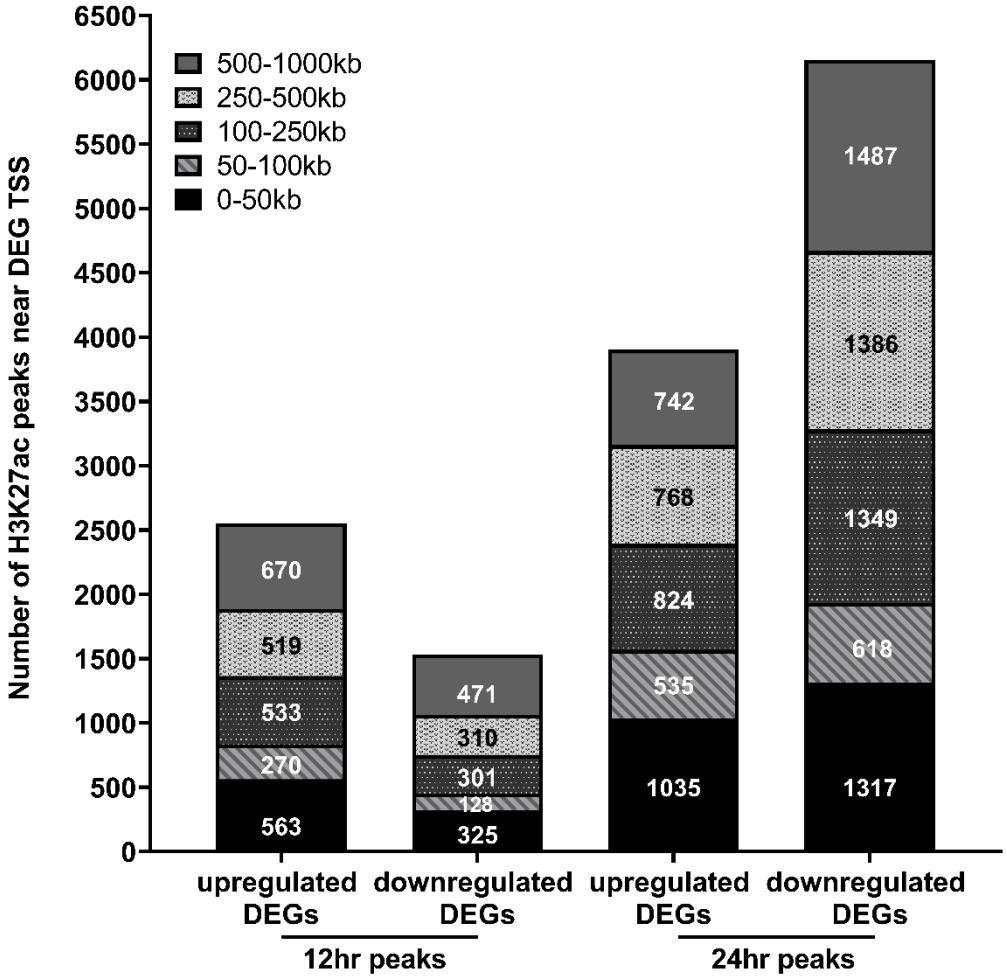

Figure 3.10: ***H3K27ac peaks near DEGs at 12hrs and 24hrs post-treatment.***

We identified thousands of H3K27ac peaks near DEGs, many as close as 50kb from the gene`s TSS. Some of these peaks may represent active regulatory regions.

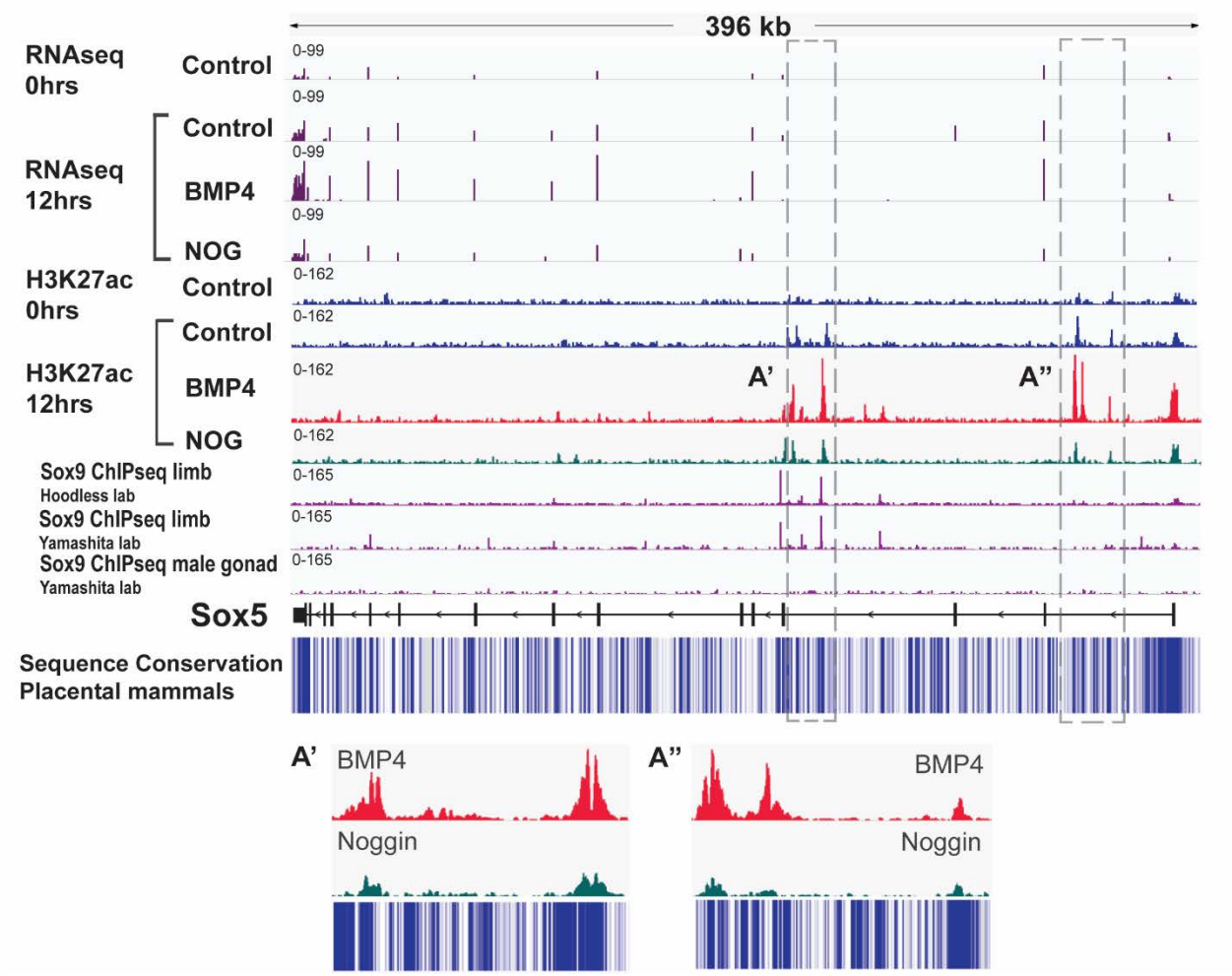

Figure 3.11: ***RNA-seq, histone modification and Sox9 ChIP-seq for Sox5.***

In the RNA-seq profiles, we observe a significant increase in exon reads for the BMP4 track compared to the Noggin track. Likewise, we note a significant increase in H3K27ac reads at multiple intronic regions (A' and A" expanded to show closeups of BMP4 and Noggin H3K27ac reads). The sequence conservation track shows that these K27ac reads are localized to well-conserved sequences across placental mammals. There also appear to be Sox9 binding sites overlapping with the K27ac marks in panel A', validating that area as a regulatory region.

Sequence conservation is represented with a heatmap of the UCSC genome browser PlyloP basewise conservation score derived from the Multiz alignment of 60 placental mammals (against the mm10 mouse genome). Exons are shown as wide bars and the 5'-3' direction of the denoted by the > symbol. Scales are shown in the top right corner for each track. SOX9 ChIP-seq data used here were from E12.5 mouse whole limb buds ((Garside et al. 2015); GEO Database (GSE73225)) and E13 mouse whole limb buds (Yamashita et al. 2019).

3.3.3 Bioinformatic Motif Discovery and Integration with Genomic Data

Using the functionally distinct motif-types identified in *Drosophila*, we scanned the mouse genome using the motif discovery tool HOMER (v4.10) (Heinz et al. 2011). These were filtered for high sequence conservation across 60 mammalian species using PhastCons scores, limiting the list to 3944 BMP-CREs with an average PhastCons score over 0.7 (Table 3.8). In all cases, over 2/3 (2764/3944) of the motifs are highly conserved with a score above 0.9.

Table 3.8: **Murine BMP-CREs with Average PhastCons Score > 0.7**

	Motif Type		
Average PhastCons Score	*BMP-SE*	*BMP-AE*	*BMP-AE2*
1	181	115	25
0.99-0.9	1358	983	102
0.89-0.8	374	200	21
0.79-0.7	345	209	30
Total	2258	1507	178

Out of these 3944 motifs, more than half (2305/3944) are located nearby genes that were differentially expressed in our RNA-seq experiment. More specifically, 52% of these motifs (2068/3944) were located within 1Mb from a DEG`s TSS (Table 3.9). Notably, 533 of these motifs were located within 50kb of a DEG`s TSS. We then excluded promoter-proximal motifs (within 250bp of the TSS) and identified 401/533 motifs that are within 50kb of the DEG`s TSS. Finally, there were more BMP-CREs in the vicinity of upregulated DEGs (1143/2068) up to 1Mb away from the TSS than downregulated DEGs (925/2068).

Table 3.9: ***BMP-CRE distance from the nearest BMP-responsive gene TSS***

	Motif Type						
	Up*regulated DEGs*			***Down****regulated DEGs*			
Distance from TSS	***BMP-SE***		***BMP-AE***		***BMP-AE2***		***Total***
	Up	*Down*	*Up*	*Down*	*Up*	*Down*	
within 50kb	158	110	151	90	13	11	533
50kb-100kb	82	56	68	30	5	5	246
100kb-250kb	157	134	131	105	12	15	554
250kb-500kb	120	131	77	86	8	10	432
500kb-1Mb	106	72	51	64	4	6	303
over 1Mb	84	61	55	27	7	3	237
Total	707	564	533	402	49	50	
	1271		935		99		**2305**

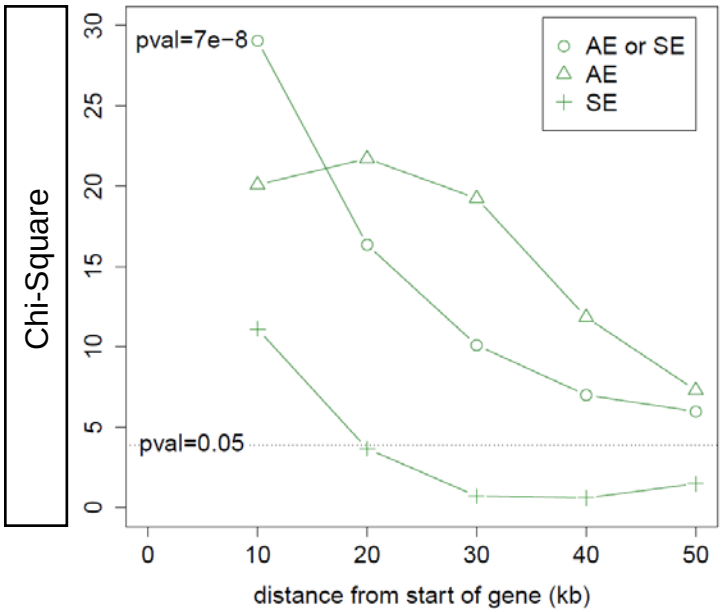

Figure 3.12: ***Putative BMP-CREs are enriched up to 50kb away from BMP-regulated genes.***
Statistical significance of the enrichment of BMP-AE and BMP-SE responsive genomic fragments near BMP up regulated genes was calculated using Pearson's Chi-Square test for count data in R (function chisq.test) with continuity correction without correcting for multiple testing. We used the non-significantly DEGs from our RNA-seq as the control gene set.

We performed a Chi-square analysis to see if there is an enrichment of BMP-CREs near upregulated DEG from our RNA-seq data (Figure 3.12). This test indicated that there was a significant enrichment of BMP-AEs up to 50kb from upregulated DEGs. The same was not true for BMP-SEs, as there was an enrichment only up to 20kb away from the TSS. When we combined both BMP-AEs and BMP-SEs, we identified a significant enrichment up to 50kb away from TSSs.

Upon review of previously identified Smad-binding sites or BMP-responsive regions in the vicinity of BMP-regulated genes (some of which have important roles in chondrogenesis) such as *Msx1*, *Msx2*, *Smad6*, *Ihh* and *Id1*, we identify canonical BMP-CRE motifs conforming to an AE- or SE- like consensus, with canonical n=5 linker site spacing (Table3.10). Many of these BMP-CREs were not identified as potential Smad-biding sites, but our bioinformatic search using the *Drosophila* BMP-CRE motifs has allowed us to identify these highly conserved motifs.

Table 3.10: **Revisiting and Examining Published Vertebrate BMP Regulatory Elements**

Experimentally Verified Vertebrate BMP-Regulatory Elements

Gene Name	*Publication Citation*	*Regulatory Element Coordinates (mm10)*	*Smad-Binding Specific Sequence*	*Comments and Observations*
Msx1	(Binato et al. 2006)	chr5:37,824,529-37,824,683	GCCGGCG	Potential Smad4 binding sites not identified in this study. CGGCGGACCCGGA**GCCGGCG**AGTGCGCCT
Id1	(Korchynskyi and Ten Dijke, 2002) (López-Rovira et al. 2002)	chr2:152,735,122-152,735,230	GGCGCC CGCC	Described as individual binding sites identified and not a Smad-complex binding site, additional putative Smad4 binding site not identified in this study. **CGCC**CGCGC**GGCGCC**AGCCTGACA
Id1	(Karaulanov, Knöchel, and Niehrs 2004)	chr2:152,739,406-152,739,488	TGGCGCCTGGCT GTCT	Identified a canonical BMP-CRE **GGCGCC**TGGCT**GTCT**
Id2	(Karaulanov, Knöchel, and Niehrs 2004)	chr12:25,098,842-25,098,933	TGGCGCCAGAG AGTCT	Identified a canonical BMP-CRE **GGCGCC**AGAGA**GTCT** Within the same fragment tested for BMP-responsiveness in this study, we identify an additional putative BMP-CRE with a GNCV Smad4 binding site GGCGCCGCTCAGGCG
Id3	(Karaulanov, Knöchel, and Niehrs 2004)	upstream: chr4:136,140,517-136,140,650 intron2: chr4:136,144,759-136,144,808	upstream: TGGCGCCAGGC TGTCT intron2: TGGCGCCGGCC AGTCT	Identified two canonical BMP-CRE motifs **GGCGCC**AGGCT**GTCT** and **GGCGCC**GGCCA**GTCT** Our analysis reveals additional putative BMP-CREs both upstream and downstream Id3.
Id4	(Karaulanov, Knöchel, and Niehrs 2004)	chr13:48,262,829-48,262,957	TGGCGCCAGTT AGTCT	Identified a canonical BMP-CRE **GGCGCC**AGTTA**GTCT**
Bambi	(Karaulanov, Knöchel, and Niehrs 2004)	chr18:3,506,976-3,507,050	TGGCGCC GTCT	Though the correct Smad1/5/9 binding site has been identified, since there was not evidence at the time that GNCV sequences excited, they were unable to identify the complete BMP-CRE. C**GTCT**CGTT**GGCGCC**

Smad7	(Karaulanov, Knöchel, and Niehrs 2004)	upstream: chr18:75,367,158-75,367,207 intron1: chr18:75,370,679-75,370,758	upstream: GGCCGGAGCC intron1: TGGCGCCAGGCGGCC	The intron1 Smad-complex binding site is almost completely resolved in this study, however, we cannot detect a canonical BMP-CRE sequence in the upstream sequence identified. intron1: **GGCGCC**AGGCGGCCT Our analysis reveals multiple putative BMP-CREs in the 5`UTR.
Smad6	(Ishida et al., 2000)	chr9:64,022,908-64,022,934	28bp GC-rich BMP-responsive fragment: GCCGCTCCTGCCCTGGA**GCCGGCGCGGC**	Mutational analysis revealed that **GCCGGCGCGGC** was the BMP-responsive sequence. Another region upstream of the fragment tested was also significantly BMP-responsive, however, that fragment was not tested further. Our bioinformatic analysis revealed a conserved putative BMP-CREs within that upstream fragment identified (Appendix, Figure S3): chr9:64,023,056-64,023,071; GGCGCCGATTGGCCC We identified additional BMP-CREs up to ~100kb from the TSS. chr9:64,021,146-64,021,159; GGCGCCGTGCAGACC chr9:64,021,029-64,021,042; ATACCCTTTGGCGCC chr9:63,968,880-63,968,893; AGACCCAGAGCCGCC chr9:63,919,401-63,919,414; AGCCACGGGGACGCC chr9:63,919,326-63,919,339; AGACTGGCTGTCGCC
Ihh	(Seki and Hata, 2004)	chr1:74,951,380-74,951,542	TGCGGGGCGGGGGC CCGGGGCCCTGGCT GGTGGCGGCGTGCT GTCCCCCTCGGCGCC TCGACTCTGAGCTGC CCGGCTCGCCGGCC GCCAATAAATAGGC CGGCCCGTTTGTTTT GGCAACGCGGCGAC GGCGGGGGGCGGCG GGCGGCGGGGCTGA GGGCCG	Multiple GC-rich motifs have been identified in this fragment as necessary and sufficient for BMP-specific up-regulation of reporter expression. A larger fragment containing the entire 5`UTR of Ihh was initially identified as BMP responsive and was able to drive almost double the reporter expression as the GC-rich motif fragment the study focused on. Looking at the excluded part of the fragment (+1 to -123 from the Ihh TSS) we identified 2 highly conserved putative BMP-CREs. chr1:74951,300-74,951,314; GGCGTCTGGGTGGCT chr1:74,951,246-74,951,260; GGCGCCTGGTGGGCT We identified additional BMP-CREs up to ~5kb from the TSS. chr1:74,951,797-74,951,811; GGCGGCCCCAAGGCT chr1:74,949,942-74,949,956; GGCGCCAGGGCGCAT

Msx2	(Brugger et al. 2004)	560bp fragment: chr13:53,475,962-53,476,524 52bp fragment: chr13:53,476,176-53,476,228	AGGCTGAGTGCCGG GCCGAGAGCAATTA ACGCGGCTCCGGCG CGGGCAGCCGC	The authors identified a 560bp BMP-responsive region with multiple GC-rich sequences. Deletion analysis revealed a 52bp BMP-responsive region with multiple "GCCG" and a homeodomain-like binding site "AATTAA" sequences that were shown to be required for BMP-responsiveness. We identified a conserved BMP-SE within the previously identified 560bp fragment. The authors recognised the GTCT part of the motif as a Smad4 binding site but did not further investigate this motif: chr13:53,476,371-53,476,385;GGCGGCCATTTGTCT

Predicted Vertebrate BMP-Regulatory Elements from (Karaulanov, Knöchel, and Niehrs 2004)

Gene Name	*Regulatory Element Coordinates (mm10)*	*Predicted Smad-Binding Specific Sequence*	*Comments and Observations*
Msx2	chr13:53,476,048-53,476,075 ~3.3kb upstream TSS	**AGAC**GGGCCAGGGCTGCG GGTA**GGCGCC**	We found a canonical BMP-CRE sequence very close to this other **predicted** Msx2 BMP response element. chr13:53,476,371-53,476,385 (~3.6kb upstream TSS); GGCGGCCATTTGTCT
Gata2	chr6:88,198,664-88,198,693	**GTCTG**TGCAGGAGTCGGC AGC**TGGCGCCAG**	We identified a canonically spaced Smad4 binding site (GNCV-type) near the **predicted** Smad1/5/9 binding site: chr6:88,198,686-88,198,700; **GGCGCC**AGGGCGGCC
Gata3	chr2:9,878,569-9,878,596	**GGCGCCA**GGCAGCTCAGT GTTCG**CAGAC**	We haven't identified a canonically spaced Smad4 binding sequence for this **predicted** motif, however, using our bioinformatic approach we have identified 3 canonical BMP-CRE upstream of Gata3: chr2:9,881,170-9,881,184; AGTCTCGCCGACGCC chr2:9,881,396-9,881,410; GGCGCCGGTCTGACC chr2:9,882,867-9,882,881; ATCCAGGCCGGCGCC

Bold and underlined sequences denote motifs sections that have been identified previously.

Grey highlight denotes Smad1/5/9 or Smad4 binding sites conforming to the canonical BMP-CRE consensus that we have identified.

More putative BMP-CRE binding sites can be seen in the UCSC browser graphic in Appendix Figure S8.

3.3.3.1 Prioritization of Regulatory Regions

We were interested to see if any of these BMP-CRE motifs we identified bioinformatically were located within regions marked with histone modifications associated with active enhancers. We decided to use H3K27ac as a proxy for active enhancer regions since it has narrow-type peaks, making it easier to confidently call as differentially "modified" with MACS2. We restricted our search to motifs within 1Mb away from the TSS of a DEG. This yielded a total of 332 H3K27ac peaks containing at least 1 motif up to 1Mb away from a DEG TSS. Out of these, 107 peaks contain at least 1 motif within 50kb of a DEG TSS (Figure 3.13; Appendix, Tables S6-S9).

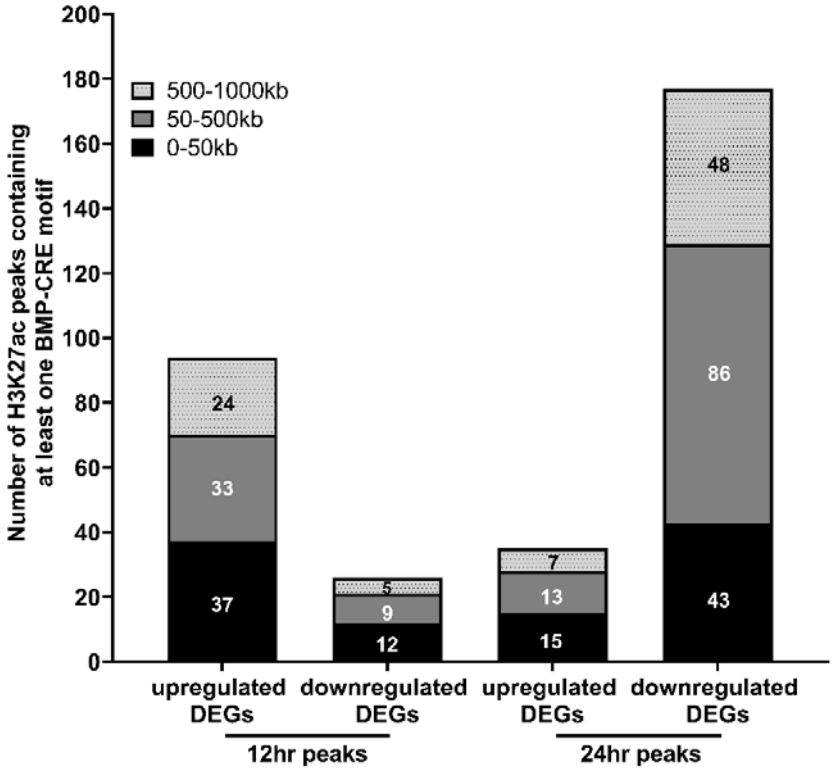

Figure 3.13: ***H3K27ac peaks with at least 1 BMP-CRE motif within 1Mb of a DEG.***
Highly conserved BMP-CREs within 1Mb from the TSS of DEGs from our RNA-seq experiments were identified within H3K27ac peaks. These regions could represent active Smad-binding sites.

We were then interested to identify BMP-CRE motifs within the regions marked by H3K27ac, H3K4me1 or H3K4me3 modifications, which could indicate potential regulation of

these genes by SMADs. We found that at least 4 of the TF/cofactors without any chondrogenic/osteogenic GO term annotations identified in Sections 3.3.1.2 and 3.3.1.3 had such histone marks and SOX9 binding sites: *Klf2*, *Grh1l*, *Wwp2* and *Jdp2* (Figures 3.14-3.16, 3.19).

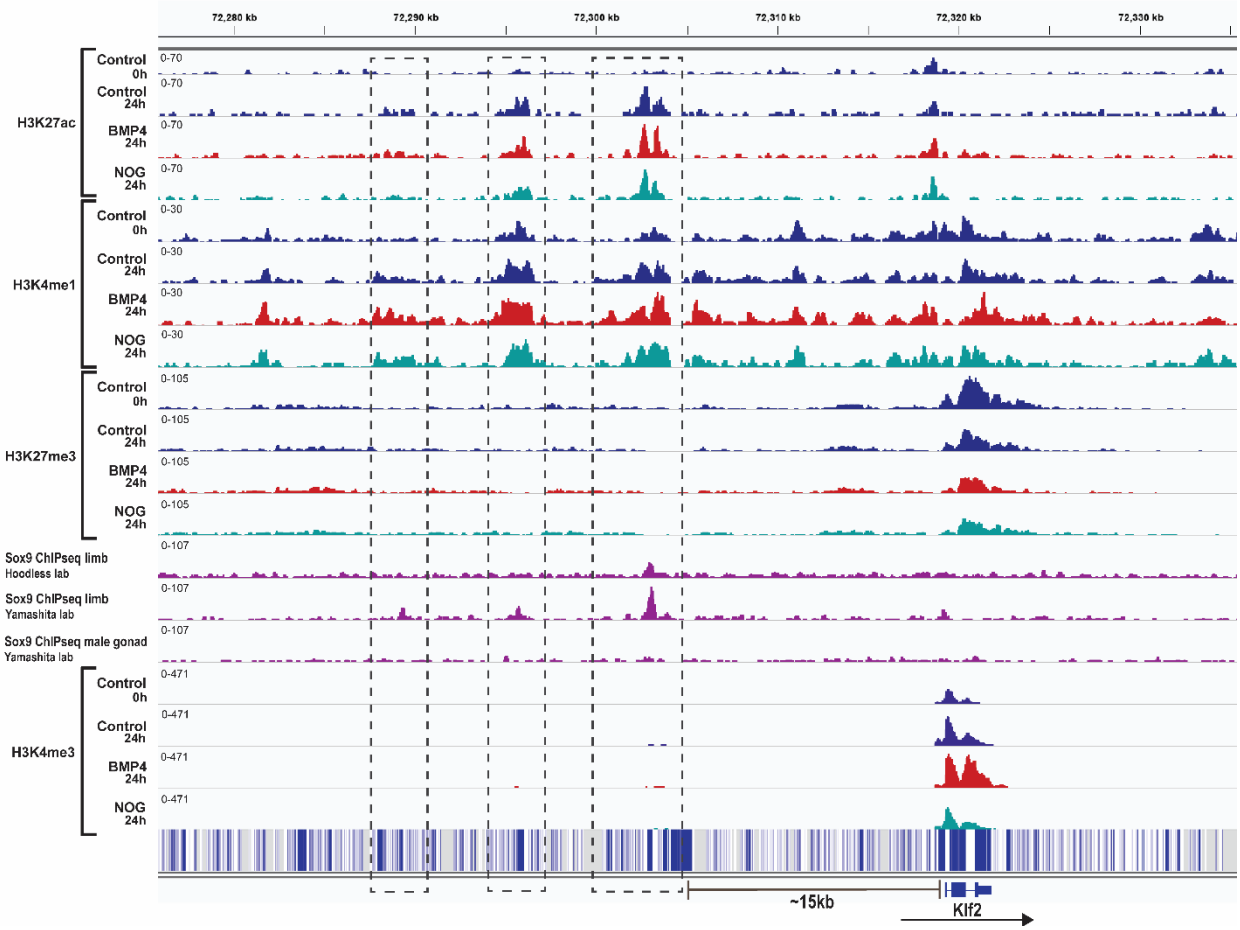

Figure 3.14: ***Histone modification marks, SOX9 ChIP-seq and BMP-CREs in the Klf2 locus.*** In agreement with our RNA-seq data, we can see a significant decrease in H3K27me3 repression-associated marks and an increase in H3K4me3 marks with BMP4 treatment at 24hrs. We noted 3 regions upstream of the *Klf2* TSS that contain an increase in H3K27ac and H3K4me1 marks, as well Sox9 binding sites. Sequence conservation is represented with a heatmap of the UCSC genome browser PlyloP basewise conservation score derived from the Multiz alignment of 60 placental mammals (against the mm10 mouse genome). Exons are shown as wide bars and the 5'-3' direction of the denoted by the > symbol. SOX9 ChIP-seq data used here were from E12.5 mouse whole limb buds ((Garside et al. 2015); GEO Database (GSE73225)) and E13 mouse whole limb buds (Yamashita et al. 2019).

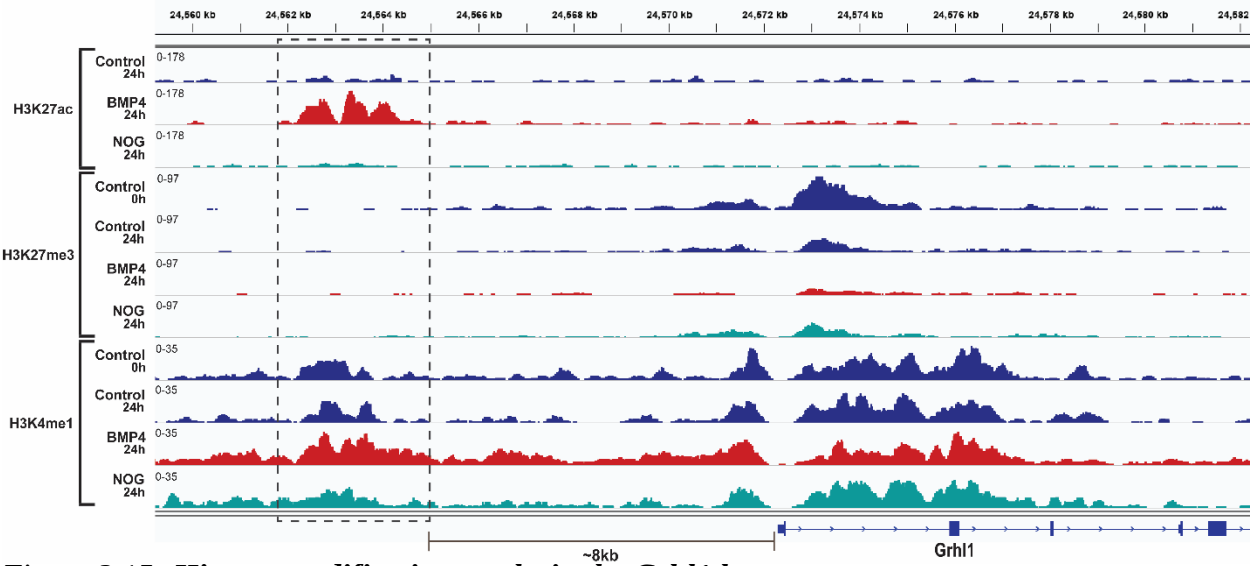

Figure 3.15: ***Histone modification marks in the Grhl1 locus.***

In the *Grh1l* locus we can see a significant reduction of the H3K27me3 repression-associated mark from time point 0h to 24hrs. The decrease in H3K27me3 occupancy is more apparent with BMP4 treatment. We can also see a significant increase in H3K27ac and H3K4me1 marks with BMP4 treatment 24hr post-induction in a region ~8kb upstream of *Grh1l* TSS. This region likely contains CREs that could regulate the expression of *Grh1l.*

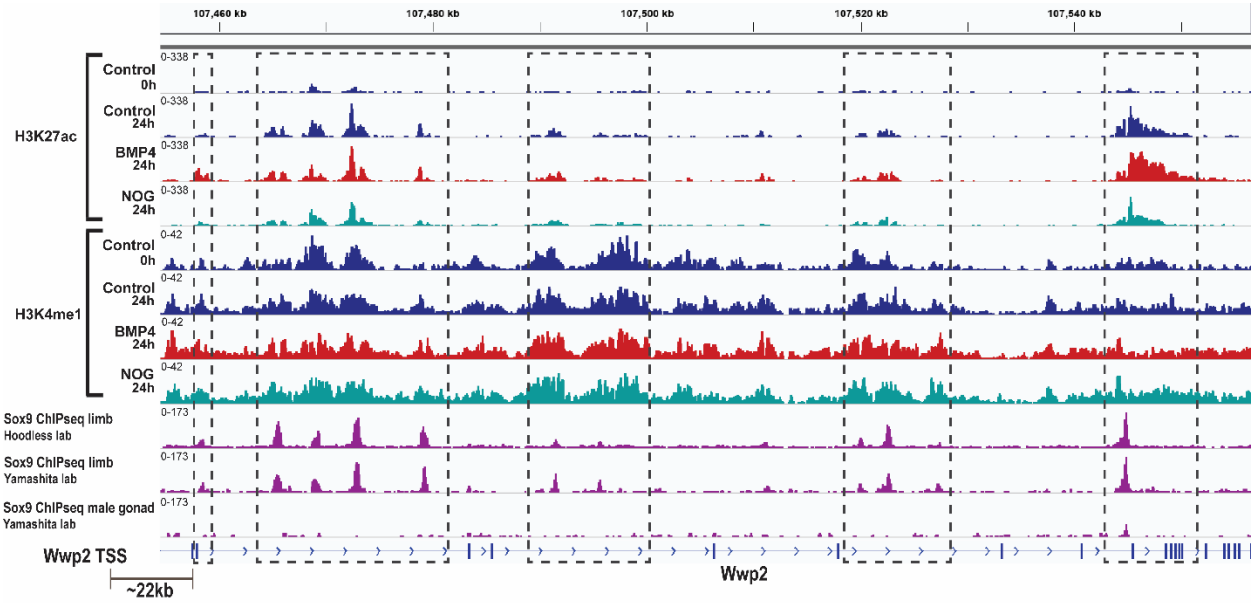

Figure 3.16: ***Histone modification marks and SOX9 ChIP-seq data in the Wwp2 locus.***

Multiple *Wwp2* introns contain increases in H3K27ac and H3K4me1 histone marks that line up with SOX9 binding sites. This result is in agreement with previously published work on *Wwp2* being a direct target of SOX9 (Nakamura et al. 2011).

We next sought to prioritize a set of regulatory regions to functionally characterize with a reporter assay in PLM cells. Regulatory regions were evaluated based on the existence of histone marks that would indicate an active regulatory site (e.g. H3K27ac or H3K4me1), their proximity to significantly upregulated DEGs from our RNA-seq data, and the existence of a conserved BMP-CRE within the region. Additionally, we searched for potential Sox9 binding sites within those regions using ChIP-seq data from previously published studies (Garside et al. 2015; Yamashita et al. 2019). Using these criteria, we selected regulatory regions near the following 3 genes: *Dlx2*, *Msx2*, *Jpd2*.

DLX2 (Distal-less homeobox 2) is a transcription factor and a member of the homeobox (Dlx) gene family, that is upregulated around E9.5-E10.5 of mouse embryonic development and plays important roles during chondrogenesis (Zhang et al. 2018; Ferguson et al. 2000). It was also demonstrated to be a downstream target of BMP signaling in early chondrogenesis (Xu et al. 2001). Several *cis*-regulatory elements regulating *Dlx2* expression in the CNS have been identified previously, though none of them was shown to be a BMP-dependent regulatory region (Ghanem et al. 2003; 2007). According to our RNA-seq data, at 24hours post-induction *Dlx2* exhibits a high upregulation (log2FoldChange=4.3) when comparing BMP4vs.NOG treatment. Additionally, we identified 3 conserved BMP-CREs (one of which was a double binding site), within areas of upregulated H3K27ac marks with BMP4 treatment compared to NOG treatment (Figure 3.17).

MSX2 (Muscle segment homeobox 2) is a homeobox transcription factor with a complex role during chondrogenic differentiation. It stimulates differentiation of mesenchymal cells into osteoblasts, inhibits adipocyte differentiation, stimulates chondrocyte maturation, but also negatively regulates chondrocyte differentiation of migratory cranial neural crest cells (Semba et

al. 2000; Takahashi et al. 2001; Cheng et al. 2003; Ichida et al. 2004; Amano et al. 2008). *Msx2* was also shown to be a direct target of embryonic BMP4 signaling (Hollnagel et al. 1999). A BMP-responsive region with substantial lacZ-reporter expression in E11.5 mouse limbs was previously identified ~3.5kb upstream of the *Msx2* gene (Brugger et al. 2004). According to our RNA-seq data, *Msx2* exhibits a high upregulation (log2FoldChange=1.52) at 24hours post-induction when comparing BMP4vs.NOG treatment. Our histone ChIP-seq data also indicates that this region contains a highly upregulated H3K27ac mark with BMP4 treatment compared to NOG treatment Further, we identified a conserved BMP-SE within the 560bp region previously identified as BMP-responsive (Brugger et al. 2004), thus we decided to use this region as an additional positive control for our reporter assay in PLM cells (Figure 3.18).

JDP2 (Jun dimerization protein 2) is a member of the AP-1 family of transcription factors and has many different functions during cell differentiation. It plays an important role during RANK-mediated osteoclast differentiation and bone homeostasis (Kawaida et al. 2003; Maruyama et al. 2012), while also being able to repress adipogenesis (Nakade et al. 2007) and inhibit retinoic-acid induced differentiation (Jin et al. 2002). JDP2 is also known to act as an epigenetic regulator of gene expression (Jin et al. 2006). Based on our RNA-seq data, *Jdp2* exhibits high upregulation (log2FoldChange=2.26) at 24hours post-induction when comparing BMP4vs.NOG treatment. Our GO term analysis and literature review revealed no chondrogenic annotations or associations. Additionally, we identified a highly conserved BMP-CRE around 50kb from the TSS of *Jdp2*, within an area with a small increase in H3K27ac marks when comparing BMP4 and NOG treatments at 24hours, as well as a SOX9 binding site (Figure 3.19).

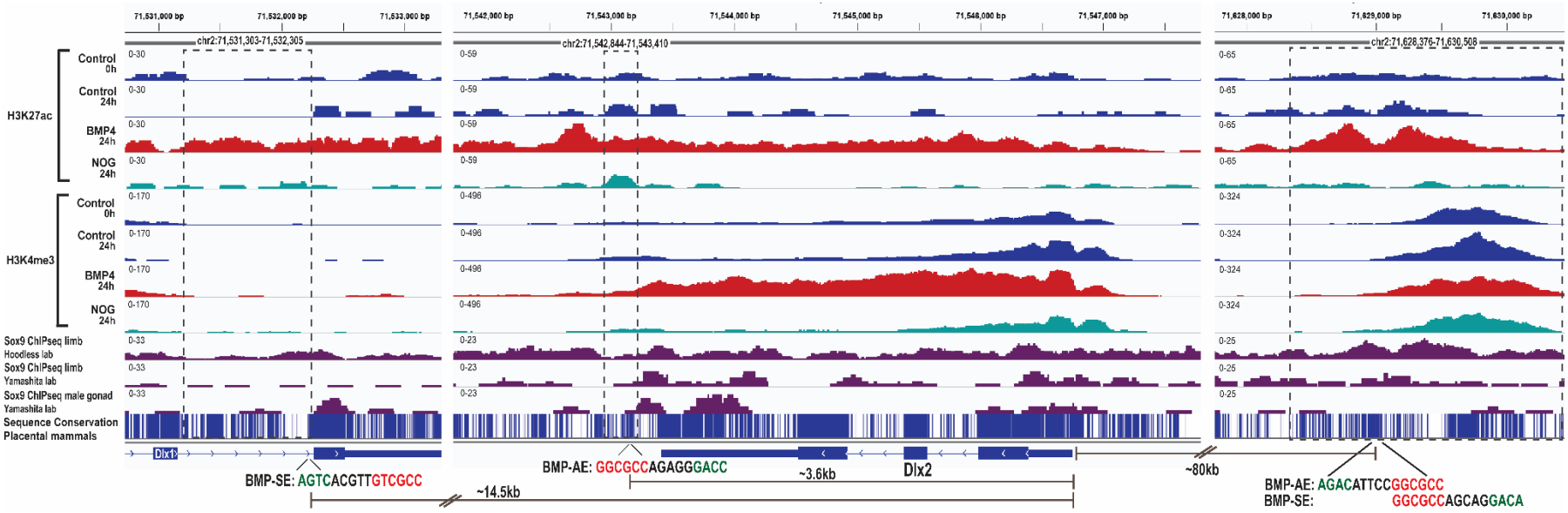

Figure 3.17: ***Histone modification marks, SOX9 ChIP-seq and BMP-CREs in the Dlx2 locus.***

In concordance with the RNA-seq data, there is great upregulation in H3K4me3 reads along the *Dlx2* locus. We also note a significant increase in H3K27ac reads at multiple regions in the vicinity of the *Dlx2* gene. The sequence conservation track shows that these K27ac reads are localized to well-conserved sequences across placental mammals. We selected 3 of these regions containing the highly conserved BMP-CREs located ~3.6kb, ~14.5kb and ~80kb from the TSS for reporter assays in PLM cell cultures.

Sequence conservation is represented with a heatmap of the UCSC genome browser PlyloP basewise conservation score derived from the Multiz alignment of 60 placental mammals (against the mm10 mouse genome). Exons are shown as wide bars and the 5'-3' direction of the denoted by the > symbol. SOX9 ChIP-seq data used here were from E12.5 mouse whole limb buds ((Garside et al. 2015); GEO Database (GSE73225)) and E13 mouse whole limb buds (Yamashita et al. 2019).

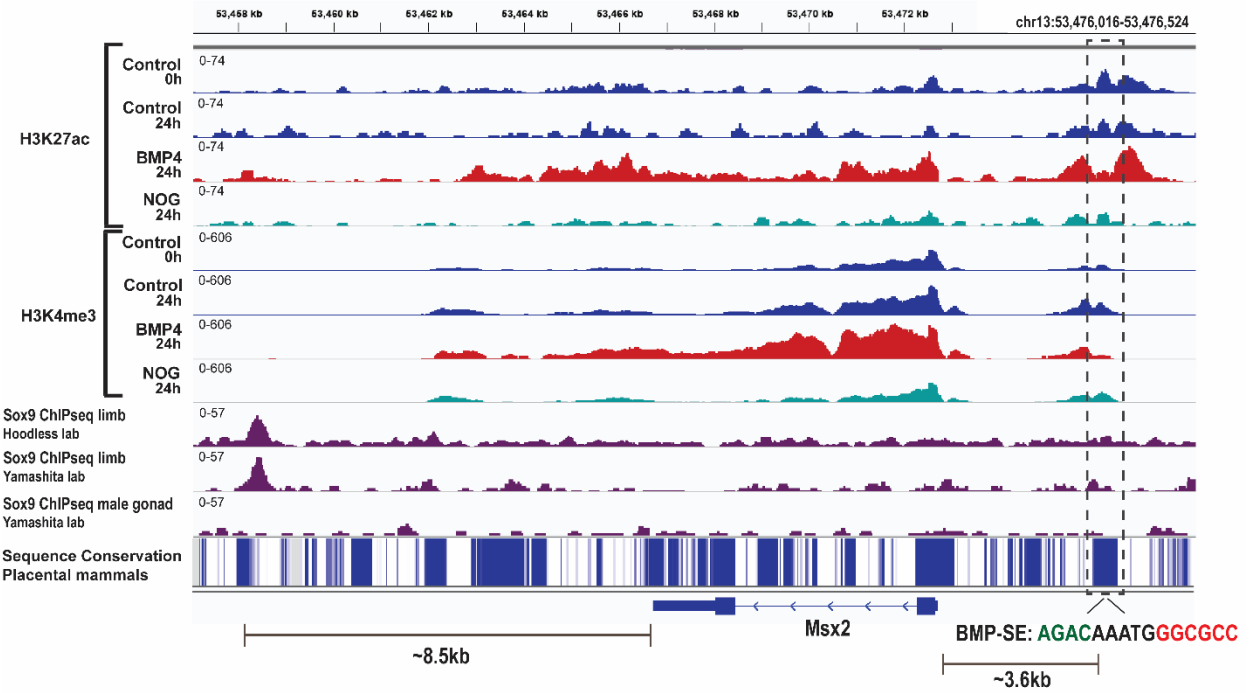

Figure 3.18: ***Histone modification marks, SOX9 ChIP-seq and BMP-CREs in the Msx2 locus.***

In agreement with the RNA-seq data, there is great upregulation in H3K4me3 and H3K27ac reads along the *Msx2* locus. There is also a significant increase in H3K27ac reads ~3.6kb upstream of the *Msx2* TSS in a region which is highly conserved according to the sequence conservation track. We also identified a conserved BMP-SE sequence in the same region, which we selected to clone and functionalize in a reporter assay in PLM cell cultures. Around 3.5kb upstream of the *Msx2* TSS is a predicted BMP-response element (Karaulanov, Knöchel, and Niehrs 2004), as well as the experimentally verified 560bp BMP-responsive region (Brugger et al. 2004). Approximately ~8.5kb downstream of the *Msx2* gene 3` end we can note a SOX9 binding site.

Sequence conservation is represented with a heatmap of the UCSC genome browser PlyloP basewise conservation score derived from the Multiz alignment of 60 placental mammals (against the mm10 mouse genome). Exons are shown as wide bars and the 5'-3' direction of the denoted by the > symbol. Sox9 ChIP-seq data used here were from E12.5 mouse whole limb buds ((Garside et al. 2015); GEO Database (GSE73225)) and E13 mouse whole limb buds (Yamashita et al. 2019).

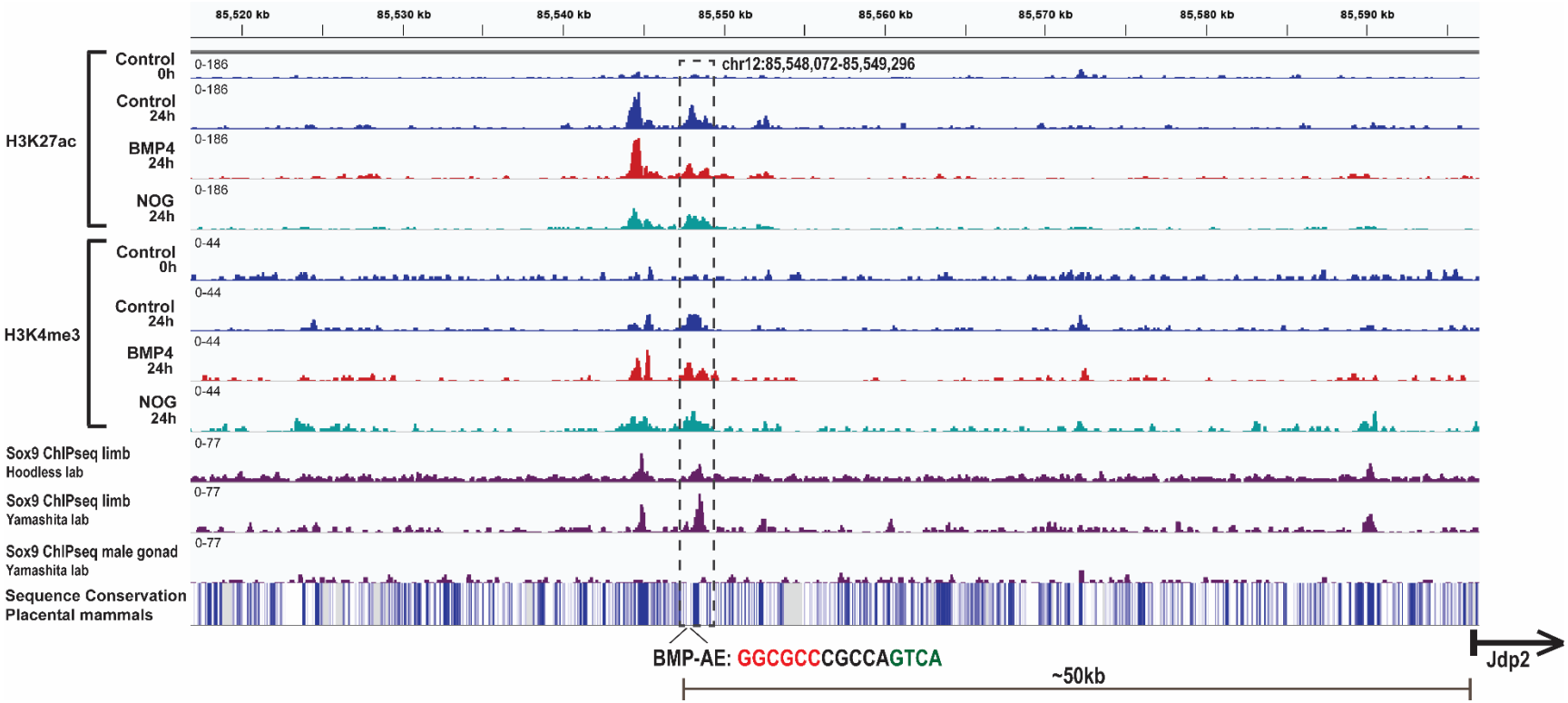

Figure 3.19: ***Histone modification marks, SOX9 ChIP-seq and BMP-CREs in the Jdp2 locus.***

We have identified a region ~50kb upstream of the *Jdp2* TSS that contains a highly conserved BMP-AE, a small increase in H3K27ac mark with BMP4 treatment (and a visible bimodal peak compared to NOG treatment sample), as well as a SOX9 binding site. We selected to clone and functionalize this boxed region with a reporter assay in PLM cell cultures.

Sequence conservation is represented with a heatmap of the UCSC genome browser PlyloP basewise conservation score derived from the Multiz alignment of 60 placental mammals (against the mm10 mouse genome). Exons are shown as wide bars and the 5'-3' direction of the denoted by the > symbol. SOX9 ChIP-seq data used here were from E12.5 mouse whole limb buds ((Garside et al. 2015); GEO Database (GSE73225)) and E13 mouse whole limb buds (Yamashita et al. 2019).

3.3.4 Preliminary Reporter Assay Experiments to Functionalize Identified CREs

Following the identification of putative regulatory regions, we wanted to test whether they were able to drive BMP-dependent reporter expression in the PLM cell culture system. We first generated the plasmid backbone that would allow us to easily add in and screen enhancer fragments, as described in the Methods Section 3.2.4. During the initial optimization phase, we opted to use a GFP read-out for our reporter, as it would be easier to quantify the number of reporter-expressing cells than it would be with the use of a luciferase reporter system, which is the most commonly used system in these assays.

Before testing any of the prioritized putative regulatory fragments, we transfected PLM cells with a positive control enhancer (7xBRE enhancer; (Javier et al. 2012), as well as the 8-times repeat concatemer of the fly dad13 BMP-AE plasmid (BMP-AE8x-EGFP) and its Mad-binding site mutant version (BMP-AE8x$^{\Delta mad}$) that were generated in the Allan lab (Vuilleumier et al. 2018). We monitored the cells for GFP expression for up to 36 hours post transfection.

As expected, the negative control plasmid (Empty mpId3-eGFP, only contains a minimal Id3 promoter) had no GFP expression, while the cultures transfected with the 7xBRE and 8xAE enhancer fragments had GFP expressing cells. The mutated Mad-binding site (8xAEmut enhancer fragment) had no GFP expressing cells. The GFP expression of both 7xBRE and 8xAE enhancer fragments was indeed BMP-driven, as we could see more GFP expressing cells with BMP4 treatment than in the control and NOG treatments (Figure 3.20). Therefore, we established that the assay was working, though we noted that the transfection efficiency was low.

We next transfected the 5 enhancer fragments we prioritized in Section 3.3.3.1. This experiment was only carried out once, and the following results are preliminary.

Two out of the 5 had no GFP-expression in our system (Dlx2-AE.SE and Dlx2-SE; data not shown). The enhancers in the fragments Dlx2-AE and Msx2-SE had few GFP-expressing cells, whereas the controls either had not reporter expression (Dlx2-AE) or had fewer reporter-expressing cells (Msx2-SE) than the BMP4 treated cultures (Appendix, Figure S9).

Jdp2-AE was the only enhancer fragment we tested that had robust BMP-driven GFP expression (Figure 3.21). We observed a noticeable upregulation of GFP-expressing cells with the addition of BMP4 compared to the Control and NOG treatments. While this experiment needs to be repeated, our assay has identified a BMP-responsive region ~50kb upstream of the *Jdp2* gene.

Taken together, this data indicates that utilizing our experimental and *in silico* methods can help us identify *bona fide* BMP-dependent regulatory regions.

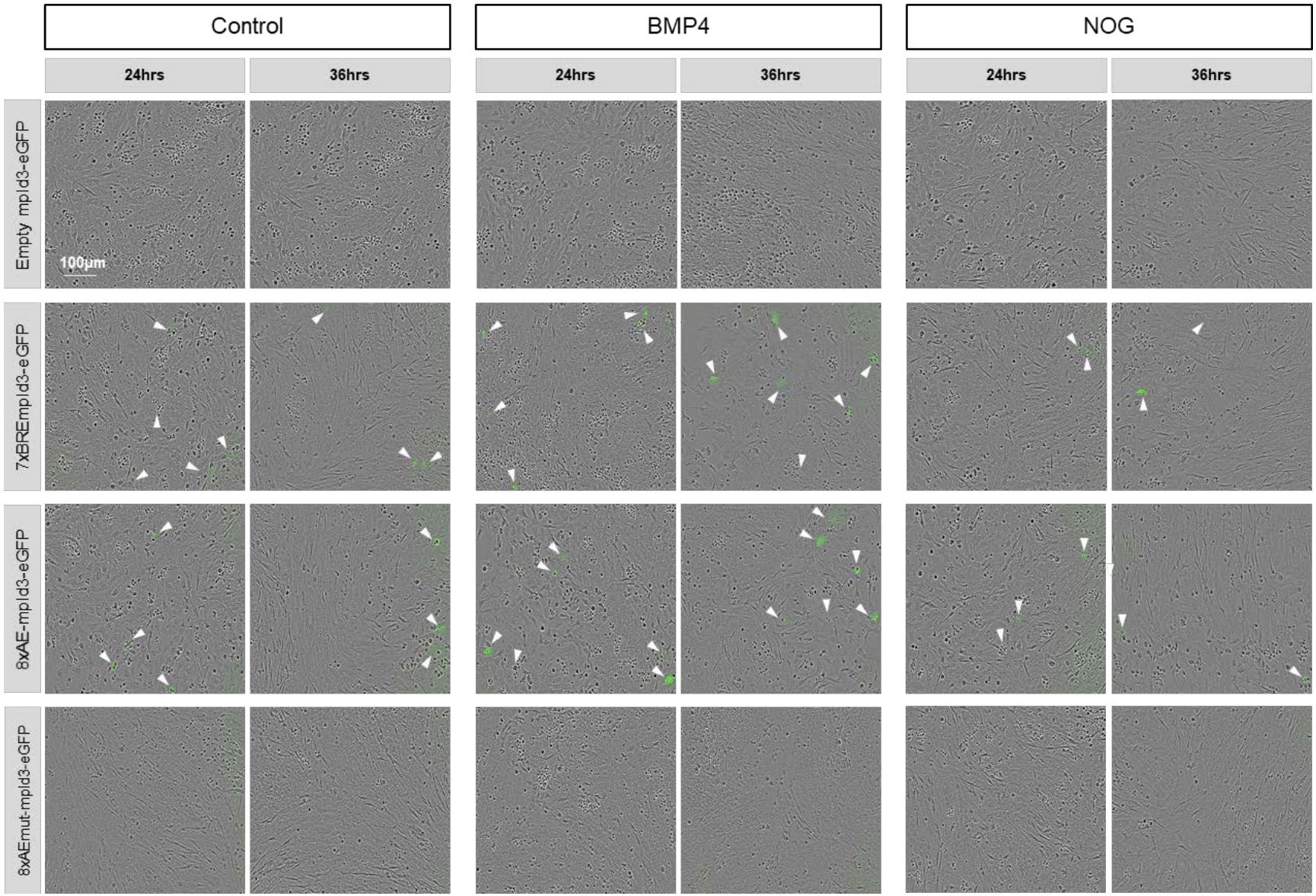

Figure 3.20: ***PLM cell transfection with positive control enhancers and minimal promoter Id3 (mpId3) driving eGFP plasmids confirms BMP-driven expression of previously used BMP-regulated enhancers.***

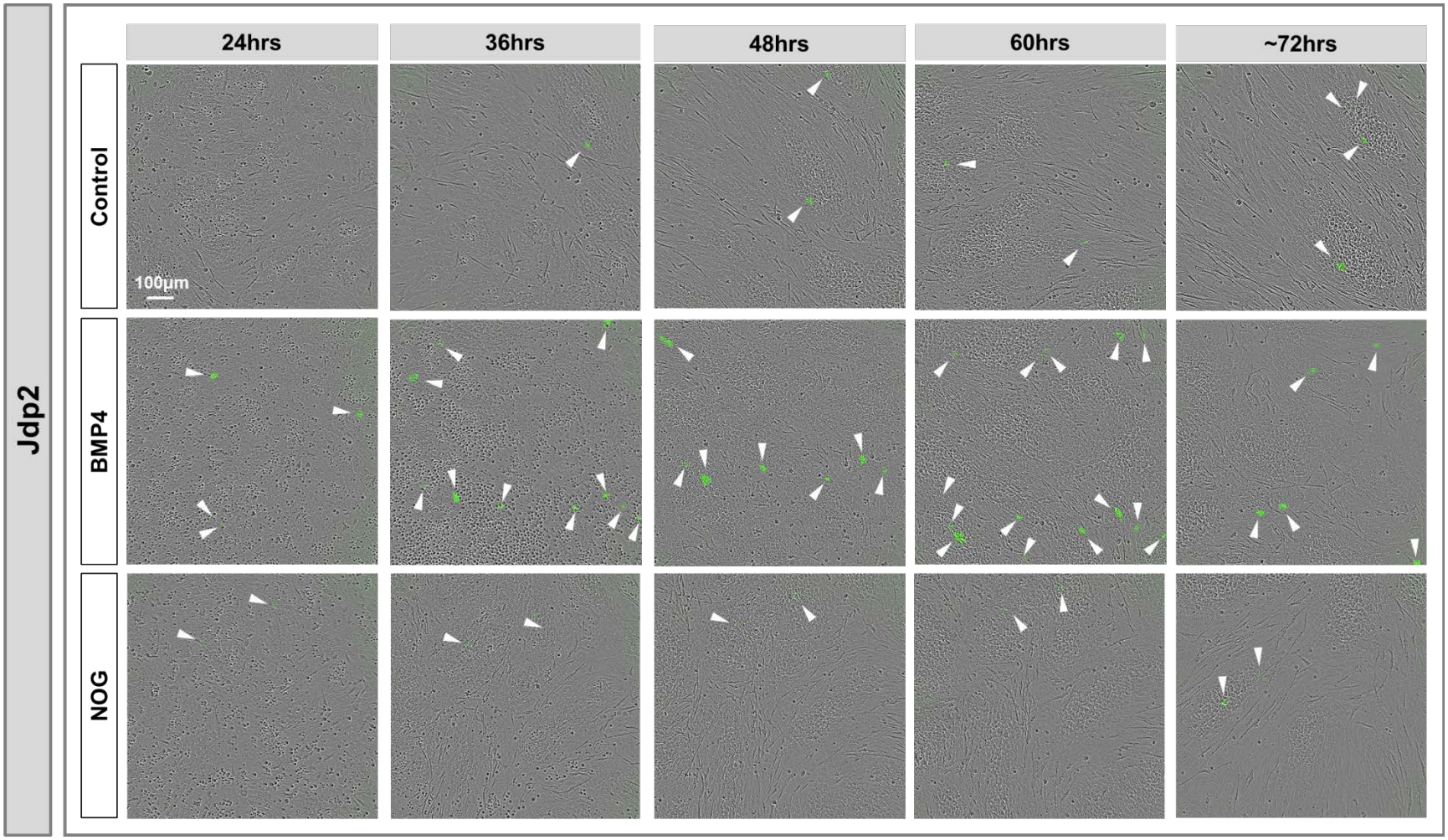

Figure 3.21: ***The Jdp2 BMP-AE drives GFP expression in differentiating chondrogenic PLM cells in a BMP4-dependent manner.***

3.4 Discussion

BMPs play a fundamental role in the chondrogenic program and are extensively involved in many/different steps of this process, from the initial commitment to terminal differentiation. Despite this, there remain unanswered questions regarding the exact mechanisms regulating BMP responsiveness and the underlying *cis*-regulatory network involved in early chondrogenesis.

To address this gap, we employed whole-transcriptome (RNA-seq) and histone ChIP-seq sequencing approaches to study BMP-driven mouse embryonic limb bud chondrogenesis. Combining these two methods with computational motif discovery and PLM cell reporter assays, we uncovered and verified the BMP-dependency of regulatory regions that most likely help coordinate chondrogenic gene expression.

Through our RNA-seq experiments, we identified genes that were differentially regulated during chondrogenesis, several of which are novel transcription factors/regulators/cofactors (Tables 3.2-3.7). Literature review revealed that some of the genes we identified were previously studied in a chondrogenic context, though they lacked chondrogenic/osteogenic GO term annotations. Furthermore, many of the genes we identified without chondrogenic GO terms have been shown to have a role in the maturation and maintenance of other MSC-derived lineages, including osteocytes, myocytes, adipocytes, and tenocytes. Therefore, it is likely that some of these genes have roles in the differentiation/maintenance of both chondrocytes and other MSC-derived lineages. Another possible explanation is that such genes are only necessary for the differentiation of alternate MSC lineages and are thus downregulated in PLM cultures to allow chondrogenic differentiation. Finally, it is also possible that some of the genes we identified have no role in chondrogenesis and are only a byproduct of the heterogeneity of our culture system (Discussed

further in Section 3.5). These results call for further investigations regarding the specific roles and regulatory processes that the genes/transcription factors/cofactors we identified play in the chondrogenic lineage.

Our histone modification ChIP-seq data has helped identify thousands of candidate regulatory regions, including the ~2000 H3K27ac regions located within 1.5-50kb from the TSS of ~1000 DEGs (Section 3.3.2; a subset of peaks listed in Appendix Tables S6-S9). While in our case we selected to focus on the H3K4me3, H3K4me1, H3K27ac and H3K27me3 marks to distinguish active/inactive promoters and enhancers (Heintzman et al. 2007, 2009; Creyghton et al. 2010; Rada-Iglesias et al. 2011; Zentner et al., 2011; Kim and Shiekhattar 2015), several other histone modifications have been implicated in influencing gene expression. According to Barski et al., active genes are characterized by high levels of H3K4me1, H3K4me2, H3K4me3, H4K9me1, and H2A.Z surrounding the TSS and elevated levels of H2BK5me1, H3K36me3, H3K27me1, and H4K20me1 throughout the entire transcribed region downstream of the TSS (Barski et al. 2007). On the other hand, inactive genes are characterized by low or negligible levels of H3K4 methylation at promoter regions, low levels of H3K36me3, H3K27me1, K3K9me1, and H4K20me1 along the gene body and high levels of H3K27me3 and H3K79me3 in the promoter and along the gene body. In the case of regulatory regions, although as described in Chapter 1, H3K4me1, H3K27ac, H3K27me3, and p300-binding are commonly used to predict enhancers and their (active/inactive) state, it is becoming increasingly clear that these marks alone do not identify all active/inactive enhancers (Karmodiya et al. 2012; Taylor et al. 2013; Pradeepa et al. 2016). Several additional histone modification marks have been found to mark active enhancers, including H4K16ac, H3K122ac, and H3K64ac (Taylor et al. 2013; Pradeepa et al. 2016). While in many cases these marks co-localize with H3K27ac, several examples of active enhancers lacking

H3K27ac, but bearing H4K16ac or H3K122ac marks have identified (Taylor et al. 2013; Pradeepa et al. 2016). Further, it was recently shown that the most active enhancers bear high levels of H3K4me3 rather than H3K4me1 marks (Henriques et al. 2018). There is also evidence to suggest that certain *cis*-regulatory elements can be active but also devoid of H3K4me1 (Dorighi et al. 2017). Thus, following the conventional use of H3K4me1 and H3K27ac marks as the identifiers of active enhancers would exclude these very active H3K4me3 bearing enhancers. Taking all this into consideration, while the histone modification marks we used in our work can help us identify several regulatory regions with high confidence, we cannot exclude the possibility that other regions (that we overlooked) may also be active enhancers in our system. Although the use of histone modifications to identify regulatory elements is a challenging and constantly evolving field, the integration of such information to this kind of work is worthwhile, as it gives a nuanced and informative view of gene regulatory mechanisms.

Using a bioinformatic motif discovery approach we identified thousands of highly conserved, candidate BMP-CRE motifs throughout the murine genome. More than 50% of these motifs were located within 1Mb of DEGs, but more importantly, 533 of these motifs were located within 50kb of DEGs TSS. In fact, BMP-AE motifs were found to be enriched up to 50kb from upregulated DEGs.

Reviewing published articles investigating vertebrate BMP-responsive elements revealed that very few of these enhancers were exhaustively studied to discover the exact Smad-binding site. Many of these studies identified large BMP-responsive fragments and did not attempt to locate the exact Smad-binding site sequence with mutational analyses. Others only identified the SMAD1/5/9 binding-site and not the SMAD4 site or simply predicted a BRE without a canonical

linker site and did not verify its BMP-responsiveness. Our results draw attention to the necessity of further characterizing enhancers. Better characterization of enhancers will enable more accurate computational motif predictions that can be used to map regulatory regions in a wide range of tissues, developmental systems, and organisms, including humans.

Finally, we prioritized and selected BMP-CREs in a pilot test to validate with a reporter assay in PLM cell cultures. We were able to identify 2 fragments containing a conserved BMP-CREs that were functional and responsive to BMP4 treatment in the cells (robust GFP expression with Jdp2-AE and low GFP expression with Dlx2-AE). We were also able to confirm reporter expression driven off the Msx2 fragment that was studied before. It will be interesting to mutate the previously identified BMP-responsive 52bp fragment (Brugger et al. 2004) to study the BMP-responsiveness of the remaining sequence in these cells. Future studies will focus on identifying more BMP-dependent regulatory regions, as well as further dissecting the specific TF binding sites that confer BMP-dependency to those regulatory regions.

3.5 Strengths and Limitations

One of the major limitations of our approach is the use of cells collected not only from whole E11.5 limb buds but also from both forelimbs and hindlimbs, ensuring a heterogeneous population (both in cell type and developmental stage) at the start of the experiment. The use of factors *in vitro*, such as BMP4 or NOG, helps "synchronize" the cells, though it is still likely that some heterogeneity persists in these cultures. In this case, it is unclear whether certain DEGs identified in our RNA-seq experiments are due to remaining blood or endothelial cells in the culture (as some of the GO terms may indicate; Appendix, Table S10) or whether these same genes

are also implicated in chondrocyte differentiation. Adopting strategies such as selecting/purifying cell types or using single-cell techniques can help provide a better picture of the regulatory and epigenetic landscape from chondrocyte lineage commitment to full differentiation.

Primary limb mesenchymal cultures are notoriously difficult to transfect (Juhász et al. 2010), prompting us to re-evaluate the transfection protocol we used in this thesis for our future experiments. While the FuGENE 6 (Promega) reagent is optimized to be gentle of the limb mesenchyme, the transfection efficiency is very low (Song et al. 2004). This was one of the reasons we opted for our initial validation experiments to be done with a GFP-reporter assay system, as opposed to the more commonly used luciferase-reporter assay. Our next experiments will likely explore the use of the Effectene (Qiagen)/trehalose transfection method developed in the Underhill lab (Karamboulas et al., 2010), as well as a pulse electroporation method (Bobick et al., 2014). Another avenue we are currently exploring is to transition the reporter assays into the mouse chondroprogenitor cell line ATDC5, which is a more robust and easier to transfect system (Chen et al. 2005). Initial validation of regulatory fragments in this system will provide a faster and more efficient screening process, allowing us to prioritize transfection of PLM cells with verified BMP-dependent regulatory regions.

A major limitation of histone modification ChIP-seq assays is that they reflect marks that have been corelated with enhancer activity, rather than directly showing that a genomic region functions as an enhancer. Therefore, despite their ability to yield genome-wide potential CREs, these genomic regions need to be further validated with functional assays (i.e. reporter assays).

Difficulties with data interpretation is another limitation when working with histone modification ChIP-seq data. Part of these difficulties rises from sample heterogeneity, but also the limited spatiotemporal information one can extract from the "snapshot" of histone/protein-DNA interactions. Therefore, many replicates or time points may be necessary to confirm results, making this a costly experimental approach. Additionally, determining and prioritizing which of the thousands of identified protein-binding sites to validate with reporter assays as biologically relevant is a daunting task. As discussed previously (Section 3.4), there is a growing body of work regarding histone modifications and their function in transcriptional regulation. Since this is still an evolving field, with the identification of novel and more nuanced roles for these marks in different contexts (Guenther et al. 2007; Liu et al. 2017), it is difficult to reliably interpret this information in isolation.

3.6 Conclusions

Using evolutionary conservation, *in silico* motif discovery tools, RNA-seq, and histone modification ChIP-seq assays, we were able to identify thousands of candidate active regulatory regions that may be involved in chondrogenesis. We then embarked on validating their functionality, confirming two novel BMP-responsive enhancers in the process, using reporter assays in primary limb mesenchymal cultures.

Chapter 4: Conclusions

The overall objectives of my thesis were to firstly characterize the use of a novel low-affinity BMP-CRE motif previously identified by our lab to be active in the *Drosophila* CNS and secondly to initiate the process of identifying the BMP-driven gene regulatory network of underlying mammalian chondrogenesis. In so doing, I have:

1) ***Identified and studied 7 conserved Drosophila BMP-CREs with the same sequence as the non-canonical FMRFa BMP-AE2 binding site, proving that this type of CRE is not only used by FMRFa but also other enhancers regions for BMP-dependent activation.*** Other studies in the Allan lab have provided evidence of the extensive use of BMP-AEs (Vuilleumier et al. 2018) and BMP-SEs (unpublished) in the *Drosophila* nervous system. My work has added to this field by identifying the use of these low-affinity BMP-regulated binding sites, which are located near BMP-regulated genes, in the *Drosophila* CNS.

2) ***Identified transcription factors and other cofactors with no previously known roles in chondrogenesis.*** Whole-transcriptome sequencing of BMP4 or NOG treated primary limb mesenchymal cultures yielded a comprehensive list of the gene regulatory network involved in the early stages of chondrogenesis. Chondrogenic GO term annotations and literature review helped narrow down this list to determine previously unidentified transcription factors/cofactors. Further investigations are required to fully elucidate their contributions to chondrogenic differentiation.

3) ***Identified thousands of potential regulatory regions in close proximity to genes that are differentially expressed during BMP-driven chondrogenesis.*** Histone ChIP-seq experiments corresponding to the timepoints and treatments of our RNA-seq experiments provided a list of ~2000 candidate regulatory regions within 1.5-50kb of ~1000 DEGs. The addition of *in silico*

methods and other high-throughput datasets will help us further refine these lists to ascertain regions most likely to be *bona fide* enhancers.

4) ***Demonstrated the BMP-dependency of regulatory regions located near upregulated differentially expressed genes during chondrogenesis.*** We prioritized candidate BMP-dependent regulatory regions based on their proximity to highly upregulated DEGs, as well as the existence of pertinent histone modification marks (H3K4me1 and/or H3K27ac upregulation with BMP4 treatment), conserved putative BMP-CREs, and SOX9 binding sites. We confirmed the BMP-dependence of two regulatory regions that are located within 50kb of highly upregulated DEGs, and one of these (*Jdp2*) was identified as a novel chondrogenic transcription factor through our RNA-seq experiments/GO term analyses.

4.1 Significance and Translation of the Study

In the era of reliable and affordable next-generation sequencing and genome-scale methods, there is renewed interest in the scientific community to decipher the non-coding regions of the human genome, discover and expand our understanding of enhancers and other regulatory regions.

One of the main arguments used to highlight the significance of identifying and studying *cis*-regulatory modules is the staggering number of genome-wide association studies (GWAS) loci identified in non-coding regions that have been associated with human diseases (Smallwood and Ren 2013; Kellis et al. 2014; Hojo et al., 2016). Seeking ways to reliably and robustly identify *cis*-regulatory modules is a very challenging goal. Concentrated efforts to map *cis*-regulatory regions in different tissues, developmental stages and diseases have been ongoing, with new techniques

added to the traditional “enhancer-bashing” methods each year. This thesis attempted to combine different high-throughput experimental techniques and *in silico* methods to identify *cis*-regulatory elements related to canonical BMP-signaling.

4.2 Future Directions

Several lines of work are currently being pursued to follow up on the work described in this thesis. Preliminary work has begun on optimizing SMAD1/5/9 ChIP-seq experiments in the PLM cultures to complement our other datasets. This will be followed by SOX9 ChIP-seq as well to confirm the data previously published in whole limb buds. These experiments will allow us to identify SMAD1/5/9 and SOX9 binding sites and potential novel binding motifs, as well as determine whether SMAD1/5/9 and SOX9 cooperatively regulated the expression of chondrogenic genes. Additional candidate enhancers could be functionally validated with reporter assays in PLM cultures following prioritization of regulatory regions based on SMAD1/5/9 and SOX9 binding.

Apart from the repetition of the Jdp2-AE, Dlx2-AE, and Msx2-SE transfection experiments, mutational analysis of the enhancer fragments will allow us to delineate the specific TF binding sites that contribute to their BMP-dependency. Specific mutation of the putative BMP-CRE binding sites would also allow us to establish the necessity of this motif for BMP-dependence and Smad-binding. Depending on the success of such experiments, we would transition these analyses from episomal plasmid reporter assays to either endogenous TF-binding site CRISPR mutations or CRISPR interference (Larson et al. 2013) in the ATDC5 chondrogenic cell line. These experiments would allow us to assess the effect of individual TF binding sites on the expression of neighboring genes via qPCR and/or western blots. The overall effect of the

chondrogenic differentiation progress of the culture could also be assessed with Alcian Blue staining and qPCR or key chondrogenic markers such as *Sox9*, *Acan*, *Col2a1*, and others.

Further, the newly identified chondrogenic transcription factors/regulators/cofactors from Section 3.3.1 could be further studied in a chondrogenesis context. The use of RNAi or CRISPR techniques would enable us to remove said genes from differentiated ATDC5 cells, allowing us to study the effects of their loss to the chondrogenic program via Alcian Blue staining and qPCR/western blots for *Col2a1*, *Acan*, *Sox9*, *Runx2*, and other chondrogenic markers.

Finally, in the long run, the work this thesis has initiated will have important repercussions for efforts to identify causal genomic loci of human musculoskeletal diseases. Transferring knowledge and lessons learned from studying murine chondrogenesis will help identify genes and gene regulatory regions that underlie chondrogenesis in the human genome. It is likely that this future work will provide a vital resource for clinical geneticists and informaticians attempting to identify causal mutations for diseases that lie in the non-coding regions (which represent ~98% of the genome) of the human genome.

To quote Shlyueva et al., 2014,

“These are exciting times to study transcriptional regulation”.

References

Aberle, Hermann, A. Pejmun Haghighi, Richard D. Fetter, Brian D. McCabe, Tiago R. Magalhães, and Corey S. Goodman. 2002. “Wishful Thinking Encodes a BMP Type II Receptor That Regulates Synaptic Growth in Drosophila.” *Neuron* 33 (4): 545–58. https://doi.org/10.1016/S0896-6273(02)00589-5.

Affolter, Markus, and Konrad Basler. 2007. “The Decapentaplegic Morphogen Gradient: From Pattern Formation to Growth Regulation.” *Nature Reviews Genetics* 8: 663–74. https://doi.org/10.1038/nrg2166.

Aki, Takashi, Ko Hashimoto, Masanori Ogasawara, and Eiji Itoi. 2018. “A Whole-Genome Transcriptome Analysis of Articular Chondrocytes in Secondary Osteoarthritis of the Hip.” *PLoS ONE* 13 (6): 1–17. https://doi.org/10.1371/journal.pone.0199734.

Akiyama, Haruhiko and Lefebvre, Véronique. 2011. “Unraveling the Transcriptional Regulatory Machinery in Chondrogenesis.” *Journal of Bone and Mineral Research* 29 (4): 390–95. https://doi.org/10.1007/s00774-011-0273-9.Unraveling.

Akiyama, Haruhiko, Marie-Christine Chaboissier, James F. Martin, Andreas Schedl, and Benoit De Crombrugghe. 2002. “The Transcription Factor Sox9 Has Essential Roles in Successive Steps of the Chondrocyte Differentiation Pathway and Is Required for Expression of Sox5 and Sox6.” *Genes & Development* 16: 2813–28. https://doi.org/10.1101/gad.1017802.overt.

Akiyama, Haruhiko, Jon P Lyons, Yuko Mori-akiyama, Xiaohong Yang, Ren Zhang, Zhaoping Zhang, Jian Min Deng, et al. 2004. “Interactions between Sox9 and β-Catenin Control Chondrocyte Differentiation.” *Genes & Development* 18: 1072–87. https://doi.org/10.1101/gad.1171104.Wagner.

Akiyama, Haruhiko, H Scott Stadler, James F Martin, Takahiro M Ishii, Philip A Beachy, Takashi Nakamura, and Benoit De Crombrugghe. 2007. “Misexpression of Sox9 in Mouse Limb Bud Mesenchyme Induces Polydactyly and Rescues Hypodactyly Mice.” *Matrix Biology* 26: 224–33. https://doi.org/10.1016/j.matbio.2006.12.002.

Akiyama, Ryutaro, Hiroko Kawakami, M Mark Taketo, Sylvia M Evans, Naoyuki Wada, Anna Petryk, and Yasuhiko Kawakami. 2014. “Distinct Populations within Isl1 Lineages Contribute to Appendicular and Facial Skeletogenesis through the β -Catenin Pathway.” *Developmental Biology* 387: 37–48. https://doi.org/10.1016/j.ydbio.2014.01.001.

Allan, Douglas W, Dongkook Park, Susan E St Pierre, Paul H Taghert, Stefan Thor, and St Louis. 2005. “Regulators Acting in Combinatorial Codes Also Act Independently in Single Differentiating Neurons.” *Neuron* 45: 689–700. https://doi.org/10.1016/j.neuron.2005.01.026.

Allan, Douglas W, and Stefan Thor. 2015. “Transcriptional Selectors, Masters, and Combinatorial Codes: Regulatory Principles of Neural Subtype Specification.” *WIREs Dev Biol* 4: 505–28. https://doi.org/10.1002/wdev.191.

Allen, Kelli D, and Yvonne M Golightly. 2015. “Epidemiology of Osteoarthritis: State of the Evidence Kelli.” *Curr Opin Rheumatol.* 27 (3): 276–83. https://doi.org/10.1097/BOR.0000000000000161.Epidemiology.

Allfrey, G, R Faulkner, and A E Mirsky. 1964. “Possible Role in the Regulation of RNA Synthesis.” *Proc. Natl. Acad. Sci U.S.A.* 315 (1938): 786–94.

Alliston, Tamara, Tien C Ko, Yanna Cao, Yao-yun Liang, Xin-hua Feng, Chenbei Chang, and Rik Derynck. 2005. “Repression of Bone Morphogenetic Protein and Activin-Inducible Transcription by Evi-1.” *Journal of Biological Chemistry* 280 (25): 24227–37. https://doi.org/10.1074/jbc.M414305200.

Almalki, Sami G, and Devendra K Agrawal. 2016. “Key Transcription Factors in the Differentiation of Mesenchymal Stem Cells.” *Differentiation* 92 (1–2): 41–51. https://doi.org/10.1016/j.diff.2016.02.005.Key.

Amano, Katsuhiko, Fumitaka Ichida, Atsushi Sugita, Kenji Hata, Masahiro Wada, Yoko Takigawa, Masako

Nakanishi, Mikihiko Kogo, Riko Nishimura, and Toshiyuki Yoneda. 2008. “Msx2 Stimulates Chondrocyte Maturation by Controlling Ihh Expression.” *The Journal of Biological Chemistry* 283 (43): 29513–21. https://doi.org/10.1074/jbc.M803681200.

Andrew, E Denker, Andrew R. Haas, Steven B Nicoll, and Rocky S Tuan. 1999. “Chondrogenic Differentiation of Murine C3H10T1/2 Multipotential Mesenchymal Cells : I. Stimulation by Bone Morphogenetic Protein-2 in High-Density Micromass Cultures.” *Differentiation* 64: 67–76. https://doi.org/10.1046/j.1432-0436.1999.6420067.x.

Angerer, H, D Krusch, A Deutsch, G Gruber, D Setznagl, M L Kremser, A Leithner, M H Stradner, and W B Graninger. 2012. “Potential Role of Nuclear Orphan Receptors NR4A1 and NR4A3 in Human Chondrocytes.” *Osteoarthritis and Cartilage* 20 (2012): S140. https://doi.org/10.1016/j.joca.2012.02.193.

Arnold, CD;, D; Gerlach, C; Stelzer, ŁM; Boryń, and A. Rath, M and Stark. 2013. “Genome-Wide Quantitative Enhancer Activity Maps Identified by STARR-Seq.” *Science (New York)* 339 (March). http://f1000.com/717973160.

Arnold, Michael A, Yuri Kim, Michael P Czubryt, Dillon Phan, John Mcanally, Xiaoxia Qi, John M Shelton, James A Richardson, Rhonda Bassel-duby, and Eric N Olson. 2007. “MEF2C Transcription Factor Controls Chondrocyte Hypertrophy and Bone Development.” *Developmental Cell* 12: 377–89. https://doi.org/10.1016/j.devcel.2007.02.004.

Asp, Julia, Maria Thornemo, Sven Inerot, and Anders Lindahl Y. 1998. “The Helix-Loop-Helix Transcription Factors Id1 and Id3 Have a Functional Role in Control of Cell Division in Human Normal and Neoplastic Chondrocytes.” *FEBS Letters* 438: 85–90.

Baburajendran, Nithya, Ralf Jauch, Clara Yueh, Zhen Tan, Kamesh Narasimhan, and Prasanna R Kolatkar. 2011. “Structural Basis for the Cooperative DNA Recognition by Smad4 MH1 Dimers” 39 (18): 8213–22. https://doi.org/10.1093/nar/gkr500.

Baburajendran, Nithya, Paaventhan Palasingam, Kamesh Narasimhan, Wenjie Sun, Shyam Prabhakar, Ralf Jauch, and Prasanna R Kolatkar. 2010. “Structure of Smad1 MH1 / DNA Complex Reveals Distinctive Rearrangements of BMP and TGF- b Effectors.” *Nucleic Acids Research* 38 (10): 3477–88. https://doi.org/10.1093/nar/gkq046.

Badis, Gwenael, Michael F Berger, Anthony A Philippakis, Shaheynoor Talukder, Andrew R Gehrke, Savina A Jaeger, Esther T Chan, et al. 2009. “Diversity and Complexity in DNA Recognition by Transcription Factors.” *Science* 324 (5935): 1720–23. https://doi.org/10.1126/science.1162327.Diversity.

Bandyopadhyay, Amitabha, Kunikazu Tsuji, Karen Cox, Brian D Harfe, Vicki Rosen, and Clifford J Tabin. 2006. “Genetic Analysis of the Roles of BMP2, BMP4, and BMP7 in Limb Patterning and Skeletogenesis.” *PLoS Genetics* 2 (12). https://doi.org/10.1371/journal.pgen.0020216.

Banerjee, Sucharita Sen, Mark W. Feinberg, Masafumi Watanabe, Susan Gray, Richard L. Haspel, Diane J. Denkinger, Rodney Kawahara, Hans Hauner, and Mukesh K. Jain. 2003. “The Krüppel-like Factor KLF2 Inhibits Peroxisome Proliferator-Activated Receptor-γ Expression and Adipogenesis.” *Journal of Biological Chemistry* 278 (4): 2581–84. https://doi.org/10.1074/jbc.M210859200.

Banerji, J.;, and W. Rusconi, S. and Schaffner. 1981. “Expression of a B-Globin Gene Is Enhanced by Remote SV40 DNA Sequences.” *Cell* 27: 299–308.

Barski, Artem;, Suresh; Cuddapah, Kairong; Cui, Tae-Young; Roh, Dustin E.; Schones, Zhibin; Wang, Gang; Wei, Iouri; Chepelev, and Keji Zhao. 2007. “High-Resolution Profiling of Histone Methylations in the Human Genome.” *Cell* 129: 823–37. https://doi.org/10.1016/j.cell.2007.05.009.

Beagrie, Robert A, and Ana Pombo. 2016. “Gene Activation by Metazoan Enhancers: Diverse Mechanisms Stimulate Distinct Steps of Transcription.” *BioEssays* 38: 881–93. https://doi.org/10.1002/bies.201600032.

Beak, Ju Youn, Hong Soon Kang, Yong-sik Kim, and Anton M Jetten. 2007. “Krüppel-Like Zinc Finger Protein Glis3 Promotes Osteoblast Differentiation by Regulating FGF18 Expression.” *Journal of Bone and Mineral Research* 22: 1234–44. https://doi.org/10.1359/JBMR.070503.

Bell, Donald M, Keith K H Leung, Susan C Wheatley, Ling Jim Ng, Sheila Zhou, Kam Wing Ling, Mai Har Sham, Peter Koopman, Patrick P L Tam, and Kathryn S E Cheah. 1997. “SOX9 Directly Regulates the Type-II Collagen Gene.” *Nature Genetics* 16: 7–11.

Benchabane, Hassina, and Jeffrey L Wrana. 2003. “GATA- and Smad1-Dependent Enhancers in the Smad7 Gene Differentially Interpret Bone Morphogenetic Protein Concentrations.” *Molecular and Cellular Biology* 23 (18): 6646–61. https://doi.org/10.1128/MCB.23.18.6646.

Bentley, George. 1975. “Articular Cartilage Studies Osteoarthrosis.” *Annals of the Royal College of Surgeons of England* 57: 86–100.

Berke, Brett, Jessica Wittnam, Elizabeth Mcneill, David L Van Vactor, and Haig Keshishian. 2013. “Retrograde BMP Signaling at the Synapse : A Permissive Signal for Synapse Maturation and Activity-Dependent Plasticity.” *Journal of Neuroscience* 33 (45): 17937–50. https://doi.org/10.1523/JNEUROSCI.6075-11.2013.

Berndt, Anthony J.E.; Tang, Jonathan C.Y.; Ridyard, Marc S.; Lian, Tianshun; Keatings, Kathleen and Allan, Douglas W. 2015. “Gene Regulatory Mechanisms Underlying the Spatial and Temporal Regulation of Target-Dependent Gene Expression in Drosophila Neurons.” *PLoS Genetics*, 1–27.

Berndt, Anthony J.E., Jonathan C.Y. Tang, Marc S. Ridyard, Tianshun Lian, Kathleen Keatings, and Douglas W. Allan. 2015. “Gene Regulatory Mechanisms Underlying the Spatial and Temporal Regulation of Target-Dependent Gene Expression in Drosophila Neurons.” *PLoS Genetics* 11 (12): 1–27. https://doi.org/10.1371/journal.pgen.1005754.

Bernstein, Bradley E., Tarjei S. Mikkelsen, Xiaohui Xie, Michael Kamal, Dana J. Huebert, James Cuff, Ben Fry, et al. 2006. “A Bivalent Chromatin Structure Marks Key Developmental Genes in Embryonic Stem Cells.” *Cell* 125 (2): 315–26. https://doi.org/10.1016/j.cell.2006.02.041.

Bi, Weimin, Jian Min Deng, Zhaoping Zhang, Richard R Behringer, and Benoit De Crombrugghe. 1999. “Sox9 Is Required for Cartilage Formation.” *Nature Genetics* 22: 85–89.

Bi, Weimin, Wendong Huang, Deanne J Whitworth, Jian Min Deng, Zhaoping Zhang, Richard R Behringer, and Benoit De Crombrugghe. 2001. “Haploinsufficiency of Sox9 Results in Defective Cartilage Primordia and Premature Skeletal Mineralization.” *Proc Natl Acad Sci USA* 98: 6698–6703 兩.

Binato, Renata, Cristina E. Alvarez Martinez, Luciana Pizzatti, Benoit Robert, and Eliana Abdelhay. 2006. “SMAD 8 Binding to Mice *Msx1* Basal Promoter Is Required for Transcriptional Activation.” *Biochemical Journal* 393 (1): 141–50. https://doi.org/10.1042/BJ20050327.

Bischof, J., R. K. Maeda, M. Hediger, F. Karch, and K. Basler. 2007. “An Optimized Transgenesis System for Drosophila Using Germ-Line-Specific C31 Integrases.” *Proceedings of the National Academy of Sciences* 104 (9): 3312–17. https://doi.org/10.1073/pnas.0611511104.

Blitz, IL Ira;, and Ken KW Cho. 2009. “Finding Partners: How BMPs Select Their Targets.” *Dev Dyn.* 238 (6): 1321–31. https://doi.org/10.1002/dvdy.21984.

Bobick, Brent E., Peter G. Alexander, and Rocky S. Tuan. 2014. “High Efficiency Transfection of Embryonic Limb Mesenchyme with Plasmid DNA Using Square Wave Pulse Electroporation and Sucrose Buffer.” *BioTechniques* 56 (2): 85–89. https://doi.org/10.2144/000114136.

Boros, Joanna, Nausica Arnoult, Vincent Stroobant, and Anabelle Decottignies. 2014. “Polycomb Repressive Complex 2 and H3K27me3 Cooperate with H3K9 Methylation To Maintain Heterochromatin Protein 1 ⎵ At.” *Molecular and Cellular Biology* 34 (19): 3662–74. https://doi.org/10.1128/MCB.00205-14.

Bradley, Elizabeth W, Lomeli R Carpio, Eric N Olson, and Jennifer J Westendorf. 2015. “Histone Deacetylase 7

(Hdac7) Suppresses Chondrocyte Proliferation and β-Catenin Activity during Endochondral." *Journal of Biological Chemistry* 290 (1): 118–26. https://doi.org/10.1074/jbc.M114.596247.

Bray, Nicolas L.;, Harold; Pimentel, Pall; Melsted, and Lior Pachter. 2016. "Near-Optimal Probabilistic RNA-Seq Quantification." *Nature Biotechnology* 34 (5): 525–28.

Bridgewater, Laura C, Marlan D Walker, Gwen C Miller, Trevor A Ellison, L Daniel Holsinger, Jennifer L Potter, Todd L Jackson, et al. 2003. "Adjacent DNA Sequences Modulate Sox9 Transcriptional Activation at Paired Sox Sites in Three Chondrocyte-Specific Enhancer Elements." *Nucleic Acids Research* 31 (5): 1541–53. https://doi.org/10.1093/nar/gkg230.

Bridgewater, Laura Clarke;, Veronique; Lefebvre, and Benoit De Crombrugghe. 1998. "Chondrocyte-Specific Enhancer Elements in the Col11a2 Gene Resemble the Col2a1 Tissue-Specific Enhancer." *Journal of Biological Chemistry* 273 (24): 14998–6.

Brocher, Jan, Benjamin Vogel, and Robert Hock. 2010. "HMGA1 Down-Regulation Is Crucial for Chromatin Composition and a Gene Expression Profile Permitting Myogenic Differentiation." *BMC Cell Biology* 11 (64): 1–12.

Brown, Carl O, Xuan Chi, Eduardo Garcia-Gras, Manabu Shirai, Xin-Hua Feng, and Robert J Schwartz. 2004. "The Cardiac Determination Factor, Nkx2-5 , Is Activated by Mutual Cofactors GATA-4 and Smad1/4 via a Novel Upstream Enhancer." *Journal of Biological Chemistry* 279 (11): 10659–69. https://doi.org/10.1074/jbc.M301648200.

Brugger, Sean M., Amy E. Merrill, Jesus Torres-Vazquez, Nancy Wu, Man Chun Ting, Jane Y.M. Cho, Sonia L. Dobias, et al. 2004. "A Phylogenetically Conserved Cis-Regulatory Module in the Msx2 Promoter Is Sufficient for BMP-Dependent Transcription in Murine and Drosophila Embryos." *Development* 131 (20): 5153–65. https://doi.org/10.1242/dev.01390.

Bulger, Michael, and Mark Groudine. 2011. "Functional and Mechanistic Diversity of Distal Transcription Enhancers." *Cell* 144 (3): 327–39. https://doi.org/10.1016/j.cell.2011.01.024.

Burke, Tara L, and Patrick A Grant. 2010. "Histone Acetylation Complexes." In *Handbook of Cell Signaling*, 2nd ed., 3:2369–78. Elsevier Inc. https://doi.org/10.1016/B978-0-12-374145-5.00285-0.

Butler, Jill S, Evangelia Koutelou, Andria C Schibler, and Sharon YR and Dent. 2012. "Histone-Modifying Enzymes: Regulators of Developmental Decisions and Drivers of Human Disease." *Epigenomics* 4 (2): 163–77. https://doi.org/10.2217/epi.12.3.Histone-modifying.

Byun, Sang Kyung, Tae Hyeon An, Min Jeong Son, Da Som Lee, Hyun Sup Kang, Eun-woo Lee, Baek Soo Han, et al. 2017. "HDAC11 Inhibits Myoblast Differentiation through Repression of MyoD-Dependent Transcription." *Molecules and Cells* 40 (9): 667–76.

Cairns, Dana M, Renjing Liu, Manpreet Sen, James P Canner, Aaron Schindeler, David G Little, and Li Zeng. 2012. "Interplay of Nkx3.2, Sox9 and Pax3 Regulates Chondrogenic Differentiation of Muscle Progenitor Cells." *PloS One* 7 (7): 1–17. https://doi.org/10.1371/journal.pone.0039642.

Calo, Eliezer;, and Joanna Wysocka. 2013. "Modification of Enhancer Chromatin: What, How and Why?" *Mol Cell* 49 (5): 1–24. https://doi.org/10.1016/j.molcel.2013.01.038.Modification.

Candia, Albert F, Jinxin Hu, Jeffrey Crosby, Peter A Lalley, Drew Noden, Joseph Nadeau, and Christopher V E Wright. 1992. "Mox-1 and Mox-2 Define a Novel Homeobox Gene Subfamily and Are Differentially Expressed during Early Mesodermal Patterning in Mouse Embryos." *Development* 116: 1123–36.

Candia, Albert F, and Christopher V E Wright. 1996. "Differential Localization of Mox-1 and Mox-2 Proteins Indicates Distinct Roles during Development." *Int. J. Dev. Biol.* 40: 1179–84.

Capdevila, Javier, Tohru Tsukui, Concepción Rodríguez Esteban, Vincenzo Zappavigna, and Juan Carlos Izpisúa Belmonte. 1999. "Control of Vertebrate Limb Outgrowth by the Proximal Factor Meis2 and Distal

Antagonism of BMPs by Gremlin." *Molecular Cell* 4: 839–49. https://doi.org/10.1016/S1097-2765(00)80393-7.

Carbon, Seth, Amelia Ireland, Christopher J Mungall, Shengqiang Shu, Brad Marshall, Suzanna Lewis, Amigo Hub, and Web Presence. 2009. "AmiGO: Online Access to Ontology and Annotation Data." *Bioinformatics* 25 (2): 288–89. https://doi.org/10.1093/bioinformatics/btn615.

Cardelli, Marco, and Jane E Aubin. 2014. "ERRgamma Is Not Required for Skeletal Development but Is a RUNX2-Dependent Negative Regulator of Postnatal Bone Formation in Male Mice." *PloS One* 9 (10): 1–11. https://doi.org/10.1371/journal.pone.0109592.

Cash, David E, Cheryl B Bock, Klaus Schughart, Elwood Linney, and T Michael Underhill. 1997. "Retinoic Acid Receptor α Function in Vertebrate Limb Skeletogenesis: A Modulator of Chondrogenesis." *Journal of Cell Biology* 136 (2): 445–57.

Chai, Nan, Wan-xin Li, Jue Wang, Zhi-xin Wang, Shi-ming Yang, and Jia-wei Wu. 2015. "Structural Basis for the Smad5 MH1 Domain to Recognize Different DNA Sequences." *Nucleic Acids Research* 43 (18): 9051–64. https://doi.org/10.1093/nar/gkv848.

Chantry, Andrew. 2011. "WWP2 Ubiquitin Ligase and Its Isoforms: New Biological Insight and Promising Disease Targets." *Cell Cycle* 10 (15): 2437–39. https://doi.org/10.4161/cc.10.15.16874.

Chen, Li, Trine Fink, Xiao-yan Zhang Peter, Ebbesen Vladimir Zachar, Li Chen, Á Trine Fink, Á Peter Ebbesen, and Á Vladimir Zachar. 2005. "Quantitative Transcriptional Profiling of ATDC5 Mouse Progenitor Cells during Chondrogenesis." *Differentiation* 73 (7): 350–63. https://doi.org/10.1111/j.1432-0436.2005.00038.x.

Chen, Weiwei, Xinli Zhang, Ronald K Siu, Feng Chen, Jia Shen, Janette N Zara, Cymbeline T Culiat, Sotirios Tetradis, Kang Ting, and Chia Soo. 2011. "Nfatc2 Is a Primary Response Gene of Nell-1 Regulating Chondrogenesis in ATDC5 Cells." *Journal of Bone and Mineral Research* 26 (6): 1230–41. https://doi.org/10.1002/jbmr.314.

Cheng, Aixin, and Paul Genever. 2010. "SOX9 Determines RUNX2 Transactivity by Directing Intracellular Degradation." *Journal of Bone and Mineral Research* 25 (12): 2680–89. https://doi.org/10.1002/jbmr.174.

Cheng, Su-li, Jian-su Shao, Nichole Charlton-Kachigian, Arleen P Loewy, and Dwight A Towler. 2003. "Msx2 Promotes Osteogenesis and Suppresses Adipogenic Differentiation of Multipotent Mesenchymal Progenitors." *The Journal of Biological Chemistry* 278 (46): 45969–77. https://doi.org/10.1074/jbc.M306972200.

Chimal-Monroy, J, J Rodriguez-Leon, J Montero, Y Ganan, D Macias, R Merino, and J Hurle. 2003. "Analysis of the Molecular Cascade Responsible for Mesodermal Limb Chondrogenesis: Sox Genes and BMP Signaling." *Developmental Biology* 257: 292–301. https://doi.org/10.1016/S0012-1606(03)00066-6.

Chintapalli, Venkateswara R, Jing Wang, and Julian A T Dow. 2007. "Using FlyAtlas to Identify Better Drosophila Melanogaster Models of Human Disease." *Nature Genetics Perspective* 39 (6): 715–20. https://doi.org/10.1038/ng2049.

Cho, Ken W.Y. 2012. "Enhancers: WIRE Review." *Wiley Interdiscip Rev Dev Biol.* 1 (4): 469–78. https://doi.org/10.1002/wdev.53.Enhancers.

Cleary, Mairéad A, Gerjo J V M Van Osch, Pieter A Brama, Catharine A Hellingman, and Roberto Narcisi. 2015. "FGF, TGF b and Wnt Crosstalk: Embryonic to in Vitro Cartilage Development from Mesenchymal Stem Cells." *Journal of Tissue Engineering and Regenerative Medicine* 9: 332–42. https://doi.org/10.1002/term.

Conrad, Willliam, Michael B Major, Michele A Cleary, Marc Ferrer, Shane Marine, Namjin Chung, William T Arthur, Randall T Moon, Jason D Berndt, and Andy J Chien. 2013. "FAM129B Is a Novel Regulator of Wnt / β-Catenin Signal Transduction in Melanoma Cells." *F1000Research* 2 (134): 1–17. https://doi.org/10.12688/f1000research.2-134.v1.

Correa, Diego, Eric Hesse, Dutmanee Seriwatanachai, Riku Kiviranta, Kei Yamana, Lynn Neff, Azeddine Atfi, et al.

2010. “Zfp521 Is a Target Gene and Key Effector of Parathyroid Hormone-Related Peptide Signaling in Growth Plate Chondrocytes.” *Developmental Cell* 19 (4): 533–46. https://doi.org/10.1016/j.devcel.2010.09.008.Zfp521.

Craymer, L. 1984. “Synthesis of a Ring Third Chormosome and Its Use in Inserting Markers into Ln(3R)C.” *Drosophila Inform. Serv.*, 3 (60): 234–36.

Creyghton, M. P.;, W.; Cheng, A., G.G.; Welstead, T.; Kooistra, B.W.; Carey, Eveline J.; Steine, Jacob; Hanna, et al. 2010. “Histone H3K27ac Separates Active from Poised Enhancers and Predicts Developmental State.” *PNAS* 107 (50): 21931–36. https://doi.org/10.1073/pnas.

Crocker, Justin, Namiko Abe, Lucrezia Rinaldi, Alistair P. Mcgregor, Nicolas Frankel, Shu Wang, Ahmad Alsawadi, et al. 2015. “Low Affinity Binding Site Clusters Confer Hox Specificity and Regulatory Robustness.” *Cell* 160: 191–203. https://doi.org/10.1016/j.cell.2014.11.041.

Crocker, Justin, Ella Preger-ben Noon, and David L Stern. 2016. “The Soft Touch: Low-Affinity Transcription Factor Binding Sites in Development and Evolution.” In *Essays on Developmental Biology Part B*, 1st ed., 117:455–69. Elsevier Inc. https://doi.org/10.1016/bs.ctdb.2015.11.018.

Csaki, Lauren S, Jennifer R Dwyer, Xia Li, Michael H K Nguyen, Jay Dewald, David N Brindley, Aldons Lusis, et al. 2014. “Lipin-1 and Lipin-3 Together Determine Adiposity in Vivo.” *Molecular Metabolism* 3: 145–54. https://doi.org/10.1016/j.molmet.2013.11.008.

D. Allan, S. St. Pierre, I. Miguel-Aliaga and S. Thor. 2003. “Specification of Neuropeptide Cell Identity by the Integration of Retrograde BMP Signaling and a Combinatorial Transcription Factor Code.” *Cell* 113: 73–86.

Dailey, Lisa. 2015. “High Throughput Technologies for the Functional Discovery of Mammalian Enhancers: New Approaches for Understanding Transcriptional Regulatory Network Dynamics.” *Genomics* 106 (3): 151–58. https://doi.org/10.1016/j.ygeno.2015.06.004.

Daish, C;, R; Blanchard, K; Fox, P; Pivonka, and E Pirogova. 2018. “The Application of Pulsed Electromagnetic Fields (PEMFs) for Bone Fracture Repair: Past and Perspective Findings.” *Annals of Biomedical Engineering* 46 (4): 525–42. https://doi.org/10.1007/s10439-018-1982-1.

Daoud, Georges, Herve Kempf, Deepak Kumar, Elena Kozhemyakina, Tamara Holowacz, Dae-won Kim, Andreia Ionescu, and Andrew B Lassar. 2014. “BMP-Mediated Induction of GATA4/5/6 Blocks Somitic Responsiveness to SHH.” *Development* 141: 3978–87. https://doi.org/10.1242/dev.111906.

Das, Pradeep, Lisa L Maduzia, Huang Wang, Alyce L Finelli, Seo-hee Cho, Marsha M Smith, and Richard W Padgett. 1998. “The Drosophila Gene Medea Demonstrates the Requirement for Different Classes of Smads in Dpp Signaling.” *Development* 125: 1519–28.

Dehne, Tilo, Rita Schenk, Carsten Perka, Lars Morawietz, Axel Pruss, Michael Sittinger, Christian Kaps, and Jochen Ringe. 2010. “Gene Expression Profiling of Primary Human Articular Chondrocytes in High-Density Micromasses Reveals Patterns of Recovery, Maintenance, Re- and Dedifferentiation.” *Gene* 462: 8–17. https://doi.org/10.1016/j.gene.2010.04.006.

Deignan, Lisa, Marco T Pinheiro, Catherine Sutcliffe, Abbie Saunders, G Wilcockson, Leo A H Zeef, Ian J Donaldson, and Hilary L Ashe. 2016. “Regulation of the BMP Signaling-Responsive Transcriptional Network in the Drosophila Embryo.” *PLoS Genetics* 12 (7): 1–23. https://doi.org/10.1371/journal.pgen.1006164.

Dobin, Alexander, Carrie A Davis, Felix Schlesinger, Jorg Drenkow, Chris Zaleski, Sonali Jha, Philippe Batut, Mark Chaisson, and Thomas R Gingeras. 2013. “STAR: Ultrafast Universal RNA-Seq Aligner.” *Bioinformatics* 29 (1): 15–21. https://doi.org/10.1093/bioinformatics/bts635.

Dong, Yufeng, Alana M Jesse, Anat Kohn, Lea M Gunnell, Tasuku Honjo, Michael J Zuscik, Regis J O Keefe, and Matthew J Hilton. 2010. “RBPjk-Dependent Notch Signaling Regulates Mesenchymal Progenitor Cell Proliferation and Differentiation during Skeletal Development.” *Development* 1471: 1461–71.

https://doi.org/10.1242/dev.042911.

Dorighi, Kristel M, Tomek Swigut, Telmo Henriques, Natarajan V Bhanu, Benjamin S Scruggs, Nataliya Nady, Christopher Still, Benjamin A Garcia, Karen Adelman, and Joanna Wysocka. 2017. “Mll3 and Mll4 Facilitate Enhancer RNA Synthesis and Transcription from Promoters Independently of H3K4 Monomethylation.” *Molecular Cell* 66: 568-576.e4. https://doi.org/10.1016/j.molcel.2017.04.018.

Douglas, Adam T., and Robert E. Hill. 2014. “Variation in Vertebrate Cis-Regulatory Elements in Evolution and Disease.” *Transcription* 5 (MAY). https://doi.org/10.4161/trns.28848.

Dréau, Gwenvael Le, Murielle Saade, Irene Gutiérrez-vallejo, and Elisa Martí. 2014. “The Strength of SMAD1/5 Activity Determines the Mode of Stem Cell Division in the Developing Spinal Cord.” *Journal of Cell Biology* 204 (4): 591–605. https://doi.org/10.1083/jcb.201307031.

Drissi, M Hicham, Xufeng Li, Tzong J Sheu, Michael J Zuscik, Edward M Schwarz, J Edward Puzas, Randy N Rosier, and Regis J O Keefe. 2003. “Runx2 / Cbfa1 Stimulation by Retinoic Acid Is Potentiated by BMP2 Signaling Through Interaction With Smad1 on the Collagen X Promoter in Chondrocytes.” *Journal of Cellular Biochemistry* 90: 1287–98. https://doi.org/10.1002/jcb.10677.

Dy, Peter, Weihuan Wang, Pallavi Bhattaram, Qiuqing Wang, Lai Wang, R. Tracy Ballock, and Véronique Lefebvre. 2012. “Sox9 Directs Hypertrophic Maturation and Blocks Osteoblast Differentiation of Growth Plate Chondrocytes.” *Developmental Cell* 22 (3): 597–609. https://doi.org/10.1016/j.devcel.2011.12.024.Sox9.

Eade, K. T., and D. W. Allan. 2009. “Neuronal Phenotype in the Mature Nervous System Is Maintained by Persistent Retrograde Bone Morphogenetic Protein Signaling.” *Journal of Neuroscience* 29 (12): 3852–64. https://doi.org/10.1523/JNEUROSCI.0213-09.2009.

El-Magd, Mohammed Abu, Steve Allen, Imelda McGonnell, Ali A Mansour, Anthony Otto, and Ketan Patel. 2015. “Shh Regulates Chick Ebf1 Gene Expression in Somite Development.” *Gene* 554: 87–95. https://doi.org/10.1016/j.gene.2014.10.028.

Evans, Nicole C, Christina I Swanson, and Scott Barolo. 2012. *Sparkling Insights into Enhancer Structure, Function, and Evolution*. *Current Topics in Developmental Biology: Transcriptional Switches During Development*. 1st ed. Vol. 98. Elsevier Inc. https://doi.org/10.1016/B978-0-12-386499-4.00004-5.

Farley, Emma K.;, Katrina M.; Olson, Wei; Zhang, Alexander J.; Brandt, Daniel S.; Rokhsar, and Michael S. and Levine. 2015. “Suboptimization of Developmental Enhancers.” *Science* 350 (6258): 325–28. https://doi.org/10.1126/science.aac6948.Suboptimization.

Ferguson, Christine A, Abigail S Tucker, and Paul T Sharpe. 2000. “Temporospatial Cell Interactions Regulating Mandibular and Maxillary Arch Patterning.” *Development* 127: 403–12.

Furumatsu, Takayuki, Masanao Tsuda, Noboru Taniguchi, Yoshitaka Tajima, and Hiroshi Asahara. 2005. “Smad3 Induces Chondrogenesis through the Activation of SOX9 via CREB-Binding Protein/P300 Recruitent.” *Journal of Biological Chemistry* 280 (9): 8343–50. https://doi.org/10.1074/jbc.M413913200.

Gadi, Jogeswar, Seung-Hyun Jung, Min-Jung Lee, Ajita Jami, Kalyani Ruthala, Kyoung-Min Kim, Nam-Hoon Cho, Han-Sung Jung, Cheol-Hee Kim, and Sung-Kil Lim. 2013. “The Transcription Factor Protein Sox11 Enhances Early Osteoblast Differentiation by Facilitating Proliferation and the Survival of Mesenchymal and Osteoblast Progenitors.” *Journal of Biological Chemistry* 288 (35): 25400–413. https://doi.org/10.1074/jbc.M112.413377.

Gao, Sheng, and Allen Laughon. 2006. “Decapentaplegic-Responsive Silencers Contain Overlapping.” *Journal of Biol* 281 (35): 25781–90. https://doi.org/10.1074/jbc.M603371200.

———. 2007. “Flexible Interaction of Drosophila Smad Complexes with Bipartite Binding Sites” 1769: 484–96. https://doi.org/10.1016/j.bbaexp.2007.05.006.

Gao, Sheng, Janet Steffen, and Allen Laughon. 2005. “Dpp-Responsive Silencers Are Bound by a Trimeric” 280

(43): 36158–64. https://doi.org/10.1074/jbc.M506882200.

García, Amaya, De Vinuesa, Salim Abdelilah-seyfried, Petra Knaus, An Zwijsen, and Sabine Bailly. 2016. "Cytokine & Growth Factor Reviews BMP Signaling in Vascular Biology and Dysfunction." *Cytokine and Growth Factor Reviews* 27: 65–79. https://doi.org/10.1016/j.cytogfr.2015.12.005.

Garside, Victoria C, Rebecca Cullum, Olivia Alder, Daphne Y Lu, Ryan Vander Werff, Mikhail Bilenky, Yongjun Zhao, et al. 2015. "SOX9 Modulates the Expression of Key Transcription Factors Required for Heart Valve Development." *Development* 142: 4340–50. https://doi.org/10.1242/dev.125252.

Gaulton, Kyle J, Takao Nammo, Lorenzo Pasquali, Jeremy M Simon, Paul G Giresi, Marie P Fogarty, Tami M Panhuis, et al. 2010. "A Map of Open Chromatin in Human Pancreatic Islets." *Nature Publishing Group* 42 (3): 255–59. https://doi.org/10.1038/ng.530.

Gazzerro, Elisabetta, and Ernesto Canalis. 2006. "Bone Morphogenetic Proteins and Their Antagonists." *Rev Endocr Metab Disord* 7: 51–65. https://doi.org/10.1007/s11154-006-9000-6.

Gerard, Deborah, Florian Schmidt, Martine Schmitz, Rashi Halder, Peter Ebert, Marcel H Schulz, Thomas Sauter, and Lasse Sinkkonen. 2019. "Temporal Enhancer Profiling of Parallel Lineages Identifies AHR and GLIS1 as Regulators of Mesenchymal Multipotency." *Nucleic Acids Research* 47 (3): 1141–63. https://doi.org/10.1093/nar/gky1240.

Ghanem, Noël, Olga Jarinova, Angel Amores, Qiaoming Long, Gary Hatch, Byung Keon Park, John L R Rubenstein, and Marc Ekker. 2003. "Regulatory Roles of Conserved Intergenic Domains in Vertebrate Dlx Bigene Clusters." *Genome Research* 13: 533–43. https://doi.org/10.1101/gr.716103.1.

Ghanem, Noel, Man Yu, Jason Long, Gary Hatch, John L R Rubenstein, and Marc Ekker. 2007. "Distinct Cis-Regulatory Elements from the Dlx1/Dlx2 Locus Mark Different Progenitor Cell Populations in the Ganglionic Eminences and Different Subtypes of Adult Cortical Interneurons." *The Journal of Neuroscience* 27 (19): 5012–22. https://doi.org/10.1523/JNEUROSCI.4725-06.2007.

Gibson, Gary. 1998. "Active Role of Chondrocyte Apoptosis in Endochondral Ossification." *MICROSCOPY RESEARCH AND TECHNIQUE* 43: 191–204.

Goldring, Mary B, Kaneyuki Tsuchimochi, and Kosei Ijiri. 2006. "The Control of Chondrogenesis." *Journal of Cellular Biochemistry* 97: 33–44. https://doi.org/10.1002/jcb.20652.

Gong, Yaoqin, Deborah Krakow, Jose Marcelino, Douglas Wilkin, David Chitayat, Riyana Babul-hirji, Louanne Hudgins, et al. 1999. "Heterozygous Mutations in the Gene Encoding Noggin Affect Human Joint Morphogenesis." *Nature Genetics* 21: 302–4.

Grabherr, Manfred, Brian Hass, Moran Yassour, Joshua Levin, Dawn Thompson, Ido Amit, Xian Adiconis, et al. 2011. "Trinity: Reconstructing a Full-Length Transcriptome without a Genome from RNA-Seq Data." *Nature Biotechnology* 29 (7): 644–52. https://doi.org/10.1038/nbt.1883.Trinity.

Greer, Eric and Shi, Yang. 2012. "Histone Methylation: A Dynamic Mark in Health, Disease and Inheritance." *Nature Reviews Genetics* 13 (5): 343–57. https://doi.org/10.1038/nrg3173.Histone.

Groth, Amy; Fish, Matthew; Nusse, Roel and Calos, Michele P. 2004. "Construction of Transgenic Drosophila by Using the Site-Specific Integrase From Phage PhiC31." *Genetics* 166: 1775–82. https://doi.org/10.1534/genetics.166.4.1775.

Guan Yang, Liang Zhu, Ning Hou, Yu Lan, Xi-Mei Wu, Bin Zhou, and Xiao Yang Yan Teng. 2014. "Osteogenic Fate of Hypertrophic Chondrocytes." *Cell Research* 24 (10): 1266–69. https://doi.org/10.1038/cr.2014.111.

Guenther, Matthew G, Stuart S Levine, Laurie A Boyer, Rudolf Jaenisch, and Richard A Young. 2007. "A Chromatin Landmark and Transcription Initiation at Most Promoters in Human Cells." *Cell* 130 (1): 77–88. https://doi.org/10.1016/j.cell.2007.05.042.A.

Guo, Fengjin, Xiaofeng Han, Zhimeng Wu, Zhi Cheng, Qin Hu, Yunpeng Zhao, and Yingxiong Wang. 2016. “ATF6a, a Runx2-Activable Transcription Factor, Is a New Regulator of Chondrocyte Hypertrophy.” *Journal of Cell Science* 129: 717–28. https://doi.org/10.1242/jcs.169623.

Guo, Haitao, and Hongwei Huo. 2017. “A New Algorithm for Identifying Cis-Regulatory Modules Based on Hidden Markov Model.” *BioMed Research International*.

Gurusinghe, Saliya, Nadeeka Bandara, Bryan Hilbert, Gareth Trope, Lexin Wang, and Padraig Strappe. 2019. “Lentiviral Vector Expression of Klf4 Enhances Chondrogenesis and Reduces Hypertrophy in Equine Chondrocytes.” *Gene* 680: 9–19. https://doi.org/10.1016/j.gene.2018.09.013.

Halfon, Marc S, Stephen Gisselbrecht, Jun Lu, Beatriz Estrada, Haig Keshishian, Alan M Michelson, and Uas-xeyfp Ah. 2002. “New Fluorescent Protein Reporters for Use With the Drosophila Gal4 Expression System and for Vital Detection of Balancer Chromosomes.” *Genesis* 138 (1–2): 135–38. https://doi.org/10.1002/gene.10136.

Hamaratoglu, Fisun, Markus Affolter, and George Pyrowolakis. 2014. “Dpp/BMP Signaling in Flies: From Molecules to Biology.” *Seminars in Cell and Developmental Biology* 32: 128–36. https://doi.org/10.1016/j.semcdb.2014.04.036.

Han, Yu, and Veronique; Lefebvre. 2008. “L-Sox5 and Sox6 Drive Expression of the Aggrecan Gene in Cartilage by Securing Binding of Sox9 to a Far-Upstream Enhancer □.” *Molecular and Cellular Biology* 28 (16): 4999–5013. https://doi.org/10.1128/MCB.00695-08.

Hanai, Jun-ichi, Lin Feng Chen, Tomohiko Kanno, Naoko Ohtani-fujita, Woo Young Kim, Wei-hui Guo, Takeshi Imamura, et al. 1999. “Interaction and Functional Cooperation of PEBP2 / CBF with Smads.” *Journal of Biological Chemistry* 274 (44): 31577–82.

Hardingham, Timothy E, Rachel A Oldershaw, and Simon R Tew. 2006. “Cartilage, SOX9 and Notch Signals in Chondrogenesis.” *Journal of Anatomy* 209: 469–80. https://doi.org/10.1111/j.1469-7580.2006.00630.x.

Hardison, R.C. and Taylor, J. 2012. “Genomic Approaches towards Finding Cis-Regulatory Modules in Animals.” *Nature Reviews Genetics* 13: 469–83.

Hardison, Ross C. and Taylor, James. 2012. “Genomic Approaches towards Finding Cis-Regulatory Modules in Animals.” *Nature Reviews Genetics* 13: 469–83.

Hassan, Mohammad Q, Rahul S Tare, Suk Hee Lee, Matthew Mandeville, Maria I Morasso, Amjad Javed, Andre J Van Wijnen, Janet L Stein, Gary S Stein, and Jane B Lian. 2006. “BMP2 Commitment to the Osteogenic Lineage Involves Activation of Runx2 by DLX3 and a Homeodomain Transcriptional Network.” *Journal of Biological Chemistry* 281 (52): 40515–26. https://doi.org/10.1074/jbc.M604508200.

Hata, Akiko, Joan Seoane, Giorgio Lagna, Ermelinda Montalvo, Ali Hemmati-brivanlou, and Joan Massague. 2000. “OAZ Uses Distinct DNA- and Protein-Binding Zinc Fingers in Separate BMP-Smad and Olf Signaling Pathways.” *Cell* 100: 229–40.

Heintzman, Nathaniel D., Rhona K. Stuart, Gary Hon, Yutao Fu, Christina W. Ching, R. David Hawkins, Leah O. Barrera, et al. 2007. “Distinct and Predictive Chromatin Signatures of Transcriptional Promoters and Enhancers in the Human Genome.” *Nature Genetics* 39 (3): 311–18. https://doi.org/10.1038/ng1966.

Heintzman, Nathaniel D, Gary C Hon, R David Hawkins, Pouya Kheradpour, Alexander Stark, Lindsey F Harp, Zhen Ye, et al. 2009. “Histone Modifications at Human Enhancers Reflect Global Cell Type-Specific Gene Expression.” *Nature* 459 (7243): 108–12. https://doi.org/10.1038/nature07829.Histone.

Heinz, Sven, Christopher Benner, Nathanael Spann, Eric Bertolino, Yin C Lin, Peter Laslo, Jason X Cheng, Cornelis Murre, Harinder Singh, and K Christopher. 2011. “Simple Combinations of Lineage-Determining Transcription Factors Prime Cis-Regulatory Elements Required for Macrophage and B Cell Identities.” *Mol Cell* 38 (4): 576–89. https://doi.org/10.1016/j.molcel.2010.05.004.Simple.

Heldin, Carl-Henrik, Kohei Miyazono, and Peter ten Dijke. 1997. “TGF-β Signalling from Cell Membrane to

Nucleus through SMAD Proteins." *Nature* 390 (December): 465. https://doi.org/10.1038/37284.

Henningfeld, Kristine A, Henner Friedle, Sepand Rastegar, and Walter Kno. 2002. "Autoregulation of Xvent-2B; Direct Interaction and Functional Cooperation of Xvent-2 and Smad1." *Journal of Biological Chemistry* 277 (3): 2097–2103. https://doi.org/10.1074/jbc.M108524200.

Henriques, Telmo, Benjamin S. Scruggs, Michiko O. Inouye, Ginger W. Muse, Lucy H. Williams, Adam B. Burkholder, Christopher A. Lavender, David C. Fargo, and Karen Adelman. 2018. "Widespread Transcriptional Pausing and Elongation Control at Enhancers." *Genes and Development* 32 (1): 26–41. https://doi.org/10.1101/gad.309351.117.

Hill, Caroline S. 2016. "Transcriptional Control by the SMADs." *Cold Spring Harbor Perspectives in Biology*.

Hippenmeyer, Simon, Ina Kramer, and Silvia Arber. 2004. "Control of Neuronal Phenotype : What Targets Tell the Cell Bodies." *Trends in Neurosciences* 27 (8). https://doi.org/10.1016/j.tins.2004.05.012.

Hobert, Oliver; Carrera, Ines; Stefanakis, Nikolaos. 2010. "The Molecular and Gene Regulatory Signature of a Neuron." *Trends in Neurosciences* 33 (10): 435–45. https://doi.org/10.1016/j.tins.2010.05.006.

Hoffman, Lisa M, Kamal Garcha, Konstantina Karamboulas, Matthew F Cowan, Linsay M Drysdale, William A Horton, and T Michael Underhill. 2006. "BMP Action in Skeletogenesis Involves Attenuation of Retinoid Signaling." *Journal of Cell Biology* 174 (1): 101–13. https://doi.org/10.1083/jcb.200604150.

Hojo, Hironori, Ung-il Chung, and Shinsuke Ohba. 2017. "Identification of the Gene-Regulatory Landscape in Skeletal Development and Potential Links to Skeletal Regeneration." *Regenerative Therapy* 6: 100–107. https://doi.org/10.1016/j.reth.2017.04.001.

Hojo, Hironori, Andrew P Mcmahon, and Shinsuke Ohba. 2016. "An Emerging Regulatory Landscape for Skeletal Development." *Trends in Genetics* 32 (12): 774–87. https://doi.org/10.1016/j.tig.2016.10.001.

Hollnagel, Angela, Verena Oehlmann, Joachim Heymer, Ulrich Ru, and Alfred Nordheim. 1999. "Id Genes Are Direct Targets of Bone Morphogenetic Protein Induction in Embryonic Stem Cells." *The Journal of Biological Chemistry* 274 (28): 19838–45.

Horton, W;, T; Miyashita, K; Kohno, J R; Hassell, and Y Yamada. 1987. "Identification of a Phenotype-Specific Enhancer in the First Intron of the Rat Collagen II Gene." *Proc Natl Acad Sci USA* 84: 8864–68.

Hou, Zhenyang, Zhen Wang, Yunxia Tao, Jiaxiang Bai, Binqing Yu, Jining Shen, Houyi Sun, et al. 2019. "KLF2 Regulates Osteoblast Differentiation by Targeting of Runx2." *Laboratory Investigation* 99 (2): 271–80. https://doi.org/10.1038/s41374-018-0149-x.

Hu, Ming Chang, and Norman D Rosenblum. 2005. "Smad1 , β-Catenin and Tcf4 Associate in a Molecular Complex with the Myc Promoter in Dysplastic Renal Tissue and Cooperate to Control Myc Transcription." *Development* 132: 215–25. https://doi.org/10.1242/dev.01573.

Hu, Xiaoming, Yuanfei Zhou, Yang Yang, Jie Peng, Tongxing Song, Tao Xu, Hongkui Wei, Siwen Jiang, and Jian Peng. 2016. "Identification of Zinc Finger Protein Bcl6 as a Novel Regulator of Early Adipose Commitment." *Open Biology* 6: 1–14.

Huang, He, Benjamin R Sabari, Benjamin A Garcia, C David Allis, and Yingming Zhao. 2014. "SnapShot: Histone Modifi Cations." *Cell* 159 (2): 458-458.e1. https://doi.org/10.1016/j.cell.2014.09.037.

Huang, Kui;, Qing; Li, Yong; Li, Zhihao; Yao, Daowen; Luo, Pengcheng; Rao, and Jingang Xiao. 2018. "Cartilage Tissue Regeneration: The Roles of Cells, Stimulating Factors and Scaffolds." *Current Stem Cell Research & Therapy* 13: 547. https://doi.org/10.2174/1574888X12666170608080722.

Hudson, John B, Steven D Podos, Kallie Keith, Susan L Simpson, and Edwin L Ferguson. 1998. "The Drosophila Medea Gene Is Required Downstream of Dpp and Encodes a Functional Homolog of Human Smad4." *Development* 125 (8): 1407–20. http://www.ncbi.nlm.nih.gov/pubmed/9502722.

Huey, Daniel J.;, Jerry C.; Hu, and Kyriacos A. Athanasiou. 2012. “Unlike Bone, Cartilage Regeneration Remains Elusive.” *Science* 338 (6109): 917–21. https://doi.org/10.1126/science.1222454.Unlike.

Hussain, S, M Sun, Y Guo, N Mushtaq, Y Zhao, Y Yuan, N Hussain, et al. 2018. “SFMBT2 Positively Regulates SOX9 and Chondrocyte Proliferation.” *Journal of Molecular Medicine* 42: 3503–12.

Ichida, Fumitaka, Riko Nishimura, Kenji Hata, Takuma Matsubara, Fumiyo Ikeda, Kunihiro Hisada, Hirofumi Yatani, et al. 2004. “Reciprocal Roles of Msx2 in Regulation of Osteoblast and Adipocyte Differentiation.” *The Journal of Biological Chemistry* 279 (32): 34015–22. https://doi.org/10.1074/jbc.M403621200.

Inoue, Fumitaka, Martin Kircher, Beth Martin, Gregory M Cooper, Daniela M Witten, Michael T Mcmanus, Nadav Ahituv, and Jay Shendure. 2017. “A Systematic Comparison Reveals Substantial Differences in Chromosomal versus Episomal Encoding of Enhancer Activity.” *Genome Research* 27: 38–52. https://doi.org/10.1101/gr.212092.116.7.

Ishida, Wataru, Toshiaki Hamamoto, Kiyoshi Kusanagi, and Ken Yagi. 2000. “Smad6 Is a Smad1/5-Induced Smad Inhibitor.” *Journal of Biological Chemistry* 275 (9): 6075–79. https://doi.org/10.1074/jbc.275.9.6075.

Ishida, Wataru, Toshiaki Hamamoto, Kiyoshi Kusanagi, Ken Yagi, Masahiro Kawabata, Kazuhiko Takehara, T Kuber Sampath, Mitsuyasu Kato, and Kohei Miyazono. 2000. “Smad6 Is a Smad1 / 5-Induced Smad Inhibitor.” *Journal of Biological Chemistry* 275 (9): 6075–79.

Ito, K, Z Maruyama, A Sakai, S Izumi, T Moriishi, C A Yoshida, T Miyazaki, et al. 2014. “Overexpression of Cdk6 and Ccnd1 in Chondrocytes Inhibited Chondrocyte Maturation and Caused P53-Dependent Apoptosis without Enhancing Proliferation.” *Oncogene*, 1862–71. https://doi.org/10.1038/onc.2013.130.

Jaeger, Savina A, Esther T Chan, Michael F Berger, Rolf Stottmann, Timothy R Hughes, and Martha L Bulyk. 2010. “Genomics Conservation and Regulatory Associations of a Wide Affinity Range of Mouse Transcription Factor Binding Sites.” *Genomics* 95 (4): 185–95. https://doi.org/10.1016/j.ygeno.2010.01.002.

James, Claudine G, C Thomas G Appleton, Veronica Ulici, T Michael Underhill, and Frank Beier. 2005. “Microarray Analyses of Gene Expression during Chondrocyte Differentiation Identifies Novel Regulators of Hypertrophy.” *Molecular Biology of the Cell* 16: 5316–33. https://doi.org/10.1091/mbc.E05.

James, Claudine G, Anita Woods, T Michael Underhill, and Frank Beier. 2006. “The Transcription Factor ATF3 Is Upregulated during Chondrocyte Differentiation and Represses Cyclin D1 and A Gene Transcription.” *BMC Molecular Biology* 11: 1–11. https://doi.org/10.1186/1471-2199-7-30.

Javier, Anna L, Linda T Doan, Mui Luong, N Soledad Reyes De Mochel, Aixu Sun, Edwin S Monuki, and Ken W Y Cho. 2012. “Bmp Indicator Mice Reveal Dynamic Regulation of Transcriptional Response.” *PloS One* 7 (9). https://doi.org/10.1371/journal.pone.0042566.

Jenkins, Elizabeth;, Jennie B.; Moss, James M.; Pace, and Laura C. Bridgewater. 2005. “The New Collagen Gene COL27A1 Contains SOX9-Responsive Enhancer Elements.” *Matrix Biology* 24 (3): 177–84. https://doi.org/10.1016/j.matbio.2005.02.004.The.

Jeong, Byung-chul, Yong-soo Lee, Yun-yong Park, In-ho Bae, Don-kyu Kim, Seung-hoi Koo, Hong-ran Choi, et al. 2009. “The Orphan Nuclear Receptor Estrogen Receptor-Related Receptor Gamma-Negatively Regulates BMP2-Induced Osteoblast Differentiation and Bone Formation.” *Journal of Biological Chemistry* 284 (21): 14211–18. https://doi.org/10.1074/jbc.M808345200.

Jeong, Juhee, Xue Li, Robert J Mcevilly, Michael G Rosenfeld, Thomas Lufkin, and John L R Rubenstein. 2008. “Dlx Genes Pattern Mammalian Jaw Primordium by Regulating Both Lower Jaw-Specific and Upper Jaw-Specific Genetic Programs.” *Development* 2916: 2905–16. https://doi.org/10.1242/dev.019778.

Ji, Quanbo, Xiaojie Xu, Lei Kang, Yameng Xu, Jingbo Xiao, Stuart B Goodman, Xiang Zhu, et al. 2019. “Hematopoietic PBX-Interacting Protein Mediates Cartilage Degeneration during the Pathogenesis of Osteoarthritis.” *Nature Communications* 10: 1–15. https://doi.org/10.1038/s41467-018-08277-5.

Jin, Chunyuan, Kohsuke Kato, Takahiko Chimura, Takahito Yamasaki, Koji Nakade, Takehide Murata, Hongjie Li, et al. 2006. “Regulation of Histone Acetylation and Nucleosome Assembly by Transcription Factor JDP2.” *Nature Structural and Molecular Biology* 13 (4): 331–38. https://doi.org/10.1038/nsmb1063.

Jin, Chunyuan, Hongjie Li, Takehide Murata, Kailai Sun, Masami Horikoshi, Robert Chiu, and Kazunari K Yokoyama. 2002. “JDP2 , a Repressor of AP-1 , Recruits a Histone Deacetylase 3 Complex To Inhibit the Retinoic Acid-Induced Differentiation of F9 Cells.” *Molecular and Cellular Biology* 22 (13): 4815–26. https://doi.org/10.1128/MCB.22.13.4815.

Jing, Junjun, Robert J Hinton, Yuji Mishina, Ying Liu, Xuedong Zhou, Q Jian, and Materials Sciences. 2014. “Critical Role of Bmpr1a in Mandibular Condyle Growth.” *Connect Tissue Res.* 55 (01): 73–78. https://doi.org/10.3109/03008207.2014.923858.Critical.

Johnson, Christopher W, Laura Hernandez-Lagunas, Weiguo Feng, Vida Senkus, Trevor Williams, and Kristin Bruk Artinger. 2011. “Vgll2a Is Required for Neural Crest Cell Survival during Zebrafish Craniofacial Development.” *Developmental Biology* 357 (1): 269–81. https://doi.org/10.1016/j.ydbio.2011.06.034.Vgll2a.

Jolma, Arttu, Yimeng Yin, Kazuhiro R Nitta, Kashyap Dave, Alexander Popov, Minna Taipale, Martin Enge, Teemu Kivioja, Ekaterina Morgunova, and Jussi Taipale. 2015. “DNA-Dependent Formation of Transcription Factor Pairs Alters Their Binding Specificity.” *Nature* 527 (7578): 384–88. https://doi.org/10.1038/nature15518.

Jones, Susan. 2004. “An Overview of the Basic Helix-Loop-Helix Proteins.” *Genome Biology* 5 (6).

Joos, Helga, Wolfgang Albrecht, Stefan Laufer, Heiko Reichel, and Rolf E Brenner. 2008. “IL-1 β Regulates FHL2 and Other Cytoskeleton-Related Genes in Human Chondrocytes.” *Mol Med* 14 (3–4): 150–59. https://doi.org/10.2119/2007-00118.Joos.

Joshi, Rohit, Jonathan M Passner, Remo Rohs, Rinku Jain, Alona Sosinsky, Michael A Crickmore, Vinitha Jacob, Aneel K Aggarwal, Barry Honig, and Richard S Mann. 2007. “Functional Specificity of a Hox Protein Mediated by the Recognition of Minor Groove Structure.” *Cell* 131: 530–43. https://doi.org/10.1016/j.cell.2007.09.024.

Juhász, Tamás, Csaba Matta, Zoltán Mészár, Georgina Nagy, Zsolt Szíjgyártó, Zsanett Molnár, Bernadett Kolozsvári, Éva Bakó, and Róza Zákány. 2010. “Optimalized Transient Transfection of Chondrogenic Primary Cell Cultures.” *Central European Journal of Biology* 5 (5): 572–84. https://doi.org/10.2478/s11535-010-0053-x.

Kamata, Mayumi, Yoko Okitsu, Tohru Fujiwara, Masahiko Kanehira, Shinji Nakajima, Taro Takahashi, Ai Inoue, et al. 2014. “GATA2 Regulates Differentiation of Bone Marrow-Derived Mesenchymal Stem Cells.” *Hematologica* 99 (11). https://doi.org/10.3324/haematol.2014.105692.

Kaplan, Tommy, Xiao-yong Li, Peter J Sabo, Sean Thomas, John A Stamatoyannopoulos, D Mark, and Michael B Eisen. 2011. “Quantitative Models of the Mechanisms That Control Genome-Wide Patterns of Transcription Factor Binding during Early Drosophila Development.” *PLoS Genetics* 7 (2). https://doi.org/10.1371/journal.pgen.1001290.

Karamboulas, Konstantina, Helen J Dranse, and T Michael Underhill. 2010. “Regulation of BMP-Dependent Chondrogenesis in Early Limb Mesenchyme by TGFb Signals.” *Journal of Cell Science*, 2068–76. https://doi.org/10.1242/jcs.062901.

Karaulanov, Emil, Walter Knöchel, and Christof Niehrs. 2004. “Transcriptional Regulation of BMP4 Synexpression in Transgenic Xenopus.” *EMBO Journal* 23 (4): 844–56. https://doi.org/10.1038/sj.emboj.7600101.

Karmodiya, Krishanpal, Arnaud R. Krebs, Mustapha Oulad-Abdelghani, Hiroshi Kimura, and Laszlo Tora. 2012. “H3K9 and H3K14 Acetylation Co-Occur at Many Gene Regulatory Elements, While H3K14ac Marks a Subset of Inactive Inducible Promoters in Mouse Embryonic Stem Cells.” *BMC Genomics* 13 (1): 1. https://doi.org/10.1186/1471-2164-13-424.

Katagiri, Takenobu, Mana Imada, Takeshi Yanai, Tatsuo Suda, Naoyuki Takahashi, and Ryutaro Kamijo. 2002. "Identification of a BMP-Responsive Element in Id1, the Gene for Inhibition of Myogenesis." *Genes to Cells* 7 (9): 949–60. https://doi.org/10.1046/j.1365-2443.2002.00573.x.

Kawaida, Reimi, Toshiaki Ohtsuka, Junichi Okutsu, Tohru Takahashi, Yuho Kadono, Hiromi Oda, Atsuhiko Hikita, Kozo Nakamura, Sakae Tanaka, and Hidehiko Furukawa. 2003. "Jun Dimerization Protein 2 (JDP2), a Member of the AP-1 Family of Transcription Factor, Mediates Osteoclast Differentiation Induced by RANKL." *Journal of Experimental Medicine* 197 (8): 1029–35. https://doi.org/10.1084/jem.20021321.

Kawakami, Yasuhiko, Merce Marti, Hiroko Kawakami, Junji Itou, Thu Quach, Austin Johnson, Setsuko Sahara, et al. 2011. "Islet1-Mediated Activation of the b-Catenin Pathway Is Necessary for Hindlimb Initiation in Mice." *Development* 138: 4465–73. https://doi.org/10.1242/dev.065359.

Kawakami, Yasuhiko, Masanao Tsuda, Shigeru Takahashi, Noboru Taniguchi, Concepcion Rordriguez Esteban, Michihisa Zemmyo, Takayuki Furumatsu, Martin Lotz, Juan Carlos Izpisua Belmonte, and Hiroshi Asahara. 2005. "Transcriptional Coactivator PGC-1α Regulates Chondrogenesis via Association with Sox9." *Proc Natl Acad Sci USA* 102 (7): 2414–19.

Kawato, Yoshitaka, Makoto Hirao, Kosuke Ebina, Kenrin Shi, Jun Hashimoto, Yui Honjo, Hideki Yoshikawa, and Akira Myoui. 2012. "Nkx3.2 Promotes Primary Chondrogenic Differentiation by Upregulating Col2a1 Transcription." *PloS ONE* 7 (4): 1–8. https://doi.org/10.1371/journal.pone.0034703.

Kellis, Manolis, Barbara Wold, Michael P Snyder, Bradley E Bernstein, Anshul Kundaje, Georgi Marinov, Lucas Ward, et al. 2014. "Defining Functional DNA Elements in the Human Genome." *PNAS Pers* 111 (17): 6131–38. https://doi.org/10.1073/pnas.1318948111.

Kim, Dae-won, and Andrew B Lassar. 2003. "Smad-Dependent Recruitment of a Histone Deacetylase/Sin3A Complex Modulates the Bone Morphogenetic Protein-Dependent Transcriptional Repressor Activity of Nkx3.2." *Molecular and Cellular Biology* 23 (23): 8704–17. https://doi.org/10.1128/MCB.23.23.8704.

Kim, Jaeseob;, Kirby; Johnson, Hui Ju; Chen, Sean; Carroll, and Allen Laughon. 1997. "Mad Binds to DNA and Directly Mediates Activation Of." *Nature* 388 (July): 1132–36.

Kim, Jonghyun, Weirong Xing, Jon Wergedal, Jefferson Y Chan, Subburaman Mohan, J Kim, W Xing, J Wergedal, Chan Jy, and Mohan S Targeted. 2010. "Targeted Disruption of Nuclear Factor Erythroid-Derived 2-like 1 in Osteoblasts Reduces Bone Size and Bone Formation in Mice." *Physiol Genomics* 40: 100–110. https://doi.org/10.1152/physiolgenomics.00105.2009.

Kim, Tae Kyung, and Ramin Shiekhattar. 2015. "Architectural and Functional Commonalities between Enhancers and Promoters." *Cell* 162 (5): 948–59. https://doi.org/10.1016/j.cell.2015.08.008.

Kimura, Hiroshi, Yoko Hayashi-Takanaka, Yuji Goto, Nanako Takizawa, and Naohito Nozaki. 2008. "The Organization of Histone H3 Modifications as Revealed by a Panel of Specific Monoclonal Antibodies." *Cell Structure and Function* 33: 61–73.

Korchynskyi, Olexander, and Peter Ten Dijke. 2002. "Identification and Functional Characterization of Distinct Critically Important Bone Morphogenetic Protein-Specific Response Elements in the Id1 Promoter." *Journal of Biological Chemistry* 277 (7): 4883–91. https://doi.org/10.1074/jbc.M111023200.

Kou, Ikuyo, and Shiro Ikegawa. 2004. "SOX9-Dependent and -Independent Transcriptional Regulation of Human Cartilage Link Protein." *Journal of Biological Chemistry* 279 (49): 50942–48. https://doi.org/10.1074/jbc.M406786200.

Kouzarides, Tony. 2007. "Chromatin Modifications and Their Function." *Cell* 128 (4): 693–705. https://doi.org/10.1016/j.cell.2007.02.005.

Kozhemyakina, Elena, Todd Cohen, Tso-Pang Yao, and Andrew B Lassar. 2009. "Parathyroid Hormone-Related Peptide Represses Chondrocyte Hypertrophy through a Protein Phosphatase 2A/Histone Deacetylase 4/MEF2

Pathway." *Molecular and Cellular Biology* 29 (21): 5751–62. https://doi.org/10.1128/MCB.00415-09.

Kozhemyakina, Elena, Andrew B Lassar, and Elazar Zelzer. 2015. "A Pathway to Bone: Signaling Molecules and Transcription Factors Involved in Chondrocyte Development and Maturation." *Development* 142: 817–31. https://doi.org/10.1242/dev.105536.

Kraan, P M van der, E N Blaney Davidson, A Blom, and W B van den Berg. 2009. "TGF-Beta Signaling in Chondrocyte Terminal Differentiation and Osteoarthritis Modulation and Integration of Signaling Pathways through Receptor-Smads." *Osteoarthritis and Cartilage* 17 (12): 1539–45. https://doi.org/10.1016/j.joca.2009.06.008.

Kraut, Norbert, Lauren Snider, C Amy Chen, Stephen J Tapscott, and Mark Groudine. 1998. "Requirement of the Mouse I-Mfa Gene for Placental Development and Skeletal Patterning." *The EMBO Journal* 17 (21): 6276–88.

Krebsbach, Paul H, Ken Nakata, Suzanne M Bernier, Osamu Hatano, Tomoyuki Miyashita, Craig S Rhodes, and Yoshihiko Yamada. 1996. "Identification of a Minimum Enhancer Sequence for the Type II Collagen Gene Reveals Several Core Sequence Motifs in Common with the Link Protein Gene." *Journal of Biological Chemistry* 271 (8): 4298–4303.

Kretzschmar, Marcus, and Joan Massagué. 1998. "SMADs: Mediators and Regulators of TGF-β Signaling." *Current Opinion in Genetics & Development* 8 (1): 103–11. https://doi.org/10.1016/S0959-437X(98)80069-5.

Kronenberg, Henry M. 2003. "Developmental Regulation of the Growth Plate." *Nature* 423: 332–36.

Kumar, Deepak, and Andrew Lassar. 2014. "FGF Maintains Chondrogenic Potential of Limb Bud Mesenchymal Cells by Modulating DNMT3A Recruitment." *Cell Research* 8 (5): 1419–31. https://doi.org/10.1016/j.celrep.2014.07.038.FGF.

Kurosaka, Marianna, Yuji Ogura, Toshiya Funabashi, and Tatsuo Akema. 2016. "Early Growth Response 3 (Egr3) Contributes a Maintenance of C2C12 Myoblast Proliferation." *Journal of Cellular Physiology* 232: 1114–22. https://doi.org/10.1002/jcp.25574.

Kusanagi, Kiyoshi, Hirofumi Inoue, Yasuhiro Ishidou, Hiromu K Mishima, Masahiro Kawabata, and Kohei Miyazono. 2000. "Characterization of a Bone Morphogenetic Protein- Responsive Smad-Binding Element." *Molecular Biology of the Cell* 11: 555–65.

Kvon Evgeny Z., Tomas Kazmar, J. Omar Yanez-Cuna Stampfel Gerald, Michaela Pagani, Schernhuber Katharina, and Dickson Barry and Stark Alexander J. 2014. "Genome-Scale Functional Characterization of Drosophila Developmental Enhancers in Vivo." *Nature Letters* 512: 91–95. https://doi.org/10.1038/nature13395.

Larson, Matthew H, Luke A Gilbert, Xiaowo Wang, Wendell A Lim, Jonathan S Weissman, and Lei S Qi. 2013. "CRISPR Interference (CRISPRi) for Sequence-Specific Control of Gene Expression." *Nature Protocols* 8 (11): 2180–96. https://doi.org/10.1038/nprot.2013.132.

Le, Tien, Zhiguo Liang, Heeren Patel, Marcus H. Yu, Gitanjali Sivasubramaniam, Matthew Slovitt, Guy Tanentzapf, et al. 2006. "A New Family of Drosophila Balancer Chromosomes with a W- Dfd-GMR Yellow Fluorescent Protein Marker." *Genetics* 174 (4): 2255–57. https://doi.org/10.1534/genetics.106.063461.

Leboy, Phoebe, Giovi Grasso-Knight, Marina D`Angelo, Susan Volk, Jane Lian, Hicham Drissi, Gary Stein, and Sherrill Adams. 2001. "Smad-Runx Interactions During Chondrocyte Maturation." *The Journal of Bone & Joint Surgery* 83-A (S1): 15–22.

Lee, Kyoung-Mi, Kwang Hwan Park, Ji Suk Hwang, Moses Lee, Dong Suk Yoon, Hyun Aae Ryu, Ho Sun Jung, et al. 2018. "Inhibition of STAT5A Promotes Osteogenesis by DLX5 Regulation." *Cell Death and Disease* 9: 1–13. https://doi.org/10.1038/s41419-018-1184-7.

Lee, Kyu-ho, Samuel Evans, Todd Y Ruan, and Andrew B Lassar. 2004. "SMAD-Mediated Modulation of YY1 Activity Regulates the BMP Response and Cardiac-Specific Expression of a GATA4/5/6- Dependent Chick

Nkx2.5 Enhancer." *Development* 131: 4709–23. https://doi.org/10.1242/dev.01344.

Lefebvre, Veronique;, Ping; Li, and Benoit De Crombrugghe. 1998. "A New Long Form of Sox5 (L-Sox5), Sox6 and Sox9 Are Coexpressed in Chondrogenesis and Cooperatively Activate the Type II Collagen Gene." *The EMBO Journal* 17 (19): 5718–33.

Lefebvre, Véronique, and Mona Dvir-Ginzberg. 2017. "SOX9 and the Many Facets of Its Regulation in the Chondrocyte Lineage." *Connect Tissue Res.* 58 (1): 2–14. https://doi.org/10.1080/03008207.2016.1183667.SOX9.

Lefebvre, Veronique, Wendong Huang, Vincent R Harley, Peter N Goodfellow, and Benoit D E Crombrugghe. 1997. "SOX9 Is a Potent Activator of the Chondrocyte-Specific Enhancer of the Proa1(II) Collagen Gene." *Molecular and Cellular Biology* 17 (4): 2336–46.

Lennartsson, Andreas, and Karl Ekwall. 2009. "Histone Modification Patterns and Epigenetic Codes." *Biochimica et Biophysica Acta* 1790: 863–68. https://doi.org/10.1016/j.bbagen.2008.12.006.

Leonard, Claire, Howard Fuld, Dorothy Frenz, Sherry Downie, Joan Massague, and Stuard Newman. 1991. "Role of Transforming Growth Factor-β in Chondrogenic Pattern Formation in the Embryonic Limb: Stimulation of Mesenchymal Condensation and Fibronectin Gene Expression by Exogenenous TGF-β and Evidence for Endogenous TGF-β-like Activity." *Developmental Biology* 145: 99–109.

Leung, Keith K H, Ling Jim Ng, Ken K Y Ho, Patrick P L Tam, and Kathryn S E Cheah. 1998. "Regulatory DNA Elements Mediate Developmental Stage- and Tissue-Specific Expression of the Human COL2A1 Gene in Transgenic Mice." *Journal of Cell Biology* 141 (6): 1291–1300.

Levine, Mike. 2010. "Transcriptional Enhancers in Animal Development and Evolution." *Current Biology* 20 (17): R754–R763. https://doi.org/10.1016/j.cub.2010.06.070.Transcriptional.

Li-Chin Yao, Ira L. Blitz*, Daniel A. Peiffer*, Sopheap Phin*, Ying Wang, Souichi Ogata, Ken W. Y. Cho, Kavita Arora† and Rahul Warrior. 2006. "Schnurri Transcription Factors from Drosophila and Vertebrates Can Mediate Bmp Signaling through a Phylogenetically Conserved Mechanism." *Development* 133 (20): 4025–34. https://doi.org/10.1242/dev.02561.

Li, Bo, and Colin N Dewey. 2011. "RSEM: Accurate Transcript Quantification from RNA-Seq Data with or without a Reference Genome." *BMC Bioinformatics* 12 (323): 1–16. https://doi.org/10.1186/1471-2105-12-323.

Li, Heng, and Richard Durbin. 2009. "Fast and Accurate Short Read Alignment with Burrows- Wheeler Transform." *Bioinformatics* 25 (14): 1754–60. https://doi.org/10.1093/bioinformatics/btp324.

Li, Ian M H, Ke Liu, Alice Neal, Peter D Clegg, Sarah De Val, and George Bou-gharios. 2018. "Differential Tissue Specific, Temporal and Spatial Expression Patterns of the Aggrecan Gene Is Modulated by Independent Enhancer Elements." *Nature Scientific Reports* 8 (950): 1–12. https://doi.org/10.1038/s41598-018-19186-4.

Li, Xuelin, Shuyi Nie, Chenbei Chang, Tao Qiu, and Xu Cao. 2006. "Smads Oppose Hox Transcriptional Activities." *Experimental Cell Research* 312 (6): 854–64. https://doi.org/10.1016/j.yexcr.2005.12.002.

Liang, Hsiao-lan, Mu Xu, Yi-chun Chuang, and Christine Rushlow. 2012. "Response to the BMP Gradient Requires Highly Combinatorial Inputs from Multiple Patterning Systems in the Drosophila Embryo." *Development* 139: 1956–64. https://doi.org/10.1242/dev.079772.

Lien, Ching-ling, John Mcanally, James A Richardson, and Eric N Olson. 2002. "Cardiac-Specific Activity of an Nkx2 – 5 Enhancer Requires an Evolutionarily Conserved Smad Binding Site." *Developmental Biology* 244: 257–66. https://doi.org/10.1006/dbio.2002.0603.

Liew, Chong Wee, Jeremie Boucher, Jit Kong Cheong, Cecile Vernochet, Ho-Jin Koh, Cristina Mallol, Kristy Townsend, et al. 2013. "Ablation of TRIP-Br2, a Novel Regulator of Fat Lipolysis, Thermogenesis and Oxidative Metabolism, Prevents Diet-Induced Obesity and Insulin Resistance." *Nature Medicine* 19 (2): 217–26. https://doi.org/10.1038/nm.3056.Ablation.

Liu, Aimin, and Lee A Niswander. 2005. “Bone Morphogenetic Protein Signaling and Vertebrate Nervous System Development.” *Nature Reviews Neuroscience* 6 (December): 945–55. https://doi.org/10.1038/nrn1805.

Liu, Chia-feng, Marco Angelozzi, Abdul Haseeb, and Veronique Lefebvre. 2018. “SOX9 Is Dispensable for the Initiation of Epigenetic Remodeling and the Activation of Marker Genes at the Onset of Chondrogenesis.” *Development* 145: 1–15. https://doi.org/10.1242/dev.164459.

Liu, Chia-Feng, and Véronique Lefebvre. 2015. “The Transcription Factors SOX9 and SOX5 / SOX6 Cooperate Genome-Wide through Super-Enhancers to Drive Chondrogenesis.” *Nucleic Acids Research* 43 (17): 8183–8203. https://doi.org/10.1093/nar/gkv688.

Liu, Chia-Feng, William E Samsa, Guang Zhou, and Veronique Lefebvre. 2017. “Transcriptional Control of Chondrocyte Specification and Differentiation.” *Seminars in Cell and Developmental Biology* 62: 34–49. https://doi.org/10.1016/j.semcdb.2016.10.004.Transcriptional.

Liu, Jiancheng, Xiwei Wu, Heying Zhang, Gerd P Pfeifer, and Qiang Lu. 2017. “Dynamics of RNA Polymerase II Pausing and Bivalent Histone H3 Methylation during Neuronal Differentiation in Brain Development.” *CellReports* 20: 1307–18. https://doi.org/10.1016/j.celrep.2017.07.046.

Long, Fanxin, and David M Ornitz. 2013. “Development of the Endochondral Skeleton.” *Cold Spring Harb Perspect Biol* 5: 1–20.

Long, Hannah K, Sara L Prescott, and Joanna Wysocka. 2016a. “Ever-Changing Landscapes: Transcriptional Enhancers in Development and Evolution.” *Cell* 167 (5): 1170–87. https://doi.org/10.1016/j.cell.2016.09.018.

———. 2016b. “Review Ever-Changing Landscapes : Transcriptional Enhancers in Development and Evolution.” *Cell* 167 (5): 1170–87. https://doi.org/10.1016/j.cell.2016.09.018.

López-Rovira, Teresa, Elisabet Chalaux, Joan Massagué, Jose Luis Rosa, and Francesc Ventura. 2002. “Direct Binding of Smad1 and Smad4 to Two Distinct Motifs Mediates Bone Morphogenetic Protein-Specific Transcriptional Activation of Id1 Gene.” *Journal of Biological Chemistry* 277 (5): 3176–85. https://doi.org/10.1074/jbc.M106826200.

Lorberbaum, David S, Andrea I Ramos, Kevin A Peterson, Brandon S Carpenter, David S Parker, Sandip De, Lauren E Hillers, et al. 2016. “An Ancient yet Flexible Cis- Regulatory Architecture Allows Localized Hedgehog Tuning by Patched / Ptch1.” *ELife* 5: 1–22. https://doi.org/10.7554/eLife.13550.

Lorda-Diez, Carlos I, Juan A Montero, Carmen Martinez-Cue, Juan A Garcia-Porrero, and Juan M Hurle. 2009. “Transforming Growth Factors β Coordinate Cartilage and Tendon Differentiation in the Developing Limb Mesenchyme.” *Journal of Biological Chemistry* 284 (43): 29988–96. https://doi.org/10.1074/jbc.M109.014811.

Lorzadeh, Alireza, Misha Bilenky, Colin Hammond, David J H F Knapp, Luolan Li, Paul H Miller, Annaick Carles, et al. 2016. “Nucleosome Density ChIP-Seq Identifies Distinct Chromatin Modification Signatures Associated with MNase Accessibility.” *CellReports* 17: 2112–24. https://doi.org/10.1016/j.celrep.2016.10.055.

Love, Michael I, Wolfgang Huber, and Simon Anders. 2014. “Moderated Estimation of Fold Change and Dispersion for RNA-Seq Data with DESeq2.” *Genome Biology* 15 (550): 1–21. https://doi.org/10.1186/s13059-014-0550-8.

Luger, Karollin; Mader A; Richmond, Robin K;, David F; Sargent, and Timothy J; Richmond. 1997. “Crystal Structure of the Nucleosome Core Particle at 2.8A Resolution.” *Nature* 7: 251–60.

Lui, Julian C, Presley Garrison, Quang Nguyen, Michal Ad, Chithra Keembiyehetty, Weiping Chen, Youn Hee Jee, et al. 2016. “EZH1 and EZH2 Promote Skeletal Growth by Repressing Inhibitors of Chondrocyte Proliferation and Hypertrophy.” *Nature Communications* 7: 1–12. https://doi.org/10.1038/ncomms13685.

Ma, Chi, Ying Zhang, Yu Qing Li, Cheng Chen, Wei Cai, and Yue Lin Zeng. 2015. “The Role of PPARγ in Advanced Glycation End Products-Induced Inflammatory Response in Human Chondrocytes.” *PLoS ONE* 10

(5): 1–12. https://doi.org/10.1371/journal.pone.0125776.

Mackie, E J, L Tatarczuch, and M Mirams. 2011. “The Skeleton : A Multi-Functional Complex Organ . The Growth Plate Chondrocyte and Endochondral Ossification.” *Journal of Endocrinology* 211: 109–21. https://doi.org/10.1530/JOE-11-0048.

Manikandan, Muthurangan, Sarah Abuelreich, Mona Elsafadi, Hussain Alsalman, Hassan Almalak, Abdulaziz Siyal, Jamil Amjad Hashmi, et al. 2018. “NR2F1 Mediated Down-Regulation of Osteoblast Differentiation Was Rescued by Bone Morphogenetic Protein-2 (BMP-2) in Human MSC.” *Differentiation* 104: 36–41. https://doi.org/10.1016/j.diff.2018.10.003.

Marqués, Guillermo. 2005. “Morphogens and Synaptogenesis in Drosophila .” *Journal of Neurobiology* . Hoboken : Wiley Subscription Services, Inc., A Wiley Company . https://doi.org/10.1002/neu.20165.

Marqués, Guillermo, Theodore E Haerry, M Lisa Crotty, Mingshan Xue, Bing Zhang, and Michael B O Connor. 2003. “Retrograde Gbb Signaling through the Bmp Type 2 Receptor Wishful Thinking Regulates Systemic FMRFa Expression in Drosophila,” 5457–70. https://doi.org/10.1242/dev.00772.

Maruyama, Kenta, Masahiro Fukasaka, Alexis Vandenbon, Tatsuya Saitoh, Takumi Kawasaki, Takeshi Kondo, Kazunari K. Yokoyama, et al. 2012. “The Transcription Factor Jdp2 Controls Bone Homeostasis and Antibacterial Immunity by Regulating Osteoclast and Neutrophil Differentiation.” *Immunity* 37 (6): 1024–36. https://doi.org/10.1016/j.immuni.2012.08.022.

Marzaioli, Viviana, Jason P Mcmorrow, Hannes Angerer, Alyssa Gilmore, Daniel Crean, Davide Zocco, Peadar Rooney, et al. 2012. “Histamine Contributes to Increased RANKL to Osteoprotegerin Ratio Through Altered Nuclear Receptor 4A Activity in Human Chondrocytes” 64 (10): 3290–3301. https://doi.org/10.1002/art.34554.

Massague, Joan, Stacy Blain, and Roger Lo. 2000. “TGFb Signaling in Growth Control , Cancer , and Heritable Disorders.” *Cell* 103: 295–309.

Massagué, Joan, Joan Seoane, and David Wotton. 2005. “Smad Transcription Factors.” *Genes & Development* 19: 2783–2810. https://doi.org/10.1101/gad.1350705.embryo.

Mathelier, Anthony, Wenqiang Shi, and Wyeth W Wasserman. 2015. “Identification of Altered Cis -Regulatory Elements in Human Disease.” *Trends in Genetics* 31 (2): 67–76. https://doi.org/10.1016/j.tig.2014.12.003.

Mccabe, Brian D, Sabrina Hom, Hermann Aberle, Richard D Fetter, Guillermo Marques, Theodore E Haerry, Hong Wan, Michael B O Connor, Corey S Goodman, and a Pejmun Haghighi. 2004. “Highwire Regulates Presynaptic BMP Signaling Essential for Synaptic Growth.” *Neuron* 41 (6): 891–905. https://doi.org/10.1016/S0896-6273(04)00073-X.

Mehler, Mark F, Peter C Mabie, Damin Zhang, and John A Kessler. 1997. “Bone Morphogenetic Proteins in the Nervous System.” *Trends in Neurosciences* 20 (7): 309–17. https://doi.org/10.1016/S0166-2236(96)01046-6.

Metsalu, Tauno, and Jaak Vilo. 2015. “ClustVis: A Web Tool for Visualizing Clustering of Multivariate Data Using Principal Component Analysis and Heatmap.” *Nucleic Acids Research* 43: 566–70. https://doi.org/10.1093/nar/gkv468.

Mi, Huaiyu, Anushya Muruganujan, Dustin Ebert, Xiaosong Huang, and D Thomas. 2019. “PANTHER Version 14: More Genomes, a New PANTHER GO-Slim and Improvements in Enrichment Analysis Tools.” *Nucleic Acids Research* 47: 419–26. https://doi.org/10.1093/nar/gky1038.

Miguel-aliaga, Irene, Douglas W Allan, Stefan Thor, and Wit Gbb. 2004. “Independent Roles of the Dachshund and Eyes Absent Genes in BMP Signaling, Axon Pathfinding and Neuronal Specification.” *Development* 131: 5837–48. https://doi.org/10.1242/dev.01447.

Minina, Eleonora, Hans Markus Wenzel, Conny Kreschel, Seth Karp, William Gaffield, Andrew P Mcmahon, and Andrea Vortkamp. 2001. “BMP and Ihh / PTHrP Signaling Interact to Coordinate Chondrocyte Proliferation

and Differentiation" 4534: 4523–34.

Miyazono K, Maeda S and Imamura T. 2006. "Smad Transcriptional Co-Activators and Co-Repressors." In *Smad Signal Transduction*, edited by Peter ten Dijke and Carl-Henrik Heldin, 5:277–93. Dordrecht: Springer Netherlands.

Miyazono, Kohei, Yuto Kamiya, and Masato Morikawa. 2010. "Bone Morphogenetic Protein Receptors and Signal Transduction." *J. Biochem.* 147 (1): 35–51. https://doi.org/10.1093/jb/mvp148.

Morikawa, Masato, Daizo Koinuma, Shuichi Tsutsumi, Eleftheria Vasilaki, Yasuharu Kanki, Carl Henrik Heldin, Hiroyuki Aburatani, and Kohei Miyazono. 2011. "ChIP-Seq Reveals Cell Type-Specific Binding Patterns of BMP-Specific Smads and a Novel Binding Motif." *Nucleic Acids Research* 39 (20): 8712–27. https://doi.org/10.1093/nar/gkr572.

Morimoto, Riyo, Akitsugu Yamamoto, Yoshihiro Akimoto, and Akiko Obinata. 2011. "Homeoprotein Hex Is Expressed in Mouse Developing Chondrocytes." *The Journal of Biochemistry* 150 (1): 61–71. https://doi.org/10.1093/jb/mvr039.

Morrell, Nicholas W, Donald B Bloch, Peter Dijke, Marie-jose T H Goumans, Jim Smith, Paul B Yu, and Kenneth D Bloch. 2016. "Targeting BMP Signalling in Cardiovascular Disease and Anaemia." *Nat Rev Cardiol.* 13 (2): 106–20. https://doi.org/10.1038/nrcardio.2015.156.Targeting.

Mu, Yabing, Shyam Kumar Gudey, and Maréne Landström. 2012. "Non-Smad Signaling Pathways." *Cell Tissue Res* 327: 11–20. https://doi.org/10.1007/s00441-011-1201-y.

Mueller, Thomas D. 2015. *Mechanisms of BMP – Receptor Interaction and Activation*. *Bone Morphogenic Protein*. 1st ed. Vol. 99. Elsevier Inc. https://doi.org/10.1016/bs.vh.2015.06.003.

Mukhopadhyay, Krish;, Veronique; Lefebvre, Guang; Zhou, Silvio; Garofalo, James H; Kimura, and Benoit De Crombrugghe. 1995. "Use of a New Rat Chondrosarcoma Cell Line to Delineate a 119-Base Pair Chondrocyte-Specific Enhancer Element and to Define Active Promoter Segments in the Mouse Pro-A1(II) Collagen Gene." *Journal of Biological Chemistry* 270 (46): 27711–19.

Mulloy, Barbara, and Chris C Rider. 2015. *The Bone Morphogenetic Proteins and Their Antagonists*. *Bone Morphogenic Protein*. 1st ed. Vol. 99. Elsevier Inc. https://doi.org/10.1016/bs.vh.2015.06.004.

Murakami, Shunichi, Mikio Kan, Wallace L Mckeehan, and Benoit De Crombrugghe. 2000. "Up-Regulation of the Chondrogenic Sox9 Gene by Fibroblast Growth Factors Is Mediated by the Mitogen-Activated Protein Kinase Pathway." *Proc Natl Acad Sci USA* 97 (3): 1113–18.

Murre, Cornelis, Patrick Schonleber McCaw, and David Baltimore. 1989. "A New DNA Binding and Dimerization Motif in Lmmunoglobulin Enhancer Binding, Daughterless, MyoD, and Myc Proteins." *Cell* 56: 777–83.

Nakade, K., J. Pan, A. Yoshiki, H. Ugai, M. Kimura, B. Liu, H. Li, et al. 2007. "JDP2 Suppresses Adipocyte Differentiation by Regulating Histone Acetylation." *Cell Death and Differentiation* 14 (8): 1398–1405. https://doi.org/10.1038/sj.cdd.4402129.

Nakahiro, Takeshi, Hisanori Kurooka, Kentaro Mori, Kazuo Sano, and Yoshifumi Yokota. 2010. "Identification of BMP-Responsive Elements in the Mouse Id2 Gene." *Biochemical and Biophysical Research Communications* 399 (3): 416–21. https://doi.org/10.1016/j.bbrc.2010.07.090.

Nakamura, Yukio, Koji Yamamoto, Xinjun He, Bungo Otsuki, Youngwoo Kim, Hiroki Murao, Tsunemitsu Soeda, et al. 2011. "Wwp2 Is Essential for Palatogenesis Mediated by the Interaction between Sox9 and Mediator Subunit 25." *Nature Communications* 2 (251): 1–23. https://doi.org/10.1038/ncomms1242.Wwp2.

Nawachi, Kumiko, Miho Inoue, Satoshi Kubota, Takashi Nishida, Gen Yosimichi, Tohru Nakanishi, Manabu Kanyama, et al. 2002. "Tyrosine Kinase-Type Receptor ErbB4 in Chondrocytes: Interaction with Connective Tissue Growth Factor and Distribution in Cartilage." *FEBS Letters* 528: 109–13. https://doi.org/10.1016/S0014-5793(02)03263-5.

Nichols, James T, Luyuan Pan, Cecilia B Moens, and Charles B Kimmel. 2013. “Barx1 Represses Joints and Promotes Cartilage in the Craniofacial Skeleton.” *Development* 140: 2765–75. https://doi.org/10.1242/dev.090639.

Nie, Yumin, Hongde Liu, and Xiao Sun. 2013. “The Patterns of Histone Modifications in the Vicinity of Transcription Factor Binding Sites in Human Lymphoblastoid Cell Lines.” *PloS One* 8 (3): 1–11. https://doi.org/10.1371/journal.pone.0060002.

Nordin, Kara, and Carole LaBonne. 2014. “Sox5 Is a DNA Binding Co-Factor for BMP R-Smads That Directs Target Specificity during Patterning of the Early Ectoderm.” *Developmental Cell* 31 (3): 374–82. https://doi.org/10.1016/j.devcel.2014.10.003.Sox5.

Norrie, Jacqueline L, Qiang Li, Swanie Co, Bau-lin Huang, Ding Ding, Jann C Uy, Zhicheng Ji, et al. 2016. “PRMT5 Is Essential for the Maintenance of Chondrogenic Progenitor Cells in the Limb Bud.” *Stem Cells and Regeneration* 143: 4608–19. https://doi.org/10.1242/dev.140715.

Oh, Chun-do, Yue Lu, Shoudan Liang, Yuko Mori-akiyama, Di Chen, and Benoit De Crombrugghe. 2014. “SOX9 Regulates Multiple Genes in Chondrocytes , Including Genes Encoding ECM Proteins, ECM Modification Enzymes , Receptors , and Transporters.” *PloS ONE* 9 (9). https://doi.org/10.1371/journal.pone.0107577.

Ohba, Shinsuke, Xinjun He, Hironori Hojo, Andrew P Mcmahon, and Edythe Broad-cirm. 2016. “Distinct Transcriptional Programs Underlie Sox9 Regulation of the Mammalian Chondrocyte.” *Cell Reports* 12 (2): 229–43. https://doi.org/10.1016/j.celrep.2015.06.013.Distinct.

Ohlen, Tonia Von, Derek Lessing, Roel Nusse, and Joan E. Hooper. 1997. “Hedgehog Signaling Regulates Transcription through Cubitus Interruptus, a Sequence-Specific DNA Binding Protein.” *PNAS* 94: 2404–9.

Ong, Chin-Tong and, and Victor Corces. 2011. “Enhancer Function: New Insights into the Regulation of Tissue-Specific Gene Expression.” *Nature Reviews Genetics* 12 (4): 283–93. https://doi.org/10.1038/nrg2957.Enhancer.

Ono, Noriaki, Wanida Ono, Takashi Nagasawa, and Henry M Kronenberg. 2014. “A Subset of Chondrogenic Cells Provides Early Mesenchymal Progenitors in Growing Bones.” *Nat Cell Biol.* 16 (12): 1157–67. https://doi.org/10.1038/ncb3067.A.

Oughtred, Rose, Chris Stark, Bobby-joe Breitkreutz, Jennifer Rust, Lorrie Boucher, Christie Chang, Nadine Kolas, et al. 2019. “The BioGRID Interaction Database : 2019 Update.” *Nucleic Acids Research* 47: 529–41. https://doi.org/10.1093/nar/gky1079.

Park, Peter J. 2009. “ChIPseq: Advantages and Challenges of a Maturing Technology.” *Nature Reviews Genetics* 10: 669–80.

Parker, David S., Michael A. White, Andrea I. Ramos, Barak A. Cohen, and Scott Barolo. 2011. “The Cis-Regulatory Logic of Hedgehog Gradient Responses: Key Roles for Gli Binding Affinity, Competition, and Cooperativity.” *Sci Signal* 4 (176): 1–16. https://doi.org/10.1126/scisignal.2002077.The.

Patro, Rob, Geet Duggal, Michael I Love, Rafael A Irizarry, and Carl Kingsford. 2017. “Salmon: Fast and Bias-Aware Quantification of Transcript Expression Using Dual-Phase Inference.” *Nature Methods* 14 (4): 417–19. https://doi.org/10.1038/nmeth.4197.Salmon.

Pepe, Anna Elena, Qingzhong Xiao, Anna Zampetaki, Zhongyi Zhang, Akira Kobayashi, Yanhua Hu, and Qingbo Xu. 2010. “Crucial Role of Nrf3 in Smooth Muscle Cell Differentiation From Stem Cells.” *Circulation Research* 106: 870–79. https://doi.org/10.1161/CIRCRESAHA.109.211417.

Pertea, Mihaela, Daehwan Kim, Geo Pertea, Jeffrey T Leek, and L Steven. 2016. “Transcript-Level Expression Analysis of RNA-Seq Experiments with HISAT, StringTie, and Ballgown.” *Nature Protocols* 11 (9): 1650–67. https://doi.org/10.1038/nprot.2016.095.Transcript-level.

Petersen, Britt-Sabina, Broder Fredrich, Marc P Hoeppner, David Ellinghaus, and Andre Franke. 2017.

"Opportunities and Challenges of Whole-Genome and -Exome Sequencing." *BMC Genetics* 18 (14): 1–13. https://doi.org/10.1186/s12863-017-0479-5.

Pfeiffer, Barret D, Arnim Jenett, Ann S Hammonds, Teri-t B Ngo, Sima Misra, Christine Murphy, Audra Scully, et al. 2008. "Tools for Neuroanatomy and Neurogenetics in Drosophila." *PNAS* 105 (28): 9715–20.

Postberg, Jan, Sakeh Forcob, Wei-jen Chang, and Hans J Lipps. 2010. "The Evolutionary History of Histone H3 Suggests a Deep Eukaryotic Root of Chromatin Modifying Mechanisms." *BMC Evolutionary Biology* 10 (259): 1–13. https://doi.org/10.1186/1471-2148-10-259.

Pouponnot, Celio; Jayaraman, Lata; and Massague, Joan. 1998. "Physical and Functional Interaction of SMADs and P300/CBP." *Journal of Biological Chemistry* 273 (36): 22865–69.

Pradeepa, Madapura M., Graeme R. Grimes, Yatendra Kumar, Gabrielle Olley, Gillian C.A. Taylor, Robert Schneider, and Wendy A. Bickmore. 2016. "Histone H3 Globular Domain Acetylation Identifies a New Class of Enhancers." *Nature Genetics* 48 (6): 681–86. https://doi.org/10.1038/ng.3550.

Pratap Singh, Pratik Narendra, Upendra Yadav Singh, Kimi Azad, Pooja Goswami, Veena Kinare, and Amitabha Bandyopadhyay. 2018. "NFIA and GATA3 Are Crucial Regulators of Embryonic Articular Cartilage Differentiation." *Development* 145: 1–12. https://doi.org/10.1242/dev.156554.

Preitschoph, ANDREA, KATHARINA SCHORGHOFER, DAVID KINSLECHNER, BIRGIT SCHUTZ, HANNES ZWICKL, MARGIT ROSNER, JOZSEF GABOR JOO, STEFAN NEHRER, MARKUS HENGSTSCHLAGER, and MARIO MIKULA. 2016. "Rapamycin-Induced Hypoxia Inducible Factor 2A Is Essential for Chondrogenic Differentiation of Amniotic Fluid Stem Cells." *Fetal and Neonatal Stem Cells* 5: 580–90.

Pundhir, Sachin, Panayiota Poirazi, and Jan Gorodkin. 2015. "Emerging Applications of Read Profiles towards the Functional Annotation of the Genome." *Frontiers in Genetics* 6: 1–11. https://doi.org/10.3389/fgene.2015.00188.

Pyrowolakis, George, Britta Hartmann, Bruno Mu, Konrad Basler, and Markus Affolter. 2004. "Widespread BMP-Induced Repression during Drosophila Development." *Developmental Cell* 7: 229–40.

Qiryaqoz, Zeena, Suraj Timilsina, Daniel Czarnowski, Paul H Krebsbach, and Luis G Villa-diaz. 2019. "Identification of Biomarkers Indicative of Functional Skeletal Stem Cells." *Orthod Craniofac Res* 22: 192–98. https://doi.org/10.1111/ocr.12260.

Rada-Iglesias, Alvaro, Ruchi Bajpai, Tomek Swigut, Samantha A Brugmann, A Ryan, and Joanna Wysocka. 2011. "A Unique Chromatin Signature Uncovers Early Developmental Enhancers in Humans." *Nature* 470 (7333): 279–83. https://doi.org/10.1038/nature09692.A.

Ramirez, Fidel, Devon P Ryan, Bjorn Gruning, Vivek Bhardwaj, Fabian Kilpert, Andreas S Richter, Steffen Heyne, Friederike Dundar, and Thomas Manke. 2016. "DeepTools2: A next Generation Web Server for Deep-Sequencing Data Analysis." *Nucleic Acids Research* 44: 160–65. https://doi.org/10.1093/nar/gkw257.

Ramos, Andrea;, and Scott Barolo. 2013. "Low-Affinity Transcription Factor Binding Sites Shape Morphogen Responses and Enhancer Evolution." *Phil Trans R Soc B* 386.

Ranger, Ann M, Louis C Gerstenfeld, Jinxi Wang, Tamiyo Kon, Hyunsu Bae, Ellen M Gravallese, Melvin J Glimcher, and Laurie H Glimcher. 2000. "The Nuclear Factor of Activated T Cells (NFAT) Transcription Factor NFATp (NFATc2) Is a Repressor of Chondrogenesis." *Journal of Experimental Medicine* 191 (1): 9–21.

Raouf, Afshin, and Arun Seth. 2000. "Ets Transcription Factors and Targets in Osteogenesis." *Oncogene* 19: 6455–63.

Rawson, Joel M, Michael Lee, Eric L Kennedy, and Scott B Selleck. 2003. "Drosophila Neuromuscular Synapse Assembly and Function Require the TGF-β Type I Receptor Saxophone and the Transcription Factor Mad."

Journal of Neurobiology 55 (2): 134–50. https://doi.org/10.1002/neu.10189.

Rebeiz, M and Williams, T. 2011. "Experimental Approaches to Evaluate the Contributions of Candidate Cis-Regulatory Mutations to Phenotypic Evolution." In *Molecular Methods for Evolutionary Genetics*, 351–75.

Rentsendorj, Otgonchimeg;, Andrea; Nagy, Iidiko; Sinko, Andreea Daraba, Endre Barta, and Ibolya Kiss. 2005. "Highly Conserved Proximal Promoter Element Harbouring Paired Sox9-Binding Sites Contributes to the Tissue- and Developmental Stage-Specific Activity of the Matrilin-1 Gene." *Biochemical Journal* 398: 705–16.

Retting, Kelsey N, Buer Song, Byeong S Yoon, and Karen M Lyons. 2009. "BMP Canonical Smad Signaling through Smad1 and Smad5 Is Required for Endochondral Bone Formation." *Development* 1104: 1093–1104. https://doi.org/10.1242/dev.029926.

Reynard, Louise N, and John Loughlin. 2013. "Insights from Human Genetic Studies into the Pathways Involved in Osteoarthritis." *Nature Publishing Group* 9 (10): 573–83. https://doi.org/10.1038/nrrheum.2013.121.

Rice, S. J., K. Cheung, L. N. Reynard, and J. Loughlin. 2019. "Discovery and Analysis of Methylation Quantitative Trait Loci (MQTLs) Mapping to Novel Osteoarthritis Genetic Risk Signals." *Osteoarthritis and Cartilage* 27 (10): 1545–56. https://doi.org/10.1016/j.joca.2019.05.017.

Robinson, James T., Wendy Thorvaldsdóttir, Helga Winckler, Mitchell Guttman, Eric S. Lander, Gad Getz, and Jill P. and Mesirov. 2011. "Integrative Genomics Viewer." *Nature Biotechnology* 29 (1): 24–26. https://doi.org/10.1038/nbt.1754.Integrative.

Robinson, Mark D, Davis J Mccarthy, and Gordon K Smyth. 2010. "EdgeR: A Bioconductor Package for Differential Expression Analysis of Digital Gene Expression Data." *Bioinformatics* 26 (1): 139–40. https://doi.org/10.1093/bioinformatics/btp616.

Rodrigo, Isabel, Paola Bovolenta, Baljinder S Mankoo, Kenji Imai, Rodrigo E T Al, and M O L C E L L B Iol. 2004. "Meox Homeodomain Proteins Are Required for Bapx1 Expression in the Sclerotome and Activate Its Transcription by Direct Binding to Its Promoter." *Molecular and Cellular Biology* 24 (7): 2757–66. https://doi.org/10.1128/MCB.24.7.2757.

Rodrigo, Isabel, Robert E Hill, Rudi Balling, Andrea Münsterberg, and Kenji Imai. 2003. "Pax1 and Pax9 Activate Bapx1 to Induce Chondrogenic Differentiation in the Sclerotome." *Development* 130: 473–82. https://doi.org/10.1242/dev.00240.

Ross, Sarah, and Caroline S Hill. 2008. "How the Smads Regulate Transcription." *IJBCB* 40: 383–408. https://doi.org/10.1016/j.biocel.2007.09.006.

Rudnicki, Julie A, and Anthony M C Brown. 1997. "Inhibition of Chondrogenesis by Wnt Gene Expression in Vivo and in Vitro." *Developmental Biology* 118: 104–18.

Rushlow, Christine, Pamela F Colosimo, Meng-chi Lin, Mu Xu, and Nikolai Kirov. 2001. "Transcriptional Regulation of the Drosophila Gene Zen by Competing Smad and Brinker Inputs." *Gene & Developent* 15: 340–51. https://doi.org/10.1101/gad.861401.Medea.

Salazar, Valerie S, Satoshi Ohte, Luciane P Capelo, Laura Gamer, and Vicki Rosen. 2016. "Specification of Osteoblast Cell Fate by Canonical Wnt Signaling Requires Bmp2." *Stem Cells and Regeneration* 143: 4352–67. https://doi.org/10.1242/dev.136879.

Santos-Rosa, Helena, Robert Schneider, Andrew J Bannister, Julia Sherriff, Bradley E Bernstein, N C Tolga Emre, Stuart L Schreiber, Jane Mellor, and Tony Kouzarides. 2002. "Active Genes Are Tri-Methylated at K4 of Histone H3." *Nature* 419: 407–11. https://doi.org/10.1038/nature01071.Published.

Schmidt, Dominic, Michael D Wilson, Benoit Ballester, Petra C Schwalie, Gordon D Brown, Aileen Marshall, Claudia Kutter, et al. 2010. "Five-Vertebrate ChIP-Seq Reveals Transcription Factor Binding." *Science (New York, N.Y.)* 328 (May): 1036–40. https://doi.org/10.1126/science.1186176.

Schmierer, Bernhard, and Caroline S Hill. 2007. “TGFβ – SMAD Signal Transduction: Molecular Specificity and Functional Flexibility.” *Nature Reviews Molecular Cell Biology* 8: 970–82. https://doi.org/10.1038/nrm2297.

Schubert, Thomas, Simone Kaufmann, Ann-kathrin Wenke, Susanne Gra, and Anja-katrin Bosserhoff. 2009. “Role of Deleted in Colon Carcinoma in Osteoarthritis and in Chondrocyte Migration.” *Rheumatology* 48: 1435–41. https://doi.org/10.1093/rheumatology/kep245.

Seki, Kenji, and Akiko Hata. 2004. “Indian Hedgehog Gene Is a Target of the Bone Morphogenetic Protein Signaling Pathway.” *Journal of Biological Chemistry* 279 (18): 18544–49. https://doi.org/10.1074/jbc.M311592200.

Sekiya, Ichiro, Tao Tang, Masaya Hayashi, Toshiyuki Morito, Young-jin Ju, Tomoyuki Mochizuki, and Takeshi Muneta. 2009. “Periodic Knee Injections of BMP-7 Delay Cartilage Degeneration Induced by Excessive Running in Rats.” *Journal of Orthopaedic Research* 27: 1088–92. https://doi.org/10.1002/jor.20840.

Semba, Ichiro, Kazuaki Nonaka, Ichiro Takahashi, Katsu Takahashi, Ralph Dashner, Lillian Shum, Glen H Nuckolls, and Harold C Slavkin. 2000. “Positionally-Dependent Chondrogenesis Induced by BMP4 Is Co-Regulated by Sox9 and Msx2.” *Developmental Dynamics* 217: 401–14.

Sensiate, Lucimara Aparecida, Debora Sobreira, Fernanda Cristina Da Veiga, Denner Jefferson Peterlini, Angelica Vasconcelos Pedrosa, Thais Rirsch, Paulo Pinto Joazeiro, et al. 2014. “Dact Gene Expression Profiles Suggest a Role for This Gene Family in Integrating Wnt and TGF- b Signaling Pathways During Chicken Limb Development.” *Developmental Dynamics* 243: 428–39. https://doi.org/10.1002/dvdy.23948.

Shen, Ming, Takeshi Kawamoto, Weiqun Yan, Kazuko Nakamasu, Mami Tamagami, Yasuhiko Koyano, Mitsuhide Noshiro, and Yukio Kato. 1997. “Molecular Characterization of the Novel Basic Helix-Loop-Helix Protein DEC1 Expressed in Differentiated Human Embryo Chondrocytes.” *Biochemical and Biophysical Research Communications* 236: 294–98. https://doi.org/10.1006/bbrc.1997.6960.

Shi, Xinge, Hui Ye, Xuedong Yao, and Yanzheng Gao. 2017. “The Involvement and Possible Mechanism of NR4A1 in Chondrocyte Apoptosis during Osteoarthritis.” *Am J Transl Res* 9 (2): 746–54.

Shi, Xingming;, Xiangli; Yang, Di; Chen, Zhijie; Chang, and Xu Cao. 1999. “Smad1 Interacts with Homeobox DNA-Binding Proteins in Bone Morphogenetic Protein Signaling.” *Journal of Biological Chemistry* 274 (19): 13711–17.

Shi, Yigong and, and Joan Massague. 2003. “Mechanisms of TGF-Beta Signaling from Cell Membrane to the Nucleus.” *Cell* 113: 685–700.

Shi, Yigong, Yan-fei Wang, Lata Jayaraman, Haijuan Yang, and Joan Massague. 1998. “Crystal Structure of a Smad MH1 Domain Bound to DNA : Insights on DNA Binding in TGF-β Signaling.” *Cell* 94 (2): 585–94.

Shlyueva, D., G. Stampfel, and and Stark A. 2014. “Transcriptional Enhancers: From Properties to Genome-Wide Predictions.” *Nature Reviews Genetics* 15: 272–86.

Shukunami, Chisa, Kiyoto Ishizeki, Tadao Atsumi, Yoshiyuki Ohta, Fujio Suzuki, and Yuji Hiraki. 1997. “Cellular Hypertrophy and Calcification of Embryonal Carcinoma-Derived Chondrogenic Cell Line ATDC5 In Vitro.” *Journal of Bone and Mineral Research* 12 (8): 1174–88.

Siepel, Adam, Gill Bejerano, Jakob S Pedersen, Angie S Hinrichs, Minmei Hou, Kate Rosenbloom, Hiram Clawson, et al. 2005. “Evolutionarily Conserved Elements in Vertebrate, Insect, Worm, and Yeast Genomes.” *Genome Research* 15: 1034–50. https://doi.org/10.1101/gr.3715005.

Silva, Iris A L, Natércia Conceição, Édith Gagnon, Helena Caiado, Jacques P Brown, Fernando Gianfrancesco, Laëtitia Michou, and M Leonor Cancela. 2018. “Effect of Genetic Variants of OPTN in the Pathophysiology of Paget ’ s Disease of Bone.” *BBA - Molecular Basis of Disease* 1864: 143–51. https://doi.org/10.1016/j.bbadis.2017.10.008.

Silva, Susana da, and Fan Wang. 2011. “Retrograde Neural Circuit Specification by Target-Derived Neurotrophins

and Growth Factors." *Curr Opin Neurobiol.* 21 (1): 61–67. https://doi.org/10.1016/j.conb.2010.07.007.Retrograde.

Sivasankaran, Rajeev, M Alessandra Vigano, Bruno Mu, Markus Affolter, and Konrad Basler. 2000. "Direct Transcriptional Control of the Dpp Target Omb by the DNA Binding Protein Brinker." *The EMBO Journal* 19 (22): 6162–72.

Slattery, Matthew, Todd Riley, Peng; Liu, Namiko; Abe, Pilar; Gomez-Alcala, Iris; Dror, Tianyin; Zhou, et al. 2011. "Cofactor Binding Evokes Latent Differences in DNA Binding Specificity between Hox Proteins." *Cell* 147 (6): 1270–82. https://doi.org/10.1016/j.cell.2011.10.053.Cofactor.

Small, Kerrin S, Åsa K Hedman, Elin Grundberg, Alexandra C Nica, Gudmar Thorleifsson, Augustine Kong, Unnur Thorsteindottir, et al. 2011. "Identification of an Imprinted Master Trans-Regulator at the KLF14 Locus Related to Multiple Metabolic Phenotypes." *Nature Genetics* 43 (6): 561–64. https://doi.org/10.1038/ng.833.Identification.

Smallwood, Andrea, and Bing Ren. 2013. "Genome Organization and Long-Range Regulation of Gene Expression by Enhancers." *Current Opinion in Cell Biology* 25: 387–94. https://doi.org/10.1016/j.ceb.2013.02.005.

Smith, Edwin, and Ali Shilatifard. 2014. "Enhancer Biology and Enhanceropathies." *Nature Structural and Molecular Biology* 21 (3): 210–2019.

Smith, James Oliver, Alexander Aarvold, Edward R Tayton, Douglas G Dunlop, and Richard O C Oreffo. 2011. "Skeletal Tissue Regeneration: Current Approaches, Challenges, and Novel Reconstructive Strategies for an Aging Population." *Tissue Engineering Part B: Reviews* 17 (5): 307–20. https://doi.org/10.1089/ten.teb.2011.0143.

Smits, Patrick, Peter Dy, Srijeet Mitra, and Véronique Lefebvre. 2004. "Sox5 and Sox6 Are Needed to Develop and Maintain Source, Columnar, and Hypertrophic Chondrocytes in the Cartilage Growth Plate." *Journal of Cell Biology* 164 (5): 747–58. https://doi.org/10.1083/jcb.200312045.

Smits, Patrick, Ping Li, Jennifer Mandel, Zhaoping Zhang, Jian Ming Deng, Richard R Behringer, Benoit De Crombrugghe, and Véronique Lefebvre. 2001. "The Transcription Factors L-Sox5 and Sox6 Are Essential for Cartilage Formation." *Developmental Cell* 1: 277–90.

Song, Buer, Kristine Estrada, and Karen Lyons. 2009. "Smad Signaling in Skeletal Development and Regeneration." *Cytokine and Growth Factor Reviews* 20 (5–6): 379–88. https://doi.org/10.1016/j.cytogfr.2009.10.010.Smad.

Song, Lin, Lillian Chau, Yoshitaka Sakamoto, Juichiro Nakashima, Masafumi Koide, and Rocky S. Tuan. 2004. "Electric Field-Induced Molecular Vibration for Noninvasive, High-Efficiency DNA Transfection." *Molecular Therapy* 9 (4): 607–16. https://doi.org/10.1016/j.ymthe.2004.01.017.

Song, Zhuoyue, Xiaolei Lian, Yang Wang, Yong Xiang, and Guangheng Li. 2017. "KLF15 Regulates in Vitro Chondrogenic Differentiation of Human Mesenchymal Stem Cells by Targeting SOX9." *Biochemical and Biophysical Research Communications* 493 (2): 1082–88. https://doi.org/10.1016/j.bbrc.2017.09.078.

Spaapen, Frank, Guus G H van den Akker, Marjolein M J Caron, Peggy Prickaerts, Celine Rofel, Vivian E H Dahlmans, Don A M Surtel, et al. 2013. "The Immediate Early Gene Product EGR1 and Polycomb Group Proteins Interact in Epigenetic Programming during Chondrogenesis." *PloS One* 8 (3): 1–16. https://doi.org/10.1371/journal.pone.0058083.

Spitz Francois and Furlong Eileen. 2012. "Transcription Factors: From Enhacer Binding to Developmental Control." *Nature Reviews Genetics* 13: 613–26.

Sun, Cheng, Hanning Liu, Ke Si, Yaru Wu, Kun Zhao, Ruixia Xu, Zhou Zhou, and Zhe Zheng. 2019. "Meis2 Represses the Osteoblastic Transdifferentiation of Aortic Valve Interstitial Cells through the Notch1/Twist1 Pathway." *Biochemical and Biophysical Research Communications* 509: 455–61. https://doi.org/10.1016/j.bbrc.2018.12.040.

Suryamohan, Kushal, and Marc S Halfon. 2015. “Identifying Transcriptional Cis -Regulatory Modules” 4 (April). https://doi.org/10.1002/wdev.168.

Swanson, Christina I.; Schwimmer, David B.; and Barolo, Scott. 2011. “Rapid Evolutionary Rewiring of a Structurally Constrained Eye Enhancer.” *Current Biology* 21 (14): 1186–96. https://doi.org/10.1016/j.cub.2011.05.056.Rapid.

Szklarczyk, Damian, Annika L Gable, David Lyon, Alexander Junge, Stefan Wyder, Jaime Huerta-cepas, Milan Simonovic, et al. 2019. “STRING V11 : Protein – Protein Association Networks with Increased Coverage, Supporting Functional Discovery in Genome-Wide Experimental Datasets.” *Nucleic Acids Research* 47: 607–13. https://doi.org/10.1093/nar/gky1131.

Takahashi, K, G H Nuckolls, I Takahashi, K Nonaka, M Nagata, T Ikura, H C Slavkin, and L Shum. 2001. “Msx2 Is a Repressor of Chondrogenic Differentiation in Migratory Cranial Neural Crest Cells.” *Developmental Dynamics* 222: 252–62. https://doi.org/10.1002/dvdy.1185.

Takeda, Shu, Jean-Pierre Bonnamy, Michael J Owen, Patricia Ducy, and Gerard Karsenty. 2001. “Continuous Expression of Cbfa1 in Nonhypertrophic Chondrocytes Uncovers Its Ability to Induce Hypertrophic Chondrocyte Differentiation and Partially Rescues Cbfa1-Deficient Mice.” *Genes & Development* 15: 467–81. https://doi.org/10.1101/gad.845101.Hypertrophic.

Taylor, Gillian C.A., Ragnhild Eskeland, Betül Hekimoglu-Balkan, Madapura M. Pradeepa, and Wendy A. Bickmore. 2013. “H4K16 Acetylation Marks Active Genes and Enhancers of Embryonic Stem Cells, but Does Not Alter Chromatin Compaction.” *Genome Research* 23 (12): 2053–65. https://doi.org/10.1101/gr.155028.113.

Teramura, T., J. Hasei, H. Asahara, and M.K. Lotz. 2015. “Krüppel-like Factors (KLFS), Novel Transcriptional Regulators of Articular Chondrocytes That Are Abnormally Expressed in Osteoarthritic Cartilage.” *Osteoarthritis and Cartilage* 23 (2015): A101. https://doi.org/10.1016/j.joca.2015.02.814.

Thomas, Paul D, Anish Kejariwal, Nan Guo, Huaiyu Mi, Michael J Campbell, Anushya Muruganujan, Betty Lazareva-ulitsky, et al. 2006. “Applications for Protein Sequence – Function Evolution Data: MRNA / Protein Expression Analysis and Coding SNP Scoring Tools.” *Nucleic Acids Research* 34: 645–50. https://doi.org/10.1093/nar/gkl229.

Tie, Feng, Rakhee Banerjee, Carl A Stratton, Jayashree Prasad-sinha, Vincent Stepanik, Andrei Zlobin, Manuel O Diaz, Peter C Scacheri, and Peter J Harte. 2009. “CBP-Mediated Acetylation of Histone H3 Lysine 27 Antagonizes Drosophila Polycomb Silencing.” *Development* 3141: 3131–41. https://doi.org/10.1242/dev.037127.

Tolkachov, Alexander, Cornelius Fischer, Thomas H Ambrosi, Melissa Bothe, Chung-ting Han, Matthias Muenzner, Susanne Mathia, et al. 2018. “Loss of the Hematopoietic Stem Cell Factor GATA2 in the Osteogenic Lineage Impairs Trabecularization and Mechanical Strength of Bone.” *Molecular and Cellular Biology* 38 (12): 1–16.

Tong, Qiang, Gokhan Dalgin, Haiyan Xu, Chao-Nan Ting, Jeffrey Leiden, and Gokhan Hotamisligil. 2000. “Function of GATA Transcription Factors in Preadipocyte- Adipocyte Transition.” *Science* 290: 134–39.

Tong, Qiang, Judy Tsai, Guo Tan, Gokhan Dalgin, and Gokhan Hotamisligil. 2005. “Interaction between GATA and the C/EBP Family of Transcription Factors Is Critical in GATA-Mediated Suppression of Adipocyte Differentiation.” *Molecular and Cellular Biology* 25 (2): 706–15. https://doi.org/10.1128/MCB.25.2.706.

Topol, Lilia, Wen Chen, Hai Song, Timothy F Day, and Yingzi Yang. 2009. “Sox9 Inhibits Wnt Signaling by Promoting β-Catenin Phosphorylation in the Nucleus.” *Journal of Biological Chemistry* 284 (5): 3323–33. https://doi.org/10.1074/jbc.M808048200.

Tsai, Sophia Y., and Ming J. Tsai. 1997. “Chick Ovalbumin Upstream Promoter-Transcription Factors (COUP-TFs): Coming of Age.” *Endocrine Reviews* 18 (2): 229–40. https://doi.org/10.1210/er.18.2.229.

Tsuda, Takeshi, Dessislava Markova, Hui Wang, Lucia Evangelisti, Te-cheng Pan, and Mon-li Chu. 2004. “Zinc Finger Protein Zac1 Is Expressed in Chondrogenic Sites of the Mouse.” *Developmental Dynamics* 229: 340–48. https://doi.org/10.1002/dvdy.10439.

Tsuji, Kunikazu, Amitabha Bandyopadhyay, Brian D Harfe, Karen Cox, Sanjeev Kakar, Louis Gerstenfeld, Thomas Einhorn, Clifford J Tabin, and Vicki Rosen. 2006. “BMP2 Activity , Although Dispensable for Bone Formation , Is Required for the Initiation of Fracture Healing.” *Nature Genetics* 38 (12): 1424–29. https://doi.org/10.1038/ng1916.

Tuli, Richard, Suraj Tuli, Sumon Nandi, Xiaoxue Huang, Paul A Manner, William J Hozack, Keith G Danielson, David J Hall, and Rocky S Tuan. 2003. “Transforming Growth Factor-β-Mediated Chondrogenesis of Human Mesenchymal Progenitor Cells Involves N-Cadherin and Mitogen- Activated Protein Kinase and Wnt Signaling Cross-Talk.” *Journal of Biological Chemistry* 278 (42): 41227–36. https://doi.org/10.1074/jbc.M305312200.

Tzchori, Itai, Timothy F Day, Peter J Carolan, Yangu Zhao, Christopher A Wassif, Liqi Li, Mark Lewandoski, et al. 2009. “LIM Homeobox Transcription Factors Integrate Signaling Events That Control Three-Dimensional Limb Patterning and Growth.” *Development* 136: 1375–85. https://doi.org/10.1242/dev.026476.

Ueda, Shogo, Ingrid Rosenburg Cordeiro, Yuuta Moriyama, Chika Nishimori, Kei-ichi Kai, Reiko Yu, Ryoichiro Nakato, Katsuhiko Shirahige, and Mikiko Tanaka. 2019. “Cux2 Refines the Forelimb Field by Controlling Expression of Raldh2 and Hox Genes.” *Biology Open* 8: 1–10. https://doi.org/10.1242/bio.040584.

Underhill, T Michael, Helen J Dranse, and Lisa M Hoffman. 2014. “Analysis of Chondrogenesis Using Micromass Cultures of Limb Mesenchyme BT -.” In *Skeletal Development and Repair: Methods and Protocols in Molecular Biolo*, edited by Matthew J Hilton, 251–65. Totowa, NJ: Humana Press. https://doi.org/10.1007/978-1-62703-989-5_19.

Urist, Marshall R. 1965. “Bone: Formation by Autoiduction.” *Science* 150 (3698): 893–99.

Valenta, Tomas, Jan Lukas, Lenka Doubravska, Bohumil Fafilek, and Vladimir Korinek. 2006. “HIC1 Attenuates Wnt Signaling by Recruitment of TCF-4 and b -Catenin to the Nuclear Bodies.” *The EMBO Journal* 25 (11): 2326–37. https://doi.org/10.1038/sj.emboj.7601147.

Verschueren, Kristin, Jacques E Remacle, Clara Collart, Harry Kraft, Betty S Baker, Przemko Tylzanowski, Luc Nelles, et al. 1999. “SIP1 , a Novel Zinc Finger/Homeodomain Repressor, Interacts with Smad Proteins and Binds to 5`-CACCT Sequences in Candidate Target Genes.” *Journal of Biological Chemistry* 274 (29): 20489–98.

Veverytsa, Lyubov, and Douglas W Allan. 2011. “Retrograde BMP Signaling Controls Drosophila Behavior through Regulation of a Peptide Hormone Battery.” *Development* 3157: 3147–57. https://doi.org/10.1242/dev.064105.

Vortkamp, Andrea, Kaechoong Lee, Beate Lanske, Gino V Segre, Henry M Kronenberg, and Clifford J Tabin. 1996. “Regulation of Rate of Cartilage Differentiation by Indian Hedgehog and PTH-Related Protein.” *Science* 273 (5275): 613–22. https://doi.org/10.1126/science.273.5275.613.

Vuilleumier, Robin, Tianshun Lian, Stephane Flibotte, Zaynah N Khan, Alisa Fuchs, George Pyrowolakis, and Douglas W Allan. 2018. “Retrograde BMP Signaling Activates Neuronal Gene Expression through Widespread Deployment of a Conserved BMP-Responsive *Cis* -Regulatory *Activation Element*.” *Nucleic Acids Research*, 1–21. https://doi.org/10.1093/nar/gky1135.

Walsh, Christopher M, and Sean B Carroll. 2007. “Collaboration between Smads and a Hox Protein in Target Gene Repression.” *Development* 134: 3585–92. https://doi.org/10.1242/dev.009522.

Wang, Lai, Yvonne Y. Shao, and R. Tracy Ballock. 2005. “Peroxisome Proliferator Activated Receptor-γ (PPARγ) Represses Thyroid Hormone Signaling in Growth Plate Chondrocytes.” *Bone* 37 (3): 305–12. https://doi.org/10.1016/j.bone.2005.04.031.

Wang, Liguo, Shengqin Wang, and Wei Li. 2012. “RSeQC: Quality Control of RNA-Seq Experiments.” *Bioinformatics* 28 (16): 2184–85. https://doi.org/10.1093/bioinformatics/bts356.

Wang, Qing, Xiaochao Wei, Tianhui Zhu, Ming Zhang, Run Shen, Lianping Xing, Regis J O Keefe, and Di Chen. 2007. “Bone Morphogenetic Protein 2 Activates Smad6 Gene Transcription through Bone-Specific Transcription Runx2.” *Journal of Biological Chemistry* 282 (14): 10742–48. https://doi.org/10.1074/jbc.M610997200.

Wang, Richard N, Jordan Green, Zhongliang Wang, Jixing Ye, Zhengjian Yan, Sahitya Denduluri, Olumuyiwa Idowu, et al. 2014. “ScienceDirect Bone Morphogenetic Protein (BMP) Signaling in Development and Human Diseases.” *Genes & Diseases* 1 (1): 87–105. https://doi.org/10.1016/j.gendis.2014.07.005.

Wang, Weiguang, Na Lian, Lingzhen Li, Heather E Moss, Weixi Wang, Daniel S Perrien, Florent Elefteriou, and Xiangli Yang. 2009. “Atf4 Regulates Chondrocyte Proliferation and Differentiation during Endochondral Ossification by Activating Ihh Transcription.” *Development* 136: 4143–53. https://doi.org/10.1242/dev.043281.

Wang, Weiguang, Buer Song, Teni Anbarchian, Anna Shirazyan, Joshua E Sadik, and Karen M Lyons. 2016. “Smad2 and Smad3 Regulate Chondrocyte Proliferation and Differentiation in the Growth Plate.” *PLoS Genetics* 12 (10): 1–25. https://doi.org/10.1371/journal.pgen.1006352.

Wang, Yi, Sika Ristevski, and Vincent R Harley. 2006. “SOX13 Exhibits a Distinct Spatial and Temporal Expression Pattern During Chondrogenesis, Neurogenesis, and Limb Development.” *The Journal of Histochemistry & Cytochemistry* 54 (12): 1327–33. https://doi.org/10.1369/jhc.6A6923.2006.

Wang, Zhao Jun, Hai Bin Zhang, Cheng Chen, Hao Huang, and Jian Xia Liang. 2018. “Effect of PPARG on AGEs-Induced AKT/MTOR Signaling-Associated Human Chondrocytes Autophagy.” *Cell Biology International* 42 (7): 841–48. https://doi.org/10.1002/cbin.10951.

Wang, Zhibin, Chongzhi Zang, Jeffrey A Rosenfeld, Dustin E Schones, Suresh Cuddapah, Kairong Cui, Tae-young Roh, Weiqun Peng, Michael Zhang, and Keji Zhao. 2008. “Combinatorial Patterns of Histone Acetylations and Methylations in the Human Genome.” *Nature Genetics* 40 (7): 897–903. https://doi.org/10.1038/ng.154.Combinatorial.

Warner, Dennis R, Justin P Wells, Robert M Greene, and M Michele Pisano. 2013. “Gene Expression Changes in the Secondary Palate and Mandible of Prdm16−/− Mice.” *Cell Ti* 351 (3): 445–52. https://doi.org/10.1007/s00441-012-1525-2.Gene.

Wasserman, Wyeth W, and Albin Sandelin. 2004. “Applied Bioinformatics for the Identification of Regulatory Elements.” *Nature Reviews Genetics* 5 (April): 276. https://doi.org/10.1038/nrg1315.

Watanabe, Naoko, Yoko Tezuka, Kenji Matsuno, Seiji Miyatani, Naoko Morimura, Masafumi Yasuda, Ryoji Fujimaki, et al. 2003. “Suppression of Differentiation and Proliferation of Early Chondrogenic Cells by Notch.” *Journal of Bone and Mineral Metabolism* 21: 344–52. https://doi.org/10.1007/s00774-003-0428-4.

Weake Vikki and Workman Jerry. 2010. “Inducible Gene Expression: Diverse Regulatory Mechanisms.” *Nature Reviews Genetics* 11: 426–37.

Weiss, Alexander; Charbonnier, Enrica; Ellertsdottir, Elin;, Aristotelis; Tsirigos, Christian; Wolf, Reinhard Schuh, George; Pyrowolakis, and Ma Affolter. 2010. “A Conserved Activation Element in BMP Signaling during Drosophila Development.” *Nature Structural and Molecular Biology.* 17: 69–77.

Weiszmann, Richard, Ann S Hammonds, and Susan E Celniker. 2009. “Determination of Gene Expression Patterns Using High-Throughput RNA in Situ Hybridization to Whole-Mount Drosophila Embryos.” *Nature Protocols* 4 (5): 605–18. https://doi.org/10.1038/nprot.2009.55.

Weston, Andrea D, Roshantha A S Chandraratna, Joseph Torchia, and T Michael Underhill. 2002. “Requirement for RAR-Mediated Gene Repression in Skeletal Progenitor Differentiation.” *Journal of Cell Biology* 158 (1): 39–

51. https://doi.org/10.1083/jcb.200112029.

Whetstine, Johnathan R. 2010. “Histone Methylation: Chemically Inert but Chromatin Dynamic.” In *Handbook of Cell Signaling*, Second Edi, 3:2389–97. Elsevier Inc. https://doi.org/10.1016/B978-0-12-374145-5.00287-4.

White, Michael A, Davis S Parker, Scott Barolo, and Barak A Cohen. 2012. “A Model of Spatially Restricted Transcription in Opposing Gradients of Activators and Repressors.” *Molecular Systems Biology* 8 (614): 1–9. https://doi.org/10.1038/msb.2012.48.

Whitman, Malcolm. 1998. “Smads and Early Developmental Signaling by the TGF ʟ Superfamily.” *Gene & Developent* 12: 2445–62.

Woods, Anita, Claudine G James, Guoyan Wang, Holly Dupuis, and Frank Beier. 2009. “Control of Chondrocyte Gene Expression by Actin Dynamics: A Novel Role of Cholesterol / Ror-a Signalling in Endochondral Bone Growth.” *J. Cell. Mol. Med.* 13 (9): 3497–3516. https://doi.org/10.1111/j.1582-4934.2009.00684.x.

Wozney, John M, Vicki Rosen, Anthony J Celeste, Lisa M Mitsock, J Matthew, Ronald W Kriz, Rodney M Hewick, et al. 1988. “Novel Regulators of Bone Formation : Molecular Clones and Activities Linked References Are Available on JSTOR for This Article : Novel Regulators of Bone Formation : Molecular Clones and Activities.” *Science* 242 (4885): 1528–34.

Wu, Jinghai, Seetha V. Srinivasan, Jon C. Neumann, and Jerry B. Lingrel. 2005. “The KLF2 Transcription Factor Does Not Affect the Formation of Preadipocytes but Inhibits Their Differentiation into Adipocytes.” *Biochemistry* 44 (33): 11098–105. https://doi.org/10.1021/bi050166i.

Xi, Yang, Wanjing Shen, Lili Ma, Ming Zhao, Jiachen Zheng, Shizhong Bu, Shinjiro Hino, and Mitsuyoshi Nakao. 2016. “HMGA2 Promotes Adipogenesis by Activating C/EBPb-Mediated Expression of PPARg.” *Biochemical and Biophysical Research Communications* 472: 617–23. https://doi.org/10.1016/j.bbrc.2016.03.015.

Xie, Wei-fen, X I N Zhang, Shinji Sakano, Veronique Lefebvre, and Linda J Sandell. 1999. “Trans-Activation of the Mouse Cartilage-Derived Retinoic Acid-Sensitive Protein Gene by Sox9.” *Journal of Bone and Mineral Research* 14 (5): 757–63.

Xu, Lan. 2006. “Regulation of Smad Activities.” *Biochim Biophys Acta.* 1759 (11–12): 503–13.

Xu, Mu, Nikolai Kirov, and Christine Rushlow. 2005. “Peak Levels of BMP in the Drosophila Embryo Control Target Genes by a Feed-Forward Mechanism.” *Development*, 1637–47. https://doi.org/10.1242/dev.01722.

Xu, Pin-Xian, Jane Cheng, Jonathan Epstein, and Richard Maas. 1997. “Mouse Eya Genes Are Expressed during Limb Tendon Development and Encode a Transcriptional Activation Function.” *Proc Natl Acad Sci USA* 94: 11974–79.

Xu, Susan C, Marie A Harris, John L R Rubenstein, Gregory R Mundy, and Stephen E Harris. 2001. “Bone Morphogenetic Protein-2 (BMP-2) Signaling to the Col2a1 Gene in Chondroblasts Requires the Homeobox Gene Dlx2.” *DNA and Cell Biology* 20 (6): 359–65.

Xu, Xiaolei, Zhizhang Yin, John B Hudson, Edwin L Ferguson, and Manfred Frasch. 1998. “Smad Proteins Act in Combination with Synergistic and Antagonistic Regulators to Target Dpp Responses to the Drosophila Mesoderm.” *Gene & Developent* 12: 2354–70.

Yamamoto, Shiori, Yuji Uchida, Tomomi Ohtani, Erina Nozaki, Chunyang Yin, Yoshihiro Gotoh, Nayuta Yakushiji-Kaminatsui, et al. 2019. “Hoxa13 Regulates Expression of Common Hox Target Genes Involved in Cartilage Development to Coordinate the Expansion of the Autopodal Anlage.” *Development, Growth & Differentiation* 61: 228–51. https://doi.org/10.1111/dgd.12601.

Yamashita, Satoshi, Kensuke Katao, Hiroto Yamamoto, Tomoko Kato, Satoshi Hara, Katsushi Yamaguchi, Claire Renard-Guillet, et al. 2019. “Comparative Analysis Demonstrates Cell Type-Specific Conservation of SOX9 Targets between Mouse and Chicken.” *Scientific Reports* 9: 1–15. https://doi.org/10.1038/s41598-019-48979-

4.

Yammani, Raghunatha R. and Loeser, Richard. 2014. “Stress Inducible Gene Nuclear Protein-1 (NUPR1/P8) Regulates MMP-13 Expression in Human Articular Chondrocytes.” *Arthritis Rheumatol.* 66 (5): 1266–71. https://doi.org/10.1002/art.38391.Stress.

Yan, Jianyun, Jun Li, Jun Hu, Lu Zhang, Chengguo Wei, Nishat Sultana, Xiaoqiang Cai, Weijia Zhang, and Chenleng Cai. 2018. “Smad4 Deficiency Impairs Chondrocyte Hypertrophy via the Runx2 Transcription Factor in Mouse Skeletal Development.” *Journal of Biological Chemistry* 293 (24): 9162–75. https://doi.org/10.1074/jbc.RA118.001825.

Yanagino, Takuya, Keizo Yuasa, Masami Nagahama, Yoshiko Matsuda, and Akihiko Tsuji. 2009. “Transcriptional Regulation of Fibrillin-2 Gene by E2F Family Members in Chondrocyte Differentiation.” *Journal of Cellular Biochemistry* 106: 580–88. https://doi.org/10.1002/jcb.22029.

Yanez-Cuna, Omar, Evgeny Kvon, and Alexander Stark. 2013. “Deciphering the Transcriptional Cis- Regulatory Code.” *Cell Trends in Genetics* 29 (1): 11–22. https://doi.org/10.1016/j.tig.2012.09.007.

Yang, Tian, Alexander Bassuk, and Bernd Fritzsch. 2013. “Prickle1 Stunts Limb Growth through Alteration of Cell Polarity and Gene Expression.” *Dev Dyn.* 242 (11): 1293–1306. https://doi.org/10.1002/dvdy.24025.Prickle1.

Yap, Kai Lee, Polina Sysa-shah, Brad Bolon, Ren-chin Wu, Min Gao, Alice L Herlinger, Francesco Faiola, et al. 2013. “Loss of NAC1 Expression Is Associated with Defective Bony Patterning in the Murine Vertebral Axis.” *PloS ONE* 8 (7): 1–16. https://doi.org/10.1371/journal.pone.0069099.

Yella, Venkata Rajesh, Devesh Bhimsaria, Debostuti Ghoshdastidar, Jose Rodriguez-Martinez, Aseem Ansari, and Manju Bansal. 2018. “Flexibility and Structure of Flanking DNA Impact Transcription Factor Affinity for Its Core Motif.” *Nucleic Acids Research* 14;46(22): 11883–97. https://doi.org/10.1093/nar/gky1057.

Yoon, Byeong S, Dmitry A Ovchinnikov, Isaac Yoshii, Yuji Mishina, Richard R Behringer, and Karen M Lyons. 2005. “Bmpr1a and Bmpr1b Have Overlapping Functions and Are Essential for Chondrogenesis in Vivo.” *PNAS* 102 (14): 1–6.

Yoshida, Carolina A., and Toshihisa Komori. 2005. “Role of Runx Proteins in Chondrogenesis.” *Critical Reviews™ in Eukaryotic Gene Expression* 15 (3): 243–54. 10.1615/CritRevEukarGeneExpr.v15.i3.60.

You, Di, Cheng Yang, Jun Huang, Haoli Gong, Mingming Yan, and Jiangdong Ni. 2019. “Long Non-Coding RNA MEG3 Inhibits Chondrogenic Differentiation of Synovium-Derived Mesenchymal Stem Cells by Epigenetically Inhibiting TRIB2 via Methyltransferase EZH2.” *Cellular Signalling* 63: 1–10. https://doi.org/10.1016/j.cellsig.2019.109379.

Yuan, Yuan, Honglue Tan, and Pengyi Dai. 2017. “Krüppel-Like Factor 2 Regulates Degradation of Type II Collagen by Suppressing the Expression of Matrix Metalloproteinase (MMP)-13.” *Cellular Physiology and Biochemistry* 42 (6): 2159–68. https://doi.org/10.1159/000479991.

Zawel, Leigh, Jia Le Dai, Phillip Buckhaults, Shibin Zhou, Kenneth W Kinzler, Bert Vogelstein, and Scott E Kern. 1998. “Human Smad3 and Smad4 Are Sequence-Specific Transcription Activators.” *Mol Cell* 1: 611–17.

Zeng, Kefeng, Hong Qi Zhang, Yong Chen, and Qile Gao. 2016. “Estradiol via Estrogen Receptor Beta Inhibits Chondrogenesis of Mouse Vertebral Growth Plate in Vitro.” *Child’s Nervous System* 32: 461–65. https://doi.org/10.1007/s00381-015-2973-2.

Zeng, Li, Herve Kempf, L Charles Murtaugh, Mie Elissa Sato, and Andrew B Lassar. 2005. “Shh Establishes an Nkx3.2/Sox9 Autoregulatory Loop That Is Maintained by BMP Signals to Induce Somitic Chondrogenesis.” *Genes & Development* 16: 1990–2005. https://doi.org/10.1101/gad.1008002.tion.

Zentner, Gabriel E, Paul J Tesar, and Peter C Scacheri. 2011. “Epigenetic Signatures Distinguish Multiple Classes of Enhancers with Distinct Cellular Functions.” *Genome Research* 21: 1273–83. https://doi.org/10.1101/gr.122382.111.21.

Zhang, Bing, Zhiyong Li, Wei Wang, Jichao Guo, Shufeng Kang, Shizhao Liu, Hongzhu Li, Depeng Wang, and Xiangbei Qi. 2018. “NCOA3 Loss Disrupts Molecular Signature of Chondrocytes and Promotes Posttraumatic Osteoarthritis Progression.” *Cellular Physiology and Biochemistry* 49: 2396–2413. https://doi.org/10.1159/000493839.

Zhang, Cui, Fan-fan Hong, Cui-cui Wang, Liang Li, Jian-ling Chen, Fei Liu, Ren-fu Quan, and Jin-Fu Wang. 2017. “TRIB3 Inhibits Proliferation and Promotes Osteogenesis in HBMSCs by Regulating the ERK1/2 Signaling Pathway.” *Scientific Reports* 7: 1–13. https://doi.org/10.1038/s41598-017-10601-w.

Zhang, Hailan, Michael Levine, and Hilary L Ashe. 2001. “Brinker Is a Sequence-Specific Transcriptional Repressor in the Drosophila Embryo.” *Gene & Developent* 15: 261–66. https://doi.org/10.1101/gad.861201.GENES.

Zhang, Jianfei, Wenbin Zhang, Jun Shi, Jiewen Dai, and Steve Guofang Shen. 2018. “Dlx2 Overexpression Enhanced Accumulation of Type II Collagen and Aggrecan by Inhibiting MMP13 Expression in Mice Chondrocytes.” *Biochemical and Biophysical Research Communications* 503: 528–35. https://doi.org/10.1016/j.bbrc.2018.05.066.

Zhang, Wei, Peichun Hsu, Biao Zhong, Shang Guo, Chi Zhang, Yukai Wang, Congfeng Luo, Yulin Zhan, and Changqing Zhang. 2018. “MiR-34a Enhances Chondrocyte Apoptosis , Senescence and Facilitates Development of Osteoarthritis by Targeting DLL1 and Regulating PI3K/AKT Pathway.” *Cellular Physiology and Biochemistry* 48: 1304–16. https://doi.org/10.1159/000492090.

Zhang, Ying E. 2009. “Non-Smad Pathways in TGF-β Signaling.” *Cell Research* 19 (1): 128–39. https://doi.org/10.1038/cr.2008.328.Non-Smad.

Zhang, Ying, Rong-lin Xie, Jonathan Gordon, Kimberly Leblanc, Janet L Stein, Jane B Lian, Andre J Van Wijnen, and Gary S Stein. 2012. “Control of Mesenchymal Lineage Progression by MicroRNAs Targeting Skeletal Gene Regulators Trps1 and Runx2.” *The Journal of Biological Chemistry* 287 (26): 21926–35. https://doi.org/10.1074/jbc.M112.340398.

Zhang, Yong, Tao Liu, Clifford A Meyer, Jérôme Eeckhoute, David S Johnson, Bradley E Bernstein, Chad Nusbaum, et al. 2008. “Model-Based Analysis of ChIP-Seq (MACS).” *Genome Biology* 9 (9): R137. https://doi.org/10.1186/gb-2008-9-9-r137.

Zhao, Chen, Wei Jiang, Nian Zhou, Junyi Liao, Mingming Yang, Ning Hu, Xi Liang, et al. 2017. “Sox9 Augments BMP2-Induced Chondrogenic Differentiation by Downregulating Smad7 in Mesenchymal Stem Cells (MSCs).” *Genes & Diseases* 4: 229–39. https://doi.org/10.1016/j.gendis.2017.10.004.

Zhao, Haixia, Wenrong Zhou, Zhengju Yao, Yong Wan, Jingjing Cao, Lingling Zhang, Jianzhi Zhao, et al. 2015. “Foxp1/2/4 Regulate Endochondral Ossification as a Suppresser Complex.” *Developmental Biology* 398 (2): 242–54. https://doi.org/10.1016/j.ydbio.2014.12.007.Foxp1/2/4.

Zhao, Yingming, and Benjamin A Garcia. 2015. “Comprehensive Catalog of Currently Documented Histone Modifications.” *Cold Spring Harb Perspect Biol* 7: 1–22.

Zhou, Bo, Lihong Chen, Xing Wu, Jing Wang, Yinliang Yin, and Guang Zhu. 2008. “MH1 Domain of SMAD4 Binds N-Terminal Residues of the Homeodomain of Hoxc9.” *Biochimica et Biophysica Acta MH1* 1784: 747–52. https://doi.org/10.1016/j.bbapap.2008.01.021.

Zhou, Guang, Qiping Zheng, Feyza Engin, Elda Munivez, Yuqing Chen, Eiman Sebald, Deborah Krakow, and Brendan Lee. 2006. “Dominance of SOX9 Function over RUNX2 during Skeletogenesis.” *Proc Natl Acad Sci USA* 103 (50): 19004–9.

Zhou, Xin, Klaus Von Der Mark, Stephen Henry, William Norton, Henry Adams, and Benoit De Crombrugghe. 2014. “Chondrocytes Transdifferentiate into Osteoblasts in Endochondral Bone during Development , Postnatal Growth and Fracture Healing in Mice.” *PLoS Genetics* 10 (12). https://doi.org/10.1371/journal.pgen.1004820.

Zhu, Haitao;, Peter; Kavsak, and Gerald Abdollah, Shirin; Wrana, Jerrey and Thomsen. 1999. “A SMAD Ubiquitin Ligase Targets the BMP Pathway and Affects Embryonic Pattern Formation.” *Nature* 400: 687–94.

Zhu, Lirong, Jian Lan Peng, Karine Harutyunyan, Monica Garcia, Monica Justice, and John Belmont. 2007. “Craniofacial, Skeletal, and Cardiac Defects Associated with Altered Embryonic Murine Zic3 Expression Following Targeted Insertion of a PGK-NEO Cassette.” *Frontiers in Bioscience* 12: 1680–90. https://doi.org/10.2741/2180.

Zou, Weiguo, Xi Chen, Jae Shim, Zhiwei Huang, Nicholas Brady, Dorothy Hu, Kirsten Sigrist, Laurie H Glimcher, and Dallas Jones. 2011. “The E3 Ubiquitin Ligase Wwp2 Regulates Craniofacial Development through Monoubiquitination of Goosecoid.” *Nat Cell Biol.* 13 (1): 59–65. https://doi.org/10.1038/ncb2134.The.

Zuscik, Michael J, Matthew J Hilton, Xinping Zhang, Di Chen, and Regis J O Keefe. 2008. “Review Series Regulation of Chondrogenesis and Chondrocyte Differentiation by Stress.” *The Journal of Clinical Investigation* 118 (2): 429–38. https://doi.org/10.1172/JCI34174.of.

Appendix

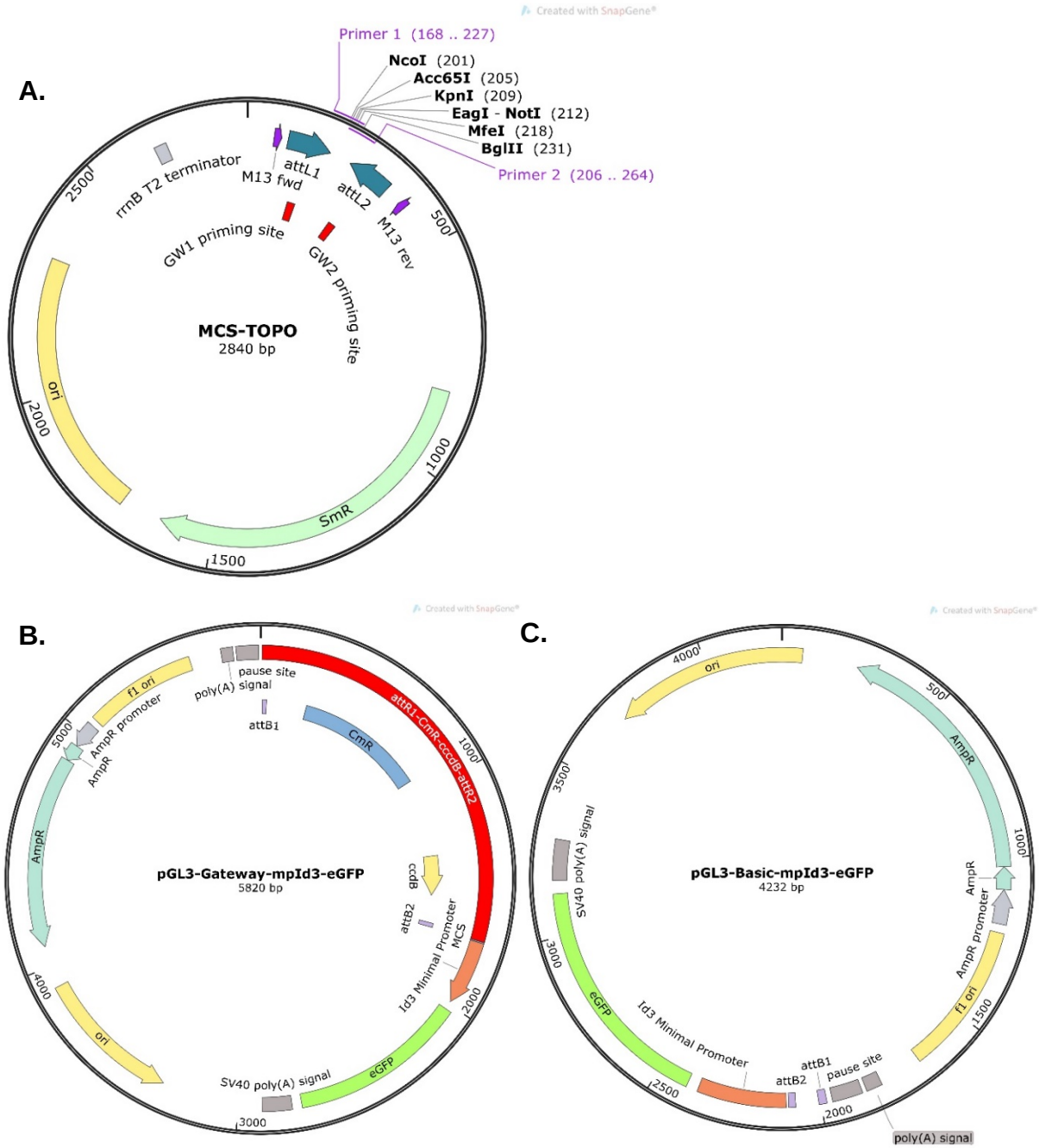

Figure S1: ***SnapGene Vector Maps***

Vector maps of (A) MCS-TOPO Gateway plasmid, (B) pGL3-Gateway-mpId3-eGFP Destination plasmid and (C) pGL2-Basic-mpId3-eGFP Negative control plasmid as exported from the SnapGene software (https://www.snapgene.com/)

A)

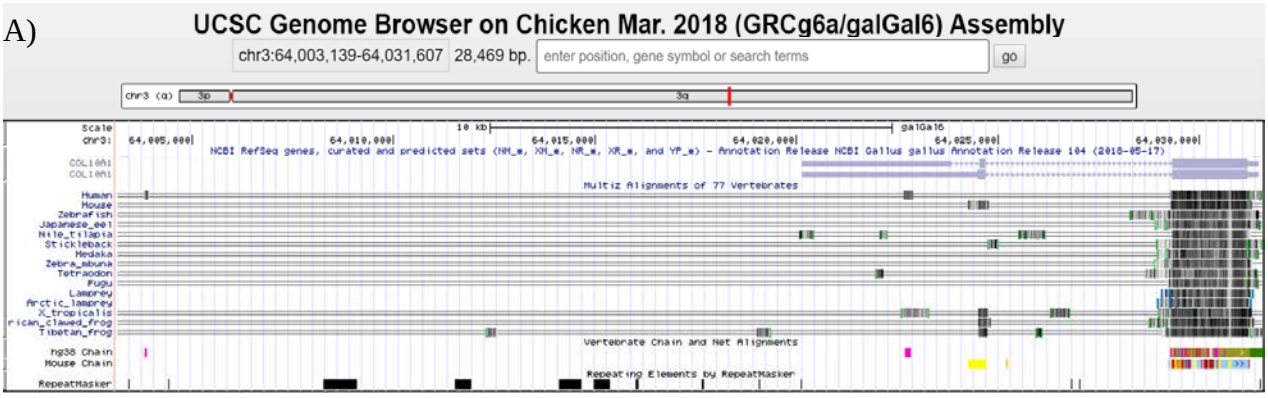

B) 560bp BMP-responsive fragment upstream of the Msx2 gene

chr13:53,475,962-53,476,524

GATCTGCCTTATCCCTCCTTCCCACAGCGCACAGGTAAAAAAAGAAAATGAGCTCAGAGAG
GTGCCATCTTTTGCCCGAAGTCACACAGCGAATGTCCACGGATTGGAGGGCAGTGGTGGAAT
TCCTGGCGGCCCTT**GGCGCCCATTTGTCT**GCCCGCTTCTGATACCCGGGTTCGGAGAATAG
GCCTCTAACAAGCGGCCCATTAGAAGGAATTGTCACTCCTCCGGGAGTGAGGTTGTCCCATT
AGGGCGAATTGTCATTCCTCCTGGAGCGAGGTTGTCCTGGCTCCGCGAAGGCTGAGTGCCGG
GCCGAGAGCAATTAACGCGGCTCCGGCGCGGGCAGCCGCCTCTGCCCCGGGCAGCGGGGGC
GGGGCGCCCGGCGCGGCTGGAGCCGGTCACCCGGCGCAGCCCCTTCCCCCGGAGCCCGCCTT
TCATCTCCCCGCGCCTGGCGCCTACCCGCAGCCCTGGCCCGTCTACAGCCTTCTCTGCCCCTC
CCCCTGCCCCTCCTAGCCTCTGGGATTCCGGCGATCCGTCCTCCGGGTTGCAAACGCCCAGG
TCTGT

Figure S2: ***Previously identified Col10a1 and Msx2 BMP-responsive regions***

A) The UCSC Genome Browser (GRCg6a/galGal6) screenshot displays the conservation of the region upstream of the *G.gallus* COL10A1 gene locus. While the region upstream of the COL10A1 gene is relatively well conserved in other bird species, there is very little conservation between the chicken and vertebrate species.

B) This is the sequence of the 560bp BMP-responsive fragment upstream of the *Msx2* gene; blue highlight indicates the 52bp region within 560bp fragment that was also shown to be BMP-responsive (Brugger et al. 2004). Yellow highlight indicates the region we cloned and used in our reporter experiment in PLM cells. **Green highlight** indicates the conserved BMP-SE we identified with our homer motif search.

UCSC Genome Browser GRCm38/mm10: chr9:64,022,728-64,023,411

-1697
GGCTCTCCCTCCTGGCGTCCTAGGCTCCTCTCAAGGCCAGGCGCTTTCTTCTCCCTTCGAGGAT
TTACCTTATGCCCCTTCGAGAGTGATAGAGGGGCGTGCTTTCCCCAGTTATGTTTCACTATAAA
AACGGGGGCAAGTTGGGGACAGACTTGGGGACCCGGCATGGGAAGGGTTAAG**GCCGCTCCTGCC**
CTGGAGCCGGCGCGGCGGGGTACCTCCTCGGGCGTGCTTGCTAGTCCGAGGGTGGCAAAAGTTC
-1911
AAGCTTGTAAAGTCAGGATTGGCCCCGCGCGGAGGGGAAAAAAGGCCTGGTTCCCCCTCCCCCT
CCCGGGCGT**GGCGCCGATTGGCCC**AGCCGCAGGGCCGGCCCCGCCCTCCCCTGGCGCGCCGCGG
CCCCACCCCCGGCGCAGCACCACGCCCCTTTCCGGGCAGGAGCGGGGCCCCGAGCTCAATGAAA
GAAATTCCGCTACTCTCATTGGCCTGGGGCTTGACGCCGCACCCCGCGGGAGGCGGAGTGGGGA
GGATGGGGCGCGGACTTGTGATCCCCTTTAGGATACCTGTGCTCTGGACTGCTGTAGCGAAGGT
GGTGTGCAAGTCCAGGAACGGGTCTGGAAGTGCGCTGGGGGAAGGGTCGTGTGTGTAGGAAAGA
TACAGACTACTTCCCTGAGTCTTACCTGGAGCCAGGTACTCCAGT
-2383

Figure S3: ***Representation and sequence of Smad6 gene regulatory region***

The illustration represents the upstream region of the *Smad6* gene containing two previously identified BMP-responsive regulatory regions (marked and cited). The sequence between -1697 to -1911 was identified by Ishida et al. as a BMP-responsive regulatory region.

Bold indicates the 28bp sequence studied by Ishida et al. with multiple potential GC-rich Smad-binding sites. **Bold underlined** indicates the palindromic GC-rich binding site identified by mutation analysis to be the most important site for BMP-responsiveness in the identified sequence.

Grey highlighted sequence represents a region identified via deletional analysis by Ishida et al. to have significant luciferase activity. (Specifically, it is the sequence between the D and E fragments studied in Figure 1B). This area was not further tested by Ishida et al. for a Smad-binding element.

Bold, red and underlined sequence is a highly conserved putative BMP-CRE, predicted through our bioinformatic analyses (Table 3.10).

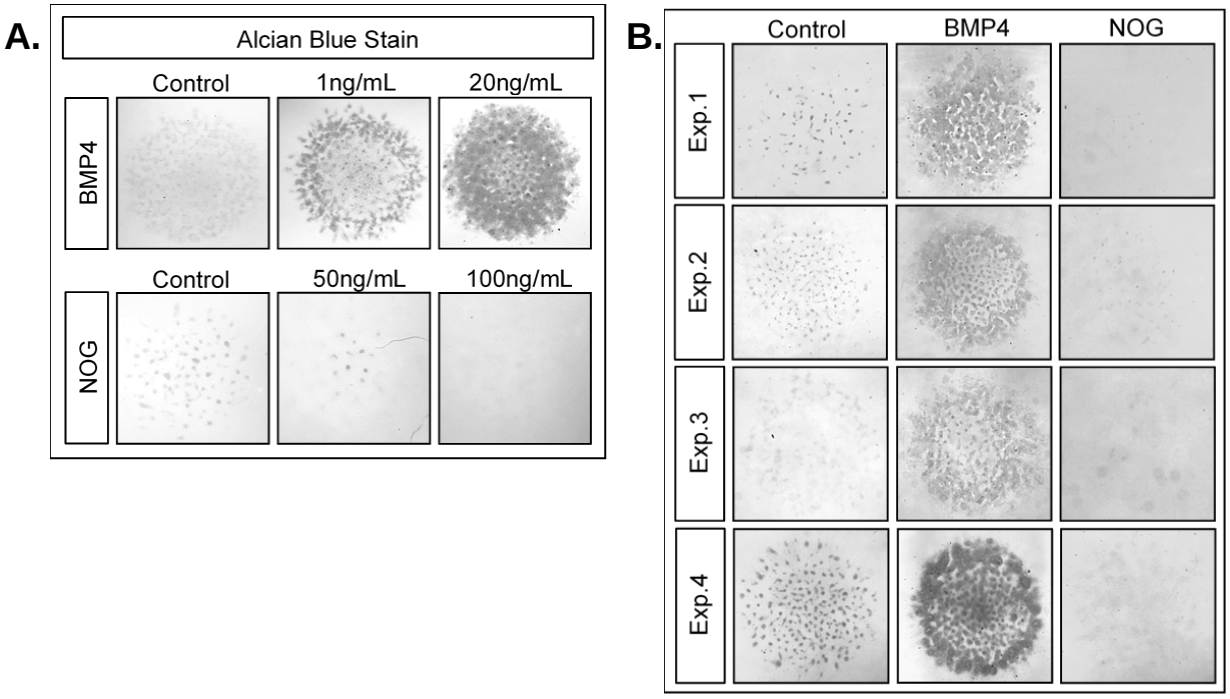

Figure S4: ***Alcian Blue stain indicates hypertrophic development of PLM cells when treated with BMP4 on Day 4 post seeding.***

A) BMP4 and NOG stimulate or block, respectively, cartilage formation in a dose-dependent manner. Alcian blue is used to stain acidic polysaccharides, which can be found in the extracellular matrix of mature chondrocytes. Here we verified the doses to use for our RNA-seq experiments.

B) Cultures from each of the experiments used for RNA-seq (Exp1., Exp2. And Exp3.) and ChIP-seq (Exp4.) were stained on Day 4 post-seeding.

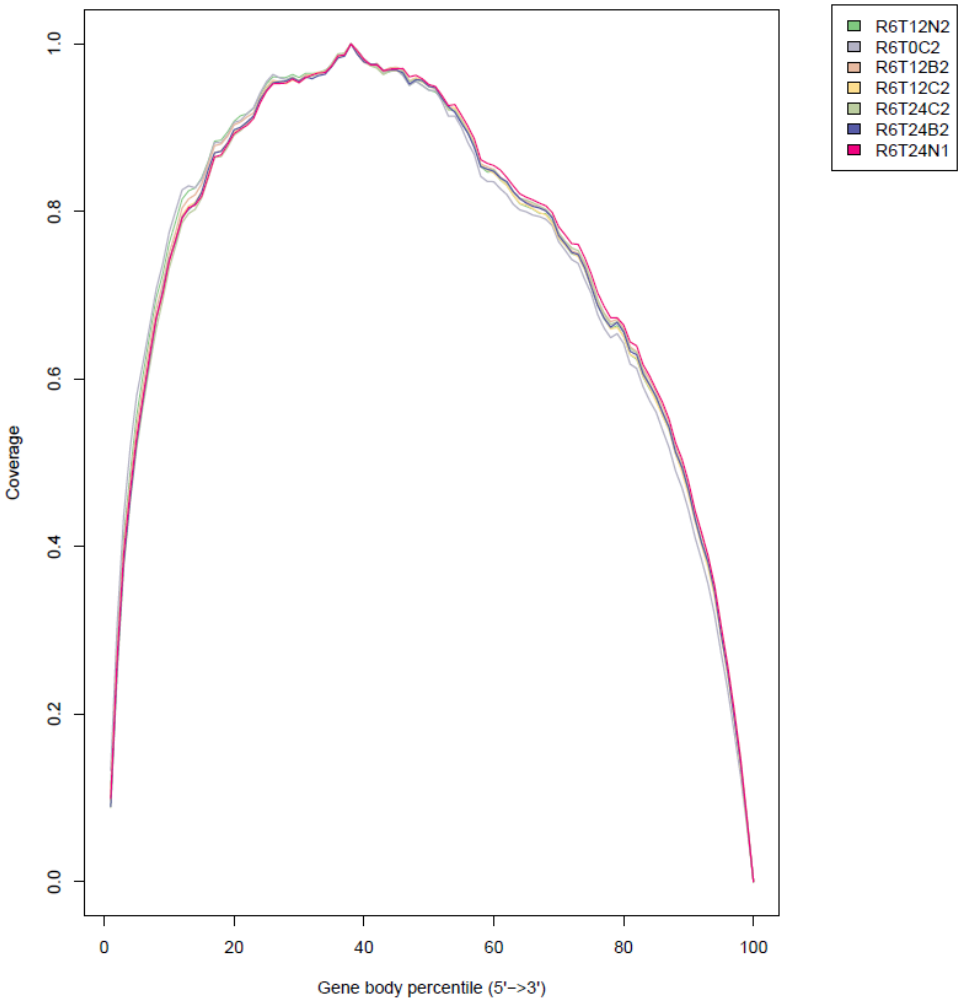

Figure S5: ***RNA-seq Gene Body Coverage Plot indicates uniform coverage profile along the gene body with no 5`/3` bias.***

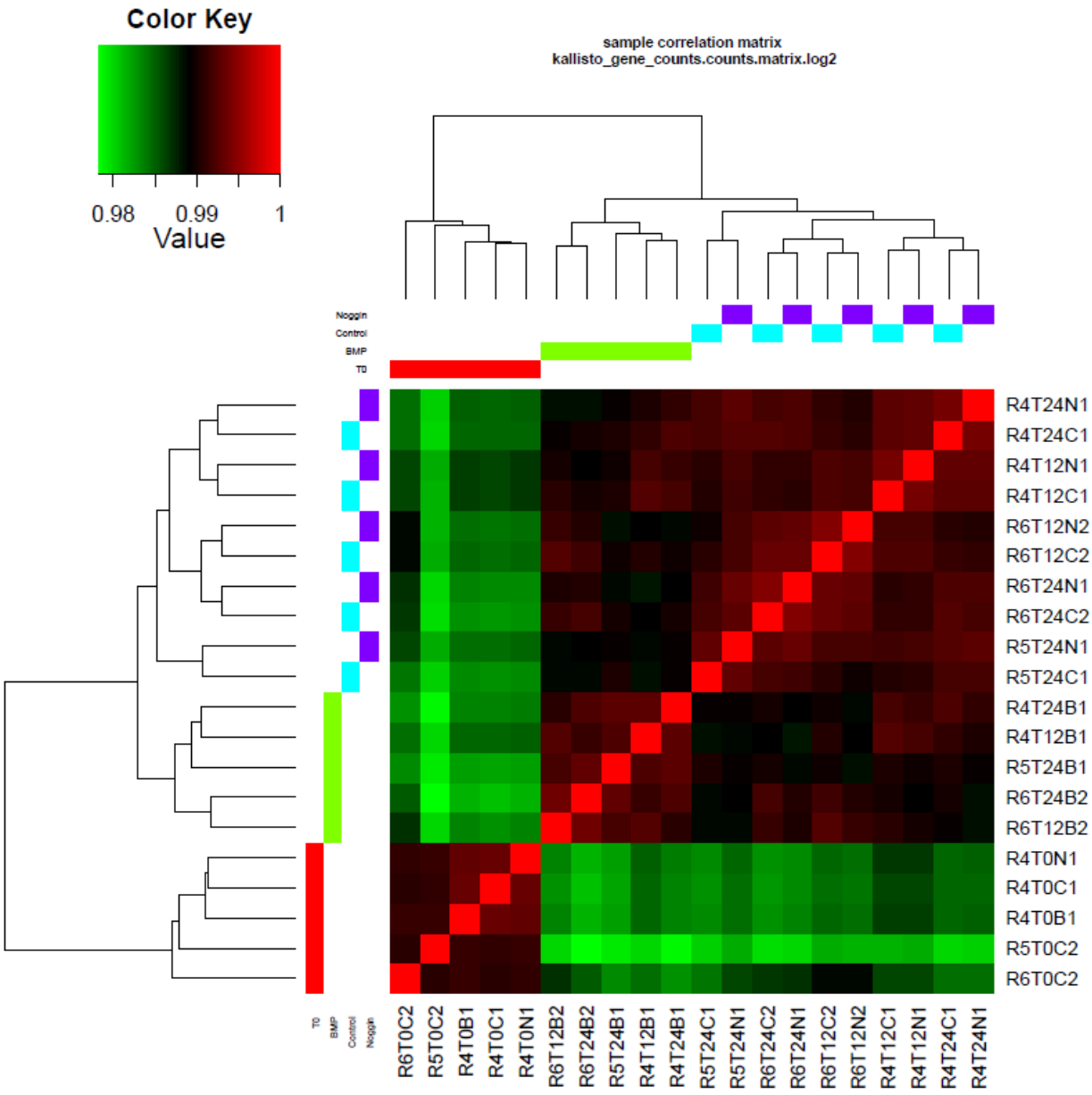

Figure S6: ***RNA-seq Sample Correlation map reveals good correlation between samples from the same time points and with the same treatment.***

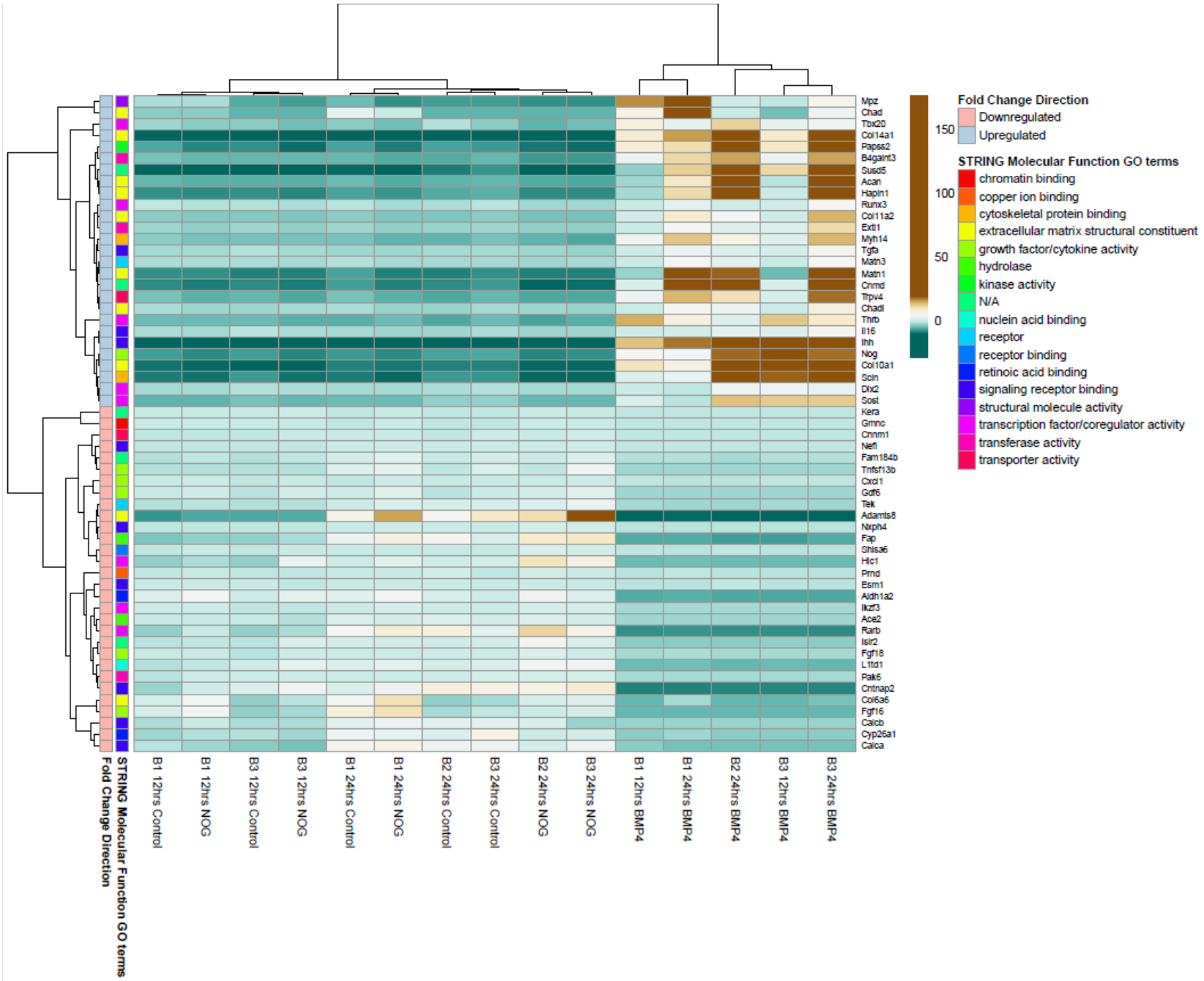
Mpz
Chad
Tbx20
Col14a1
Papss2
B4galnt3
Susd5
Acan
Hapln1
Runx3
Col11a2
Ext1
Myh14
Tgfa
Matn3
Matn1
Cnmd
Trpv4
Chadl
Thrb
Il16
Ihh
Nog
Col10a1
Scin
Dlx2
Sost
Kera
Gmnc
Cnnm1
Nefl
Fam184b
Tnfsf13b
Cxcl1
Gdf6
Tek
Adamts8
Nxph4
Fap
Shisa6
Hlc1
Prnd
Esm1
Aldh1a2
Ikzf3
Ace2
Rarb
Islr2
Fgf18
L1td1
Palk6
Cntnap2
Col6a6
Fgf16
Calcb
Cyp26a1
Calca
B1 12hrs Control
B1 12hrs NOG
B3 12hrs Control
B3 12hrs NOG
B1 24hrs Control
B1 24hrs NOG
B2 24hrs Control
B3 24hrs Control
B2 24hrs NOG
B3 24hrs NOG
B1 12hrs BMP4
B1 24hrs BMP4
B2 24hrs BMP4
B3 12hrs BMP4
B3 24hrs BMP4
Fold Change Direction
STRING Molecular Function GO terms
150
100
50
0
Fold Change Direction
Downregulated
Upregulated
STRING Molecular Function GO terms
chromatin binding
copper ion binding
cytoskeletal protein binding
extracellular matrix structural constituent
growth factor/cytokine activity
hydrolase
kinase activity
N/A
nuclein acid binding
receptor
receptor binding
retinoic acid binding
signaling receptor binding
structural molecule activity
transcription factor/coregulator activity
transferase activity
transporter activity

Figure S7: ***Heatmap of top 30 upregulated and top 30 downregulated genes from RNA-seq.***
We selected the top 1500 genes from the RNA-seq list with the highest confidence score (median ranking from the 10 differential expression pipelines). We sorted them based on their |fold change| and selected the top 30 upregulated and top 30 downregulated genes with the highest change (|fold change|>3). We took the CPM counts from the Kallisto pipeline and normalized each sample with their respective control (Control 0h). For the upregulated top30, we ended up using only the top27 genes, as the following genes were eliminated from the list for having 0 CPM counts as per Kallisto: Gm7265, BC006965 and 2600014E12Rik. Using the ClustVis web tool we plotted these genes with a heatmap. No scaling was applied, and both rows and columns were clustered using correlation distance and complete linkage. Samples with the same treatment are clustered, but we can also observe samples from the same biological experiments clustering (slight bias). STRING Molecular Function GO terms were used to annotate all the genes in the heatmap. In the upregulated list, there are more genes with “extracellular matrix structural constituent” (8 genes) and “transcription factor/coregulator activity” (5 genes) annotations vs in the downregulated list, there are more genes with “signaling receptor binding” (6 genes) and “growth factor/cytokine activity” (5 genes) annotations.

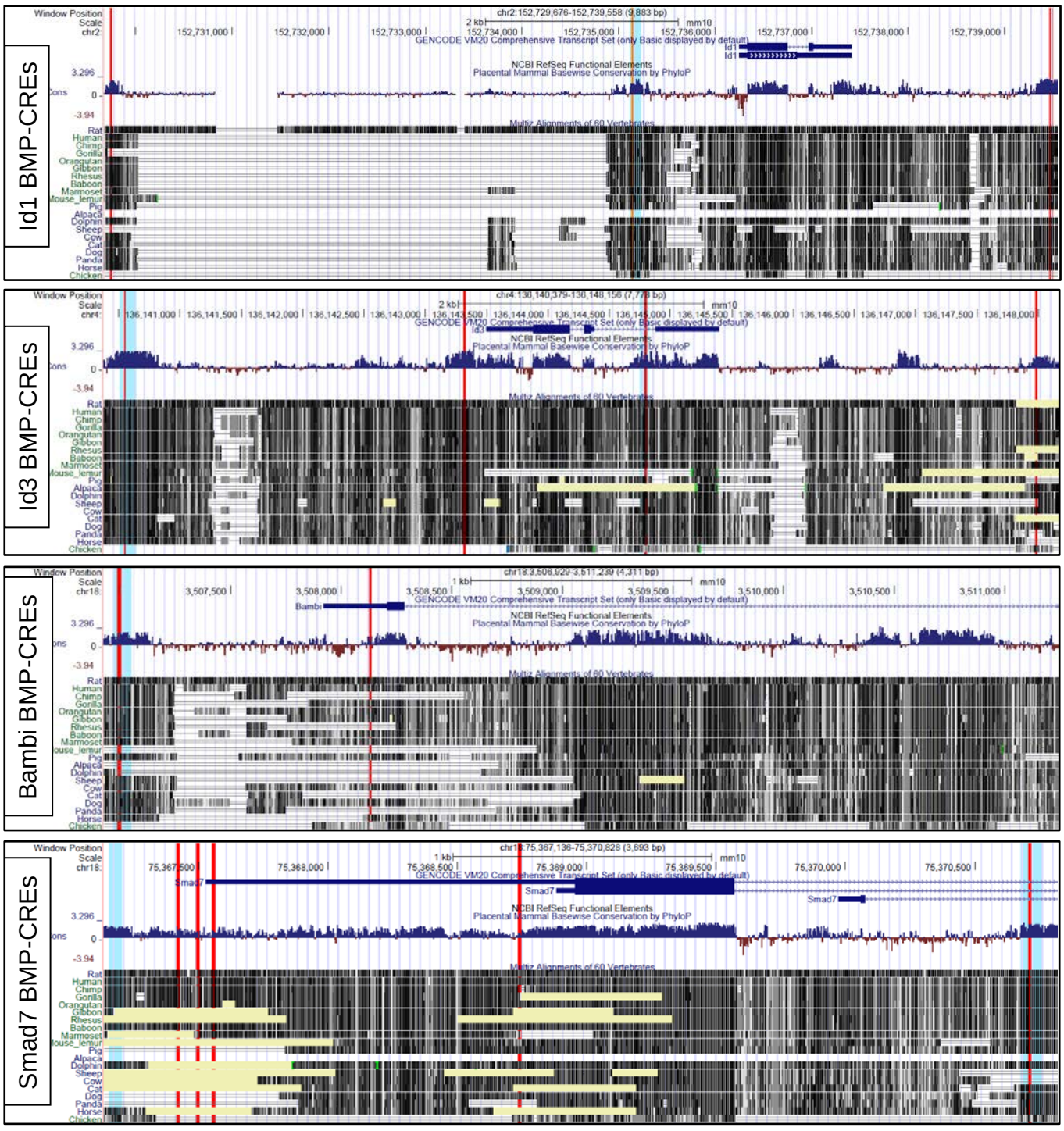

Figure S8: **Putative BMP-CREs.** Screenshots of the USCS browser indicating putative BMP-CREs in red highlight for the genes *Id1*, *Id3*, *Bambi* and *Smad7*. Blue highlights indicate the previously reported BMP-responsive regions (as per description in Table3.10)

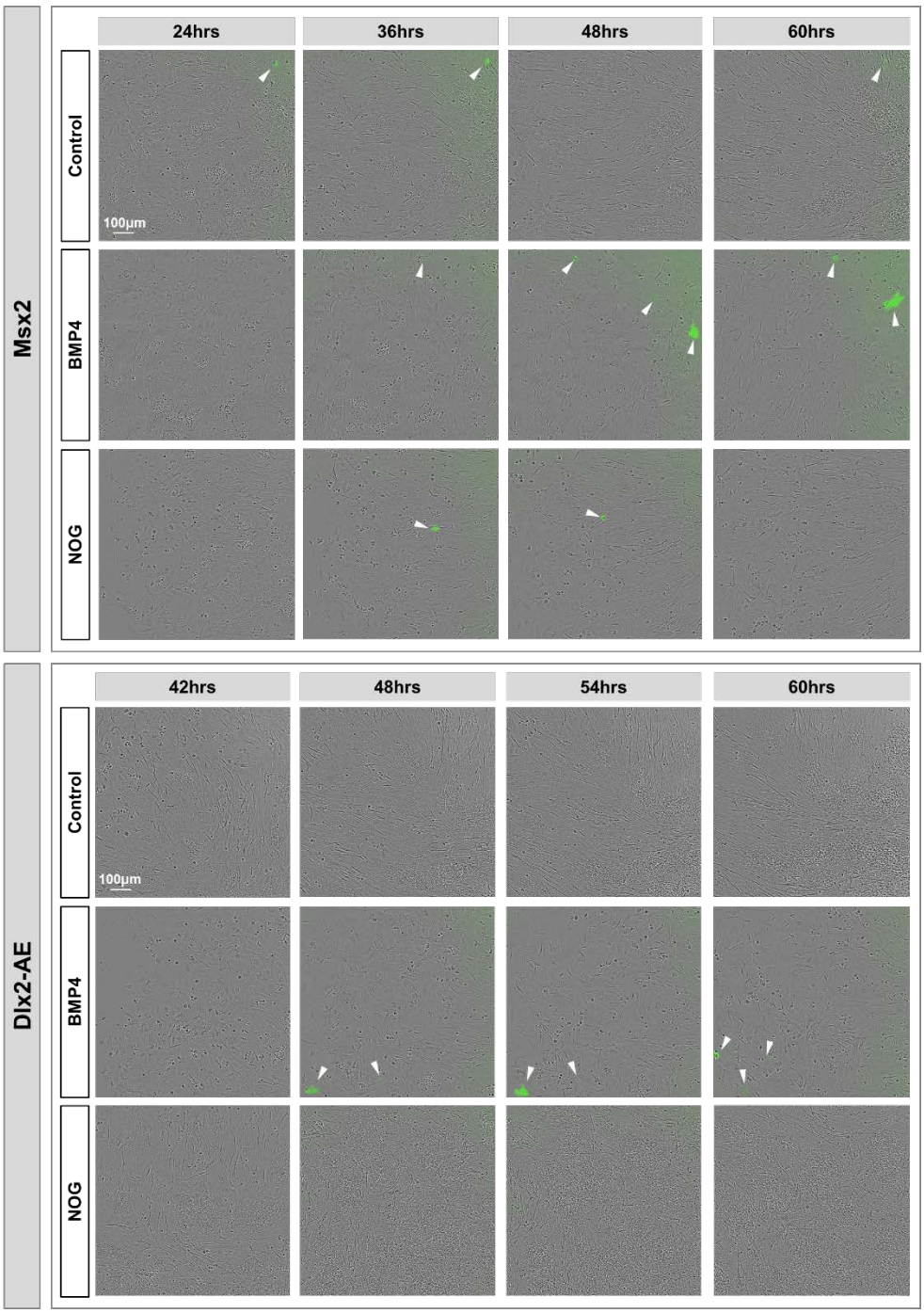

Figure S9: ***PLM cell transfection with GFP reporter plasmids containing the Msx2 BMP-SE or Dlx2 BMP-AE reveals a BMP4-regulated GFP expression.***

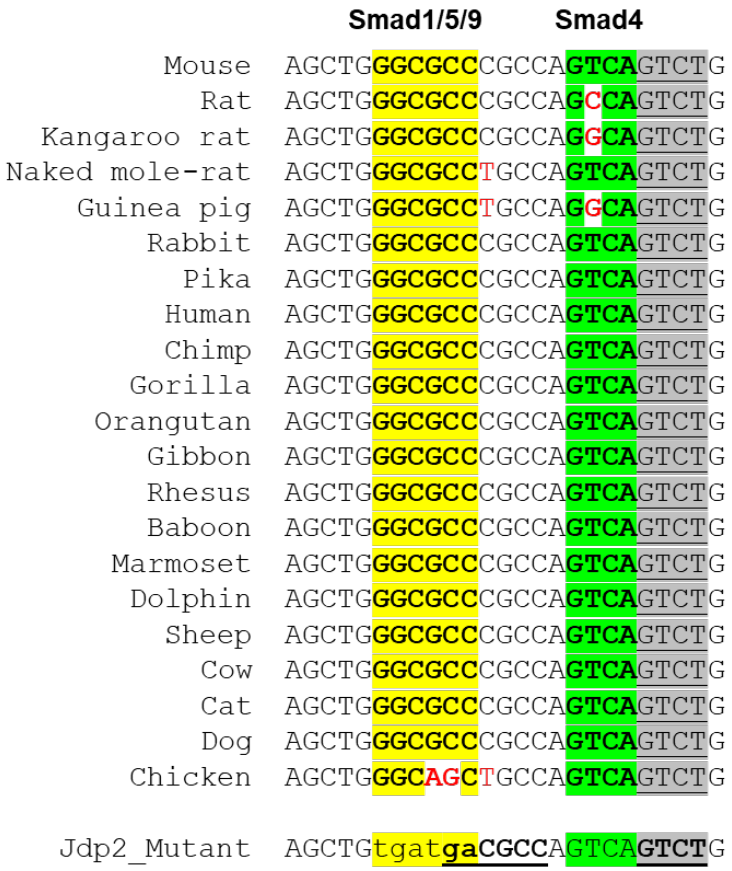

Figure S10: ***The unusual linker region and flanking sequence of Jdp2 BMP-AE resulted in the generation of an additional Jdp2 BMP-SE binding site with the generation of the Smad1/5/9 mutant.***

We mutated the SMAD1/5/9 binding site to the usual 'tgatga' sequence; however, due to the unusually high GC-rich sequence in the linker site and the conserved 'GTCT' sequence right next to the Smad4 binding site, we generated a new "almost perfect" BMP-CRE binding site with a canonical n=5 linker. This could explain why did not see any reporter-expression loss with the mutant Jdp2-AEmut enhancer fragment.

Bold letters denote the bipartite BMP-CRE. Yellow highlight indicates the SMAD1/5/9 binding site, green highlight the Smad4 binding site and grey underlined the additional Smad4 binding site. Lowercase indicates the mutated base pairs. Red denotes non-conserved base pairs. **Bold and underlined** indicates the new BMP-CRE binding site we generated with the SMAD1/5/9 site mutation.

Table S1: **Identified BMP-AE2 motifs in the Drosophila genome with an average PhastCons score > 0.55**

Atyp# name or Gene/Location	Chr	Motif Start	Motif Stop	Average PhastCONS
Atyp1	**chr2R**	**9905662**	**9905676**	**1**
Atyp2	chr3R	17053115	17053129	1
Atyp5	chr3R	28698786	28698800	1
Atyp9	chr3L	14589744	14589758	1
Atyp10	chr3R	9836926	9836940	1
Atyp11	**chr2L**	**9319175**	**9319189**	**1**
Atyp13	chr3R	15594263	15594277	1
Atyp15	**chr2R**	**19199705**	**19199719**	**1**
Atyp18	**chr2L**	**11595431**	**11595445**	**1**
Atyp23	chr3L	15776762	15776776	1
Rtnl1 intron 3	chr2L	4997220	4997234	1
Trim9 intron 8	chr2L	10625774	10625788	1
Pka-R2 intron 2	chr2R	10011600	10011614	1
bru3 intron 3	chr3L	13604317	13604331	1
twi intron 2	chr2R	22993220	22993234	1
tow intron 2	chr3L	6945724	6945738	1
dally intron 1	chr3L	8871078	8871092	1
tna intron 1	chr3L	10865636	10865650	1
olf413 intron 1	chr3L	22172305	22172319	1
TyrRII intron 4	chr3R	17742553	17742567	1
Eip93F intron 3	chr3R	21993235	21993249	1
Fur1 intron 3	chr3R	25407474	25407488	1
CG42594 intron 1	chrX	4858114	4858128	1
dpr8 intron 3	chrX	14403502	14403516	1
Frq2 intron 1	chrX	18189557	18189571	1
Poxm 5`UTR	chr3R	8333334	8333348	1
Dop1R1 3`UTR	chr3R	14177245	14177259	1
intergenic CG10814	chr2R	13381992	13382006	1
intergenic CG13197	chr2R	11698415	11698429	1
intergenic CG3483	chr2R	24447895	24447909	1
intergenic kek1	chr2L	12796326	12796340	1
intergenic CR44449	chr2R	8297798	8297812	1
intergenic CG33669	chrX	6401404	6401418	1
intergenic Lim1	chrX	8817329	8817343	1
intergenic Ten-a	chrX	12344815	12344829	1
Atyp12	chr3R	18357071	18357085	0.999929
CG43778 intron 1	chr2L	13318639	13318653	0.999929
CG43187 3`UTR	chr2R	16383772	16383786	0.999929
CR45381 intergenic	chr3L	22643174	22643188	0.999929
CG1677 intron 1	chrX	7384251	7384265	0.999929
His3.3B intron 1	chrX	9156120	9156134	0.999929
Atyp4	chr3R	18498566	18498580	0.999857
Arabido CDC48 intron 3	chr2R	10078209	10078223	0.999857
put intron 1	chr3R	14625155	14625169	0.999786
B-H1 3`UTR	chrX	17401928	17401942	0.999786
Atyp16	**chr2R**	**24694131**	**24694145**	**0.999643**
esn intron 1	chr2R	7098405	7098419	0.999571
intergenic CG14861	chr3R	15017832	15017846	0.999429
fas intron 1	chr2R	13624759	13624773	0.999357
ctp intron 2	chrX	4696943	4696957	0.999286
intergenic CR46206	chr2L	12769249	12769263	0.999214
bru3 intron 4	chr3L	13652625	13652639	0.999143
Dys intron 20	chr3R	19531223	19531237	0.999143
fz2 intron 3	chr3L	19195036	19195050	0.999071
Pde9 intron 4	chrX	12811496	12811510	0.998929
dpr8 intron 6	chrX	14428012	14428026	0.998929
Kdm4B intron 7	chr2R	13181632	13181646	0.998786
Atyp3	**chrX**	**15616808**	**15616822**	**0.998643**
sima intron 7	chr3R	30099041	30099055	0.998571
tai intron 2	chr2L	9183827	9183841	0.998429
DIP-theta intron 2	chr2L	5646986	5647000	0.998357
intergenic ttm3	chr2L	22078344	22078358	0.998143
SKIP intron 4	chr3R	22206280	22206294	0.997857
eys intron 1	chr2L	2317671	2317685	0.997786
Atyp22	chr2R	13835553	13835567	0.997357
Atyp14	chr3L	2836246	2836260	0.997214
Atyp25	chrX	1649111	1649125	0.997143
Sdc intron 2	chr2R	21439469	21439483	0.997071
CG44153 intron 1	chr2L	10101019	10101033	0.996071
slo intron 8	chr3R	24680334	24680348	0.996071
CG13577 intergenic	chr2R	24266317	24266331	0.995857
intergenic Tsp42Er	chr2R	7066733	7066747	0.995714
intergenic CG42581	chrX	20098187	20098201	0.994143
bru3 intron 2	chr3L	13594870	13594884	0.993857
stops intron 6	chr3R	31163405	31163419	0.9935
CR46251	chr3L	12807820	12807834	0.993357
intergenic CR44610	chr2L	7170701	7170715	0.992929
intergenic Or56a	chr2R	19776586	19776600	0.992714
intergenic CG6142	chr3R	26149877	26149891	0.991143
CG13954 intron 1	chr2R	9386790	9386804	0.989214
Atyp6	chr2L	15189633	15189647	0.988429
NPFR intron 2	chr3R	6190654	6190668	0.985714
intergenic Osi10	chr3R	6263630	6263644	0.979786
dpr1 intron 1	chr2R	20701999	20702013	0.974571
intergenic CG1421	chr2L	21902091	21902105	0.9715
Atyp20	chr3R	10449056	10449070	0.969214
shot intron 8	chr2R	13899555	13899569	0.9685
bbx/waw intron 2	chrX	21367618	21367632	0.967
intergenic babi	chr3L	1109827	1109841	0.964786
Lar intron 5	chr2L	19696813	19696827	0.962714
intergenic CG6836	chr3L	18968777	18968791	0.96
Axn intron 6	chr3R	30032613	30032627	0.959857
Imp intron 2	chrX	10802908	10802922	0.957286
Atyp7	chrX	14450410	14450424	0.957214
intergenic CG14317	chr3R	18074272	18074286	0.955286
CG8176 intron 1	chr3R	9520576	9520590	0.952714
intergenic CR46198	chr3L	5089499	5089513	0.949
dpr3 intron 1	chr2L	2100027	2100041	0.939071
Rbfox1 intron 2	chr3L	10543590	10543604	0.930214
CG17816 intron 1	chr3R	7886205	7886219	0.926429
CG34354 intron 2	chr3R	28157542	28157556	0.923571
Atyp21	chr2R	23517681	23517695	0.922
CG31140 intron 1	chr3R	23965098	23965112	0.921571
Epac intron 1	chr2R	6798202	6798216	0.886143
intergenic CG17560	chr2L	20267907	20267921	0.843
Pde8 intron 2	chr2R	23663087	23663101	0.839571
bru1 intron 1	chr2L	12246540	12246554	0.824643
wnd intron 2	chr3L	19630521	19630535	0.807214
Pde6 intron 2	chr3R	14549351	14549365	0.795286
rg intron 24	chrX	5244930	5244944	0.790357
CG43367 intron 16	chr3L	4212273	4212287	0.778571
Syt7 intron 7	chr4	281385	281399	0.771929
intergenic CG1142	chr3R	7477674	7477688	0.765286
Atyp26	**chr3L**	**13570864**	**13570878**	**0.756857**
intergenic CG2016	chr3R	4962832	4962846	0.732786
intergenic Or85b	chr3R	8502500	8502514	0.712357
CG2942 intron 2	chrX	2267732	2267746	0.712143
luna intron 2	chr2R	10991400	10991414	0.6965
Mob2 3`UTR	chr3L	11523467	11523481	0.691143
intergenic Fancm	chr3R	21482021	21482035	0.636214
Lar intron 6	chr2L	19675206	19675220	0.630357
Tchao intron 1	chr2L	13437095	13437109	0.619857
Atyp17	chr3L	11348427	11348441	0.6135
Gfr1 3`UTR	chr3R	20381142	20381156	0.613143
Atyp24	chrX	10180864	10180878	0.588214
intergenic phy1	chr2R	14427124	14427138	0.560071
CG32698 intron 2	chrX	9824969	9824983	0.559357
Atyp8	**chrX**	**14696740**	**14696754**	**0.554643**

* Red indicates enhancers tested and functionalized *in vivo* with reporter assays in transgenic flies

Table S2: **Strict BMP4-upregulated DEG list**

BMP4-upregulated DEGs									
2610035D17Rik	Cacna1a	Dlx3	Gm17315	Kctd4	Nkx3-2	Ptch1	Sort1	Tspoap1
2810025M15Rik	Cacna1h	Dlx5	Gm43196	Kif26b	Nmu	Ptch2	Sox10	Tuba4a
4930402H24Rik	Cadm3	Dlx6	Gm45837	Klf15	Nol4l	Ptger2	Sox13	Tunar
5730508B09Rik	Cadps	Dnajb11	Gm7265	Klf3	Notum	Ptger4	Sox5	Txndc11
5930412G12Rik	Calml3	Doc2a	Gm7902	Klf4	Npc1	Pthlh	Sox9	Uap1l1
G630022F23Rik	Calml4	Dock6	Gnb4	Klhl21	Npnt	Rab11fip4	Sp7	Unc80
AW551984	Camsap3	Dok4	Gng2	Krt8	Nr4a3	Rab28	Spata1	Vdr
Abtb2	Capn6	Dusp15	Gnptg	Krtcap3	Nrarp	Rab32	Sphk1	Vgll2
Acan	Ccdc157	Ebf4	Golga5	Lamb2	Nrxn1	Rab33b	Spon1	Vps37b
Acvr1	Ccndbp1	Efcab1	Golim4	Limd1	Ntng1	Rag1	Srgap1	Wfikkn2
Adamts3	Cd9	Efna1	Gp1bb	Litaf	Nup210	Rep15	Srprb	Wipi1
Adamtsl2	Cdc42ep3	Efna3	Gramd1a	Lpar4	Nupr1	Rftn2	Ssbp2	Yipf5
Adcy9	Cdh11	Ehd3	Grem1	Lrrc1	Nxpe3	Rgcc	Ssc4d	Zc3h12d
Adgra3	Cdh19	Emp2	Grhl1	Lrrc55	Optn	Rhbdd1	Ssh3	Zdhhc12
Adgrb3	Cdkl4	Enc1	Grhl2	Lrrc8b	Otogl	Rnf11	St3gal4	Zfp28
Ahr	Chadl	Enpp2	Gria4	Lrrc8d	Pappa2	Rnf144a	St8sia4	Zfyve21
Amt	Chrdl1	Entpd1	Grid2	Lsr	Papss1	Robo2	Stk32a	Zfyve27
Angel1	Chrdl2	Entpd7	Grid2ip	Maf	Pde10a	Rorc	Stra6l	
Ank2	Chrna7	Epb41l4b	Grik3	Man2a1	Pde4a	Rrbp1	Strip2	
Ankrd50	Chsy3	Eps8l2	Gsg1l	Map1a	Pde4dip	Runx3	Stxbp1	
Anks1	Clcn5	Epyc	Gulo	Map6	Peli2	Rxfp1	Stxbp2	
Ap5z1	Cldn19	Ets2	Hapln3	Map7d2	Penk	S100a1	Sumf1	
Apmap	Clec14a	Ezh1	Harbi1	Matn1	Pex11a	Samd9l	Surf4	
Arhgef1	Cmtm8	Fam19a5	Hcn1	Matn3	Phactr1	Scamp2	Sytl4	
Arhgef16	Col11a2	Fam20b	Hdlbp	Mbnl1	Phldb1	Sdf4	Tacc1	
Arhgef5	Col15a1	Fam63a	Hey2	Mboat1	Phospho1	Sec14l2	Tcaf1	
Arl4a	Col17a1	Farp1	Hip1r	Mboat2	Pik3ip1	Sec23a	Tcaf2	
Art3	Col20a1	Fat4	Hopx	Mbp	Pim3	Sec31a	Tcp11l2	
Asap1	Col4a1	Fbxl20	Hoxa11os	Mef2d	Pir	Sec61a1	Tex2	
Asap2	Comp	Fermt2	Hoxc13	Meltf	Plac8	Sec62	Tgfa	
Aspg	Cpt1b	Fgf15	Hs3st3a1	Mest	Plagl1	Selenok	Thrb	
Atf4	Cracr2a	Fgfr4	Hyou1	Mfsd1	Plcl1	Sema3g	Thsd4	
Atf6	Crip2	Fhdc1	Icos	Mgat5	Pld2	Sema6d	Tlr3	
Atp1b2	Ctdspl	Ficd	Ifitm10	Miat	Plec	Serpini1	Tm9sf2	
Atp6v0a2	Cux2	Foxf2	Igf2os	Mical1	Plekhb1	Setdb2	Tmem151a	
B3galt5	Cyb5d2	Frs2	Igsf1	Micall1	Plekhm3	Sh3tc2	Tmem158	
B3gat1	Cyb5r1	Fryl	Il16	Mid2	Plod2	Shc4	Tmem2	
BC006965	Cyp26b1	Fut9	Il6ra	Mrgpre	Plod3	Sipa1l1	Tmem246	
BC064078	Cyp2j9	Btbd3	Impdh1	Msx2	Plpp6	Slc25a13	Tmem266	
BC065397	Dcaf12l2	Gab1	Isl2	Mtss1l	Plxnb1	Slc25a45	Tmem40	
Baiap2l1	Ddb1	Gadd45b	Ism1	Mxra8	Pou3f3	Slc26a2	Tmem59	
Baiap2l2	Ddhd1	Gal3st1	Itga1	Myh14	Ppargc1a	Slc35d1	Tmem64	
Bbs9	Dennd3	Gata4	Itga10	Myo1e	Ppm1e	Slc37a4	Tnfrsf11b	
Bcam	Depdc7	Gcnt1	Itpr2	Nacc2	Ppp1r16b	Slc39a14	Tob2	
Bcl2	Dgke	Gfpt1	Jph1	Ndrg4	Prex1	Slc39a7	Tox2	
Bmf	Dhh	Gfpt2	Kcnj12	Necab3	Prickle1	Slc45a4	Trank1	
Bmp5	Dhx35	Ginm1	Kcnj3	Nfe2l1	Prkag3	Slc4a2	Trim25	
Bsn	Dhx57	Gja3	Kcnk5	Nim1k	Prkcz	Slc6a4	Trim46	
C030037D09Rik	Dlc1	Gli1	Kcnmb4	Nin	Proser2	Slc9a3r1	Trim62	
C130050O18Rik	Dlx2	Gm10561	Kcns1	Nkain4	Psen1	Smox	Tspan11	

Table S3: **Strict BMP4-downregulated DEG list**

BMP4-downregulated DEGs							
	1190002N15Rik	Car12	Dtx4	Gpr4	Micalcl	Rab30	Tcf20
	1700025A08Rik	Ccna2	Dusp16	Gprc5a	Mki67	Rad1	Tcf24
	2610307P16Rik	Ccnb1	Ebf2	Gpsm2	Mmaa	Rad51ap1	Tead3
	2810021J22Rik	Cd38	Ebf3	Gsc	Mpp3	Ran	Tek
	2810408I11Rik	Cd47	Edn1	Gsg2	Mpped1	Ranbp6	Tjp1
	2810474O19Rik	Cdc25c	Efemp1	H2afy	Mrps22	Rapgef5	Tlr2
	6820408C15Rik	Cdc7	Efna5	Has3	Msh6	Rarb	Tmem164
	A730020E08Rik	Cdca2	Efnb3	Hdac7	Mycn	Rasef	Tmem200b
	B130024G19Rik	Cdca3	Egfem1	Hdgfrp3	Myo1b	Rassf2	Tmem51
	C130021I20Rik	Cdca7	Elmod1	Hic1	Ncapg	Raver2	Tnfsf13b
	D030056L22Rik	Cdca8	Emilin3	Hmgb1	Ncaph2	Ret	Tpm4
	D930015E06Rik	Cdh2	Eml4	Hpse2	Ncbp1	Rhobtb2	Tpx2
	AI314180	Celsr1	Emx2	Hunk	Ncoa3	Rnd3	Trio
	Abca12	Cenpf	Enox1	Id3	Nectin2	Rnf128	Ttc27
	Abcd2	Cenpn	Epb41l2	Igfbp2	Nefl	Rnf150	Ttk
	Abhd6	Cenpv	Epb41l3	Il1rap	Neu3	Rpap3	Ttpa
	Adm	Cenpw	Epha3	Ipo5	Nhs	Sae1	Tuba1b
	Afap1	Cep19	Epha4	Irx3	Nlrp10	Scrt1	Tuba1c
	Afdn	Chst2	Ephb2	Islr2	Nop16	Sema3f	Tube1
	Ahsa1	Ckap2	Ermp1	Jak1	Notch4	Senp1	Twistnb
	Aldh1a2	Ckap2l	Esm1	Jazf1	Nrip1	11-Sep	Txnrd1
	Amigo1	Cldn1	Etv4	Kalrn	Ntf3	06-Sep	Uba2
	Amigo2	Clec2l	Etv6	Kars	Nuf2	Sesn3	Usp1
	Ank3	Cntnap2	Exoc6	Kat6b	Nxnl2	Sf3a3	Vav3
	Anln	Col3a1	Ezr	Kbtbd11	Nxpe2	Sfxn5	Vcam1
	Anp32a	Colec12	Fam107b	Kcnab1	Nxph4	Sgpl1	Vcl
	Apcdd1	Cped1	Fam184b	Kif11	Osr1	Sh2d3c	Vgll3
	Apela	Crabp1	Fdps	Kif23	Otud7b	Shb	Vps13a
	Arhgap10	Crabp2	Fgf16	Kif2c	Pbk	Shisa3	Wdr12
	Arhgap18	Crispld2	Fgf18	Kif4	Pcdh18	Shmt1	Wwc1
	Arhgap19	Csn3	Fhl3	Klhl14	Pcdh9	Six1	Ybx3
	Arhgap26	Ctsk	Filip1l	Kpna2	Pcsk5	Slc22a23	Zbtb44
	Arhgap28	Cttnbp2	Flrt1	Kpna3	Pdgfb	Slc30a10	Zcchc12
	Arhgef39	Cxcl12	Flt4	L1td1	Phf6	Slco2a1	Zfp395
	Aspm	Cxcl14	Fzd7	Lgi1	Pip4k2b	Slco4a1	Zfp422
	Atp2b1	Cxcl5	Gatc	Lgr6	Pla2g16	Smad1	Zfp512b
	Aurka	Dchs2	Gdf6	Lmnb1	Plk2	Snrnp40	Zfp608
	Avpr1a	Dgkd	Gkap1	Lpar1	Pls1	Sox12	Zfp618
	BC037039	Dhcr7	Gli3	Lsm3	Pmf1	Spata5	Zfp90
	BC055324	Dio3	Glis3	Magee2	Polr2m	Spred2	
	Bard1	Diras2	Gm1000	Magi1	Prkcb	Stambpl1	
	Blnk	Dkk2	Gm16216	Man1a	Prkce	Stard10	
	Btbd10	Dleu2	Gm21596	Map2k6	Prlr	Stip1	
	Bub1b	Dlg1	Gm27010	Mcm10	Prnd	Stom	
	C1s1	Dmd	Gm42752	Mcoln3	Prokr1	Stox2	
	C1s2	Dock5	Gm5620	Mcph1	Prom1	Stra6	
	Cacna2d2	Dpf3	Gm5860	Megf11	Ptchd1	Strbp	
	Cacna2d3	Dph3	Gpi1	Mex3b	Ptn	Stx1a	
	Cadm1	Dsc2	Gpr161	Mfhas1	Ptprj	Stxbp6	
	Camk1d	Dsc3	Gpr21	Mgst1	Pttg1	Tcerg1l	

Table S4: **Strict NOG-upregulated DEG list**

NOG-upregulated DEGs			
9430020K01Rik	Ecscr	Nuak2	
Abca12	Eml4	Otud7b	
Adcyap1r1	Enox1	Oxnad1	
Anks1b	Fjx1	Pcdhgc3	
Apba2	Fzd7	Pik3r3	
Apitd1	Gimap9	Prickle2	
Arhgap10	Gm10125	Ptchd4	
Arhgap20	Gm26507	Rab30	
Astn1	Gpi1	Rcc1l	
Begain	Gpr4	Rrp1b	
Bmp6	Gsc	Rtkn2	
C130021I20Rik	Hunk	Ruvbl1	
Cacna1e	Idh3b	Sdk1	
Cacna2d3	Itga8	Sept6	
Cd1d1	Kalrn	Slc9a9	
Cd38	Lgi1	Spred2	
Cdh2	Lgr6	Stom	
Cebpa	Lpar1	Stox2	
Dennd5b	Lrch1	Stra6	
Dicer1	Macc1	Suclg2	
Dock5	Magee2	Tacr1	
Dsc2	Mfhas1	Tpd52	
Dtnb	Mpp2	Trio	
Ebf2	Nek6	Tuba1c	
Ebf3	Nfkbia	Zyx	
F730043M19Rik	Nsdhl		

Table S5: **Strict NOG-downregulated DEG list**

NOG-downregulated DEGs			
1500009L16Rik	Gal	Lmna	Sh3tc2
2310030G06Rik	Gata2	Maf	Shc4
A730089K16Rik	Gcnt1	Maoa	Slc1a3
Arhgef5	Gfpt2	Matn1	Slc9a2
Arl4a	Gli1	Mical1	Sod2
B230354K17Rik	Gm10561	Mmp15	Ssbp2
Cacna1a	Gm17315	Msantd1	Susd6
Ccdc186	Gm20632	Msx2	Tgfa
Cd9	Gm28309	Nebl	Timp4
Chrna7	Gm44250	Optn	Tmem151a
Clec14a	Gm7265	Penk	Tmem246
Col11a2	Gria4	Pim3	Tmem30a
Col15a1	Grik3	Pitpnm1	Tmem64
Crip1	Hapln3	Plscr4	Tunar
Cyth1	Hcn1	Pnp	Upf3b
Cyyr1	Hecw2	Pou3f3	Wrnip1
Dlx3	Hey1	Prickle1	Ywhah
Ebf4	Icos	Ptch1	Zmpste24
Eno2	Id4	Ptch2	
Enpp2	Itgb3	Ptger4	
Ets2	Jph1	Rasl11b	
Faah	Kcnj13	Rhof	
Fam46a	Kcnmb4	Rspo2	
Fgfr4	Kdsr	Runx3	
Fhdc1	Klhl21	Serpini1	

Table S6: **BMP-CRE motifs within H3K27ac peaks (12hrs) up to 1Mb from upregulated DEGs**

#	Gene Name	RNAseq log2FoldChange	chr	peak start	peak end	peak name	Number of motifs in peak	Distance of peak to TSS
1	4930412O13Rik	2.76	2	9880396	9881889	H3K27ac_BMP12_vs_Noggin12_up.bed2255	2	0
2	Tmeff1	0.67	4	48584499	48585519	H3K27ac_BMP12_vs_Noggin12_up.bed2889	2	0
3	Chst3	0.64	10	60219167	60219440	H3K27ac_BMP12_vs_Noggin12_up.bed406	1	0
4	Ckap4	0.55	10	84533808	84534508	H3K27ac_BMP12_vs_Noggin12_up.bed477	1	0
5	Id4	1.3	13	48261212	48261820	H3K27ac_BMP12_vs_Noggin12_up.bed1132	1	0
6	Nin	0.77	12	70111612	70111952	H3K27ac_BMP12_vs_Noggin12_up.bed928	1	0
7	Ppp3ca	0.59	3	136669969	136670207	H3K27ac_BMP12_vs_Noggin12_up.bed2779	1	0
8	Smad9	0.92	3	54755187	54757017	H3K27ac_BMP12_vs_Noggin12_up.bed2631	1	0
9	Slc44a1	0.58	4	53440430	53440662	H3K27ac_BMP12_vs_Noggin12_up.bed2896	1	18
10	Slc2a13	1.1	15	91572853	91573231	H3K27ac_BMP12_vs_Noggin12_up.bed1558	1	30
11	Ctnnbip1	0.46	4	149518299	149518688	H3K27ac_BMP12_vs_Noggin12_up.bed3065	1	64
12	Grin3a	1.27	4	49845881	49846298	H3K27ac_BMP12_vs_Noggin12_up.bed2891	1	138
13	Ubxn4	0.34	1	128244175	128244460	H3K27ac_BMP12_vs_Noggin12_up.bed178	1	212
14	Rab2a	0.34	4	8535864	8536295	H3K27ac_BMP12_vs_Noggin12_up.bed2825	1	221
15	Klf4	1.54	4	55532736	55533483	H3K27ac_BMP12_vs_Noggin12_up.bed2902	1	271
16	Bambi	1.25	18	3507017	3507674	H3K27ac_BMP12_vs_Noggin12_up.bed1948	1	283
17	Jdp2	2.36	12	85599452	85600633	H3K27ac_BMP12_vs_Noggin12_up.bed964	1	348
18	P4hb	0.37	11	120572614	120572866	H3K27ac_BMP12_vs_Noggin12_up.bed831	1	387
19	Fgfr3	1.83	5	33722245	33722514	H3K27ac_BMP12_vs_Noggin12_up.bed3123	1	572
20	Cadps	2.25	14	12822014	12822468	H3K27ac_BMP12_vs_Noggin12_up.bed1288	1	611
21	Id4	1.3	13	48262081	48263250	H3K27ac_BMP12_vs_Noggin12_up.bed1133	1	655
22	Gpc6	0.76	14	116926044	116928027	H3K27ac_BMP12_vs_Noggin12_up.bed1447	1	748
23	Smad7	0.86	18	75368310	75369071	H3K27ac_BMP12_vs_Noggin12_up.bed2078	1	782
24	Nr3c1	1.18	18	39489949	39490470	H3K27ac_BMP12_vs_Noggin12_up.bed2012	1	831
25	4930412O13Rik	2.76	2	9882688	9882993	H3K27ac_BMP12_vs_Noggin12_up.bed2256	1	1437
26	Smad7	0.86	18	75369232	75374268	H3K27ac_BMP12_vs_Noggin12_up.bed2079	3	1704
27	Nog	4.61	11	89298858	89299427	H3K27ac_BMP12_vs_Noggin12_up.bed723	1	2905
28	Msx2	1.7	13	53476318	53477248	H3K27ac_BMP12_vs_Noggin12_up.bed1158	1	3245
29	Dlx2	3.77	2	71542550	71543147	H3K27ac_BMP12_vs_Noggin12_up.bed2375	1	3607
30	Cyp26b1	1.24	6	84587495	84588389	H3K27ac_BMP12_vs_Noggin12_up.bed3459	1	5519
31	Wwp2	2.21	8	107424775	107425000	H3K27ac_BMP12_vs_Noggin12_up.bed3958	1	11398
32	Copa	0.34	1	172063533	172064153	H3K27ac_BMP12_vs_Noggin12_up.bed247	1	18376
33	Met	0.68	6	17490863	17491153	H3K27ac_BMP12_vs_Noggin12_up.bed3361	1	27064
34	Stx5a	0.45	19	8713505	8714110	H3K27ac_BMP12_vs_Noggin12_up.bed2131	3	27303
35	Cnn1	0.99	9	22071009	22071379	H3K27ac_BMP12_vs_Noggin12_up.bed4028	1	27902
36	Dnajc12	0.94	10	63338426	63339013	H3K27ac_BMP12_vs_Noggin12_up.bed416	1	43430
37	Tmeff1	0.67	4	48540393	48540670	H3K27ac_BMP12_vs_Noggin12_up.bed2888	1	44504
38	Cdr2	0.44	7	121034783	121035175	H3K27ac_BMP12_vs_Noggin12_up.bed3763	2	52472
39	Dlx3	2.02	11	95182329	95182664	H3K27ac_BMP12_vs_Noggin12_up.bed753	1	62211
40	Spryd3	0.47	15	102203677	102203912	H3K27ac_BMP12_vs_Noggin12_up.bed1605	1	67444
41	Tmem59	0.37	4	107253207	107253420	H3K27ac_BMP12_vs_Noggin12_up.bed2973	1	74809
42	Dlx2	3.77	2	71628560	71628907	H3K27ac_BMP12_vs_Noggin12_up.bed2376	2	81807
43	Gal3st4	0.81	5	138187177	138187408	H3K27ac_BMP12_vs_Noggin12_up.bed3315	1	85432
44	Ypel2	1.16	11	87086483	87086717	H3K27ac_BMP12_vs_Noggin12_up.bed712	2	92777
45	Ptger4	1.23	15	5143892	5144120	H3K27ac_BMP12_vs_Noggin12_up.bed1466	3	100067
46	Atp1b2	1.55	11	69766018	69766261	H3K27ac_BMP12_vs_Noggin12_up.bed665	2	160077
47	Tpd52l1	1.28	10	31608849	31609160	H3K27ac_BMP12_vs_Noggin12_up.bed355	1	162929
48	Mitf	1.23	6	97981287	97981861	H3K27ac_BMP12_vs_Noggin12_up.bed3499	1	174236
49	Mpz	2.53	1	171329226	171329529	H3K27ac_BMP12_vs_Noggin12_up.bed244	1	178516

50	Gm53	1.19	11	96064636	96065357	H3K27ac_BMP12_vs_Noggin12_up.bed758	1	185748
51	Fgfr2	0.99	7	132931238	132931513	H3K27ac_BMP12_vs_Noggin12_up.bed3798	1	191837
52	Nxph3	1	11	95712916	95713279	H3K27ac_BMP12_vs_Noggin12_up.bed755	1	198347
53	Frs2	0.86	10	117376573	117376960	H3K27ac_BMP12_vs_Noggin12_up.bed524	1	228100
54	Neat1	0.72	19	5609785	5609986	H3K27ac_BMP12_vs_Noggin12_up.bed2111	1	235492
55	Depdc7	1.12	2	104494040	104494766	H3K27ac_BMP12_vs_Noggin12_up.bed2427	2	248112
56	Rab33b	0.67	3	51225023	51225503	H3K27ac_BMP12_vs_Noggin12_up.bed2618	1	258417
57	Vps37b	0.62	5	123748985	123749376	H3K27ac_BMP12_vs_Noggin12_up.bed3291	1	282894
58	Col9a3	2.36	2	180273187	180273406	H3K27ac_BMP12_vs_Noggin12_up.bed2564	2	324384
59	Kdelr2	0.41	5	143731888	143732173	H3K27ac_BMP12_vs_Noggin12_up.bed3321	1	328051
60	Sost	4	11	102296039	102296777	H3K27ac_BMP12_vs_Noggin12_up.bed771	1	329025
61	Slc7a3	0.81	X	101420021	101420329	H3K27ac_BMP12_vs_Noggin12_up.bed4276	1	334002
62	Lrrc75b	1.29	10	75212112	75212361	H3K27ac_BMP12_vs_Noggin12_up.bed442	1	347969
63	B3gnt8	1.73	7	25248113	25248410	H3K27ac_BMP12_vs_Noggin12_up.bed3621	1	379214
64	Adam17	0.29	12	21783962	21784165	H3K27ac_BMP12_vs_Noggin12_up.bed867	1	410331
65	Plekhm3	0.66	1	64532965	64533242	H3K27ac_BMP12_vs_Noggin12_up.bed107	1	423582
66	Col9a3	2.36	2	180171689	180171906	H3K27ac_BMP12_vs_Noggin12_up.bed2563	1	425884
67	Ccdc71l	0.71	12	31949613	31950179	H3K27ac_BMP12_vs_Noggin12_up.bed889	1	428525
68	Gm20633	1.39	3	96697077	96697386	H3K27ac_BMP12_vs_Noggin12_up.bed2704	1	450698
69	Pcyt1b	0.81	X	94122087	94122544	H3K27ac_BMP12_vs_Noggin12_up.bed4267	1	467225
70	Vstm2l	3.03	2	157424298	157424576	H3K27ac_BMP12_vs_Noggin12_up.bed2522	1	490077
71	Cux2	1.55	5	121545719	121545932	H3K27ac_BMP12_vs_Noggin12_up.bed3286	1	504170
72	Rag1	2.3	2	102185754	102186315	H3K27ac_BMP12_vs_Noggin12_up.bed2424	2	536254
73	Wwp2	2.21	8	106893004	106893582	H3K27ac_BMP12_vs_Noggin12_up.bed3954	1	542816
74	Gdf10	1.35	14	34502997	34503909	H3K27ac_BMP12_vs_Noggin12_up.bed1339	1	579411
75	Npnt	1.18	3	133544432	133544671	H3K27ac_BMP12_vs_Noggin12_up.bed2771	1	594142
76	Slc6a4	2.37	11	77607205	77607408	H3K27ac_BMP12_vs_Noggin12_up.bed686	1	608603
77	Rhou	0.46	8	123041909	123042238	H3K27ac_BMP12_vs_Noggin12_up.bed3988	1	611691
78	Grik3	2.03	4	126102828	126103690	H3K27ac_BMP12_vs_Noggin12_up.bed3011	1	612129
79	Ankrd6	0.64	4	32304661	32305401	H3K27ac_BMP12_vs_Noggin12_up.bed2860	1	645440
80	Zbtb8a	0.46	4	128727497	128727802	H3K27ac_BMP12_vs_Noggin12_up.bed3015	1	650314
81	Dock9	0.56	14	122452544	122454499	H3K27ac_BMP12_vs_Noggin12_up.bed1462	1	654811
82	Sox6	1.17	7	115381543	115382113	H3K27ac_BMP12_vs_Noggin12_up.bed3745	1	656631
83	Adam17	0.29	12	22030484	22030839	H3K27ac_BMP12_vs_Noggin12_up.bed868	1	656853
84	Trp53inp2	0.42	2	156065298	156065575	H3K27ac_BMP12_vs_Noggin12_up.bed2518	1	684240
85	Aspg	1.44	12	111377450	111377681	H3K27ac_BMP12_vs_Noggin12_up.bed1001	1	729002
86	Ncmap	1.65	4	136143413	136143784	H3K27ac_BMP12_vs_Noggin12_up.bed3031	1	745187
87	Ncmap	1.65	4	136144387	136144703	H3K27ac_BMP12_vs_Noggin12_up.bed3033	1	746161
88	Ptx3	0.51	3	66985694	66985918	H3K27ac_BMP12_vs_Noggin12_up.bed2659	1	765785
89	Zeb2	0.52	2	44270901	44272354	H3K27ac_BMP12_vs_Noggin12_up.bed2319	1	845041
90	Stard8	1.1	X	99853381	99853685	H3K27ac_BMP12_vs_Noggin12_up.bed4274	1	850134
91	Serinc5	0.83	13	93499462	93499794	H3K27ac_BMP12_vs_Noggin12_up.bed1223	1	888325
92	Ncmap	1.65	4	136310437	136310724	H3K27ac_BMP12_vs_Noggin12_up.bed3037	1	912211
93	Wnk4	1.3	11	100319997	100320334	H3K27ac_BMP12_vs_Noggin12_up.bed764	1	940233
94	Ankrd6	0.64	4	31963980	31964225	H3K27ac_BMP12_vs_Noggin12_up.bed2855	2	986616

Table S7: **BMP-CRE motifs within H3K27ac peaks (12hrs) up to 1Mb from downregulated DEGs**

#	Gene Name	RNAseq log2FoldChange	chr	peak start	peak end	peak name	Number of motifs in peak	Distance of peak to TSS
1	Vcl	-0.53	14	20929391	20929971	H3K27ac_BMP12_vs_Noggin12_down.bed751	1	0
2	Gas1	-1.7	13	60175594	60177184	H3K27ac_BMP12_vs_Noggin12_down.bed677	1	181
3	Hmga2	-0.75	10	120475013	120476237	H3K27ac_BMP12_vs_Noggin12_down.bed248	1	232
4	Bmp2	-3.29	2	133552460	133552770	H3K27ac_BMP12_vs_Noggin12_down.bed1415	1	302
5	Lmx1b	-1.04	2	33639416	33640027	H3K27ac_BMP12_vs_Noggin12_down.bed1328	1	484
6	1190002N15Rik	-0.8	9	94537217	94537552	H3K27ac_BMP12_vs_Noggin12_down.bed2555	1	529
7	Sema3f	-0.9	9	107709371	107709899	H3K27ac_BMP12_vs_Noggin12_down.bed2573	2	576
8	Pard3	-0.47	8	127064650	127064943	H3K27ac_BMP12_vs_Noggin12_down.bed2419	1	758
9	Bcl11a	-1.13	11	24075843	24076597	H3K27ac_BMP12_vs_Noggin12_down.bed279	1	1459
10	Zfp608	-0.92	18	54987767	54988489	H3K27ac_BMP12_vs_Noggin12_down.bed1163	1	1691
11	1700021F13Rik	-1.56	5	119797779	119798342	H3K27ac_BMP12_vs_Noggin12_down.bed1902	1	9527
12	Tbx15	-0.71	3	99254037	99256813	H3K27ac_BMP12_vs_Noggin12_down.bed1573	1	13657
13	Dnph1	-0.8	17	46555320	46555761	H3K27ac_BMP12_vs_Noggin12_down.bed1077	1	58532
14	Podnl1	-1.29	8	84197466	84198547	H3K27ac_BMP12_vs_Noggin12_down.bed2351	1	71478
15	Spry1	-1.41	3	37723995	37724554	H3K27ac_BMP12_vs_Noggin12_down.bed1496	1	84049
16	Mthfd1	-0.42	12	76370519	76370758	H3K27ac_BMP12_vs_Noggin12_down.bed544	3	115288
17	Nek6	-0.47	2	38348135	38348343	H3K27ac_BMP12_vs_Noggin12_down.bed1337	1	163300
18	Gpsm2	-0.5	3	108911018	108911356	H3K27ac_BMP12_vs_Noggin12_down.bed1588	1	188710
19	Gas1	-1.7	13	59971788	59972033	H3K27ac_BMP12_vs_Noggin12_down.bed673	1	205332
20	Myo16	-0.83	8	9977819	9978173	H3K27ac_BMP12_vs_Noggin12_down.bed2271	1	294399
21	H2afy	-0.64	13	55831695	55832003	H3K27ac_BMP12_vs_Noggin12_down.bed660	1	304358
22	Podnl1	-1.29	8	84662240	84662820	H3K27ac_BMP12_vs_Noggin12_down.bed2357	1	536252
23	H2afy	-0.64	13	55512458	55512774	H3K27ac_BMP12_vs_Noggin12_down.bed655	1	623587
24	Gemin5	-0.45	11	58949180	58949384	H3K27ac_BMP12_vs_Noggin12_down.bed331	1	780642
25	Podnl1	-1.29	8	84976055	84976427	H3K27ac_BMP12_vs_Noggin12_down.bed2361	1	850067
26	Esrrb	-1.64	12	85485347	85486063	H3K27ac_BMP12_vs_Noggin12_down.bed567	2	875054

Table S8: **BMP-CRE motifs within H3K27ac peaks (24hrs) up to 1Mb from upregulated DEGs**

#	Gene Name	RNAseq log2FoldChange	chr	peak start	peak end	peak name	Number of motifs in peak	Distance of peak to TSS
1	4930412O13Rik	2.38	2	9880669	9881876	H3K27ac_BMP24_vs_Noggin24_up.bed2661	2	0
2	G630022F23Rik	1.96	5	33722934	33723580	H3K27ac_BMP24_vs_Noggin24_up.bed3775	1	89
3	Smad9	0.52	3	54755685	54756307	H3K27ac_BMP24_vs_Noggin24_up.bed3183	1	104
4	Jdp2	2.26	12	85599372	85599799	H3K27ac_BMP24_vs_Noggin24_up.bed1125	1	268
5	Ldlrad3	0.6	2	102185753	102186099	H3K27ac_BMP24_vs_Noggin24_up.bed2877	2	286
6	Dlx2	4.3	2	71544092	71546357	H3K27ac_BMP24_vs_Noggin24_up.bed2805	1	397
7	Dlx6	2.18	6	6863842	6864712	H3K27ac_BMP24_vs_Noggin24_up.bed4066	1	509
8	Slc6a8	0.48	X	73674575	73674837	H3K27ac_BMP24_vs_Noggin24_up.bed5146	1	1426
9	Dlx2	4.3	2	71543195	71543990	H3K27ac_BMP24_vs_Noggin24_up.bed2804	1	2764
10	Nog	4.28	11	89298845	89299398	H3K27ac_BMP24_vs_Noggin24_up.bed809	1	2934
11	Msx2	1.52	13	53476420	53477204	H3K27ac_BMP24_vs_Noggin24_up.bed1317	1	3347
12	Frs2	1.07	10	117152251	117152509	H3K27ac_BMP24_vs_Noggin24_up.bed581	1	3778
13	Foxf2	0.96	13	31619826	31620208	H3K27ac_BMP24_vs_Noggin24_up.bed1239	2	5608
14	Plec	0.86	15	76208629	76209049	H3K27ac_BMP24_vs_Noggin24_up.bed1783	1	23525
15	Atp1a2	1.53	1	172326591	172327178	H3K27ac_BMP24_vs_Noggin24_up.bed317	1	28528
16	Col11a1	2.65	3	113949656	113950022	H3K27ac_BMP24_vs_Noggin24_up.bed3316	1	80518
17	Dlx2	4.3	2	71628523	71629696	H3K27ac_BMP24_vs_Noggin24_up.bed2806	2	81770
18	Synpo	0.71	18	60748329	60748627	H3K27ac_BMP24_vs_Noggin24_up.bed2381	1	88188
19	Chd7	0.69	4	8535835	8536136	H3K27ac_BMP24_vs_Noggin24_up.bed3428	1	154270
20	Trim62	0.55	4	128727599	128727878	H3K27ac_BMP24_vs_Noggin24_up.bed3658	1	155702
21	Mitf	0.73	6	97980981	97981949	H3K27ac_BMP24_vs_Noggin24_up.bed4231	1	173930
22	Mmp14	0.38	14	54631406	54631717	H3K27ac_BMP24_vs_Noggin24_up.bed1598	1	199795
23	Myo10	0.3	15	25364339	25364620	H3K27ac_BMP24_vs_Noggin24_up.bed1722	1	257905
24	Abca1	0.7	4	53440439	53440661	H3K27ac_BMP24_vs_Noggin24_up.bed3511	1	280545
25	Arhgef1	0.97	7	25247748	25248423	H3K27ac_BMP24_vs_Noggin24_up.bed4350	1	344837
26	Tm9sf2	0.28	14	122452972	122454254	H3K27ac_BMP24_vs_Noggin24_up.bed1701	1	345935
27	Ptprn2	1.98	12	116047698	116047924	H3K27ac_BMP24_vs_Noggin24_up.bed1184	1	437796
28	Anxa8	2.15	14	34549059	34549282	H3K27ac_BMP24_vs_Noggin24_up.bed1562	1	463079
29	Fbxl20	0.28	11	97628072	97628305	H3K27ac_BMP24_vs_Noggin24_up.bed889	1	522098
30	Tmem200c	1.13	17	69383481	69383786	H3K27ac_BMP24_vs_Noggin24_up.bed2201	1	546346
31	Dbx2	2.46	15	96286910	96287500	H3K27ac_BMP24_vs_Noggin24_up.bed1852	1	630951
32	Ankrd6	0.76	4	32304641	32304878	H3K27ac_BMP24_vs_Noggin24_up.bed3469	1	645963
33	Sox6	1.66	7	115381582	115382106	H3K27ac_BMP24_vs_Noggin24_up.bed4526	1	656638
34	Fbln2	1.03	6	92091450	92091747	H3K27ac_BMP24_vs_Noggin24_up.bed4217	1	878996
35	Myo5b	0.52	18	75370742	75371486	H3K27ac_BMP24_vs_Noggin24_up.bed2423	1	929807

Table S9: **BMP-CRE motifs within H3K27ac peaks (24hrs) up to 1Mb from downregulated DEGs**

#	Gene Name	RNAseq log2FoldChange	chr	peak start	peak end	peak name	Number of motifs in peak	Distance of peak to TSS
1	Atp2b1	-0.78	10	98914990	98915193	H3K27ac_BMP24_vs_Noggin24_down.bed903	2	0
2	Rai14	-0.32	15	10714011	10714696	H3K27ac_BMP24_vs_Noggin24_down.bed2828	1	0
3	Wee1	-0.52	7	110122056	110122855	H3K27ac_BMP24_vs_Noggin24_down.bed7441	1	0
4	Mpped2	-1.11	2	106693072	106694078	H3K27ac_BMP24_vs_Noggin24_down.bed4721	1	0
5	Lmx1b	-1.26	2	33639398	33640584	H3K27ac_BMP24_vs_Noggin24_down.bed4553	1	0
6	Tnfrsf21	-1.15	17	43016555	43016897	H3K27ac_BMP24_vs_Noggin24_down.bed3638	1	1
7	Vcl	-0.77	14	20929468	20930308	H3K27ac_BMP24_vs_Noggin24_down.bed2527	1	36
8	Gas1	-2.03	13	60174484	60177318	H3K27ac_BMP24_vs_Noggin24_down.bed2317	1	47
9	Nectin2	-0.61	7	19748946	19749502	H3K27ac_BMP24_vs_Noggin24_down.bed7146	1	71
10	Id3	-0.66	4	136143102	136143404	H3K27ac_BMP24_vs_Noggin24_down.bed5954	1	93
11	Fam60a	-0.43	6	148944066	148946370	H3K27ac_BMP24_vs_Noggin24_down.bed7071	1	97
12	Smad3	-0.48	9	63757619	63757888	H3K27ac_BMP24_vs_Noggin24_down.bed8278	1	106
13	Aes	-0.86	10	81559670	81559956	H3K27ac_BMP24_vs_Noggin24_down.bed827	1	177
14	Gsc	-2.37	12	104472798	104473152	H3K27ac_BMP24_vs_Noggin24_down.bed1946	1	178
15	Pdlim7	-0.8	13	55511691	55513491	H3K27ac_BMP24_vs_Noggin24_down.bed2257	1	185
16	Skida1	-0.58	2	18047643	18048840	H3K27ac_BMP24_vs_Noggin24_down.bed4429	1	211
17	Bnc2	-0.83	4	84674307	84675012	H3K27ac_BMP24_vs_Noggin24_down.bed5710	1	263
18	Uck2	-0.36	1	167283722	167285041	H3K27ac_BMP24_vs_Noggin24_down.bed478	1	279
19	Dusp7	-0.5	9	106368969	106369873	H3K27ac_BMP24_vs_Noggin24_down.bed8420	1	338
20	Bmp2	-2.75	2	133552503	133554390	H3K27ac_BMP24_vs_Noggin24_down.bed4804	1	345
21	1190002N15Rik	-0.86	9	94536566	94537730	H3K27ac_BMP24_vs_Noggin24_down.bed8377	1	351
22	Id3	-0.66	4	136143873	136145119	H3K27ac_BMP24_vs_Noggin24_down.bed5955	1	377
23	Cacna1g	-0.51	11	94473433	94473728	H3K27ac_BMP24_vs_Noggin24_down.bed1481	2	470
24	Sema3f	-0.83	9	107709368	107709978	H3K27ac_BMP24_vs_Noggin24_down.bed8433	2	497
25	Tead3	-0.46	17	28349856	28350268	H3K27ac_BMP24_vs_Noggin24_down.bed3567	1	537
26	Sox12	-0.5	2	152396765	152397425	H3K27ac_BMP24_vs_Noggin24_down.bed4841	1	638
27	Zfp608	-0.77	18	54985966	54989404	H3K27ac_BMP24_vs_Noggin24_down.bed3998	1	776
28	Aebp2	-0.47	6	140623664	140624043	H3K27ac_BMP24_vs_Noggin24_down.bed7050	1	1002
29	Ubtf	-0.4	11	102318198	102318739	H3K27ac_BMP24_vs_Noggin24_down.bed1552	1	1003
30	Mex3b	-0.87	7	82868342	82870121	H3K27ac_BMP24_vs_Noggin24_down.bed7348	1	1010
31	Cul1	-0.33	6	47454488	47454755	H3K27ac_BMP24_vs_Noggin24_down.bed6714	1	1091
32	Bcl11a	-1.11	11	24075736	24076326	H3K27ac_BMP24_vs_Noggin24_down.bed1122	1	1730
33	Ubtf	-0.4	11	102317064	102317784	H3K27ac_BMP24_vs_Noggin24_down.bed1551	1	1958
34	Bcl2l11	-0.66	2	128128268	128128547	H3K27ac_BMP24_vs_Noggin24_down.bed4777	1	2231
35	Anp32a	-0.26	9	62344123	62344555	H3K27ac_BMP24_vs_Noggin24_down.bed8267	2	2831
36	Id3	-0.66	4	136148001	136148822	H3K27ac_BMP24_vs_Noggin24_down.bed5956	1	4505
37	Sae1	-0.26	7	16400332	16401407	H3K27ac_BMP24_vs_Noggin24_down.bed7122	2	12536
38	Tpx2	-0.44	2	152830229	152831343	H3K27ac_BMP24_vs_Noggin24_down.bed4857	1	16621
39	Notch4	-1.18	17	34586098	34587456	H3K27ac_BMP24_vs_Noggin24_down.bed3613	1	21831
40	Ubtf	-0.4	11	102297306	102297558	H3K27ac_BMP24_vs_Noggin24_down.bed1549	1	22184
41	Nxnl2	-2.11	13	51202622	51203025	H3K27ac_BMP24_vs_Noggin24_down.bed2202	1	31598
42	Tcf15	-1.43	2	152105499	152105735	H3K27ac_BMP24_vs_Noggin24_down.bed4840	1	37826
43	Crabp2	-1.51	3	87905949	87906164	H3K27ac_BMP24_vs_Noggin24_down.bed5248	1	42502
44	Six1	-0.44	12	73112350	73113149	H3K27ac_BMP24_vs_Noggin24_down.bed1819	1	58464
45	Fblim1	-0.46	4	141537877	141538381	H3K27ac_BMP24_vs_Noggin24_down.bed5979	2	67715
46	Aifm2	-0.64	10	61783521	61784393	H3K27ac_BMP24_vs_Noggin24_down.bed723	1	68259
47	Cdon	-0.48	9	35342177	35342542	H3K27ac_BMP24_vs_Noggin24_down.bed8129	1	78586
48	2810021J22Rik	-0.37	11	58948996	58949293	H3K27ac_BMP24_vs_Noggin24_down.bed1239	1	81781
49	Ccnf	-0.36	17	24168980	24169421	H3K27ac_BMP24_vs_Noggin24_down.bed3518	1	81988

50	Ddx47	-0.24	6	134926890	134928501	H3K27ac_BMP24_vs_Noggin24_down.bed7024	1	83111
51	Npm3	-0.47	19	45659773	45660227	H3K27ac_BMP24_vs_Noggin24_down.bed4329	1	89364
52	Ets1	-0.48	9	32540202	32543034	H3K27ac_BMP24_vs_Noggin24_down.bed8114	1	93187
53	Ttc28	-0.46	5	110978711	110979545	H3K27ac_BMP24_vs_Noggin24_down.bed6325	1	98909
54	Eln	-2.18	5	134638830	134639277	H3K27ac_BMP24_vs_Noggin24_down.bed6461	1	108046
55	Efnb3	-0.68	11	69671370	69672225	H3K27ac_BMP24_vs_Noggin24_down.bed1320	1	111166
56	Sept11	-0.43	5	93205755	93206250	H3K27ac_BMP24_vs_Noggin24_down.bed6281	1	112319
57	Otud7b	-0.57	3	96219874	96220732	H3K27ac_BMP24_vs_Noggin24_down.bed5322	2	115348
58	Barx1	-1.88	13	48546145	48546454	H3K27ac_BMP24_vs_Noggin24_down.bed2188	2	116544
59	Otud7b	-0.57	3	96221128	96221697	H3K27ac_BMP24_vs_Noggin24_down.bed5323	1	116602
60	Gm13781	-1.29	6	30692928	30693749	H3K27ac_BMP24_vs_Noggin24_down.bed6655	1	116894
61	Birc5	-0.44	11	117968714	117968946	H3K27ac_BMP24_vs_Noggin24_down.bed1650	1	119464
62	Glrb	-0.52	3	81036669	81038445	H3K27ac_BMP24_vs_Noggin24_down.bed5204	1	123010
63	Cdkn3	-0.62	14	46884142	46884488	H3K27ac_BMP24_vs_Noggin24_down.bed2621	1	123602
64	Hmgb1	-0.41	5	149052387	149052957	H3K27ac_BMP24_vs_Noggin24_down.bed6549	1	131532
65	Ikzf3	-3.13	11	98682708	98683039	H3K27ac_BMP24_vs_Noggin24_down.bed1509	2	136678
66	Tcirg1	-0.45	19	3768139	3768471	H3K27ac_BMP24_vs_Noggin24_down.bed4171	1	138662
67	Larp1b	-1.27	3	40800005	40800647	H3K27ac_BMP24_vs_Noggin24_down.bed5088	1	149707
68	Ecscr	-1.67	18	35562386	35562925	H3K27ac_BMP24_vs_Noggin24_down.bed3935	1	159431
69	Tnnt3	-0.67	7	142659110	142659388	H3K27ac_BMP24_vs_Noggin24_down.bed7615	1	160275
70	Stx1a	-0.85	5	135187335	135188048	H3K27ac_BMP24_vs_Noggin24_down.bed6465	1	163854
71	Ecscr	-1.67	18	35889148	35889832	H3K27ac_BMP24_vs_Noggin24_down.bed3943	1	166793
72	Cdca3	-0.37	6	125009255	125009514	H3K27ac_BMP24_vs_Noggin24_down.bed6989	1	179709
73	Zbtb44	-0.94	9	31211443	31211751	H3K27ac_BMP24_vs_Noggin24_down.bed8109	1	180800
74	Gypc	-0.67	18	32377285	32377573	H3K27ac_BMP24_vs_Noggin24_down.bed3919	1	182461
75	Hmgb2	-0.44	8	57328381	57328714	H3K27ac_BMP24_vs_Noggin24_down.bed7776	1	183129
76	Smyd4	-0.43	11	75531688	75531901	H3K27ac_BMP24_vs_Noggin24_down.bed1368	1	183256
77	Esr2	-1.61	12	76370197	76371001	H3K27ac_BMP24_vs_Noggin24_down.bed1843	3	192939
78	Nfib	-0.96	4	82503769	82505240	H3K27ac_BMP24_vs_Noggin24_down.bed5685	1	200510
79	Cdc25c	-0.4	18	34953908	34954322	H3K27ac_BMP24_vs_Noggin24_down.bed3932	1	202376
80	Acy3	-1.08	19	4192247	4192487	H3K27ac_BMP24_vs_Noggin24_down.bed4174	1	205587
81	Saal1	-0.31	7	46919696	46920023	H3K27ac_BMP24_vs_Noggin24_down.bed7242	1	209017
82	Npr1	-1.79	3	90248199	90248836	H3K27ac_BMP24_vs_Noggin24_down.bed5291	1	217030
83	Cep85l	-0.89	10	53596919	53597967	H3K27ac_BMP24_vs_Noggin24_down.bed685	2	217069
84	Prkcb	-1.22	7	122067489	122067972	H3K27ac_BMP24_vs_Noggin24_down.bed7477	2	220779
85	Zkscan4	-0.96	13	21715022	21716135	H3K27ac_BMP24_vs_Noggin24_down.bed2027	1	236116
86	Fzd8	-0.71	18	9449689	9450004	H3K27ac_BMP24_vs_Noggin24_down.bed3854	1	236834
87	Itgb6	-1.88	2	60962755	60963220	H3K27ac_BMP24_vs_Noggin24_down.bed4608	1	240113
88	Zkscan4	-0.96	13	21722283	21722929	H3K27ac_BMP24_vs_Noggin24_down.bed2031	1	243377
89	Rrp1b	-0.33	17	32284197	32284687	H3K27ac_BMP24_vs_Noggin24_down.bed3602	2	248098
90	Zfp618	-0.56	4	63215417	63215728	H3K27ac_BMP24_vs_Noggin24_down.bed5653	1	249845
91	Ctps	-0.55	4	120825315	120825536	H3K27ac_BMP24_vs_Noggin24_down.bed5860	1	255040
92	Mtss1	-0.92	15	58823038	58823471	H3K27ac_BMP24_vs_Noggin24_down.bed2913	2	258555
93	Prokr1	-1.25	6	87849995	87850967	H3K27ac_BMP24_vs_Noggin24_down.bed6864	1	259253
94	Smad3	-0.48	9	64020969	64021997	H3K27ac_BMP24_vs_Noggin24_down.bed8291	2	262976
95	Plekha2	-1.02	8	25368342	25368835	H3K27ac_BMP24_vs_Noggin24_down.bed7698	1	266149
96	Tns1	-0.41	1	74392110	74392576	H3K27ac_BMP24_vs_Noggin24_down.bed184	1	267662
97	Slco2a1	-1.45	9	102717155	102718366	H3K27ac_BMP24_vs_Noggin24_down.bed8407	1	270346
98	Gm13781	-1.29	6	30304138	30304445	H3K27ac_BMP24_vs_Noggin24_down.bed6636	1	271590
99	Begain	-0.87	12	108793728	108794121	H3K27ac_BMP24_vs_Noggin24_down.bed1969	1	274096
100	Nsmce2	-0.38	15	59648461	59649920	H3K27ac_BMP24_vs_Noggin24_down.bed2918	1	274264

101	Zkscan4	-0.96	13	21754158	21754795	H3K27ac_BMP24_vs_Noggin24_down.bed2039	1	275252
102	Pmf1	-0.47	3	88685796	88686363	H3K27ac_BMP24_vs_Noggin24_down.bed5270	1	275466
103	H2afy	-0.71	13	55837212	55837457	H3K27ac_BMP24_vs_Noggin24_down.bed2269	1	298904
104	Megf11	-1.62	9	64084810	64085162	H3K27ac_BMP24_vs_Noggin24_down.bed8293	1	300464
105	Pdlim7	-0.8	13	55212697	55213089	H3K27ac_BMP24_vs_Noggin24_down.bed2250	1	300587
106	Snrnp40	-0.26	4	130663627	130664440	H3K27ac_BMP24_vs_Noggin24_down.bed5904	1	303496
107	H2afy	-0.71	13	55831656	55831866	H3K27ac_BMP24_vs_Noggin24_down.bed2265	1	304495
108	Zkscan4	-0.96	13	21787604	21788271	H3K27ac_BMP24_vs_Noggin24_down.bed2047	1	308698
109	H2afy	-0.71	13	55826222	55826464	H3K27ac_BMP24_vs_Noggin24_down.bed2262	1	309897
110	Ncbp1	-0.27	4	46451124	46451644	H3K27ac_BMP24_vs_Noggin24_down.bed5605	3	312512
111	Col26a1	-0.42	5	136566207	136566483	H3K27ac_BMP24_vs_Noggin24_down.bed6472	1	316726
112	Spag5	-0.4	11	77983488	77984505	H3K27ac_BMP24_vs_Noggin24_down.bed1394	1	317024
113	Zkscan4	-0.96	13	21809353	21810123	H3K27ac_BMP24_vs_Noggin24_down.bed2048	1	330447
114	Hic1	-5.64	11	74837918	74838337	H3K27ac_BMP24_vs_Noggin24_down.bed1348	1	331182
115	Hic1	-5.64	11	74837360	74837765	H3K27ac_BMP24_vs_Noggin24_down.bed1347	2	331754
116	0610007P14Rik	-0.33	12	85485125	85486032	H3K27ac_BMP24_vs_Noggin24_down.bed1906	2	338518
117	Zkscan4	-0.96	13	21833767	21834832	H3K27ac_BMP24_vs_Noggin24_down.bed2054	1	354861
118	Cbln1	-2.42	8	87834225	87834451	H3K27ac_BMP24_vs_Noggin24_down.bed7900	1	361634
119	Wnt5b	-1.6	6	119175343	119175659	H3K27ac_BMP24_vs_Noggin24_down.bed6965	1	368688
120	Fndc5	-0.45	4	129513789	129514013	H3K27ac_BMP24_vs_Noggin24_down.bed5893	2	376791
121	Iah1	-0.43	12	20920644	20921199	H3K27ac_BMP24_vs_Noggin24_down.bed1737	1	395193
122	Xrcc6	-0.4	15	81585603	81586024	H3K27ac_BMP24_vs_Noggin24_down.bed3020	1	401811
123	Sult1a1	-1.2	7	126272967	126273194	H3K27ac_BMP24_vs_Noggin24_down.bed7490	1	403238
124	Fmo2	-3.62	1	163314691	163314900	H3K27ac_BMP24_vs_Noggin24_down.bed466	1	415966
125	Gpi1	-0.51	7	34653672	34654022	H3K27ac_BMP24_vs_Noggin24_down.bed7208	1	423384
126	Gpi1	-0.51	7	34654505	34655670	H3K27ac_BMP24_vs_Noggin24_down.bed7209	2	424217
127	Dync2li1	-0.54	17	84184101	84185840	H3K27ac_BMP24_vs_Noggin24_down.bed3805	1	440656
128	Kctd1	-0.49	18	14682809	14683246	H3K27ac_BMP24_vs_Noggin24_down.bed3887	1	468200
129	Spon2	-2.94	5	33692376	33692667	H3K27ac_BMP24_vs_Noggin24_down.bed6146	1	473922
130	Stmn1	-0.41	4	133967557	133967976	H3K27ac_BMP24_vs_Noggin24_down.bed5929	1	500344
131	Pced1b	-0.77	15	96709117	96709702	H3K27ac_BMP24_vs_Noggin24_down.bed3060	2	537405
132	Clec2l	-1.3	6	39206174	39206529	H3K27ac_BMP24_vs_Noggin24_down.bed6701	1	543106
133	Kcnab1	-1.35	3	65665826	65666123	H3K27ac_BMP24_vs_Noggin24_down.bed5170	1	556443
134	Zkscan4	-0.96	13	22035905	22037038	H3K27ac_BMP24_vs_Noggin24_down.bed2056	1	556999
135	Scube3	-0.47	17	27556765	27557124	H3K27ac_BMP24_vs_Noggin24_down.bed3557	1	585192
136	Fam78b	-0.97	1	166409525	166409798	H3K27ac_BMP24_vs_Noggin24_down.bed477	1	591619
137	Ttc28	-0.46	5	110269409	110269820	H3K27ac_BMP24_vs_Noggin24_down.bed6321	1	609983
138	Stox2	-0.59	8	46740537	46741204	H3K27ac_BMP24_vs_Noggin24_down.bed7746	2	611144
139	Slco4a1	-1.26	2	179842765	179842984	H3K27ac_BMP24_vs_Noggin24_down.bed5005	1	613261
140	Efna5	-0.71	17	63499782	63500137	H3K27ac_BMP24_vs_Noggin24_down.bed3707	1	618466
141	Acy3	-1.08	19	4615085	4615486	H3K27ac_BMP24_vs_Noggin24_down.bed4179	1	628425
142	Myl4	-0.79	11	105181968	105182565	H3K27ac_BMP24_vs_Noggin24_down.bed1575	1	631306
143	Notch4	-1.18	17	33889859	33890595	H3K27ac_BMP24_vs_Noggin24_down.bed3608	1	673673
144	Stip1	-0.27	19	6363927	6364539	H3K27ac_BMP24_vs_Noggin24_down.bed4200	1	675487
145	Myf5	-0.69	10	108161644	108161987	H3K27ac_BMP24_vs_Noggin24_down.bed916	1	675511
146	Tcf7	-0.69	11	51606030	51606908	H3K27ac_BMP24_vs_Noggin24_down.bed1209	1	676106
147	Flt4	-1.83	11	50292056	50292261	H3K27ac_BMP24_vs_Noggin24_down.bed1204	1	682794
148	Gatc	-0.46	5	116024062	116024409	H3K27ac_BMP24_vs_Noggin24_down.bed6357	1	682885
149	Nuf2	-0.36	1	170214957	170215432	H3K27ac_BMP24_vs_Noggin24_down.bed493	1	683494
150	Oxnad1	-0.45	14	31385867	31386079	H3K27ac_BMP24_vs_Noggin24_down.bed2596	1	699295
151	Rpia	-0.64	6	71493941	71494696	H3K27ac_BMP24_vs_Noggin24_down.bed6811	1	701710
152	Ankle1	-0.59	8	70698978	70700277	H3K27ac_BMP24_vs_Noggin24_down.bed7820	1	705733

153	Stmn1	-0.41	4	133752722	133753314	H3K27ac_BMP24_vs_Noggin24_down.bed5925	1	715006
154	Etv4	-1.26	11	101063567	101064184	H3K27ac_BMP24_vs_Noggin24_down.bed1540	1	721187
155	Pole4	-0.33	6	83456506	83457010	H3K27ac_BMP24_vs_Noggin24_down.bed6846	1	751142
156	Bcl11a	-1.11	11	23307054	23307344	H3K27ac_BMP24_vs_Noggin24_down.bed1120	2	770712
157	Ube2c	-0.35	2	163995177	163995716	H3K27ac_BMP24_vs_Noggin24_down.bed4915	1	774182
158	Nfib	-0.96	4	83486085	83486328	H3K27ac_BMP24_vs_Noggin24_down.bed5697	1	780336
159	Rtp4	-1.22	16	24393509	24394349	H3K27ac_BMP24_vs_Noggin24_down.bed3247	1	783591
160	Ccna2	-0.39	3	35754122	35754497	H3K27ac_BMP24_vs_Noggin24_down.bed5070	2	817653
161	Npm3	-0.47	19	44931166	44931521	H3K27ac_BMP24_vs_Noggin24_down.bed4321	2	818070
162	Tnfaip6	-1.48	2	52857771	52858617	H3K27ac_BMP24_vs_Noggin24_down.bed4588	3	819763
163	0610007P14Rik	-0.33	12	84996703	84996908	H3K27ac_BMP24_vs_Noggin24_down.bed1898	1	827642
164	Fam65b	-1.05	13	23746762	23748051	H3K27ac_BMP24_vs_Noggin24_down.bed2101	1	834138
165	Snx9	-0.32	17	4995209	4995560	H3K27ac_BMP24_vs_Noggin24_down.bed3464	1	845768
166	Dgkd	-0.24	1	88701734	88702032	H3K27ac_BMP24_vs_Noggin24_down.bed227	1	848448
167	Jazf1	-0.75	6	52203935	52204159	H3K27ac_BMP24_vs_Noggin24_down.bed6735	1	864472
168	Notch4	-1.18	17	33684827	33685067	H3K27ac_BMP24_vs_Noggin24_down.bed3605	1	879201
169	Rtkn2	-0.76	10	67096532	67096832	H3K27ac_BMP24_vs_Noggin24_down.bed738	1	882738
170	Irx3	-1.38	8	90907940	90908188	H3K27ac_BMP24_vs_Noggin24_down.bed7917	1	893728
171	Fam65b	-1.05	13	23684267	23685765	H3K27ac_BMP24_vs_Noggin24_down.bed2096	1	896424
172	Slc14a2	-1.05	18	79109456	79109838	H3K27ac_BMP24_vs_Noggin24_down.bed4138	1	900363
173	Btbd11	-1.53	10	86295626	86296287	H3K27ac_BMP24_vs_Noggin24_down.bed858	1	908813
174	Fam65b	-1.05	13	23621479	23622502	H3K27ac_BMP24_vs_Noggin24_down.bed2094	1	959687
175	Vgll3	-1.12	16	64852578	64852874	H3K27ac_BMP24_vs_Noggin24_down.bed3375	1	962759
176	Pdgfb	-2.26	15	79028347	79028895	H3K27ac_BMP24_vs_Noggin24_down.bed3003	2	985913
177	Fam65b	-1.05	13	23585286	23585895	H3K27ac_BMP24_vs_Noggin24_down.bed2090	1	996294

Table S10: **Differentially regulated RNA-seq genes with endothelial-related GO term**

GO:0010594 regulation of endothelial cell migration	GO:0001936 regulation of endothelial cell proliferation	GO:0003158 endothelium development	GO:0001938 positive regulation of endothelial cell proliferation	GO:0010595 positive regulation of endothelial cell migration	GO:0045446 endothelial cell differentiation	GO:0043542 endothelial cell migration
Amot	Ecm1	Ctnnb1	Ecm1	Amot	Ctnnb1	Amot
Itgb3	Itgb3	Afdn	Itgb3	Itgb3	Afdn	Rab13
Slit2	Flt1	Rhoa	Agtr1a	Prkca	Heg1	Slit2
Klf4	Agtr1a	Heg1	Pgf	Gata2	Tmem100	Rhoa
Prkca	Pgf	Tmem100	Prkca	Map3k3	Acvrl1	Hmgb1
Pparg	Prkca	Acvrl1	Hmgb2	Smoc2	Plod3	Paxip1
Gata2	Pparg	Plod3	Gata2	Ets1	Col23a1	Cyp1b1
Map3k3	Hmgb2	Col23a1	Aplnr	Hdac7	Tnmd	Fap
Rhoa	Gata2	Tnmd	Cxcl12	Fgf18	Notch4	Emp2
Smoc2	Aldh1a2	Notch4	Acvrl1	Gata3	Myadm	Nr4a1
Ets1	Aplnr	Myadm	Aggf1	Nrp1	Tjp1	Nrp1
Acvrl1	Cxcl12	Tjp1	Nr4a1	Flt4	Nr2f2	Loxl2
Hdac7	Acvrl1	Bmp4	Flt4	Fgf16	Ezr	Kdr
Car10	Aggf1	Nr2f2	Fgfr3	Plpp3	Cldn1	Pik3r3
Fgf18	Nr4a1	Ezr	Adora2b	Adora2b	Dll1	Grem1
Gata3	Tnmd	Foxc2	Bmp4	Bmp4	Acvr1,Tgfb1	Clec14a
Emp2	Flt4	Cldn1	Vegfc	Sparc	Prox1	Lemd3
Dnaja4	Fgfr3	Dll1	Bmp2	Foxc2	Arhgef26	Efnb2
Nrp1	Adora2b	Acvr1,Tgfb1	Apela	Vegfc	Kdr	Stard13
Glul	Bmp4	Prox1	Nrarp	Plk2	Stc1	
Flt4	Sparc	Arhgef26	Igf2	Igf2	Hey2	
Fgf16	Nr2f2	Kdr	Prox1	Calr	CNMD	
Plpp3	Foxc2	Stc1	Ccl2	Prox1	Fas	
Bmper	Vegfc	Hey2	Kdr	Lgmn	Ppp1r16b	
Adora2b	Bmp2	CNMD	Stat5a	Kdr	Rapgef3	
Bmp4	Apela	Fas	Dysf	Stat5a	Tek	
Sparc	Nrarp	Ppp1r16b	Igf1	Ccbe1	Hey1	
Adgrb1	Igf2	Rapgef3	Ppp1r16b	Igf1	Col18a1	
Nr2f2	Prox1	Tek	Apln	Tek	Dmd	
Foxc2	Ccl2	Stard13	Bmp6	Tgfb1		
Vegfc	Kdr	Hey1	Vegfd	Anxa3		
Plk2	Stat5a	Col18a1	Pdgfb	Pdgfb		
Igf2	Ptprm	Dmd	Sema5a	Sema5a		
Calr	CNMD	Pdgfb				
Prox1	Dysf					
Lgmn	Igf1					
Kdr	Ppp1r16b					
Stat5a	Mef2c					
Ptprm	Rgcc					
Ccbe1	Apln					
Stc1	Tek					
Efna1	Bmp6					
Igf1	Vegfd					
Mef2c	Pdgfb					
Rgcc	Sema5a					
Tek						
Stard13						
Tgfb1						
Adamts9						
Anxa3						
Meox2						
Pdgfb						
Sema5a						